STICKING PROBABILITIES OF HYDROGEN ON EVAPORATED METAL FILMS

A thesis submitted for the degree of Doctor of Philosophy of the University of London

by

Norman Taylor B.Sc., A.R.C.S.

Department of Chemistry,
Imperial College,
London, S.W.7.

1967

ABSTRACT

The 'Wagener' flow technique is developed to give accurate measurements of the sticking probability of hydrogen on evaporated metal films.

Initial values are invariably high (>0.1) and are independent of flow rate and temperature. On sintered films the following initial sticking probabilities are obtained: molybdenum (o.75), nickel (0.38), titanium (0.29), tantalum (0.45) and palladium (0.99). Values obtained using unsintered films are generally somewhat higher due to the rougher surface enhancing the probability of multiple collisions.

At 78 and 90°K the adsorbed layer builds up on the 'outer' surface of the film and comes into pseudo-equilibrium with the gas phase. The kinetics of the resulting slow pressure decays on interrupting gas flow are characterized, and a gas phase process is proposed for the redistribution at low uptakes. At higher uptakes a similar model is applicable to molybdenum and nickel, the other metals absorb hydrogen and the redistribution is different in form. The rate determining step in absorption may be at or near the surface (palladium) or within the bulk (titanium and tantalum).

At 195 and 300°K the adsorbed layer is highly mobile and is near to an equilibrium distribution even during

gas flow. Titanium absorbs hydrogen in this temperature range with an almost constant sticking probability until the hydride composition TiH is approached whereas tantalum does so at 300°K only when there is a relatively high pseudo-equilibrium pressure (10^{-3} torr) above the film. Palladium does not absorb hydrogen appreciably at 300°K within the pressure range studied.

Isotherms are constructed for the saturated layers and are found to approximate to the Temkin form.

'Desorption spectra' are used to examine the energetics and population density of the adsorbed state. It is concluded that many of the adsorbed 'phases' which have been reported are merely due to surface rearrangements of the adsorbate and are not reflections of changes in population density with binding energy.

ACKNOWLEDGEMENTS

I wish to thank Professor R. M. Barrer for the provision of laboratory and other facilities in the Department of Physical Chemistry, Imperial College and also the Ministry of Aviation for the provision of a bursary.

It is a pleasure to record my gratitude to Professor F. C. Tompkins and Dr. D. O. Hayward for their help and guidance in this work.

I also wish to thank Mr. A. E. Madell and Mr. J. Preston whose glassblowing skill made this work possible.

CONTENTS

INTRODUCTION

The velocities of adsorption of gases onto clean metal surfaces are found to approach the maximum possible rate i.e. an atom or molecule adsorbs at nearly every collision between gas and surface. For this reason the kinetics of such processes are most elegantly discussed in terms of the sticking probability - defined loosely for the purpose of this introduction as the ratio of the rate of adsorption and the rate of collision of the gas atoms or molecules with the metal surface, both terms being expressed in units of atoms or molecules per unit area of surface per unit time. Thus, for a gas at a pressure P in contact with the surface, the rate of adsorption is SZP molecules per cm^2 per second where S is the sticking probability and Z the Hertz-Knudsen collision factor - $(2\pi mkT)^{-\frac{1}{2}}$.

The first reasonable model of the adsorption process was produced by Langmuir in 1918 who introduced the concept of sites for adsorption existing in the vicinity of each surface metal atom. On this basis Langmuir derived kinetically the form of the isotherm bearing his name by assuming that a necessary condition

for adsorption was collision with a vacant site. However, Langmuir later suggested that in the case of oxygen adsorption on tungsten it was possible for adsorption to occur on top of the primary chemisorbed layer thus discarding the necessity of vacant surface sites. Experimental evidence in support of this concept was obtained by Taylor and Langmuir in 1933 in a study of the adsorption of caesium on tungsten. They found that the sticking probability was unity until nearly a complete monolayer of caesium atoms had been deposited thus concluding that the caesium condensed with unit efficiency and then migrated around in a precursor state until a vacant site was reached whence transfer to the strongly held layer occurred. It may be noted at this stage that, in contrast to much work on adsorption at this time, the results of Langmuir for this system are still considered essentially correct; in fact it is relatively recently that similar results have been obtained for strontium and barium on tungsten (Moore and Allison, 1955) and for barium and magnesium on tungsten (Zingerman and Morozovskii, 1961).

Further evidence for a precursor state during the adsorption of oxygen on tungsten was presented by

Morrison and Roberts (1939) who found that the sticking probability did not fall as rapidly with increasing coverage as expected if adsorption occurred only by gas molecules colliding with vacant sites. However, the evidence cited by Morrison and Roberts is convincing only if the initial value of sticking probability is unity (as indeed they reported), otherwise the less steep fall with increasing coverage may be attributed to an activation energy of adsorption decreasing with increasing coverage. More recent work on the oxygen-tungsten system has not substantiated the unity sticking probability at zero coverage and it must be concluded that the work of Morrison and Roberts is not a convincing demonstration of the existence of a precursor to chemisorption of oxygen on tungsten.

The first reasonably reliable data suggesting the existence of a precursor to chemisorption of diatomic molecules was obtained by Becker and Hartmann (1953) in a study of the nitrogen-tungsten system. These workers found a constant sticking probability up to a certain critical coverage dependent on the temperature, and a rapid decrease beyond this point. Again, since S is less than unity (0.55 at 300°K) the constant value may be due to a fortuitiously decreasing

activation energy with increasing coverage. However, the initial S decreases with increasing adsorbent temperature and this eliminates the possibility of a simple activated process, but makes attractive the concept of a precursor state whose concentration decreases with increasing temperature. A similar negative temperature coefficient of S has been observed by Ehrlich (1961) for the same system at lower temperatures but where comparable (300°K to 400°K) Ehrlich's values of initial S are lower e.g. 0.15 at 300°K, and furthermore are strongly dependent on coverage at all temperatures above about 115°K. To add further confusion Kisliuk (1951) and Saini, Nasini and Ricca (1959) find initial values of S of 0.3 and 0.03 respectively which are temperature independent in the range 100°K (200°K in the case of Saini et al) to 500°K. The situation is as yet unresolved but the work of Hayward, King and Tompkins (1967) suggests for adsorption of nitrogen on both molybdenum and tungsten that S is independent of coverage only at temperatures below about 150°K and that there is a small negative temperature coefficient of S up to the highest temperatures used (about 350°K).

The situation with carbon monoxide on tungsten is

similarly unresolved. Redhead (1961) finds an initial S of 0.3 independent of temperature in the range 300°K to 600°K and likewise Nasini, Ricca and Saini (1961) find a constant value between 90°K and 500°K. Initial S values of 0.36, 0.18, 0.62 and 0.3 have been found around 300°K by Becker (1958), Eisinger (1957), Schlier (1958) and Ehrlich (1961) respectively. However, both King (1966) and Gomer (1966) have obtained values of unity at 78°K and 90°K by sensitive techniques measuring essentially (1 - S) thus casting doubt on the earlier results.

For the hydrogen tungsten system no significant variation of S with temperature has been recorded in studies up to 700°K and in fact calculations from atomisation data indicate an essentially constant value up to at least 2500°K (Brennan and Fletcher, 1959). Initial values of 0.1, 0.3, 0.32 and 0.24 have been obtained around 300°K by Hickmott (1960), Eisinger (1958), Rigby (1965) and Redhead (1962) respectively and 0.35 by Pasternak and Wiesendanger (1961) for hydrogen on molybdenum.

It thus appears that the negative temperature coefficient of S may be confined to the nitrogen tungsten system. However, the existence of a precursor

is suggested in the other systems by the independence of S on coverage. Fortunately, by a modification of technique, the flash filament experiments used to obtain much of the reported data can be used to supply information about the binding energies of the adsorbed species and thus about precursor states - tentatively identifying these with the most weakly held adsorbed states present. This so-called 'flash desorption' technique was developed mainly by Ehrlich (1961) and used subsequently by Hickmott, Rigby, Kasini and others to detect weakly bound species. Such species have been found for nitrogen, carbon monoxide and hydrogen on tungsten at low temperatures. For hydrogen adsorption it appears, from isotopic exchange and other data, that the most strongly bound states are atomic; Hickmott (1960) concludes that at 78°K the most weakly held hydrogen arises from a molecular type layer and thus identifies this with the precursor to chemisorption of the hydrogen as atoms.

Apart from experimental evidence the existence of a precursor may be established from the very nature of the gas-surface reaction since, as pointed out by Lennard Jones, the potential energy of a molecule approaching the surface must show two minima - a rather shallow one at a distance comparable with the hard sphere

diameter of the gas and a more pronounced one closer to the surface corresponding to the strongly held adsorbed state. Thus, if the outer shallow minimum corresponds to the precursor state, then the lifetime of molecules and the process of trapping of molecules in physically adsorbed layers is intimately connected with the kinetics of chemisorption.

Factors influencing the magnitude of S.

The values of initial sticking probability do not appear to vary significantly for the different gas-metal combinations previously considered. This has led Ehrlich (1956) and later Hayward and Trapnell (1964) to consider that the surface is essentially patch-like in adsorptive efficiency having regions where S is essentially unity balanced by others where S is very low. Strong evidence to support such a theory was obtained by Ehrlich who found that different but entirely reproducible values of S could be obtained using different samples of tungsten wire. Ehrlich considered that the 'active patches' were isolated atoms of high adsorptive efficiency perhaps situated at defects or dislocations in the surface structure. However, this can be discounted since the density of such sites is probably too low to explain values of S around 0.3 and

furthermore if such a density of sites existed then the whole of the surface could be reached by a precursor of only moderate stability and S might be expected to rise in constant. An alternative suggestion has been put forward by Hayward and Trapnell namely that the active patches are certain crystal planes. This does appear to be a more logical conclusion although it conflicts with Eisinger (1958) who claims to expose only the 311 plane of tungsten and finds the sticking probability less than unity and similar to that for other metals. There is some reasonable doubt, however, that a single plane is exposed in the latter work.

The reason for a high efficiency of adsorption on certain planes is probably associated with the process of energy transfer between gas and solid during the initial interaction with the surface. Unfortunately, in strongly interacting systems the efficiency of energy transfer is difficult to measure experimentally and comparison must be made with results obtained for the rare gases. However, since we envisage a weakly held precursor to chemisorption of the 'active gases' such a comparison may be helpful.

Energy transfer

The classical model for trapping considers the gas atoms or molecules in the surface force field both prior

and subsequent to collision with the lattice. An atom or molecule must give up some of its kinetic energy perpendicular to the surface in order to be captured i.e. remain within the range characteristic of the surface forces; failing this a molecule will rebound from the surface with little or no diminution of energy. The situation at impact is fundamentally different from that during vibrational energy transfer in gas phase collisions since the energy of compression produced in the lattice at the point of impact may be propogated through the lattice as a phonon thus making energy transfer more efficient. After trapping the atom or molecule may lose further energy to the lattice and come to thermal equilibrium. At some stage, either prior or subsequent to equilibration, the adsorbed entity may receive sufficient energy from the lattice to cause desorption. Exact treatments of simple classical models have, for example, been carried out by Ehrlich and McCarrol (1963) for a one dimensional lattice and by Goodman (1962) for both one and three dimensional lattices. In early work all collisions were head on with surface atoms in a lattice initially at rest, Goodman (1966), in his latest work, considers the removal of such restrictions. Some treatments, for

example, McCarrol (1963) and Goodman (1966) have included the effect of surface or lattice impurities on the lattice relaxation. In general the results of the simple classical treatments are interesting although not directly applicable to any reaction system. The lattice is found to relax easily giving an efficiency of energy transfer which increases as the mass ratio of gas and surface atoms or molecules approaches unity. This trend has been observed experimentally by Roberts (1939) and Thomas and Brown (1950) for a range of inert gases on platinum and tungsten. There is a second prediction from the model which has as yet not been experimentally verified. As the mass of the gas atom or molecule decreases the critical energy for capture decreases and one might expect reflexion of the lightest molecules even when there is an appreciable interaction with the surface. In early atomic beam studies reflexion phenomena were well documented for helium as well as for atomic hydrogen (Frisch and Stern 1933) but not for systems where there was a strong surface interaction. (We shall return to more modern atomic beam experiments at a later stage). Beryllium deposition on tungsten has been studied by Zingerman and Morozovskii (1961) who found unit sticking probability showing that, if

important at all, reflexions must be limited to the very lightest atoms or to cases where the interaction is negligible.

Quantum mechanical treatments of energy transfer have been carried out mainly for collisions involving the production of a single phonon, the lattice being considered as a set of Debye oscillators. Various interaction potentials have been applied but in no case can the accommodation coefficients be calculated a priori since agreement with experimental values is obtained only after judicious adjustment of several 'constants' in the final formulae. The equations derived by Devonshire (1937) are the most general and include those of Jackson and Mott (1932) and Jackson and Howarth (1933) as special cases. As a consequence of limiting the treatment to single phonon excitation the maximum allowed energy transfer is limited to $k\theta_D$, where θ_D is the Debye temperature of the lattice. Thus only weakly interacting systems are within the range of comparison and no account can be given of the highly efficient energy transfer between for example a metal atom and its own lattice where as many as ten phonons may be excited per collision. Furthermore, both the classical and the quantal theories do not

consider the accommodation of internal energy but are, with the exception of that of Feur (1963), strictly applicable only to atom-lattice collisions.

So far the consideration of energy transfer has been mainly confined to the initial act of trapping of the gas atom or molecule and not to subsequent equilibration with the lattice which must occur for any permanent adsorption. The simple treatment of Ehrlich and McCarrol (1963) indicates that the decay to the equilibrium state is rapid - for atoms colliding with their own lattice only around 4% of the initial energy is retained in the surface link after two vibrations; for different mass ratios the efficiency of energy transfer may be less but even in the worst cases a few hundred vibrations should be sufficient for equilibration. The rapidity of this approach to equilibrium makes its experimental verification very difficult but Ehrlich (1964) was able to show in the field ion microscope that tungsten atoms at 3000°K impinging on a tungsten tip at 20°K made less than one hundred surface hops before immobilisation. Unfortunately there is no similar work for more varied systems. A view of condensation in which the initial act of trapping is not important has been put forward by

Kisliuk (1956) and Sears and Cahn (1960). They consider that the limiting factor in adsorption is a slow energy transfer in the adsorbed layer which is thus at some temperature intermediate between that of gas and surface. However, recent work by Shade (1964) does not reveal any significant effect of gas temperature on the condensation of cadmium on polystyrene as might be expected if the majority of the energy transfer did not occur at a single step. Likewise the experiments of Josephy (1933) showed that mercury vapour was specularly reflected from cleaved rocksalt held at essentially the same temperature as the vapour indicating that despite the non-requirement of energy accommodation there was negligible interaction.

It is now necessary to turn from the various theories of energy accommodation and considerations of broad trends in energy accommodation to a more detailed consideration of the magnitudes of accommodation coefficients which have been experimentally determined and the effect of adsorbed layers and temperature on these values. The result of a unit sticking probability and thus unit energy accommodation for atoms depositing on their own lattice appears universal except perhaps for argon (Foner 1959) where the sticking probability

is found to be 0.6 for gas and surface temperatures of 300°K and 4.2°K respectively. McCarrol (1963), however, attributes this low value to the scattering of the lattice waves by the many defects frozen into the lattice structure which thus reduce the efficiency of energy propogation away from the point of impact.

More important in considering the relationship between sticking probability and energy transfer efficiency are those systems where the efficiency is less than unity, thus allowing the effects of temperature and adsorbed layers to be discerned. Much of the early experimental work must be discarded because of unknown surface composition; the work of Roberts (1939) is an exception and is entirely comparable with modern work. Most measurements have been performed with the rare gases since adsorption effects are thereby minimised; results for substantially clean platinum surfaces indicate an energy accommodation varying from near unity for xenon to around 10^{-2} for helium with a slight negative temperature coefficient for a given difference of gas and surface temperature (Thomas and Olmer, 1943). The situation appears more complex in recent work of Thomas and Silvernail (1966) and Roach and Thomas (1966) who found, using the temperature

jump method, a minimum in the values of the accommodation coefficient of neon at about 250°K.

For the active gases the accommodation coefficient cannot be measured by the classical techniques until the adsorbed layer is effectively saturated. This precludes the determination of a temperature coefficient of the accommodation coefficient since the surface coverage itself varies with temperature. Thus, Wachman (1966) found for nitrogen on tungsten in the temperature range 300°K to 500°K a decrease in accommodation coefficient from 0.7 to 0.4 and this is simply explained by a falling surface coverage with increase of temperature and thus a decrease in the number of surface species of similar mass to that of the impinging gas.

In a similar study of hydrogen and deuterium on tungsten Wachman (1957) found accommodation coefficients of 0.16 and 0.21 respectively and a value of 0.04 for helium accommodation on a hydrogen covered tungsten surface.

The methods of Thomas, Wachman and others are gradually being replaced by sophisticated molecular beam type work in which gas molecular speed and flux density distributions are measured directly using an essentially plane surface. Thus both a diffuse and a

specular reflection of beams of hydrogen, helium and deuterium on platinum (Datz, Moore and Taylor 1962) have been observed, and also for the last two gases on silver (Smith and Salzberg 1966) and for hydrogen and argon on tungsten and nickel (Smith and Fite 1962). It is surprising that these systems show specular reflection to such a degree since the de Broglie wavelength of the incoming molecules is of the same order as the lattice spacing and scattering of the incident beam might be expected (except at very small angles of incidence) as the surfaces are undoubtedly atomically rough. If these results are correct they give considerable insight into the process of trapping since the observation of a specularly reflected beam indicates a negligible life-time on the surface. There is much evidence in the above work that the transition from diffuse to specular reflection with increasing temperature depends critically on the degree of surface contamination. In particular Datz et al found a large decrease in the transition temperature when the platinum surface was exposed to oxygen, a fourfold change in oxygen concentration having the equivalent effect to a 1000^{o} change in temperature. Likewise Smith and Fite found, in addition to the effect of oxygen, that the carbon content of the nickel adsorbent

had a profound influence. It is reasonable to connect the diffuse behaviour at low temperatures (around 300°K) with the adsorption of some impurity since it was definitely proved by Datz that the adsorption of the hydrogen or deuterium on the platinum was not the cause and Smith and Fite were able to show that various treatments of a nickel surface had precisely the same effect on the behaviour of argon and hydrogen beams suggesting that there was a surface effect independent of the nature of the impinging gas. The LEED work of Tucker (1962) and Germer and McRae (1961) on oxygen adsorption on platinum and nickel respectively shows that the surface structures have unit cells several times bigger than that of the clean surface thus suggesting that the enhancement of diffuse reflection could be due to a roughening of the surface structure during oxygen adsorption from the 'background' gas. In support of the general idea of a specular reflection at a really clean surface Hinchen and Shepherd (1966) have observed such reflection at 400°K in the argon-platinum system and Smith and Saltsburg (1966) have obtained specularity for hydrogen, deuterium and argon on a clean silver surface at 300°K.

Another important effect has been observed during

the beam scattering experiments - that of accommodation of the gas velocity normal to the surface but not in the plane of the surface. Thus, for gas impinging as a beam onto a surface at a higher temperature it is found that the specularly reflected ray is shifted towards the normal and vice versa for a gas temperature higher than that of the surface. It thus appears that the angle of approach of gas to the surface is a parameter to be considered since it was not possible to explain the observed effect by a combination of diffuse and specular scattering.

Energy accommodation and the sticking coefficient.

Atoms or molecules which adsorb into strongly held layers will necessarily be fully accommodated to the surface; the more enlightening aspect is whether all the impinging gas is at least partially accommodated or if part is immediately reflected on impact. For the active gases the magnitudes of the sticking probability at zero coverage and the accommodation coefficient near saturation are remarkably similar thus making attractive the concept of the proportion of active patches determining the magnitudes of both sticking probability and accommodation coefficient. This picture of either full or zero accommodation of the incoming gas is in direct contrast to that of Kisliuk (1956) who

considered that there was a slow exchange of energy in the precursor state and that the majority of molecules not adsorbed came from this layer prior to complete equilibration. Kisliuk in a later publication (1958) did, however, include the case of reflection on impact but retained the concept of an essentially homogeneous surface.

The negligible temperature dependence of both the accommodation coefficient and the sticking probability is readily explained on the basis of a patched surface if the unit efficiencies are maintained irrespective of temperature. More difficult to explain is the observation of increasing accommodation coefficients with increasing coverage which are not paralleled by increases in S. This behaviour probably indicates that the inactive patches become covered with gas by surface diffusion from the active regions and, by virtue of the adsorbed layer, show an increase in energy accommodation efficiency whilst retaining a low adsorptive efficiency for molecules direct from the gas phase.

If adsorption were restricted to the 'active patches' then the sticking probability might be expected to fall rapidly at coverages corresponding to saturation of the active regions. This has been observed in the case of oxygen adsorption on tungsten

by Becker (1953) but the result may be ascribed to experimental artefacts introduced by interaction of the gas and the pressure gauge used rather than to the reason previously discussed. There does appear to be some correspondence in some systems between the value of the initial sticking probability and the fractional coverage at which S starts to fall (Hayward and Trapnell, 1964); the total coverage generally extends to that expected from the known density of surface sites. If the negative temperature coefficient of sticking probability for the nitrogen-tungsten system (Ehrlich, 1961) is accepted then this may be ascribed to a decrease in the mean distance diffused by the precursor from the active regions as the temperature is raised. Likewise, a decrease in S with increasing coverage may be attributed to the increasing probability of desorption as the precursor has to diffuse greater distances to reach vacant sites in the 'inactive' regions.

Sticking probability measurements on metal films.

It has been judicious so far to almost completely neglect most of the work performed using evaporated metal films although the latter have been widely used in rate measurements. This has been necessary because

the values of S obtained for a rough porous surface such as that of an evaporated film are not directly comparable with those obtained using smooth surface adsorbents such as filaments. Experimentally the sticking probability is measured as the ratio of the rate of adsorption and the rate of collision, both terms being expressed in units of atoms or molecules per unit area of adsorbent per unit time. For a smooth adsorbent surface the collision rate is unambiguously defined but for a porous structure this is not so since a molecule may make a number of collisions before being either adsorbed or reflected back into the void of the reaction vessel where it may be registered by the gauge. Thus, only the rate of approach to the surface may be determined and sticking probabilities calculated from this are higher than would be observed for a chemically identical smooth adsorbent surface. There are, however, two extremes at which agreement should be obtained. Thus when the true sticking probability is unity, the same value should be obtained for a rough surface. A second circumstance when the ambiguity disappears is when the sticking probability is so low that on average the atom or molecule penetrates the whole surface structure many times before being adsorbed. In this situation the gas pressure is approximately constant

throughout the porous structure and corresponds to that measured in the void of the reaction vessel in a constant temperature system. Substitution of this pressure in the Hertz-Knudsen equation yields a collision rate per unit of true surface area and providing the rate of adsorption is also expressed in the same units then a sticking probability equivalent to that for a plane surface is obtained. Normally the 'true' sticking is neither unity nor sufficiently low for the above treatment to apply and can only be obtained by estimating from some model of the porous surface the enhancement of the collision rate over and above that of the rate of approach of the gas atoms or molecules to unit geometric area of the adsorbent.

There is a second ambiguity, not hitherto specifically mentioned, relating to the term rate of adsorption. This rate is clearly understood only when adsorption occurs directly from the gas phase into a strong chemisorbed state where the atoms or molecules are permanently retained. It has been demonstrated, however, that adsorption in many cases occurs via a precursor state from which desorption may be appreciable. The rate of adsorption as normally measured refers only to atoms or molecules entering the chemisorbed state and

strictly this should be noted in the definition of sticking probability. There is a similar, but more widespread confusion when, due to a falling heat of adsorption, there is appreciable desorption from the chemisorbed state as evidenced by the appearance of equilibrium pressures of gas above the adsorbent. If the total rate of collision is obtained from, for example, an ambient pressure of gas above the film then the corresponding rate of adsorption must include terms for the rate of supply of 'new' gas and the rate of adsorption of gas previously desorbed from the chemisorbed layer if the sticking probability is to have physical significance. In many rate measurements, particularly in flash filament studies, the latter term has been ignored and the rapid fall in the calculated sticking probability as the layer approaches saturation is merely due to an increasing equilibrium pressure. The value obtained in this way still describes the overall kinetics of adsorption via the expression S.Z.P. but has no significance as regards the average number of collisions made before an atom or molecule can enter the chemisorbed state.

Although evaporated films may be seen to have certain disadvantages for rate measurements they have

the great advantage of versatility in that practically any metal may be used. Furthermore, many metals e.g. nickel, palladium, readily sinter to approximately smooth surfaces and should give data directly comparable with that for a wire or sheet. Also the rough porous films have a fairly sharp division between an outer surface which is directly accessible to the gas phase of the reaction vessel void, and an internal surface which is reached only by diffusion processes. It was found possible in this work to utilize this situation to gain insight into the phenomenon of surface migration and also to obtain the kinetics of various redistribution processes.

There is a second and much more serious reason why values for evaporated films have not been discussed at length in this introduction namely, that with few exceptions, the magnitudes of S measured are subject to large errors due to bad apparatus design and the failure to conform to certain fundamental conditions. It is hoped that the following section will outline the deficiencies of previous measurements and also invoke the necessary conditions for a successful design of experiment.

EXPERIMENTAL SYSTEMS WHICH HAVE BEEN USED TO MEASURE STICKING PROBABILITIES

Classically the amount of gas adsorbed on a solid is measured by ascertaining the pressure diminution in the system during adsorption. In principle the kinetics of the adsorption step may be followed by measuring the pressure as a function of time; in practice this has been difficult to do. With clean metal surfaces the rate of adsorption is of the same magnitude as the collision rate from the gas phase and gas pressures must be very low for the adsorption to last for many seconds or minutes. More precisely, there are about 10^{15} sites for adsorption per cm^2 of metal surface; according to the Hertz-Knudsen equation this number of collisions will be made in about $10^{-6}\ P^{-1}$ seconds, where P is the ambient pressure in torr above the metal surface. Thus, pressures less than 10^{-8} torr must be used.

In general, pressure detectors of this sensitivity have become available only recently in the form of inverted ionization gauges or various types of partial pressure devices. However, there is ample evidence that pressures as low as 10^{-8} torr were achieved in the 1920's and in fact Langmuir and co-workers did have, in one

particular system (Cs/W), a means of measuring pressures of caesium vapour of 10^{-15} torr. Langmuir, by measuring the ion current produced by ionization of the caesium atoms at a hot tungsten wire was able to estimate the sticking probability of caesium atoms on tungsten with an accuracy as good as that of modern techniques. However, the method used by Langmuir was limited to readily ionizable metal atoms. This limitation was removed by Apker who used an electron beam to ionize the gas in the system whence it became possible to measure 'pressures' of electronegative gases as well. With the development of the inverted ionization gauge by Alpert the measurement of pressures of 10^{-10} torr became routine. Various methods of estimating sticking probabilities have been developed using this gauge.

As mentioned earlier the measurement of sticking probability depends on the separate or simultaneous measurement of the rate of adsorption and the rate of collision of gas molecules at the surface (assumed smooth at this stage to avoid unnecessary complication). The rate of collision is obtained in nearly all methods from the Hertz-Knudsen equation relating the pressure P at a surface to the rate of collision per unit area:-

$$N(\text{No. of collisions per cm}^2 \text{ per sec.}) = \frac{P}{(2\pi mkT)^{\frac{1}{2}}} = ZP$$

This expression, however, presupposes a state of complete molecular chaos since the concentration of gas is given in terms of pressure and the collision frequency has been derived using the mean velocity of a completely random distribution of molecular velocities throughout the gas. As will be seen subsequently, molecular chaos cannot be assumed even approximately when the sticking probability is high and the area of adsorbent large.

The rate of adsorption has been obtained by a variety of methods. The rate of adsorption of a metal on its own lattice may be obtained by direct weighing of the deposit. In this way Rapp et al. were able to measure the rate of adsorption of zinc and cadmium on their own lattices. It so happens that the sticking probability is near unity for these systems and the small amount of material reflected could be estimated by direct weighing of a 'catch electrode'. A similar experimental set up has been used by von Goeler and co-workers to measure S during the condensation of gold on its own lattice. Here, however, a radioactive tracer (Au^{197}) was used to measure the adsorbed and reflected amounts by bringing each deposit separately near a scintillation counter.

The preceding methods have been applied to systems in which many monolayers may be deposited from the vapour phase at near unit efficiency thus making 'macroscopic' techniques feasible. Direct measurement of rate of adsorption in systems in which one or a few monolayers are adsorbed is experimentally much more difficult and only recently have vacuum microbalances been developed of sufficient sensitivity to detect several per cent of a monolayer of a gas of moderate molecular weight (say 50). A direct method for systems involving low molecular weight gases has, however, been developed using ellipsiometry. Archer and Gobelli (1965) have obtained an estimated accuracy of 2% of a monolayer for the adsorption of oxygen on silicon and in conjunction with collision rates obtained via the Hertz-Knudsen equation have obtained detailed sticking probability-coverage curves.

However, of far more importance to the present work, are the more indirect methods of estimating the kinetics of adsorption. The two major techniques in this field are the flash filament method and the flow method as developed by Wagener (1950). The former has been widely used by Becker and Hartman (1953), Ehrlich (1961 etc.), Redhead (1961) and others mainly to study gas adsorption on tungsten filaments. The experiment, briefly, consists of cleaning the adsorbent by high temperature heating in

ultra high vacuum conditions until virtually no gas is evolved on 'flashing'. Then, with the filament held at a high temperature, a steady flow of gas is set up by suitable adjustment of the inlet and outlet conductances of the reaction vessel. On cooling the filament, gas is adsorbed from the ambient gas and the steady state pressure is thus disturbed. From the resulting pressure-time profile the sticking probability can be found as a function of coverage. By rapidly heating the filament and examining the resulting pressure-time profile a check can be made on the total amount adsorbed up to any particular point.

The flow technique as developed mainly by Wagener differs from the flash filament method in that gas is not introduced to the adsorbent until a clean surface is generated. Thus, the method may be used with a wide variety of adsorbents and particularly with evaporated metal films.

Since the major part of this thesis is concerned with a flow method of the latter type only a sufficient description will be given at this stage to enable some comparisons to be made. The principles and practice of adsorption measurements using flow systems with metal films were outlined by Wagener (1950, 1951, 1952, 1956, 1957) and extended by Clausing (1961), Della Porta and

Ricca (1960), Elsworth and Holland (1963), Bergsnov-Hansen, Endow and Pasternak (1963, 1966) and others. In the basic method the rate of flow of gas to the adsorbent is controlled by interposing a capillary between a gas storage vessel and the reaction vessel. The magnitude of this rate is obtained from the pressure drop across a capillary of known conductance provided that the sole pumping agency is the adsorbent and that the rate of increase of gas molecules above the adsorbent is small compared with the rate of adsorption. The rate of collision has normally been obtained from the 'pressure' of gas above the adsorbent by utilizing the Hertz-Knudsen equation.

The method has the great advantage of versatility in that practically any material that can be evaporated may be used. The scope is not necessarily restricted to evaporated films as surfaces generated by such varied means as crystal cleavage or high temperature flashing may similarly be used. The large areas of surface normally involved restricts the degree of contamination during an experiment whereas in flash filament experiments the small area used ($\sim 1 cm^2$) demands the ultimate in vacuum conditions. Since the film is usually evaporated onto the walls of the reaction vessel temperature control is easy. This contrasts

with flash filament work in which the filament is adsorbing the ambient gas during cooling to a desired temperature thus making useful measurements near zero coverage impossible. There is a further advantage of the flow method namely that a constant pressure may be maintained above the surface during adsorption. This simplifies treatment of diffusion phenomena by maintaining a constant surface condition if a pseudo-equilibrium exists between surface and gas phase (Della Porta and Ricca, 1960). The flash filament studies should give S values of more fundamental significance than those obtained with a rough porous film and furthermore should be capable of good reproducibility as effectively the same surface is generated for each experiment. As mentioned earlier, the demarcation of the surface of a film into an inner and an outer component is not necessarily a disadvantage since it allows a sensitive method of studying both surface and gas phase diffusion phenomena.

Flash filament studies have been extended, mainly by Ehrlich, to obtain information on the population of various energy states on the surface. This is performed by presorbing gas to some desired extent and then raising the temperature of the filament at a known rate while examining the resultant pressure-time profile of

the desorbed gas. In principle such desorption may occur from equilibrated or non-equilibrated surface states depending upon the rate of heating; in practice the former may be performed using films (e.g. Hayward, Taylor and Tompkins,1966), whilst the latter may not be possible to perform even with filaments.

3. THE FLOW TECHNIQUE FOR MEASURING STICKING PROBABILITIES

Sticking probabilities of gases on evaporated metal films are usually obtained by establishing a known constant rate of flow of gas to the film and measuring the pressure P above the film surface. The rate of adsorption is equated to the rate of flow of gas (n_A molecules sec^{-1}) and the apparent rate of collision of molecules with the surface (n_c molecules sec^{-1}) is calculated from the Hertz-Knudsen equation,

$$n_c = \frac{AP}{(2\pi mkT)^{\frac{1}{2}}} \qquad (1)$$

where A is the geometric area occupied by the film, m is the mass of a molecule, k is the Boltzmann constant and T is the absolute temperature.

Hence,

$$s = \frac{n_A}{n_c} = \frac{n_A}{ZAP} \qquad (2)$$

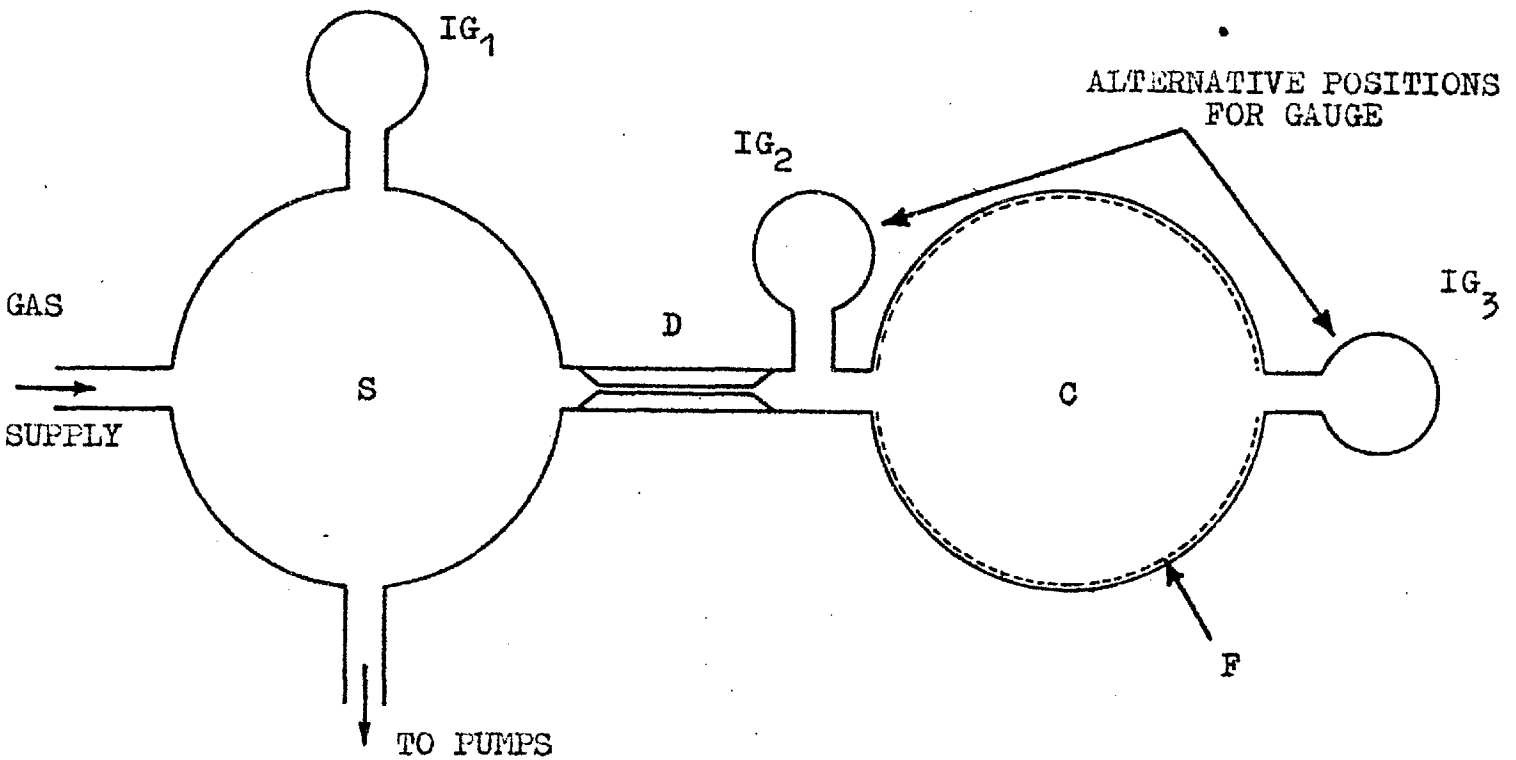

FIGURE 1. Schematic representation of apparatus commonly used to measure sticking probabilities. S - gas reservoir, C - reaction vessel, F - film, D - capillary, IG - ionization gauge.

where $Z = (2\pi mkT)^{-\frac{1}{2}}$.

The rate of flow of gas to the film is adjusted so that the film continues to adsorb for a suitable length of time; normally between 10 and 1000 minutes. If the sticking probability is high P will be in the range 10^{-7} to 10^{-10} torr and an ionization gauge or sensitive mass spectrometer must be used to record it.

The majority of workers in this field have used the same basic design of apparatus and this is shown in figure 1. The film is thrown onto the inner wall of the cell and the pressure in the cell is measured by an ionization gauge placed in one or other of the positions indicated (in some systems the gas passes through IG_2 rather than past it as shown). The rate of flow of gas to the adsorbent is given simply by $F(P_1 - P_2)$, where F is the conductance of the capillary in molecules sec^{-1} $torr^{-1}$, P_1 is the pressure in the storage bulb and P_2 is the pressure at the far end of the capillary. Normally P_2 is very much less than P_1 and can be neglected. The net rate of adsorption can be equated to the rate of flow through the capillary without significant error as pumping by IG_2 or IG_3 is usually negligible and the rate of increase in the number of gas phase molecules in the cell is always extremely small compared with the rate of uptake. Thus, measurement of the rate of adsorption

presents no difficulties except, perhaps, when the primary chemisorbed layer is weakly held and corrections must be applied for desorption (see later).

The basic problem with this method is to obtain a meaningful pressure reading from which the rate of collision of molecules with the film surface can be calculated. The pressure measured with IG_2 will always be too high because the adsorbate passes through part of the tubulation connecting gauge and cell, resulting in a pressure drop across this section. Thus, during the adsorption of carbon monoxide on a barium film at room temperature, Wagener (1956) found that the pressure registered by IG_2 was five times higher than that registered by IG_3. Similarly McKee and Roberts (1965) have shown that, in the earlier work of Roberts (1963) using a gauge between capillary and film, the initial sticking probability reported for nitrogen on molybdenum was too low by a factor of 50. In principle the pressure drop between gauge and film can be reduced to negligible proportions by increasing the conductance of the tubulation between them, although it is clearly better to place the gauge after the film.

However, the problem of obtaining a meaningful pressure reading is not necessarily solved simply by having the gauge in a certain position. When s is low

the molecules entering the cell collide on average many times with the film before they are adsorbed, and their motions are thus largely random. Under these conditions a definitive pressure exists above the surface of the film, perturbed only to a small extent by the motion of molecules emerging from the gas inlet, and the apparent collision rate is correctly given by ZAP. But when s approaches unity and the film covers most of the wall area of the containing vessel the motions of the molecules are no longer random for, at any given moment, a significant proportion of them are merely in transit between the gas inlet and the adsorbent surface. Thus a pressure cannot be defined within the cell volume and the collision rate cannot be calculated even approximately from a 'pressure' reading simply by using equation (1). Furthermore, the rate of collision is not uniform across the surface except for certain geometrical arrangements of gas inlet and adsorbent surface.

One solution of these problems is to reduce the geometric area occupied by the film to a small fraction of the total wall area. In this way the motions of molecules within the cell are largely randomised by reflection at the cell wall. Experimentally this has been achieved by throwing film onto a glass plate which is then isolated from the evaporator filament and from any

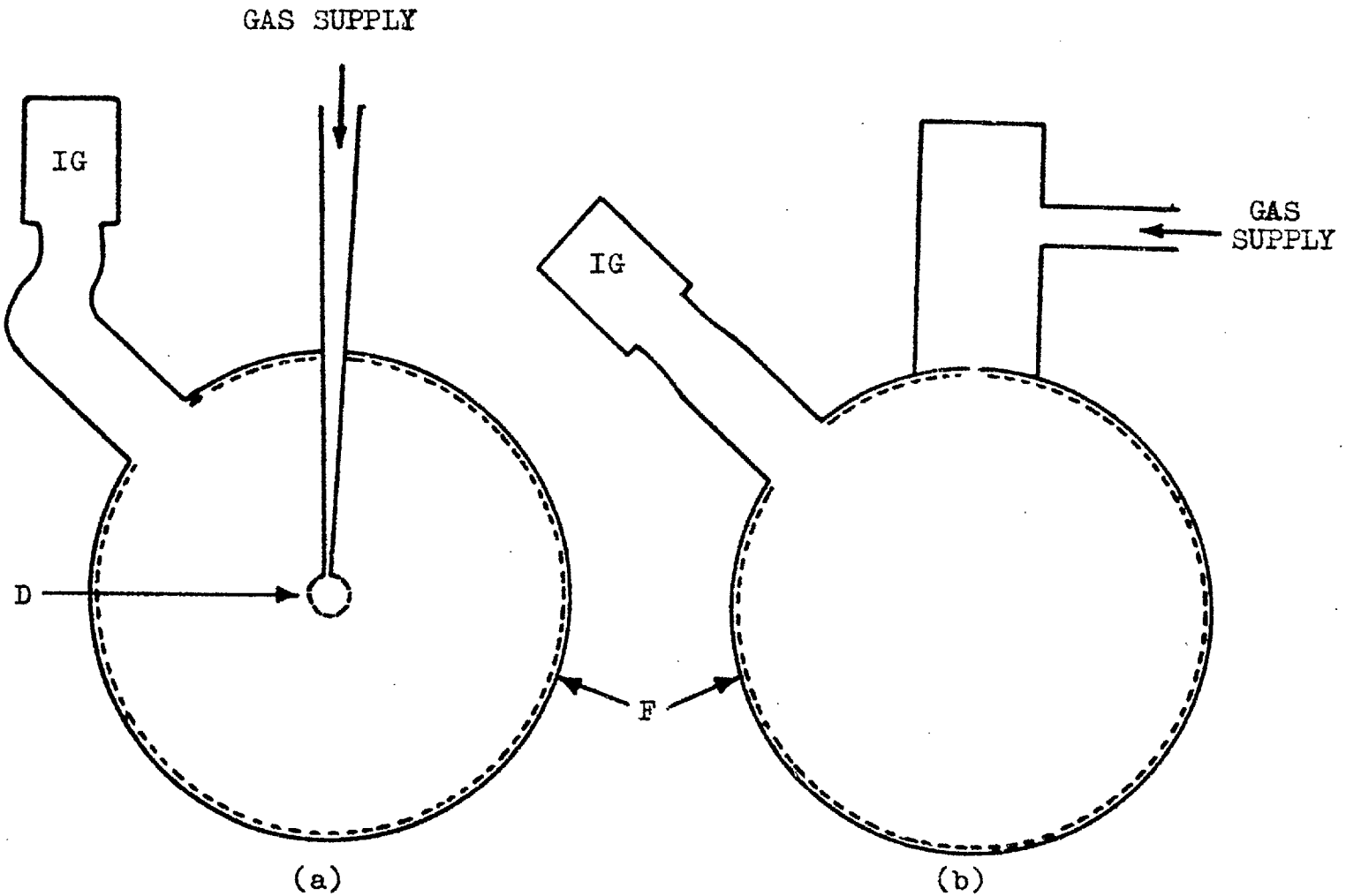

FIGURE 2. Two ways of obtaining a uniform flux over the surface of the film. D - small glass sphere punctured with many holes, F - film, IG - ionization gauge.

stray film before admission of gas (Gibson, Bergsnov-Hansen, Endow and Pasternak 1963; McKee and Roberts 1965; and Pasternak, Endow and Bergsnov-Hansen 1966). A disadvantage of this method is that adsorption is likely to occur onto the walls of the freshly outgassed system during the initial stages of an experiment, and this could easily lead to erroneous results.

Meaningful sticking probabilities can still be obtained, however, without reducing the geometric area of the film if certain designs of gas inlet and ionization gauge port are used. In general such systems must satisfy the following three conditions, otherwise the problem of relating the pressure recorded by the ionization gauge to the sticking probability becomes intractable.

(1) The molecular collision rate must be uniform over the exterior surface of the film. This can be achieved by throwing the film onto the inner wall of a spherical bulb and introducing the gas either uniformly in all directions from the centre of the sphere, as in figure 2a, or from a small orifice acting as a cosine-law emitter, as in figure 2b. The latter method has two disadvantages: first, small deviations from spherical geometry near the gas inlet lead to disproportionately large

variations in the collision rate across the surface, and secondly, the angle of incidence varies from 0 to 90 degrees so that the molecules do not 'see' equivalent sections of a rough film surface.

(2) Molecules must not enter the grid structure of the ionization gauge direct from the gas inlet, but only after their motions have been to a large extent randomised by collisions with the cell wall; hence the bend in the tubulation leading to the ionization gauge in figure 2a. This point is important because the calibration of the ionization gauge in terms of pressure is meaningful only under conditions of random motion.

(3) There must be no uptake of gas within the side arm containing the ionization gauge. This can be achieved by preventing the deposition of film onto the walls of the gauge tubulation during evaporation and by reducing gauge pumping to negligible proportions.

4. CALCULATION OF THE STICKING PROBABILITY

For a system conforming to the requirements listed above, a general equation can be derived relating s to P, the pressure registered by the ionization gauge.

First, we define α as the fraction of the total number of molecules entering the cell (n_A per second) that reach the side-arm of the ionization gauge direct from the gas inlet. As sticking probability measurements are normally carried out at very low pressures ($< 10^{-7}$ torr) where the mean free path in the gas phase is very large compared with the dimensions of the apparatus, the molecules move independently of one another and the total rate of collision with the film, n_c, may be divided into two components; one due to molecules arriving direct from the gas inlet and equal to $(1-\alpha)n_c$, and the other, n_c, due to molecules which have already suffered one collision or more with the film surface. Thus

$$s = \frac{n_A}{n_c} = \frac{n_A}{(1-\alpha)n_A + n_B} \qquad (3)$$

The molecules contributing to n_B will have a completely random distribution of velocities (i.e. as in a constant pressure reservoir) provided they are re-emitted from the film surface after collision according to the cosine law. Thus, the total molecular flux across the orifice, of area (a) leading to the ionization gauge consists of a random component, $n\,a/A$, and a directed component, αn_A. Now the rate at which molecules enter the gauge side-arm is also the rate at which they leave

under steady-state conditions and in the absence of pumping. The latter rate would be equal simply to ZaP if a uniform pressure were maintained in the side arm. However, it has been pointed out by L. Holland (private communication) that the molecules entering direct from the gas inlet penetrate a considerable way up the gauge tubulation before colliding with the walls, and they then diffuse out randomly, giving rise to a concentration gradient along this section of the tubulation. This problem is best analysed by regarding the random and directed components of the molecular flux entering the gauge side arm as independently giving rise to pressures P_B and P_A respectively within the gauge envelope. Equating the rates of arrival and departure, we have for the random component

$$ZaP_B = n_B a/A, \tag{4}$$

and for the directed component

$$ZaP_A = \alpha n_A \beta, \tag{5}$$

where β corrects for the molecular beaming effect and is a constant for a given arrangement of gas inlet and ionization gauge tubulation. Thus

$$ZaP = Za(P_A + P_B) = \alpha\beta n_A + n_B a/A$$

and

$$n_B = ZAP - \alpha\beta n_A A/a.$$

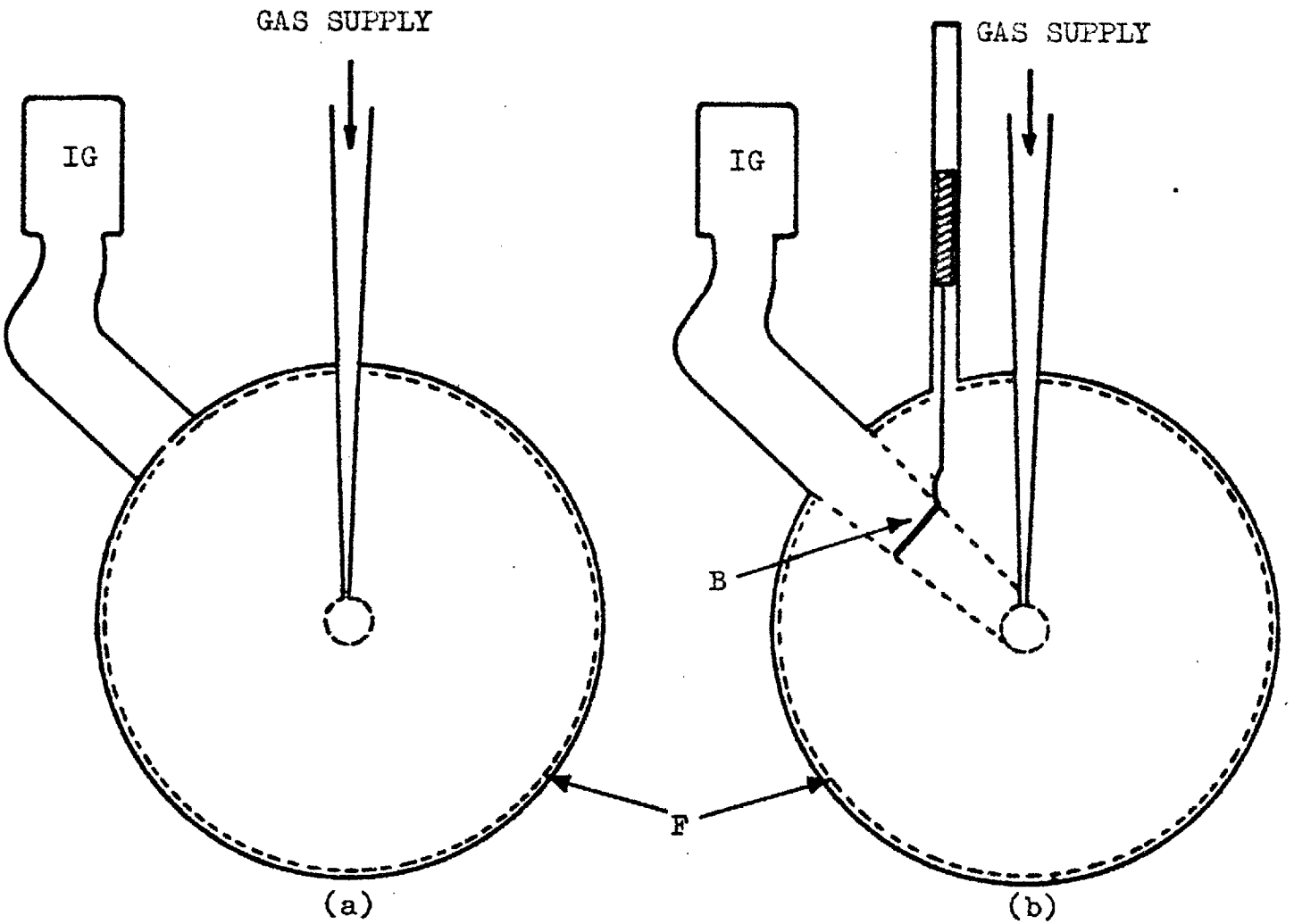

FIGURE 3. Schematic representation of two cells used to measure sticking probabilities. B - baffle plate, F - film, IG - ionization gauge.

Substituting for n_B in equation (3)

$$s = \frac{n_A}{ZAP + n_A\left\{1-\left(\frac{a + A\beta}{a}\right)\alpha\right\}} \qquad (6)$$

Three types of cell have been used in the present investigation to which this equation is applicable. The first is shown schematically in figure 2a. It suffers from the disadvantage that β must be known before sticking probabilities can be calculated accurately. β can be obtained either by calculation or by calibration against the second type of cell, which is shown in figure 3a. Here the orifice leading to the ionization gauge has been reduced to a very small hole about 2 m.m. in diameter. It will be shown later that β is effectively one for this type of cell. However, gauge pumping can be a problem with such a small hole. The third type of cell is shown schematically in figure 3b; it is similar to the first cell except for the insertion of a retractable baffle plate, just large enough to prevent molecules entering the gauge tubulation direct from the gas inlet. Thus, α is zero and the term containing β in equation (6) disappears. So far this type of cell has not given completely satisfactory results; the reasons for this will be discussed later.

The three cells will now be described in greater detail.

5. STICKING PROBABILITY CELL - TYPE I

In the first type of cell, shown schematically in figure 2a, the fraction of the incoming molecules that enter the ionization gauge compartment direct from the gas inlet is simply a/(a+A). This, substituted for α in equation (6), gives

$$s = \frac{n_A}{ZAP + An_A(1-\beta)/(A+a)} \qquad (7)$$

In earlier work (Hayward, Taylor and Tompkins 1966; Hayward, King and Tompkins, (1967) sticking probabilities were calculated for this cell using the conventional equation (2) rather than equation (7). This is tantamount to assuming that $\beta = 1$. Obviously the error involved in this assumption becomes smaller as s decreases because, at a given value of n_A, the pressure P registered by the gauge increases and finally the term ZAP in the denominator of equation (7) dominates the second term. However, at high s the error can be appreciable and it is necessary to use equation (7) and hence to calculate β.

5.1. CALCULATION OF β

We consider, first of all, a beam of molecules entering the gauge tubulation of cross-sectional area a at a rate of n molecules per second and striking the wall

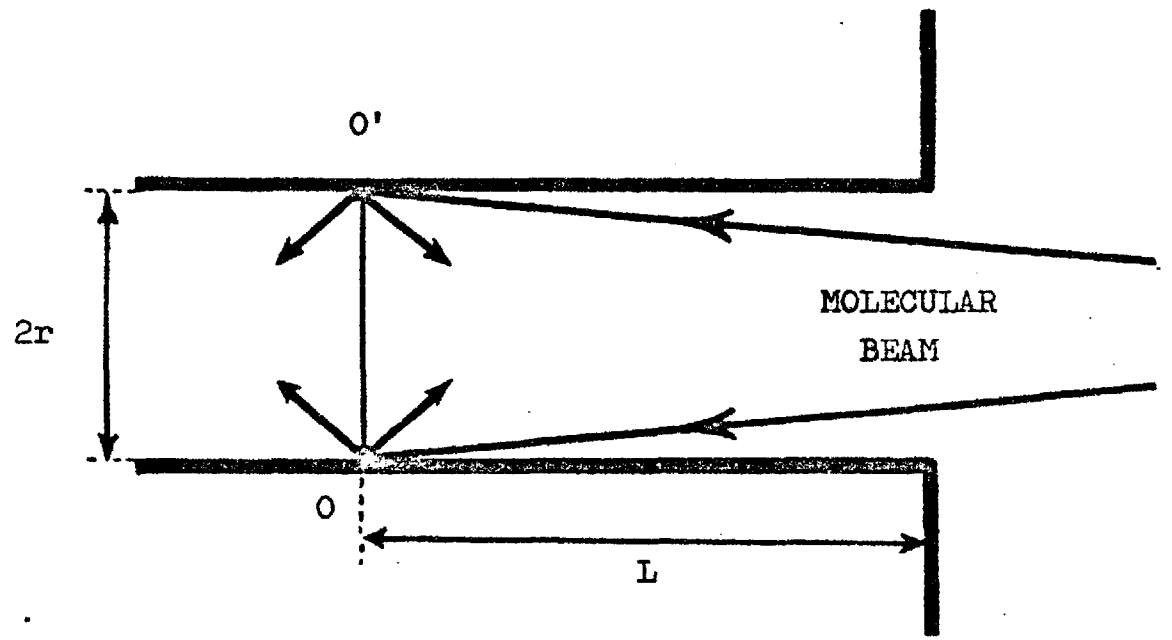

FIGURE 4. Cross section of a molecular beam striking the wall of a cylindrical tube.

at a fixed distance ℓ within the tube, as shown in figure 4. It is assumed that the beam is reflected at the wall according to the cosine law, one half of the molecules moving further up the tube and the other half moving towards the outlet. For our present purpose the beam may be regarded as a source of gas along the circumference OO'. The molecules diffuse out of the tube randomly so that there is a net free molecular flow of n molecules per second from OO' to the outlet, and this results in a concentration gradient down this length of the tube. To the left of OO' there is complete molecular chaos characterized by a constant pressure P, the pressure measured by the ionization gauge. We may consider the tubulation from OO' to the outlet as an independent tube of conductance F molecules sec^{-1} $torr^{-1}$. The rate at which molecules enter this tube is the sum of two terms; ZaP for molecules crossing OO' from left to right, and $\frac{1}{2}n$ for molecules 'originating' at OO' due to dispersion of the beam. The ratio between the rate at which molecules strike the inlet of a tube and that at which they leave the outlet is simply Za/F, provided the molecules arrive at the inlet in an entirely random manner, as they do when coming from a reservoir at constant pressure. Thus

$$\frac{ZaP + \frac{1}{2}n}{n} = \frac{Za}{F} ,$$

and

$$n = \frac{ZaP}{Za/F - \frac{1}{2}} \qquad (8)$$

As the velocities of the molecules dispersed at OO' do not have exactly the same angular and spacial distributions as those of molecules arriving from a constant pressure source, this formula involves an approximation. However, this also means that the pressure to the left of OO' is not entirely constant and the two approximations tend to cancel one another.

In the more general case where the molecular beam strikes the wall at various distances along the tube, we may consider a number of molecules dn, all striking the wall at a particular distance l from the outlet and contributing dP to the overall pressure P recorded by the gauge. Equation (8) then becomes

$$dn = \frac{ZadP}{Za/F - \frac{1}{2}}$$

On integration

$$\int_0^n (Za/F - \tfrac{1}{2})dn = ZaP \qquad (9)$$

For a short tube F is given approximately by $Za/(1+3l/8r)$, where r is the radius of the tube (Dushman 1921). Substituting this in equation (9) and integrating

$$ZaP = (\tfrac{1}{2} + 3\bar{\ell}/8r)n \qquad (10)$$

where $\bar{\ell} = 1/n \int_0^n \ell \, dn$ and is the mean distance penetrated by the beam. Comparison of equations (5) and (10), with αn put equal to n, shows that

$$\beta = \tfrac{1}{2} + 3\bar{\ell}/8r \qquad (11)$$

For our experimental system $\bar{\ell}$ can be calculated from the dimensions of the reaction vessel as indicated in the appendix, and to a good approximation is equal to RL/(R+L), where R is the radius of the spherical reaction vessel and L is the length of the gauge tubulation up to the bend (see figure 2a).

The accuracy of this formula for β will vary with $\bar{\ell}$ and also with the distribution in the values of ℓ. It involves three approximations (two in deriving equation (8) and one in the formula for F), but as these do not all operate in the same direction the overall error may be less than that involved in any one approximation. A good check on the formula is to calculate the value of β obtained when the molecules enter the gauge tubulation randomly rather than as a beam. It can readily be shown from kinetic theory that in this case $\bar{\ell} = 4r/3$ and substitution of this in equation (11) gives $\beta = 1$. Thus, the equation is exact in this instance even though $\bar{\ell} = 4r/3$ the error in using the

Dushman formula for the conductance of a short tube is about 10% (P. Clausing 1932). The equation has also been tested experimentally and it will be shown later that it is generally accurate to better than 3% for the systems used in this work.

6. STICKING PROBABILITY CELL - TYPE II

In the second type of cell access to the ionization gauge is through a small hole in a platinum sheet, which is sealed across the end of the ionization gauge tubulation. The platinum sheet is 0.05 mm thick and was used in preference to glass because the 'thickness' of the hole has to be small compared to its diameter (2 mm) in the present application.

The great advantage of this cell is that the molecular beaming effect can be ignored provided the area of the hole is very small compared to the cross-sectional area of the gauge tubulation. When this is so most of the molecules entering the gauge tubulation through the hole make many collisions with the walls before finding their way out again. Thus, the motion of molecules within the gauge tubulation is largely random and the pressure is very nearly constant. This results in a value of β close to one.

6.1 CALCULATION OF β

β may be calculated from equation (9) by substituting for F the formula for the conductance of a short tube restricted at one end by a diaphragm containing a small hole. This formula is, approximately (Dushman 1962 p. 96)

$$F = \frac{Za}{3\bar{\ell}/8r + a/a_o}$$

where a_o is the area of the hole.
Equation (10) then becomes

$$ZaP = (3\bar{\ell}/8r + a/a_o - \tfrac{1}{2})n.$$

In this case βis defined by the equation

$$Za_oP = \beta n$$

Thus

$$\beta = 1 + (3\bar{\ell}/8r - \tfrac{1}{2})a_o/a. \qquad (12)$$

In the cells we have constructed $a/a_o \simeq 300$, $r = 1.7$ cm and $\bar{\ell} < 5$ cm. Substituting these values in equation (12) we see that the error in putting $\beta = 1$ is considerably less than 1%. Thus the conventional equation (2) can be used to calculate sticking probabilities.

7. STICKING PROBABILITY CELL - TYPE III

The third cell is basically a type I cell but with the addition of a retractable baffle, as shown schematically in figure 3b. When lowered into position the baffle is just large enough to prevent molecules from entering the side arm leading to the ionization gauge direct from the gas inlet at the centre of the sphere. However, it has a negligible effect on the random component of the molecular flux and equation (6) may therefore still be used, but with β put equal to zero; that is

$$s = \frac{n_A}{ZAP_1 + n_A} , \qquad (13)$$

where P_1 is the pressure measured by the ionization gauge when the baffle is down. This method of obtaining sticking probabilities is essentially that used by R.E. Clausing (1961).

The sticking probability may also be calculated from P_2, the pressure measured with the baffle withdrawn, and P_1. n_A may be eliminated from the formula for s by combining equations (7) and (13). Thus

$$s = \frac{P_2 - P_1}{P_2 - A(1-\beta)P_1/(A+a)} \qquad (14)$$

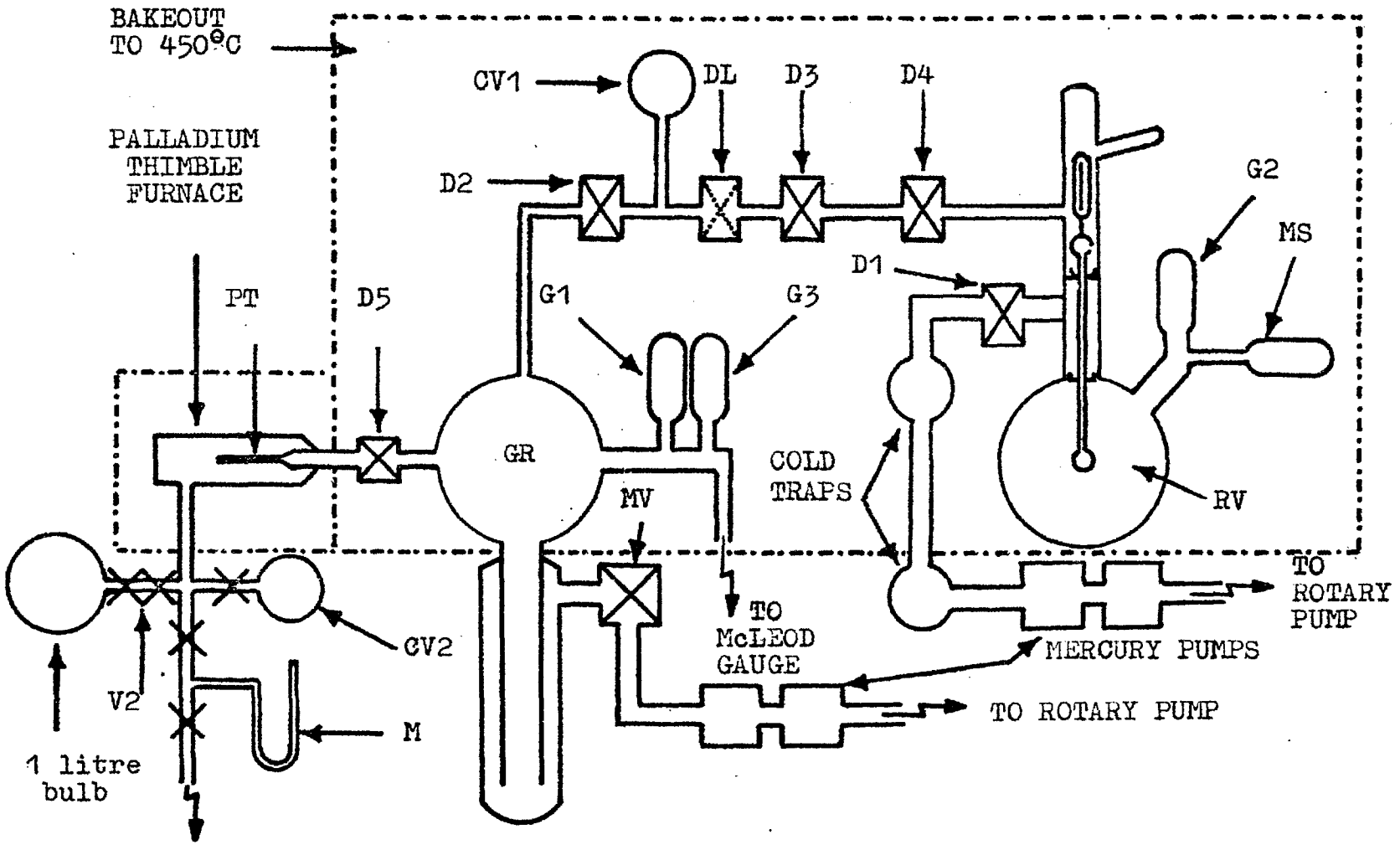

FIGURE 5. The Vacuum System

This method has the advantage that neither the absolute conductance of the gas inlet system nor the sensitivities of the gauges need be known. In all other methods discussed in this thesis the absolute conductance of the gas inlet system is required if the calculation of s is to be independent of gauge sensitivity.

8. HYDROGEN ON METAL FILMS - EXPERIMENTAL

8.1. The Ultra-High Vacuum System

The main vacuum system is shown schematically in figure 5. It is constructed entirely of glass and consists of two separately pumped chambers - the gas reservoir GR and the reaction vessel RV - interconnected by a chain of small decker valves D2, D3, D4 (Decker, 1954) and a magnetically operated capillary leak DL (see page 84). Pumping is effected by single stage high speed mercury diffusion pumps each backed by three stage diffusion pumps. The pumping speeds at 10^{-6} torr are approximately 60 l sec^{-1} and 20 l sec^{-1} on RV and GR. Cold traps are inserted between the pumps and the vacuum chambers to prevent diffusion of mercury into the main system. The pumping speed on GR may be varied by a variable-aperture mercury cut off MV; a large decker valve D1 is used when necessary to isolate RV

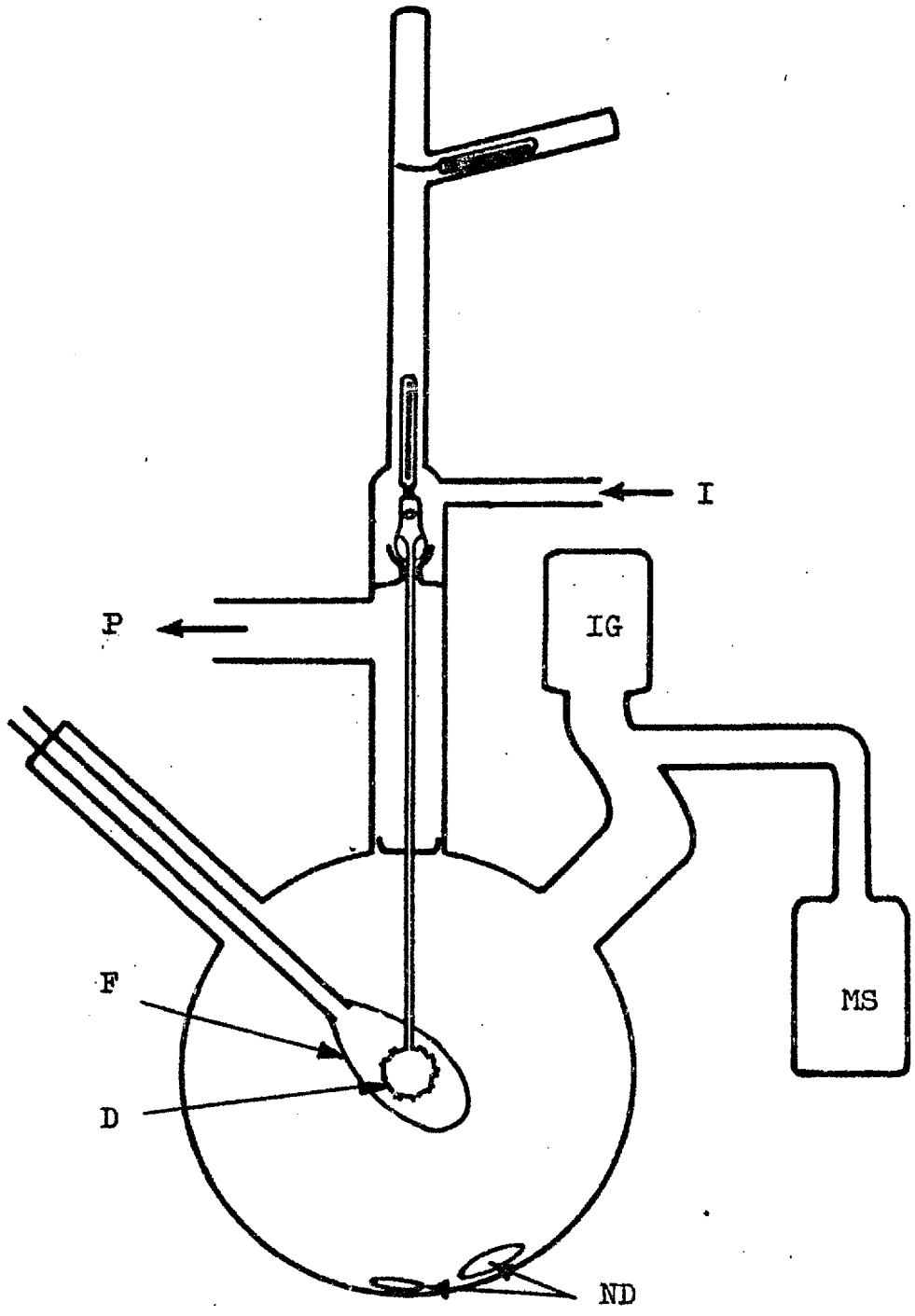

FIGURE 6. Sticking probability cell type I.

from the pumps. A calibrated volume CV1 is included in the chain of small decker valves to facilitate calibration of various volumes. The gas storage system is comprised of a 1 litre hydrogen bulb, a dosing volume V2, a mercury manometer M and a second calibrated volume CV2. Gas leaves the storage system via the palladium thimble PT and enters GR via a small decker valve D5. Pressures are measured in the main system by inverted ionization gauges G1, G2 (Alpert and Bayard, 1950) or at large gas pressures (10^{0} to 10^{-5}torr) by a high pressure ionization gauge G3 (Schulz and Phelps, 1957). A sensitive 180^{0} magnetic deflection mass spectrometer MS is connected to RV allowing partial pressures down to about 5×10^{-12}torr to be measured. For various gauge calibrations a Mcleod gauge was connected via a cold trap and capillary (see Leck 1964) to GR. The forepump is a two stage rotary pump (Edwards 28C20) which pumped on about 15 litres of ballast volume. About 5 litres of the latter volume could be isolated to operate the Mcleod gauge and the mercury cut-off.

8.2. The reaction vessels

Figure 6 is a more detailed representation of the type I cell. Gas is introduced symmetrically from

the centre of the cell via a diffuser D, which consists of a small glass sphere punctured regularly with about 20 holes and connected to the gas supply by a fine capillary. The total area of the holes is only a small fraction of the area of the diffuser sphere so that, on average, the incoming gas molecules make many collisions with the walls of the diffuser before emerging through the holes. This ensures that there is a uniform gas distribution over the film as a whole, although there may be some local variation due to the directional properties of the flux from any one hole.

The metal film is deposited onto the walls of the cell from the filament F, with the gas inlet system withdrawn from the cell and the nickel discs ND held magnetically over the orifices leading to the ionization gauge and to the retracted diffuser in the vertical sidearm. The prevention of film deposition in the gauge sidearm is of extreme importance since (see page68) even minute amounts lead to serious errors in pressure measurement. After film deposition the nickel discs are removed, the diffuser is lowered into position and gas is introduced from the gas reservoir GR through the chain of decker valves. (The pressure in GR may be set to any desired value by altering either the

temperature of the palladium thimble, the hydrogen pressure behind it, or the setting of the variable mercury cut-off MV). The cell may be isolated from the pumps by closure of the decker valve D1. Normally this remained closed during measurements although the pressure recorded by the ionization gauge was little different when it was open, except at low sticking probability. For a discussion of the effect of D1 on recorded pressure in terms of gas purity and conductance between cell and pumps see page 78.

Cells II and III were similar in basic structure and operation to cell I. The differences have been discussed previously.

8.3. The measurement of pressure with the ionization gauges.

8.3(a) Construction

The inverted ionization gauges used were the commercial types 10G3 (Mullard Ltd.) and IG3 (Edwards High Vacuum Ltd.) modified by replacing one of the tungsten filaments by a rhenium filament which was then coated with lanthanum hexaboride using a cataphoretic technique. The deposition technique has been previously described (Hayward and Taylor, 1966).

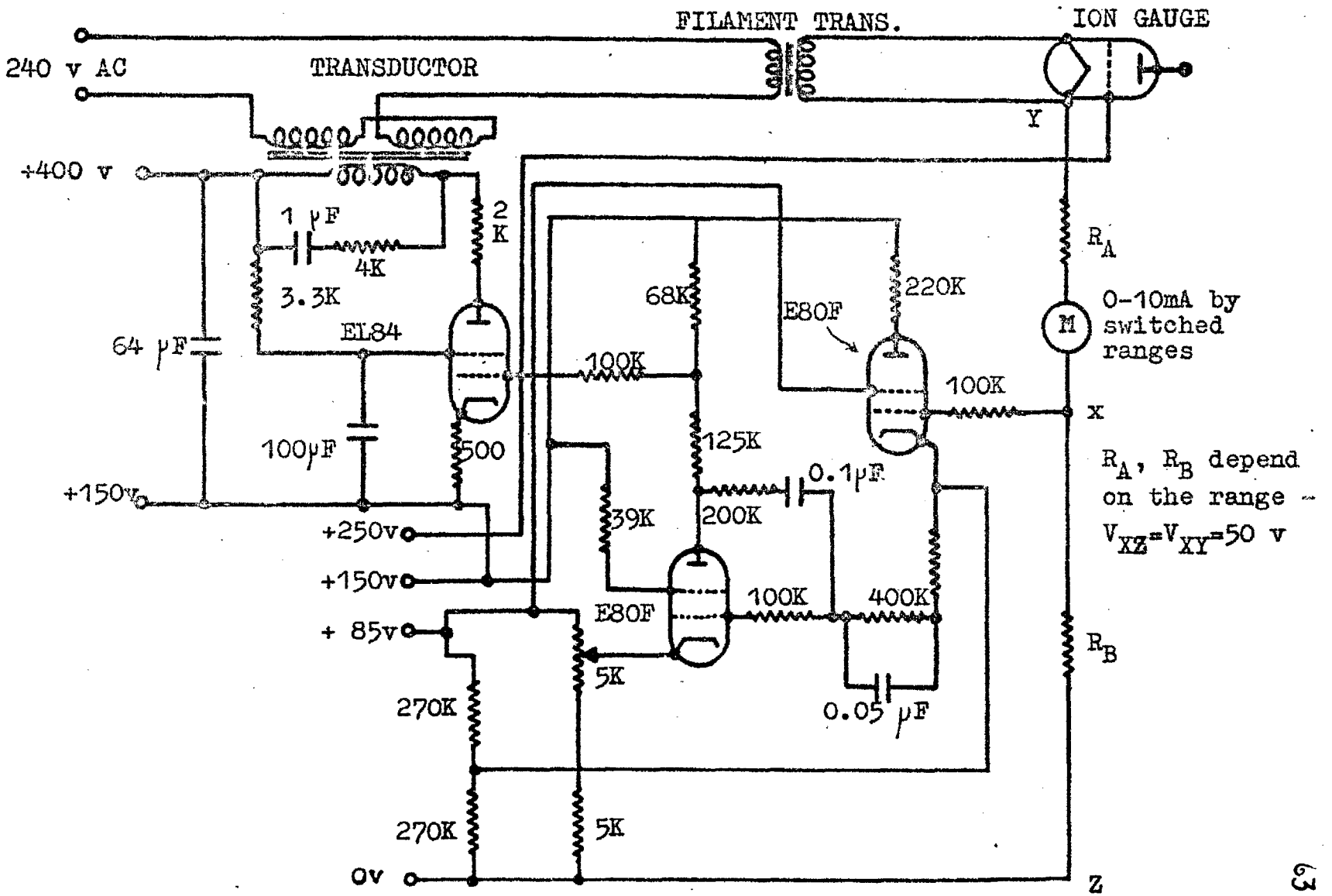

FIGURE 7. The ionization gauge emission controller.

The high pressure ionization gauges were constructed in a similar manner to that described by Schulz and Phelps (1954). In early designs the grid and collector were fabricated from polished molybdenum sheet; later platinum was used with the great advantage of a maintained surface finish. The cathodes were rhenium filaments coated with lanthanum hexaboride.

8.3(b) Operation

The electron emission of the ionization gauges was stabilized using the circuit given in figure 7. The range of control was 1 μA to 10 mA and the grid-cathode and cathode-collector potentials were maintained at the maker's recommended values - +150V and +30V respectively. The high pressure gauge operated perfectly satisfactorily from the same circuit although as pointed out by Schulz and Phelps there may be an advantage in operating with the cathode potential mid-way between grid and collector.

Ion currents were measured using 'Knick' picoammeters (maximum sensitivity 8 x 10^{-12}A f.s.d.), an 'Ekco' vibrating reed electrometer (maximum sensitivity 3 x 10^{-15}A f.s.d.) and a 'Keithley Model 417' high speed picoammeter (maximum sensitivity 1 x 10^{-13}A f.s.d.). Each unit had certain advantages; the backing off facility of the Keithley was found

particularly useful.

The inverted ionization gauges were outgassed by induction heating or by electron bombardment using the tungsten cathode only. When using the latter method the lanthanum hexaboride-rhenium cathode had to be completely disconnected from the tungsten filament otherwise radiation from the grid was sufficient to start the coated cathode emitting and thus initiate a thermal runaway. The high pressure gauge was outgassed by induction heating only.

8.3(c) Perturbations produced by the ionization gauges

Ionization gauges exhibit a pumping action due to the collection of ions and to the presence of a hot filament. Hickmott (1960) has demonstrated the serious drawbacks of using hot tungsten cathodes in ionization gauges when attempting to measure hydrogen pressures; in this work it was necessary to check that the substitution of low work function cathodes had completely alleviated such effects.

The pumping action of the ionization gauges (and the mass spectrometer) was estimated by observing the hydrogen pressure diminution in a closed volume. In general, the pressure was found initially to fall logarithmically over about 2 orders of magnitude and

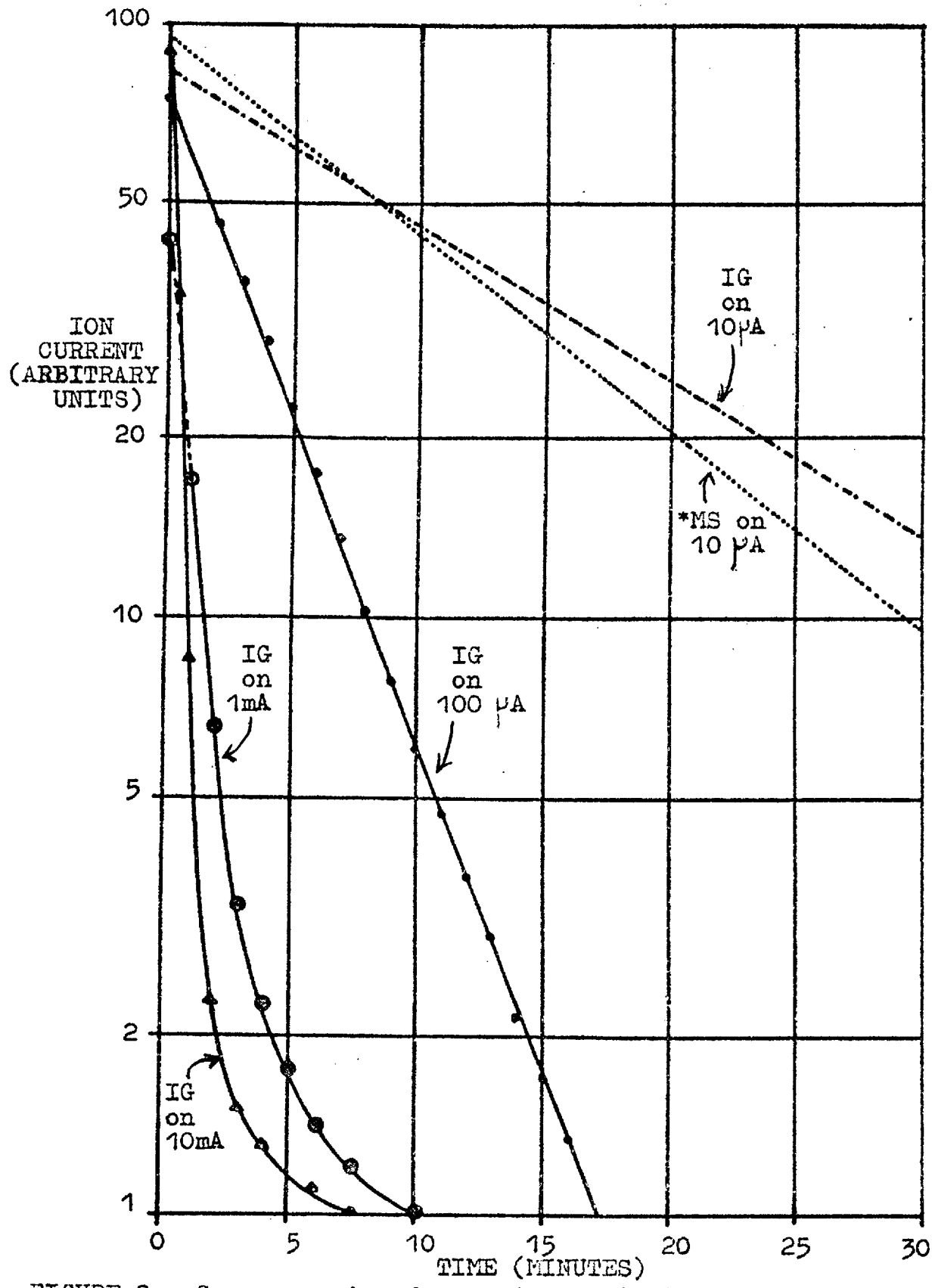

FIGURE 8. Gauge pumping for various emission currents.

then fall less steeply as the gauge approached saturation with gas. Typical curves illustrating this for emissions between 10 μA and 10 mA are shown in figure 8. The initial pumping speeds have been calculated from the latter curves; the results are given in the following table.

GAUGE USED	EMISSION CURRENT	INITIAL PUMPING SPEED OF HYDROGEN (a) in l sec^{-1}	INITIAL PUMPING SPEED OF HYDROGEN (b) in molecules sec^{-1} $torr^{-1}$
ALPERT	10 mA	0.09	3.0×10^{18}
"	1 mA	3.2×10^{-2}	1.0×10^{18}
"	100 μA	1.3×10^{-2}	4.0×10^{17}
"	10 μA	2.1×10^{-3}	7.0×10^{16}
MASS SPECTROMETER	10 μA*	2.7×10^{-3}	9.0×10^{16}

*refers to trap current.

The results may be compared with those obtained by Winters, Denison and Bills (1962) for the pumping rates of hydrogen by a tungsten filament inverted ionization gauge. These workers obtained 5 l sec^{-1} at 10 mA emission which demonstrates the great reduction in chemical pumping of hydrogen by the use of low work function cathodes. In fact the value given in the table for 10 mA emission is about that expected

for purely ion pumping; it is not clear why the pumping rate does not fall linearly with emission current.

There is a third source of pumping not hitherto mentioned, namely that due to the presence of outgassed metal parts in the gauge or to film inadvertently deposited during outgassing. Alpert (1961) has shown that heating of the molybdenum electrodes of an ionization gauge to 1870°K increases the initial pumping speeds for nitrogen by an order of magnitude; even more drastic effects may be expected if any film is deposited - 1 cm^2 of molybdenum film has a pumping speed of around 10^4 times that for normal operation at 100 μA emission current.

The pumping rates discussed above lead to low estimates of the pressure in the system to which the gauge is connected due to a pressure drop in the connecting tubulation. The effect can be estimated from the expression

$$F\Delta P = F(P_S - P_G) = GP_G$$

$$\text{or} \quad \frac{\Delta P}{P_G} = \frac{G}{F}$$

where F, G are the conductance of the tubulation and the pumping speed of the gauge respectively - both in units of molecules sec^{-1} $torr^{-1}$; P_S and P_G are the

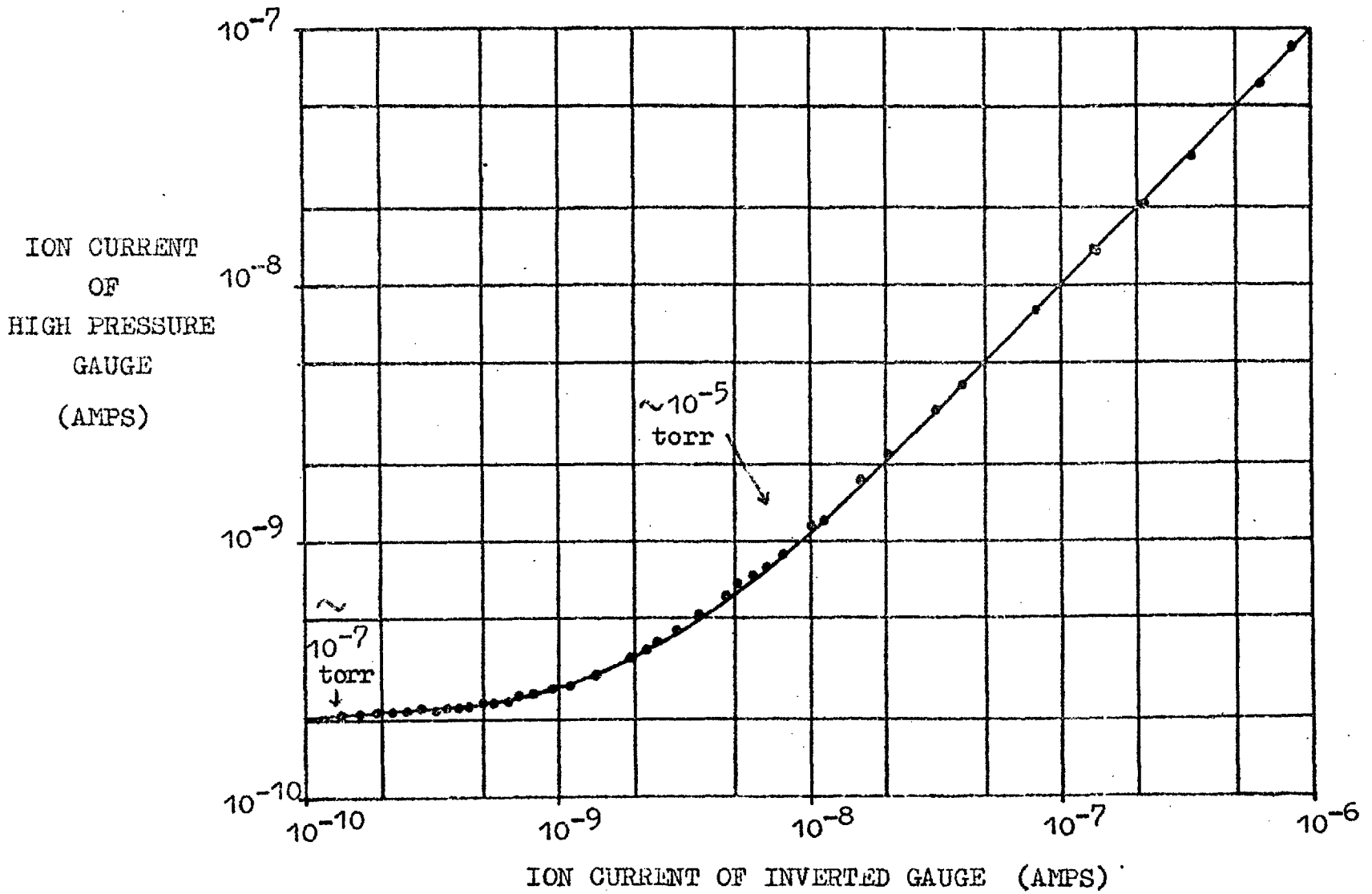

FIGURE 9. Log. Log. plot of ion currents of high pressure and inverted gauges (both on 100 μ A emission current).

pressures in the system and gauge.

In the gas reservoir, cell type I, and cell type II the tubulations have conductances of 5×10^{20}, 6×10^{21} and 3×10^{19} molecules $sec^{-1}torr^{-1}$ respectively and thus at 10 mA emission ($G \sim 3 \times 10^{18}$ molecules $sec^{-1}torr^{-1}$) the relative error in pressure measurement - $\frac{\Delta P}{P_G}$ - is about 0.6%, 0.05% and 10%. The maximum emission used in experiments was normally 100 μA and errors even with cell II should be 1% or less.

8.3(d) The linearity of the ionization gauges

The low pressure departure of ionization gauges from linearity is generally thought to be caused by soft X-rays, which are emitted from the grid during electron capture, striking the collector and causing emission of electrons - this appearing to the electrometer as an ion current. Since the X-ray current is proportional to emission current there appears a 'pressure' limit which is independent of the emission current - this is the X-ray limit.

With the high pressure ionization gauge the probability of the emitted X-rays striking the collector is very high. Figure 9 is a log plot of the ion currents at 100 μA emission current of the

high pressure ionization gauge and the inverted ionization gauge extending to the region of the X-ray limit of the high pressure gauge. The linear characteristic extends down to about 3×10^{-5}torr, the X-ray limit is at about 2×10^{-7}torr.

The mechanical design of the inverted ionization gauge greatly reduces the fraction of the X-rays which strike the collector and correspondingly reduces the X-ray limit. For gauges of average dimensions X-ray limits of between 2×10^{-10}torr and 5×10^{-11}torr have been quoted. However, Redhead (1963) has compared the readings of the inverted gauge with those of an inverted magnetron gauge (no X-ray limit) and concludes that the sorption of gas onto the grid profoundly alters the value of the pressure limit. Carbon monoxide and oxygen are quoted as increasing the limit by factors of up to 400 whereas hydrogen and nitrogen had negligible effects. The X-ray limit may be thus expected to vary with the condition of the grid; the following evidence has been obtained to support such a view.

1) In several experiments the mass spectrometer was used in an attempt to analyse the residual gas in the system. However, with gauge readings of $1 - 7 \times 10^{-10}$torr (the normal indicated

pressures after bakeout) no residuals could be detected by the spectrometer although it was shown in the same experiments that a hydrogen pressure of 5×10^{-11} torr was easily detected.

2) The lowest pressures recorded in the system ($6 - 7 \times 10^{-11}$ torr) were obtained after the gauges had been heated in an atmosphere of pure hydrogen thus suggesting that a clean grid structure is a prerequisite to a low X-ray limit.

3) The tungsten filament of the ionization gauge could be used as a desorption-spectrometer in the manner described by Redhead (1959). Results indicated pressures of 'active' gases of 10^{-11} torr or less.

4) The proximity of a magnetic field greatly influenced the recorded ion currents presumably by altering the mean path of electrons and ions in the gauge. However, the effect on ion currents near the background values was very small as would be expected for a gauge at the X-ray limit.

It is concluded that many, if not all, of the recorded background ion currents were due to X-ray emission and thus the true pressure in the system was perhaps 10^{-11} torr or lower.

The high pressure limit of ionization gauges is caused by space charge effects limiting the electron

and ion collector efficiencies and by the collection of secondary electrons thus limiting the average path length per electron collected.

In the high pressure ionization gauge the electron path is kept short and direct and the electron and ion collector efficiency is high. Simple consideration shows that providing these efficiencies remain constant for both primary and secondary ions and electrons then the maximum ion current has the magnitude of the measured emission current. (This is because each collision produces one additional ion and one additional electron). For the gauges of the dimensions used here (sensitivity about 1 per torr) Schulz and Phelps were able to show that the theoretical limit of several torr was approached.

The linearity of these high pressure gauges was checked by leaking gas at a constant rate into a closed volume. This was performed by holding the palladium thimble at a constant temperature and observing the pressure build up in GR when the mercury cut off was closed. Unfortunately an exactly constant flow rate could not be maintained over the time required to approach 1 torr. However, the non-linearity in the rate of build up of pressure could be shown to be due to a changing flow rate by rapidly

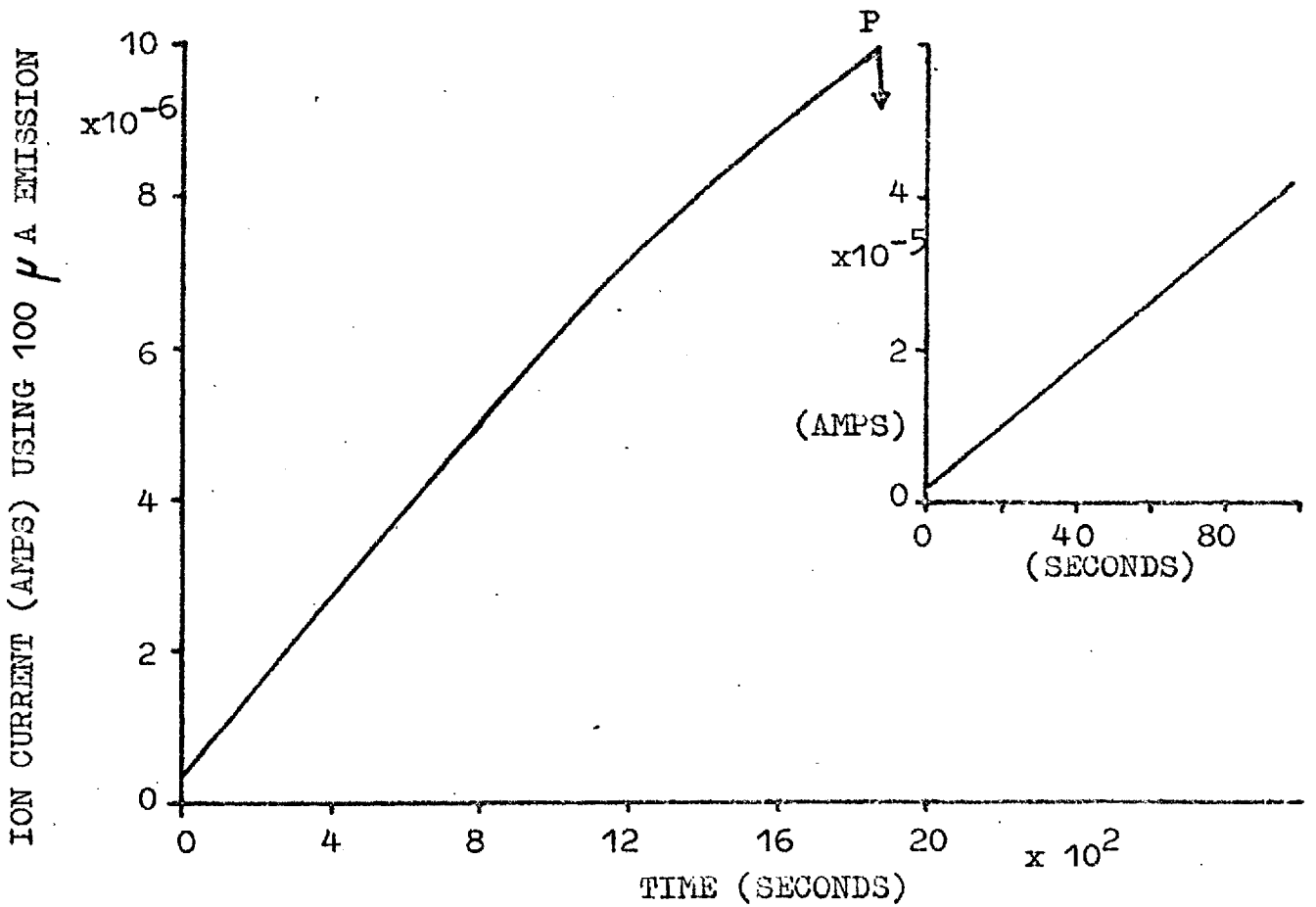

FIGURE 10. The linearity of the high pressure gauge (see text) [At P some gas was pumped off.]

pumping the system and then repeating the experiment, whence a new pressure-time slope was obtained similar to that just before pumping. Figure 10 shows the result of one such experiment showing linearity into the 10^{-1} torr range.

The saturation of inverted ionization gauges occurs at well below the high pressure limit discussed by Schulz and Phelps indicating that space charge effects probably limit the ion collector efficiency by creating a net drift out of the grid volume. (Nottingham, 1954, describes a gauge with the grid ends closed for a slightly different reason than that discussed here). A second effect is created by the charging of the glass walls of the gauge envelope; Carter and Leck (1959) showed that two stable states existed corresponding to the glass walls either at grid or collector potential. This phenomenon was observed in several experiments in this work; the change over from one state to the other occurred abruptly, generally in the 5×10^{-3} to 2×10^{-2} torr pressure range, and was accompanied by a 30% change in sensitivity. The wide variation in the pressures at change over was probably due to various amounts of conducting coating on the glass walls.

8.3 (e) The sensitivity of the ionization gauges

The only convenient absolute standard with which a direct calibration of ionization gauges can be made is the Mcleod gauge. However, calibration against the Mcleod gauge has the disadvantages of a restricted range and the presence of outgassing and pumping effects. For these reasons a check on direct calibrations was made using flow methods and absolute conductances. For simplicity the methods will be considered separately.

Calibration of sensitivity using a Mcleod gauge.

The main uncertainty in making pressure measurements with a Mcleod gauge lies in the failure to attain readily the equilibrium height of mercury in the capillary, due to a combination of surface charge and tension effects. In practice the capillary must have a bore greater than 1 mm in diameter for these effects to be reduced to an acceptable level, thus restricting the minimum pressure which can be measured to a little less than 10^{-4}torr. There is a second disadvantage of the Mcleod gauge which arises because of the pumping effect of the vapour stream between gauge and cold trap. However, this effect is at a minimum with hydrogen (and helium) and should not exceed 5% at 300°K (Gaede, 1915, Ishü and Nakayama, 1961). The effect was reduced even

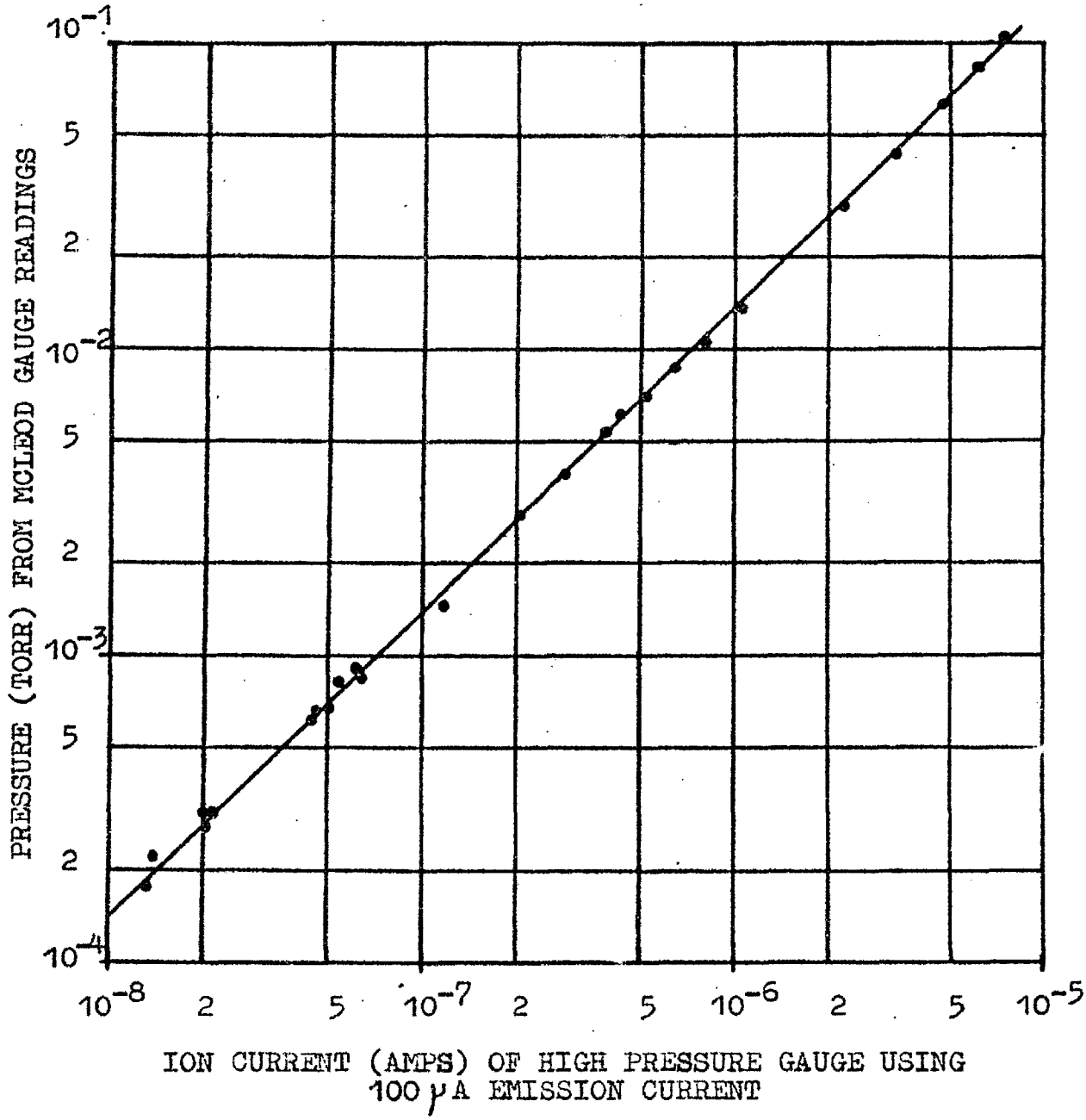

FIGURE 11. Calibration of high pressure gauge against the McLeod gauge.

further by placing a capillary between gauge and trap in the manner described by Leck (1964). When the Mcleod gauge was attached to the gas reservoir it was necessary to perform a number of degassing cycles to attain vacua of less than about 7×10^{-10}torr; sensitivities did not appear to differ in these instances from those measured with background pressures as high as 3×10^{-9}torr.

Two Mcleod gauges were used in this work; the critical dimensions and the calibration factors are given in the following table

Mcleod	Capillary Diam.	Bulb Vol.	Cal. Factor*C.
A	1.003 mm	254.5 ml	3.08×10^{-6}
B	1.020 mm	325.4 ml	2.43×10^{-6}

* $C.\ h_1(\text{mm}).\ h_2(\text{mm}) = \text{Pressure (torr)}.$

The high pressure ionization gauges covered the whole range of the Mcleod gauge and calibration was thus straightforward. Figure 11 shows the calibration curve of the high pressure gauge used in most of this work; the indicated sensitivity in this instance is around 0.79 per torr*.

* (This is the normally accepted unit for ionization gauge sensitivity - more correctly the unit is

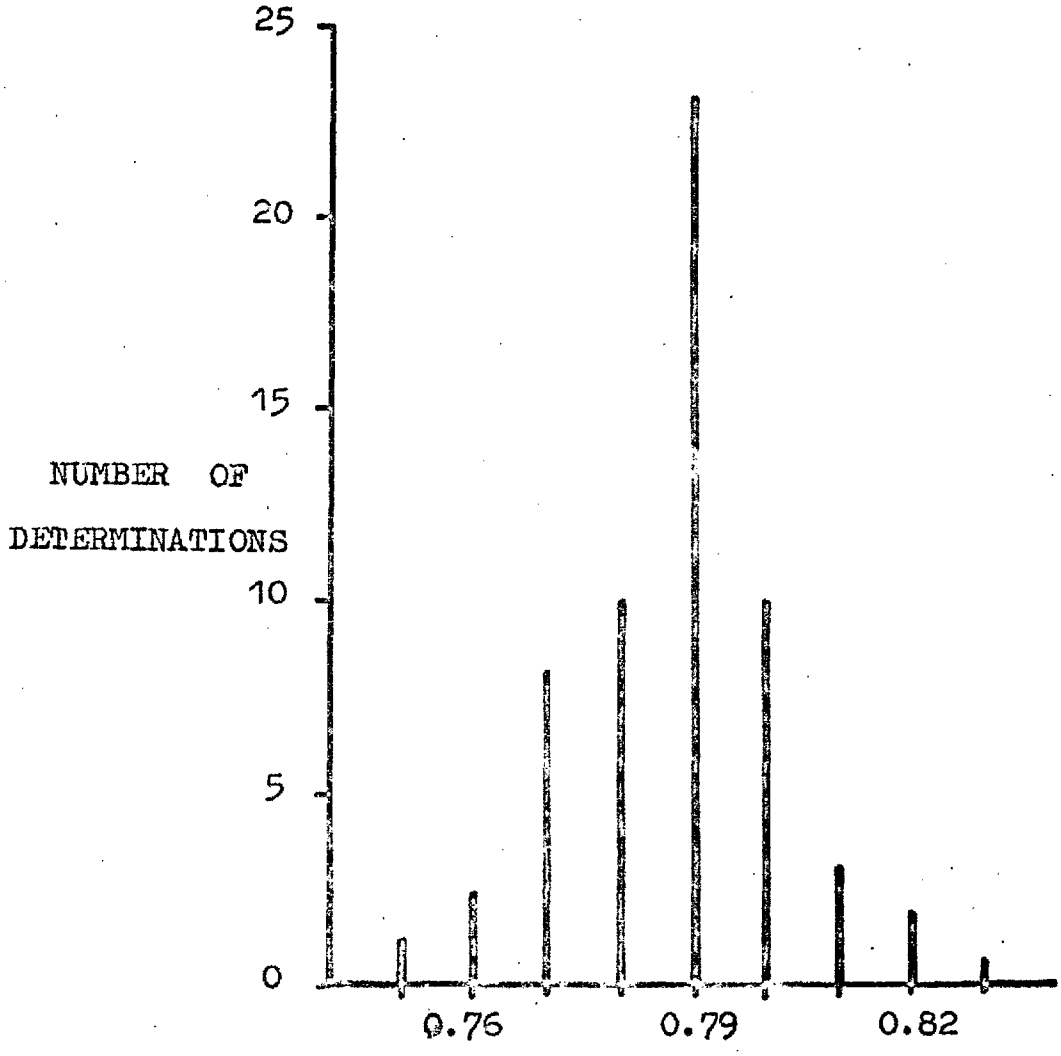

(A mean of 10 determinations of the relative sensitivity of inverted and high pressure gauges gave a factor of 10.20, i.e. sensitivity of inverted gauge $\sim$ 8.10 torr^{-1},)

FIGURE 12. Calibration of the high pressure gauge against the McLeod gauge in the range 1 - 2 x 10^{-2} torr.

$\frac{\text{ion current (A)}}{\text{emission current(A)}}$ per torr).

The inverted gauge may be calibrated directly against the Mcleod gauge over something less than 1 order of magnitude of pressure change and even in this range the Mcleod readings were found to be subject to random errors of ± 15%. On the whole, direct calibration was unsatisfactory and an alternative procedure was used in which the high pressure gauge was calibrated against the Mcleod in the range 10^{-1}torr to 10^{-3}torr and then used as a secondary standard to calibrate the inverted gauge down to 3×10^{-5}torr. Normally the sensitivity of the high pressure gauge was obtained by treating statistically a large number of readings at a fixed pressure in the range $1 - 3 \times 10^{-2}$torr; figure 12 shows the result of one such treatment giving in this instance sensitivities of 0.79 and 8.1 per torr for the high pressure and the inverted ionization gauge respectively. Other data obtained by this method will be presented at the end of the section together with the results of the flow experiments.

Calibration of sensitivity by flow methods

The magnitude of the absolute conductance of a capillary may be obtained from the physical dimensions using the expressions derived by Knudsen (1914).

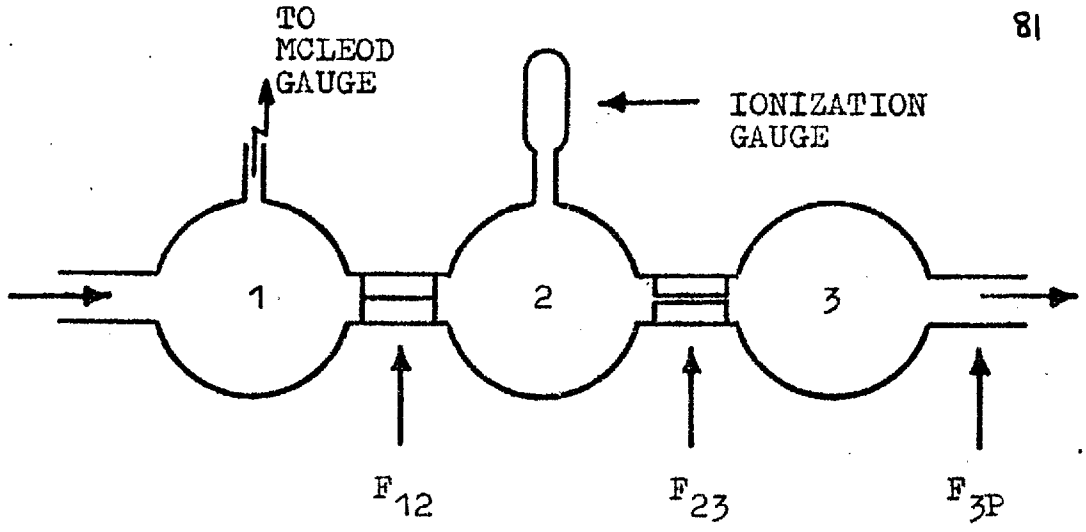

FIGURE 13(a).

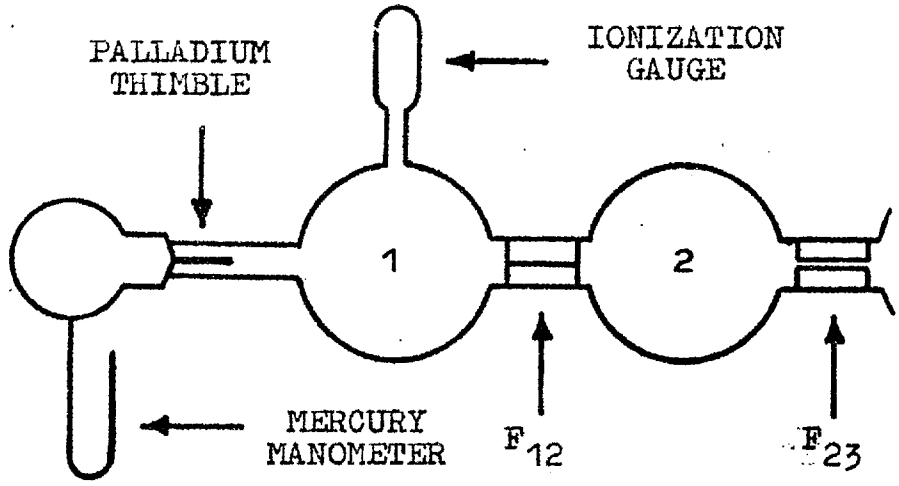

FIGURE 13(b)

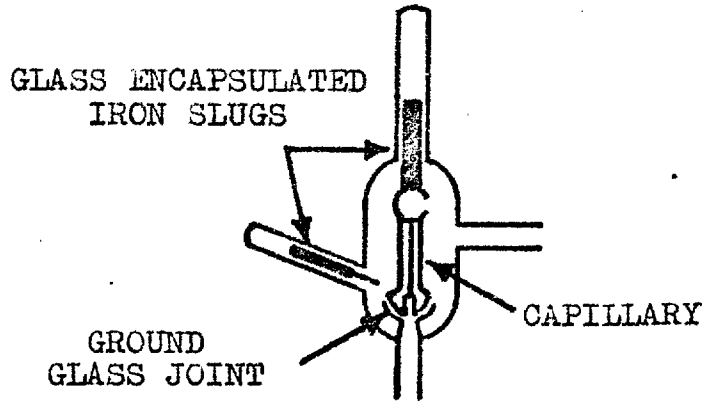

FIGURE 13(c) The construction of the capillary leaks.

Standardised conductances may be used in a variety of ways to calibrate gauges - figures 13(a) and 13(b) illustrate two methods which were used in the present work.

In 13(a) gas enters chamber 1 (here the gas reservoir GR) at a fixed flow rate (from the palladium thimble) and leaves to the pumps via chambers 2 and 3 (RV and bakeable trap). If the standard conductances F_{12} and F_{23} are so designed that $F_{12} < F_{23}$ ($< F_{3P}$) then flow rate (molecules sec^{-1}) $= \frac{dN}{dt} = F_{12}P_1 = F_{23}P_2$ where P_1 and P_2 are the absolute pressures (in torr) in chambers 1 and 2, the units of F are molecules $sec^{-1} torr^{-1}$.

Since any change in pumping speed has little effect on P_2, by measuring P_1 using the McLeod gauge, the value of P_2 in torr is obtained from

$$P_2 = \frac{F_{12}}{F_{23}} \cdot P_1,$$ and thus the sensitivity of a gauge connected to chamber 2 is determined.

A second method and one readily applicable to the present vacuum system is shown in 13(b). The flow rate through chambers 1, 2 and 3 is measured using the manometer on the high pressure side of the palladium thimble. Since $F_{12} < F_{23}$ $P_1 < P_2$ and flow rate (molecules sec^{-1}) $= F_{12}P_1$.

The measurement of F_{12}, F_{23} and of the flow rate will be considered separately.

(a) The flow rate.

The volume of the system behind the palladium thimble (see figure 5) was obtained by successive expansions into and evacuations of the calibrated volume CV2, pressures being measured on the mercury manometer M. A mean of 10 values gave the volume as 73.7 ml. To calculate the number of molecules in this volume with the thimble at the operating temperature requires a correction for a non-isothermal system. This was obtained as follows. The pressure of hydrogen was measured with the thimble at operating temperature and then the furnace around the thimble was quickly removed and the whole system cooled to room temperature, a new (lower) pressure being recorded. The ratio of the measured pressures with the thimble hot and cold was found to have a mean value of 1.16. The measured pressures during an experiment can thus be converted to an equivalent pressure in an isothermal system using this factor.

The flow rate was obtained by observing the manometer pressure as a function of time - the full expression is

$$\text{flow rate (molecules sec}^{-1}) = \frac{3.23 \times 10^{16} \times 73.7}{1.16} \times \frac{\Delta P}{\Delta t}$$ where

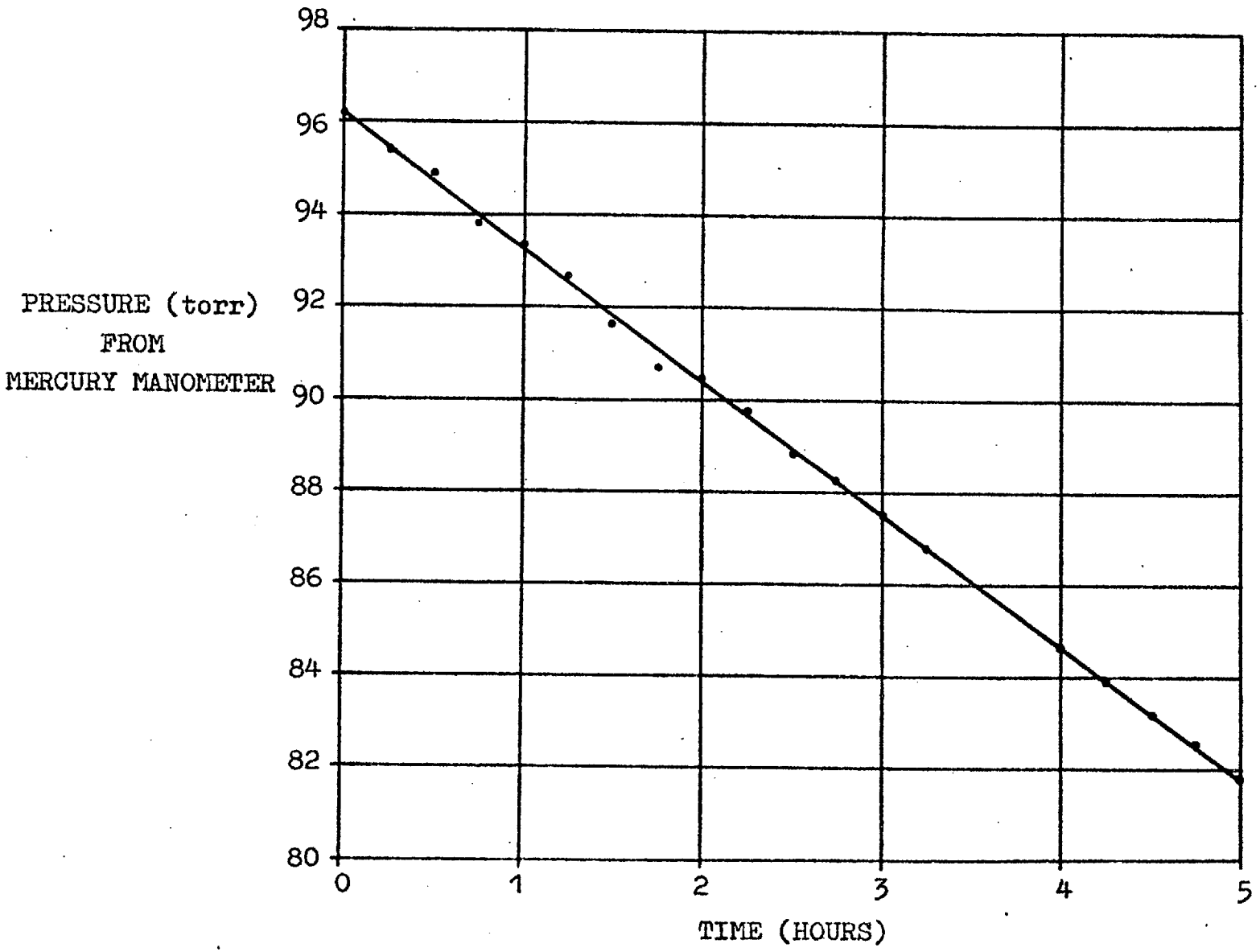

FIGURE 13(d). Pressure versus time at the palladium thimble.

$\frac{\Delta P}{\Delta t}$ is the rate of change of pressure in torr with time in seconds. To measure the $\frac{\Delta P}{\Delta t}$ term accurately required several hours and a continuous adjustment of palladium thimble to correct any deviations from pressure-time linearity. Figure 13d illustrates how effectively the latter could be performed.

(b) The Standard Conductance and F_{12}

The construction of the capillary leaks is outlined in figure 13c. Various dimensions were used - these are given in the following table together with the calculated conductances.

Capillary	Radius	Length	Calculated Conductance
1	1.01mm	12.00cm	1.006×10^{18} molecules
2	0.61mm	5.00cm	7.0×10^{16} $sec^{-1}torr^{-1}$
3	1.50mm	5.00cm	1.03×10^{18}

For the total conductance between gas reservoir and reaction vessel (corresponding to chambers 1 and 2 respectively) it is necessary to include the contribution of the remainder of the tubulation. The latter tubulation had a conductance estimated (see later) to be 1 to 1.5×10^{19} molecules $sec^{-1}torr^{-1}$ thus giving total conductances of 9.1 to 9.4×10^{17} molecules $sec^{-1}torr^{-1}$ for the '10^{18}' capillary leaks and about

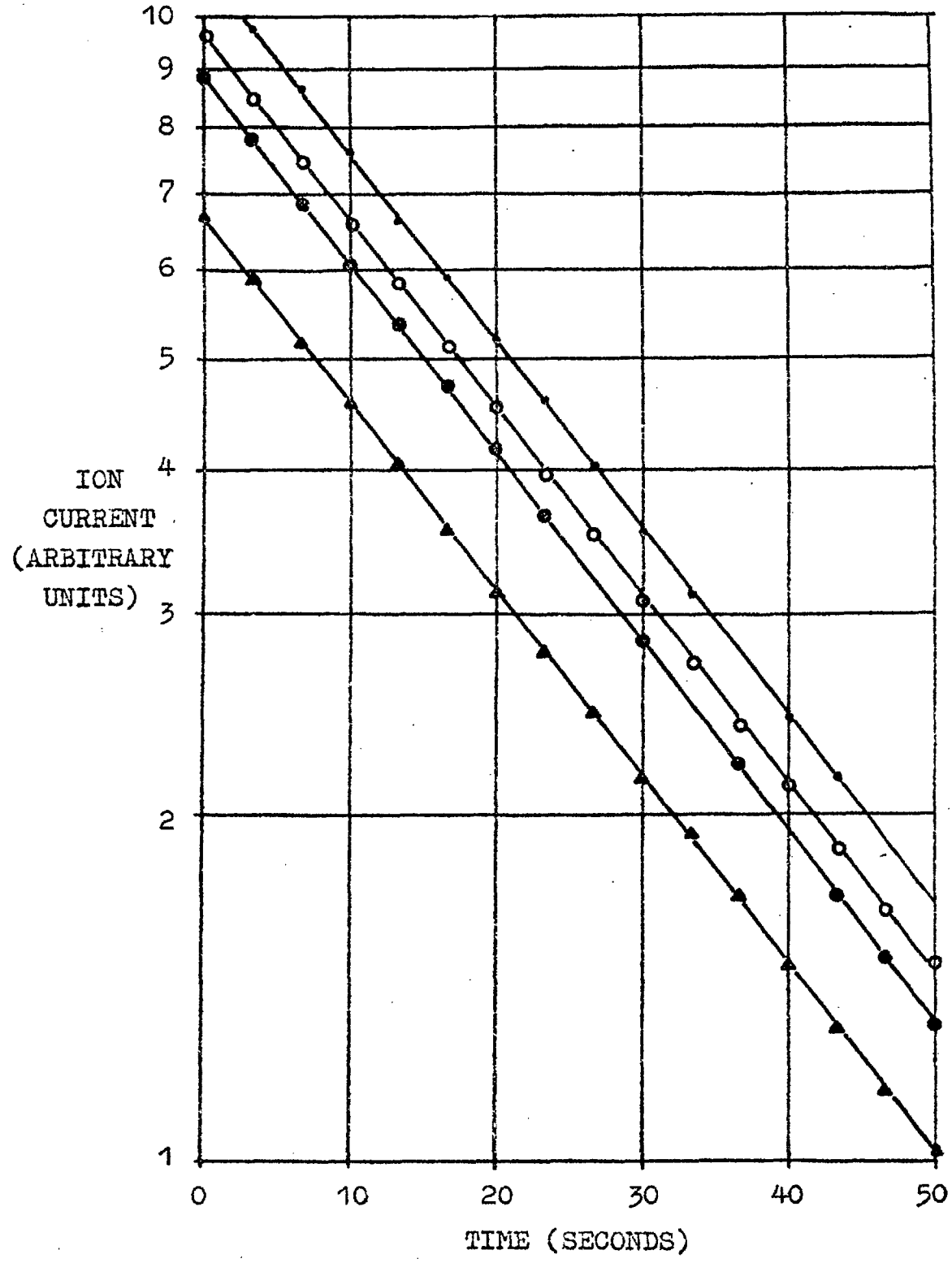

FIGURE 14. Logarithmic decay in ion current on pumping out RV through a '10^{18}' calibrated leak.

6.95×10^{16} for the leak number 2.

This total conductance was checked experimentally by observing the logarithmic decay in pressure when hydrogen in the reaction vessel was pumped out via the capillary leak. The relevant equation, if $P_2 >> P_1$ (attained by removing furnace from around thimble after trapping sufficient gas in RV), is

$$\frac{d \ln P_2}{dt} = F'_{12} \cdot V_{RV}^{-1} \cdot (3.23 \times 10^{19})^{-1}$$ where

V_{RV} is the volume of the reaction vessel up to the capillary leak and 3.23×10^{19} is the number of molecules at 300°K per litre per torr pressure. In the latter expression F'_{12} includes a term for gauge pumping as the gauges were operated continuously - in particular $F'_{12} = F_{12} + G$ all terms being in units of molecules sec^{-1} $torr^{-1}$. G was estimated from the rate of pressure decay before letting gas through D3 to the capillary leak. The volume of the reaction vessel was obtained by direct measurement from the dimensions and also by expanding gas into CV1, which was then re-evacuated and the procedure repeated. A mean of 15 expansions using the latter method gave 2.18 litres for the reaction vessel volume at this time. Figure 14 displays a typical set of 'log plots' during the pressure decay on pumping through the leak using the high pressure

ionization gauge on 100μA emission current. The values of F'_{12}, F_{12} and G for a number of runs are given in the table; the leak number 1 was in use.

Run	F'_{12}	G	F_{12}
7.10.65	9.95×10^{17}	2.8×10^{16}	9.67×10^{17}
12.10.65	1.00×10^{18}	3.6×10^{16}	9.64×10^{17}
16.10.65	9.85×10^{18}	3.0×10^{16}	9.55×10^{17}
16.10.65	9.95×10^{18}	3.0×10^{16}	9.65×10^{17}

F_{12}, G, F'_{12} are expressed in molecules $sec^{-1}torr^{-1}$

(c) The Calibration of F_{23}

The value of F_{23} was obtained by measuring pressures P_1 and P_2 while gas flowed from the reservoir to the pumps via the reaction vessel. Since the pressure in chamber 3 (see figure 13(a)) may be ignored we have

$$\underset{(\text{molecules sec}^{-1})}{\text{flow rate}} = F_{12}P_1 = F_{23}P_2$$

$$\text{i.e. } F_{23} = F_{12}\frac{P_1}{P_{12}}$$

The ratio P_1 to P_2 was obtained as the ion current ratio of similar inverted gauges in RV and GR - a mean of 8 values gave 68 when F_{12} was 2.6×10^{18} molecules $sec^{-1}torr^{-1}$ i.e. $F_{23} = 1.77 \times 10^{20}$ molecules $sec^{-1}torr^{-1}$.

The sensitivity of the ionization gauges - a collection of results.

The following table gives the results obtained in various calibration experiments. Suffix (a) or (b) in the method column indicates which of the experimental set ups of figure 13 was used. For the calculations F_{12} and F_{23} were taken as 9.50×10^{17} and 1.77×10^{20} molecules $sec^{-1}torr^{-1}$ respectively. The sensitivities of the inverted gauge which bear an asterisk are those obtained using the high pressure gauge as a secondary standard.

A mean value of 8.1 per torr is thus obtained for the hydrogen sensitivity of the inverted ionization gauge (neglecting the 9.2 reading). Assuming a relative sensitivity of hydrogen and nitrogen of 0.4 the value quoted by Edwards Ltd. is 5 per torr and that by Mullard Ltd. 7.4 per torr for gauges of identical basic construction. The disagreement with the former is serious; that with the latter may be due to the value of the relative sensitivities of hydrogen and nitrogen which is taken for comparison; the mean of the values for this factor quoted in Leck (1964) is 0.435 which gives a Mullard figure for hydrogen of 8.05 per torr.

RUN	METHOD	RANGE (torr)*	G	S_{HP}	S_{IG}
28.9.65	Flow(b)	2.90×10^{-4}	IG	-	8.6
5.10.65	Flow(b)	5.08×10^{-3}	HP	0.92	8.2*
5.10.65	Flow(b)	1.04×10^{-3}	HP	0.90	7.9*
27.10.65	Flow(b)	1.40×10^{-3}	Both	0.70	7.5*
27.10.65	Flow(b)	1.40×10^{-3}	Both	0.70	8.2*
27.10.65	Flow(a)	1.20×10^{-3}	Mcleod and I.	-	8.4
27.10.65	Mcleod	$\sim 1.40 \times 10^{-3}$	HP	0.76	8.0*
28.10.65	Mcleod	$\sim 2 \times 10^{-2}$	HP	0.77	7.9*
31.10.65	Mcleod	1.50×10^{-3}	IG	-	9.2
31.10.65	Mcleod	3.50×10^{-3}	HP	0.90	8.1*
3.10.65	Mcleod	10^{-1} to 10^{-4}	HP	0.79	8.1*

* Pressure range (torr) for primary measurements

G - Gauge used for primary measurements

S_{HP}, S_{IG} - sensitivities of high pressure and inverted gauge respectively.

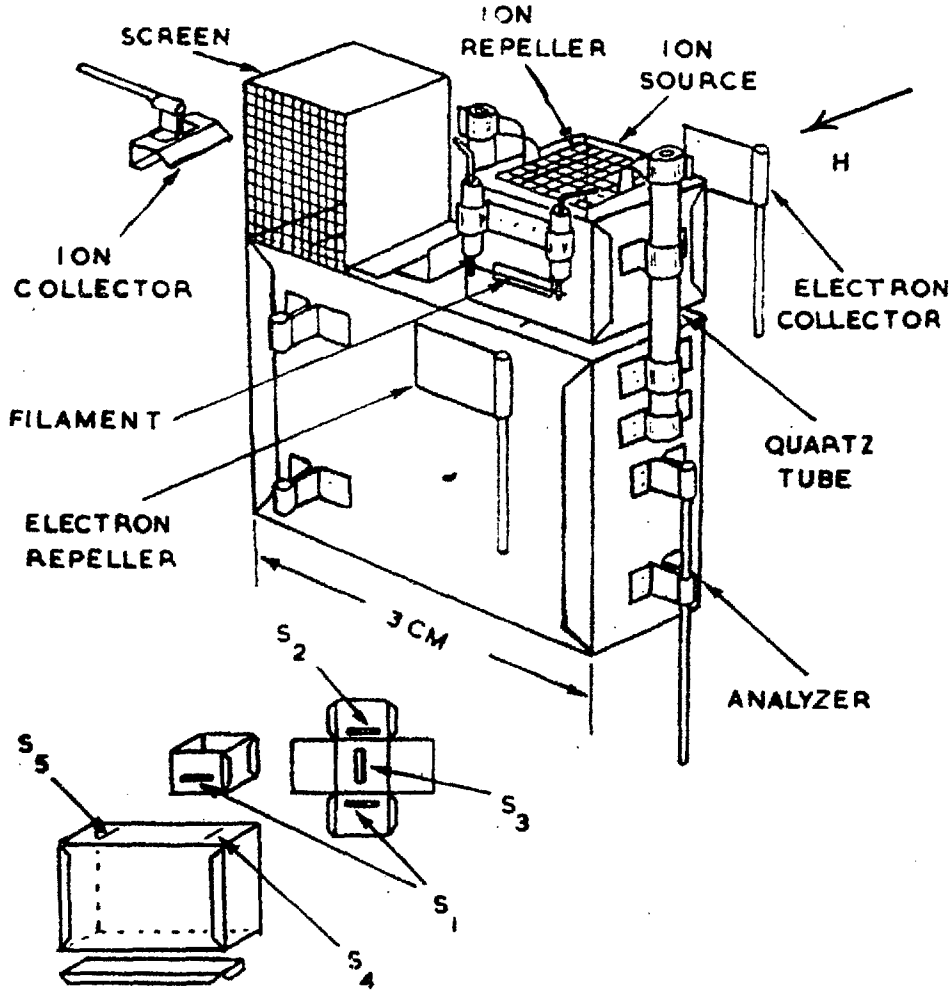

Fig. 15. Mass spectrometer electrode structure.

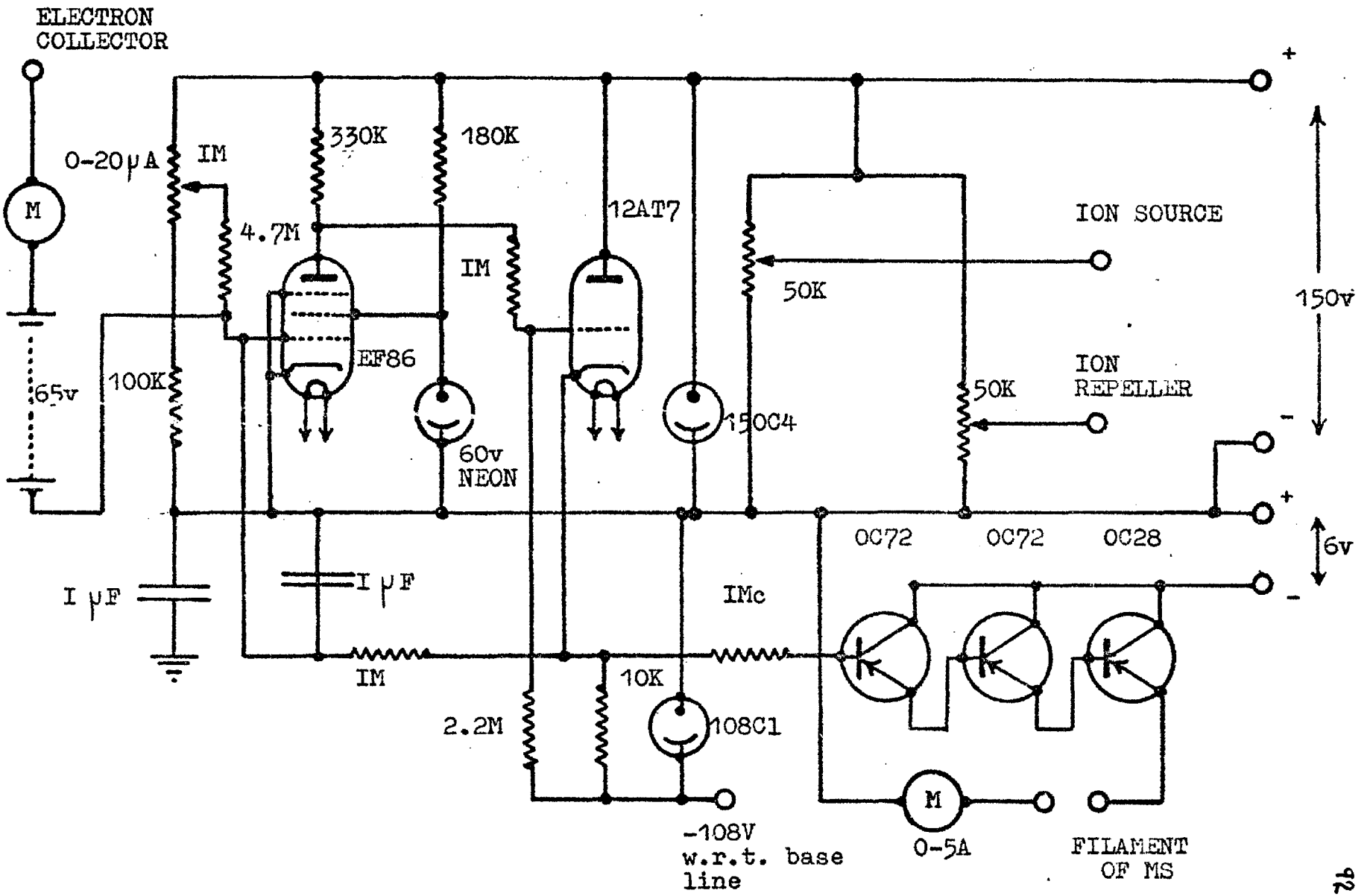

FIGURE 16. The mission controller

8.4. The measurement of partial pressures with the mass-spectrometer

The presence of non-adsorbable impurities in the gas flow to the reaction vessel may lead to serious errors in the measured sticking probability if a total pressure gauge is used (e.g. see Hayward, King and Tompkins, 1965). For this reason small 180° magnetic deflection mass spectrometers were constructed. The design is basically that of Goldstone (1964) but modified to incorporate a readily removeable lanthanum hexaboride-rhenium cathode. Figure 15 illustrates the general design. A 3000 gauss magnet served both to deflect the ions and collimate the electron beam. The magnitude of the latter was stabilised between 1 and 50 μA using the circuit shown in figure 16. The operating potentials with respect to the cathode were as follows:- ion source +100V, ion repeller +101V, electron collector +65V. The scanning potential - 0 to 215V - was applied between the ion source and the analyser; the relationship between mass number and scanning potential was approximately

$$\text{Mass number} = \frac{400}{\text{scanning potential (V)}}$$

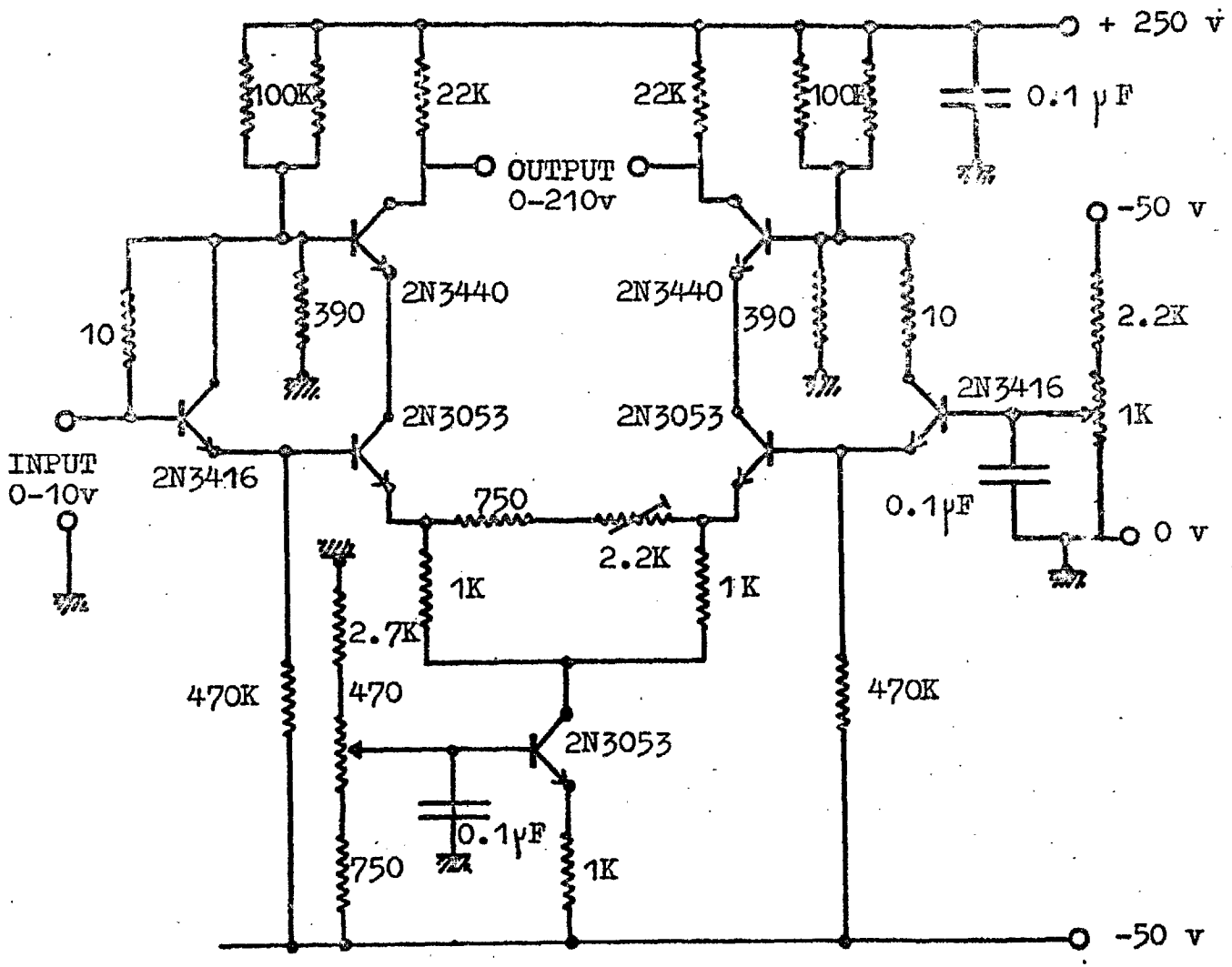

FIGURE 17. The scanning voltage amplifier

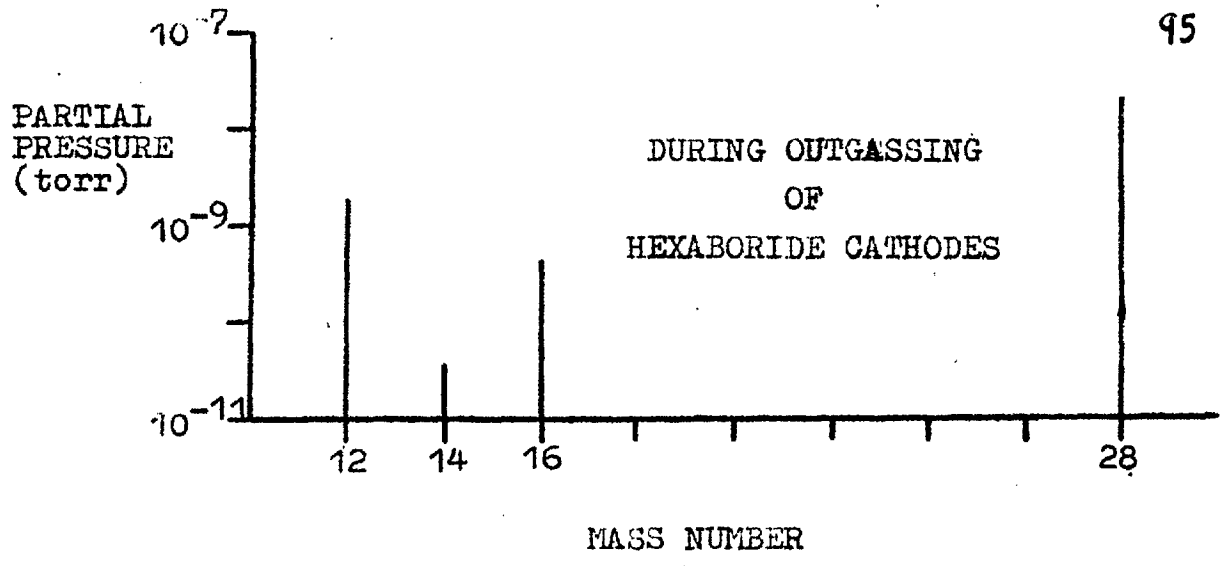

(a)

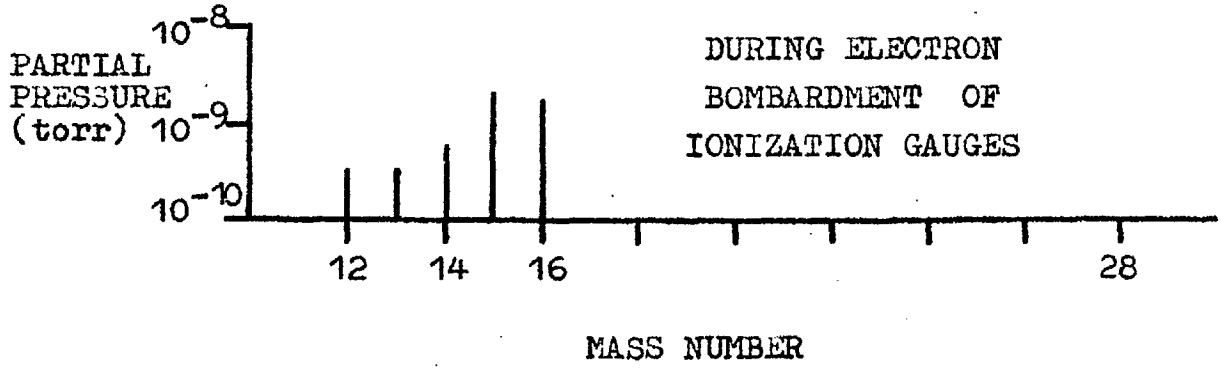

(b)

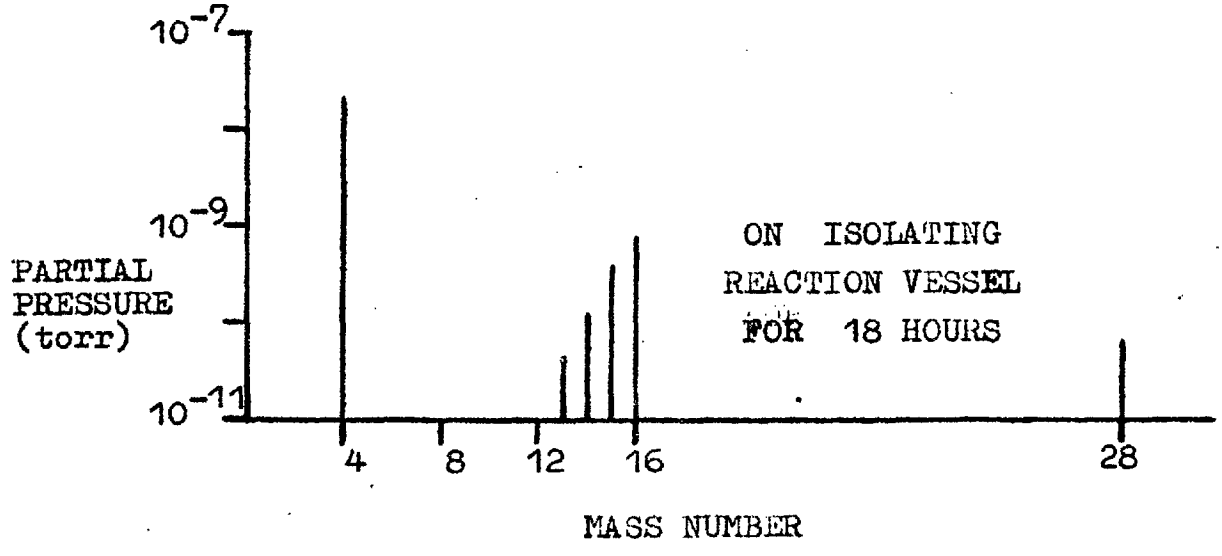

(c)

FIGURE 18 Typical results with the mass spectrometer.

Initially a motor driven potentiometer connected across a high voltage source served as a scan generator. This was later replaced by a fully transistorised D.C. amplifier with an overall voltage gain of 100, driven by a 10 speed motor-potentiometer assembly. The latter unit has the advantage that scans up to several thousand times a second are possible by incorporating an electronic ramp generator to supply the input (now being developed). Figure 17 shows the general circuitry.

The sensitivity of the mass spectrometer was a function of the operating conditions and recalibration against an ionization gauge was performed in each experiment; in general the sensitivity was 0.5 to 2A per torr. The Ekco electrometer was used for ion current measurement - using the $10^{12}\Omega$ input resistor about 5×10^{-16}A could be detected under ideal conditions thus allowing partial pressure measurement down to 5×10^{-12}torr.

Apart from monitoring hydrogen pressures the mass spectrometer was used to analyse the gas composition under various conditions. Figure 18 displays several of interest; in (a) and (b) the mass 12 peak is relatively larger than quoted for pure CO and CH_4 respectively by AEI Ltd. The resolution of the instruments was around 30 for a 10% valley.

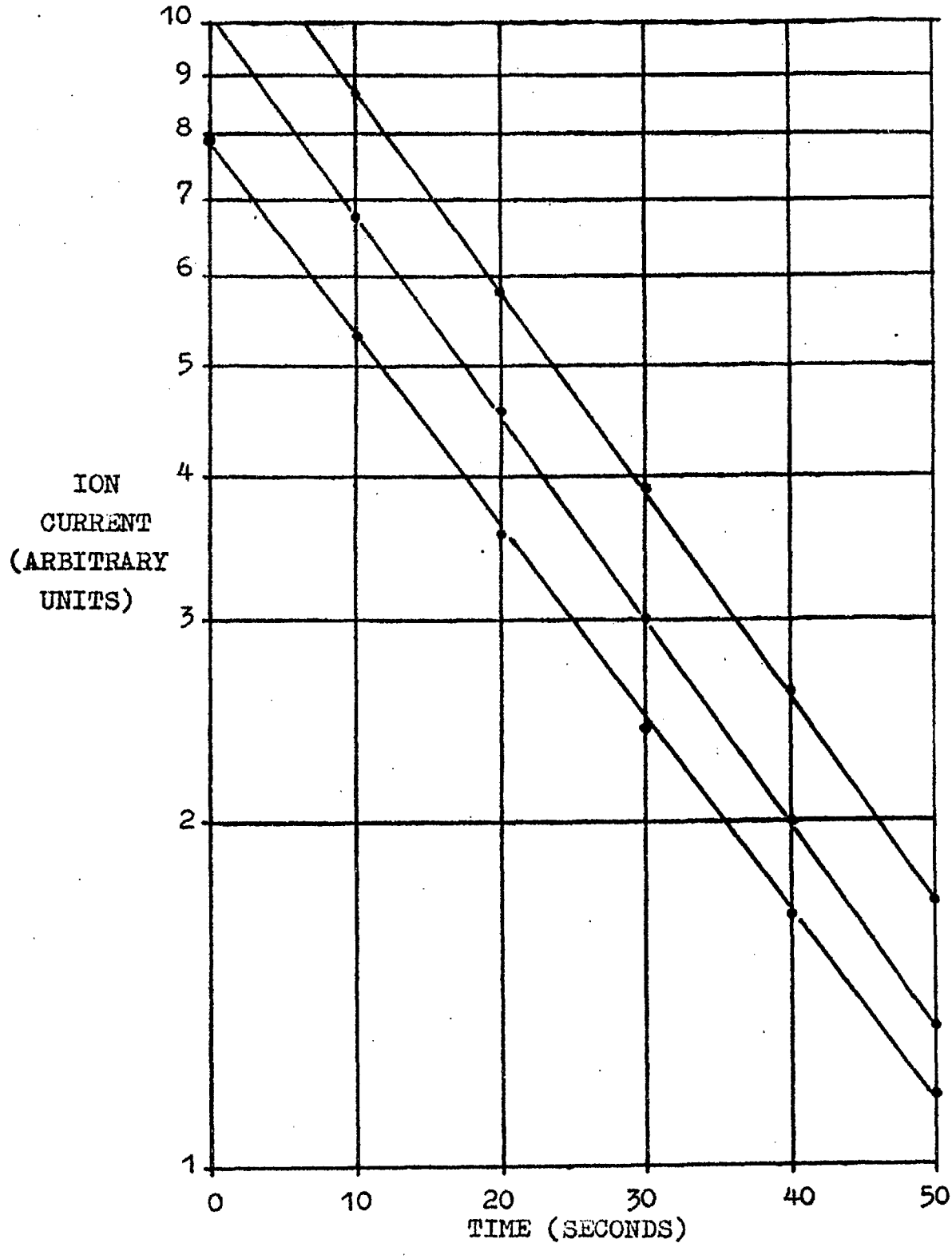

FIGURE 19. Logarithmic decay in ion current on pumping out RV through the 'diffuser' conductance.

8.5. The measurement of hydrogen flow rate to the reaction vessel.

The conductance between gas reservoir and the reaction vessel was estimated in 3 ways.

(a) By following the pressure changes with time on the high pressure side of the palladium thimble a flow rate in absolute units was obtained (see page 83). With the mercury cut off NV in the closed position all the gas flowed through the diffuser and the reaction vessel. Under these conditions (since $P_1 >> P_2$)

flow rate (molecules sec^{-1}) $= (F + G)P_1$ where F is the conductance between GR and NV, G is the pumping speed of the gauge (here 3×10^{16} molecules $sec^{-1} torr^{-1}$) and P_1 is the gas reservoir pressure in torr.

Hence F is obtained.

(b) F may also be obtained from the logarithmic decay in pressure which occurs on pumping out the reaction vessel via the diffuser and gas reservoir in exactly the same way as described on page 85. Since the major restriction to gas flow is in the capillaries of the diffuser only the volume of the reaction vessel up to the diffuser need be known; this was estimated to be 2.065 litres for the cell used in these experiments. Typical decays are shown in figure 19; a high pressure

gauge was used in these particular measurements.

(c) The standard capillary leaks were used in the following way to measure F. A steady flow rate was set up from GR to RV with the mercury cut off raised. By alternately having the standard conductance and the 'diffuser' conductance between GR and RV and measuring the gas pressures in the two cases we have, since $P_1 >> P_2$.

$(F + G)P_1 = (F_{12} + G)P_1^{12}$ where F, F_{12} and G have previously been defined, P_1 (torr) is the gas reservoir pressure with the diffuser lowered and the capillary leak raised and P_1^{12} (torr) is that when the diffuser is raised and the leak lowered.

The values of F obtained by the various methods are given in the following table.

Run	Method	Gauge used	F(molecules / (sec^{-1}torr^{-1}))	Pressure torr
5.10.65	(a)	high pressure	2.71×10^{18}	1.50×10^{-3}
27.10.65	(a)	inverted gauge	2.79×10^{18}	4.60×10^{-4}
"	(a)	"	2.60×10^{18}	2.90×10^{-4}
16.10.65	(b)	high pressure	2.64×10^{18}	10^{-3} range
"	(b)	"	2.59×10^{18}	10^{-4} range
"	(b)	"	2.71×10^{18}	10^{-3} range
"	(b)	"	2.55×10^{18}	10^{-4} range
28.9.65	(c)	inverted gauge	2.59×10^{18}	10^{-7}, 10^{-5} range
5.10.65	(c)	high pressure	2.71×10^{18}	10^{-4} range
"	(c)	"	2.70×10^{18}	10^{-4} range
27.10.65	(c)	"	2.48×10^{18}	10^{-3} range
"	(c)	"	2.45×10^{18}	10^{-3} range

Mean value - 2.62×10^{18} molecules sec^{-1}torr^{-1}

This particular diffuser was used for the majority of the results presented in this thesis. An earlier type was similarly calibrated - F was 1.78×10^{18} molecules sec^{-1} torr^{-1}.

It is convenient in this section to consider the extent of the leakage across the seats of the decker

valves when the latter are closed. With a pressure of about 10^{-4}torr in the gas reservoir and with a single decker valve closed between GR and RV the pressure in the reaction vessel could be maintained near the background by pumping via D1. On closing D1 the pressure in RV rises rapidly indicating an initial build up of gas at about 10^{11} molecules sec^{-1}. From this a conductance across the seat of about 10^{15} molecules sec^{-1} $torr^{-1}$ can be calculated. This low leakage rate can be ignored in an average experiment.

8.6. The procedure to obtain an ultra-high vacuum

The basic requirements for the attainment of ultra-high vacuum ($<10^{-9}$torr) have been described extensively in the literature and will not be repeated here. However it is useful to describe the various steps taken with this particular apparatus. The metal films were generally removed by a 5% solution of hydrofluoric acid. After washing the cell with distilled water several times the nickel discs and the evaporation filament were replaced and the following sequence observed

(1) The system was pumped down to about 10^{-1} torr by the rotary pump and the system tested for leaks with a high frequency tester. If no leaks were detected the

diffusion pumps were started and deckers D2, D3 and D4 closed.

(2) The main furnace was then lowered and switched on together with the furnace around the palladium thimble and various heating tapes wrapped around the cold traps below the table.

(3) After about three hours the lower parts of the two cold traps below the table were cooled with liquid nitrogen and shortly afterwards the furnaces and tapes were switched off.

(4) When the main furnace temperature had fallen to 200°C the furnace was removed, the cold traps were raised and the ionization gauges were immediately connected to the control units. The gauges were initially operated on 10mA emission using the low temperature cathodes; this allowed the cathodes to degas, the pressure falling to 10^{-7} to 10^{-8} torr.

(5) The inverted ionization gauges were then outgassed by electron bombardment or induction heating, the pressure in general now falling to the 10^{-9} torr range with the gauges on low emission.

(6) Next, nickel discs were held in position magnetically over the annuli leadding to the gauges and the diffuser. The evaporation filament was slowly raised to a dull red heat and left at this temperature until

the pressure which rose initially had fallen to the 10^{-8} torr range. The filament temperature was then raised to just below the evaporation point, remaining there for up to 20 hours.

(7) Steps (2) to (6) were then repeated except that the bakeout was longer (>10 hours) and that the temperature of the furnace around the palladium thimble was carefully set during the cooling process to give the required flow rate. The rosebowl cold trap was usually filled with liquid nitrogen although in the vast majority of experiments it made no difference to the background pressure in the cell.

The deposition of the metal films

When preparing sintered films the reaction vessel was not cooled and large rises in cell temperature occurred because of heating from the evaporation source; temperatures ranged from 100°C for tantalum to about 40°C for nickel and palladium. Except for certain specific experiments, films were deposited until a light source became invisible when viewed through the film. In several experiments, especially those concerned with the stoichiometry of hydrides the weight of film was obtained by the weight loss of the filament, the filament being held in a pair of nickel clips to allow removal.

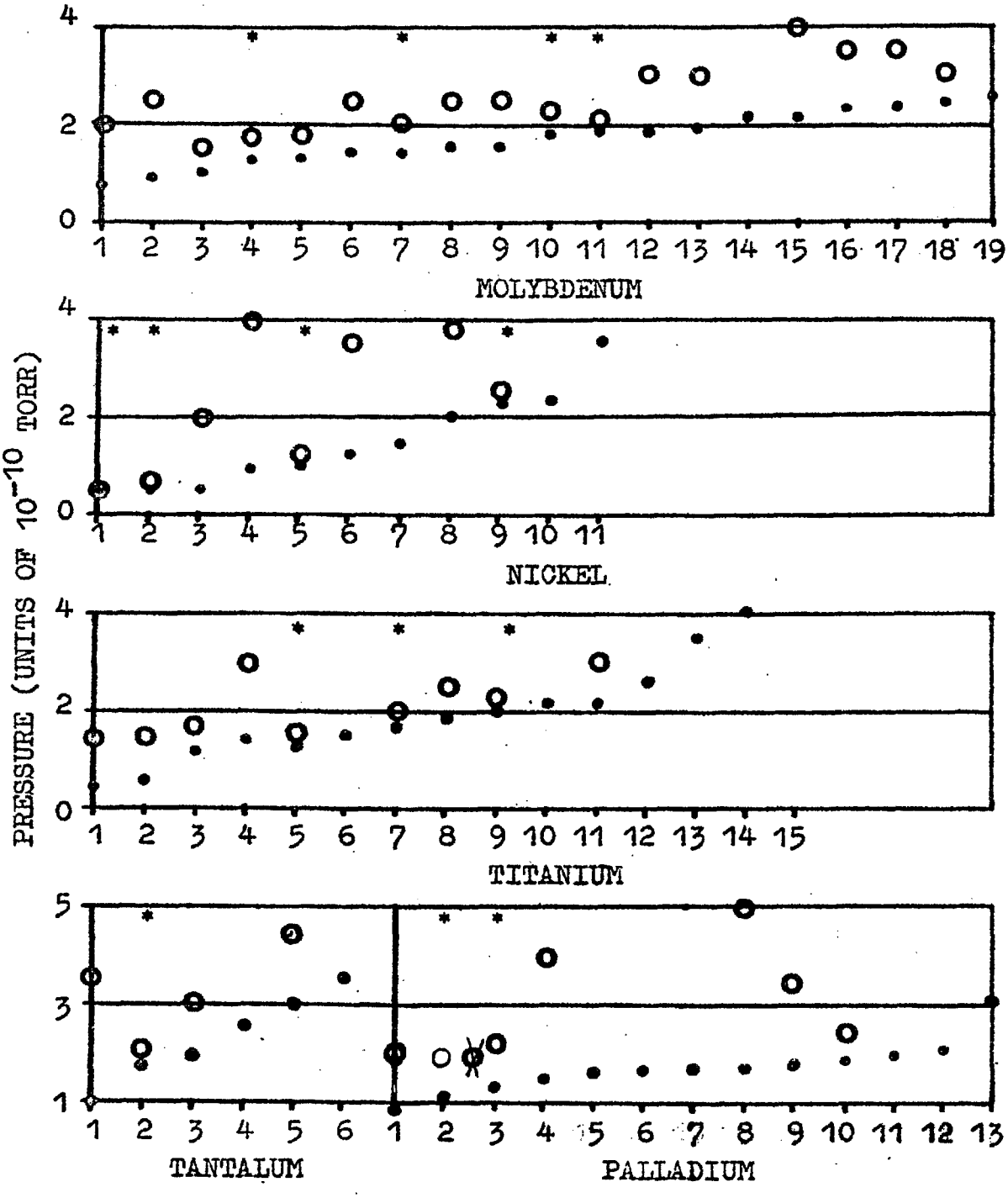

FIGURE 20. Final deposition pressures (O) and background pressures (•). [*indicates film deposited at 78°K]

8.7. The contamination of clean metal surfaces in vacuum

A metal surface, initially clean, is contaminated in a pressure of P torr of adsorbable gas in a time t seconds given by the approximate relation.

$$t(\text{seconds}) = \frac{10^{-6}}{P\ (\text{torr})}$$

The situation during the deposition process is complicated since film deposition and contamination occur simultaneously but providing there is no net migration of contaminants trapped in the metal to the final surface the above equation may be applied.

The principal sources of gas during film deposition are the degassing of the vacuum system itself and gas evolution from the evaporating metal, the former is very low and for reasons discussed elsewhere may usually be neglected. The outgassing of the metal during evaporation is reduced by the lengthy degassing procedure but particularly in the case of nickel and palladium it may be very difficult to keep the pressure during the final stages of deposition to less than 10^{-9} torr. Figure 20 shows the relative final backgrounds and deposition pressures for various runs with each of the metals. It is observed that when deposition is at 78°K or 90°K the pressure during deposition is always close to the background value.

This does not necessarily indicate that unsintered films are less contaminated but that the sticking coefficient or the lifetime on the surface of contaminant species is enhanced at the low temperature. Both King (1966) and Gomer (1966) have indicated that $S \sim 1$ for carbon monoxide on tungsten at 78°K; in the latter situation the flux of contaminant molecules from the evaporating filament would be undetected by the gauge. King (1966) has shown that large pressures of gas are produced on sintering nickel films originally deposited at 78°K. This had previously been observed in this work with palladium - an analysis of the gas evolved in one particular experiment was CO_2 - 1×10^{-9} torr, CO - 1.5×10^{-7} torr, $H_2O \sim 1.5 \times 10^{-10}$ torr, CH_4 - 5×10^{-8} torr. In the latter experiment the film was deposited with a background pressure of 2×10^{-9} torr, it was found subsequently that the main source of gas in this instance was the lanthanum hexaboride - rhenium cathode of the ionization gauge. It is, however, possible that contaminants may be trapped in the film when deposition is at 78°K but may diffuse to the surface on sintering; in the latter situation the degree of contamination of unsintered films may be lower than sintered films.

9. COMPARISON OF METHODS

9.1. Experimental

Sticking probabilities calculated by the three methods have been compared for the adsorption of hydrogen on palladium at 78°K. This system was chosen because the initial value of sticking probability at zero coverage, s_o, was very reproducible and was independent of the degree of sintering of the film; this was not found for the other metals studied (titanium, tantalum, molybdenum and nickel). All the palladium films mentioned in this section were thrown with the wall of the cell uncooled, and were therefore highly sintered. To avoid extraneous factors from entering the comparison of sticking probabilities the same gas inlet system was used with all three cells.

In all the experiments described in this section the ionization gauge was effectively at room temperature or a little above whereas the reaction vessel and film were cooled in liquid nitrogen. It has been shown elsewhere (Hayward, King and Tompkins, 1965) that the correct temperature to use in the collision factor Z [$= (2\pi mkT)^{-\frac{1}{2}}$] is the temperature of the gauge envelope and not that of the film. This principle has been followed in the present calculations.

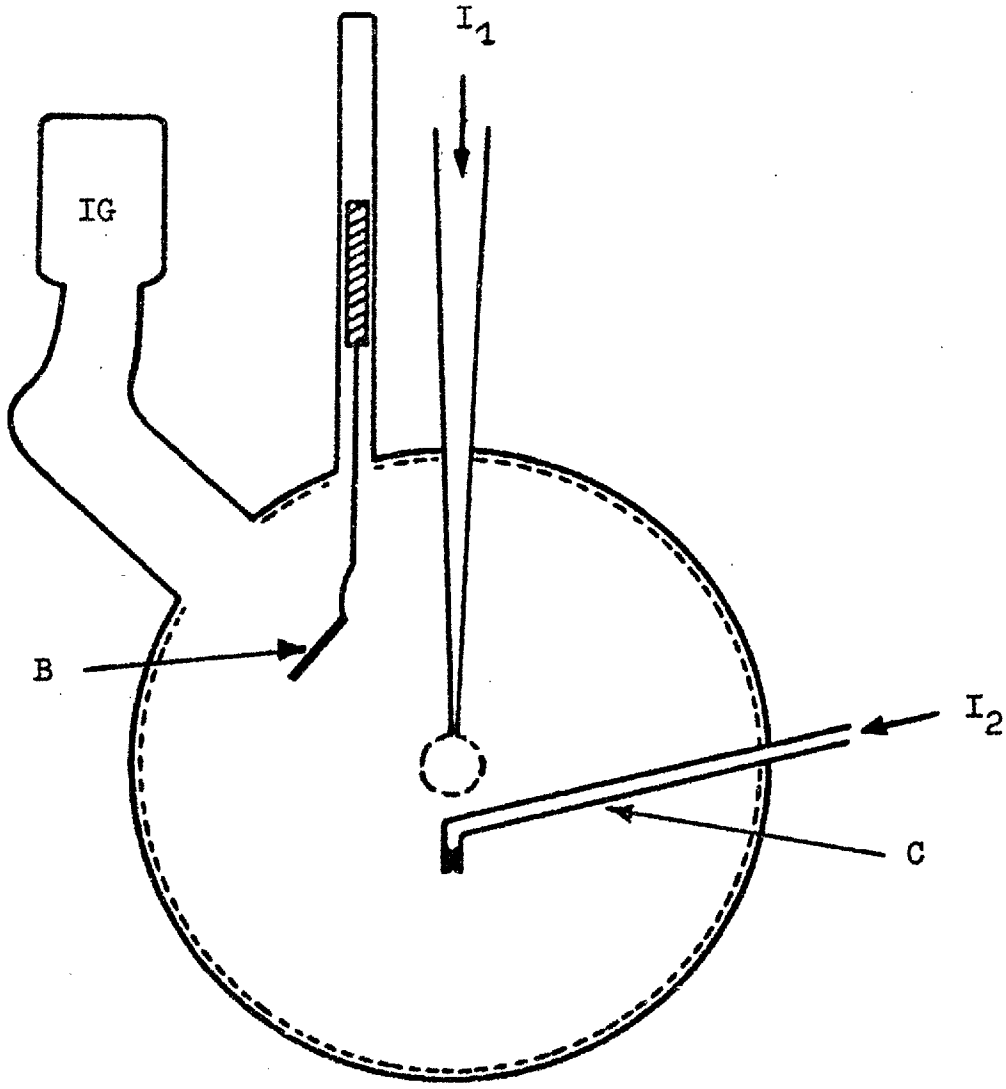

FIGURE 21. Sticking probability cell with alternative modes of gas entry. B - baffle plate, C - capillary inlet, I_1, I_2 - alternative gas entrances.

From the dimensions of the type I cell (R = 6.4 cm, L = 7.0 cm, r = 1.70 cm) β was calculated to be 1.24.

9.2. Results

Using the data given above the following sticking probabilities were calculated for the adsorption of hydrogen on palladium at zero coverage and 78°K:-

type I cell	s_o = 1.02
type II cell	s_o = 0.99(5)
type III cell	s_o = 0.93

Each of these values is the mean of three separate determinations on different films. The first two methods are in good agreement, but the sticking probability given by the third method is significantly lower, despite the fact that this method should be the most accurate at high s since essentially it measures (1-s). One explanation of this discrepancy is that the baffle does not completely prevent molecules from entering the gauge compartment before they have collided with the film. This is possible since molecules can be reflected into the gauge compartment from the vertical tube that leads to the diffuser. To test this possibility the baffle cell was modified by addition of a second mode of gas entry, shown in figure 21 which makes it impossible for molecules to enter the gauge

compartment without first colliding with the film surface. The pressure rises recorded by the ionization gauge for the two modes of gas entry and with a flow rate of 7.25×10^{14} molecules sec^{-1} are given in table 1 (the lowest pressure rises could only be recorded accurately by using a 'backing-off' potential to counteract the X-ray current).

Although the gas is distributed asymmetrically when it enters the cell via the capillary, the incidence of second and higher collisions with the film should be constant over the whole surface because molecules are likely to leave the rough surface after collision according to the cosine law. Therefore, the same number of molecules should enter the ionization gauge compartment in both methods, the only difference being that, with the baffle, these molecules come from entirely random directions, whereas in the capillary method they come preferentially from the bottom of the cell and molecular beaming has to be taken into account. However, rough calculation shows that β is close to one for the latter method. Thus, if the baffle method were working correctly the pressure recorded when the molecules enter the cell via the capillary would be approximately equal to that recorded when they enter via the diffuser, whereas the latter is about ten times the

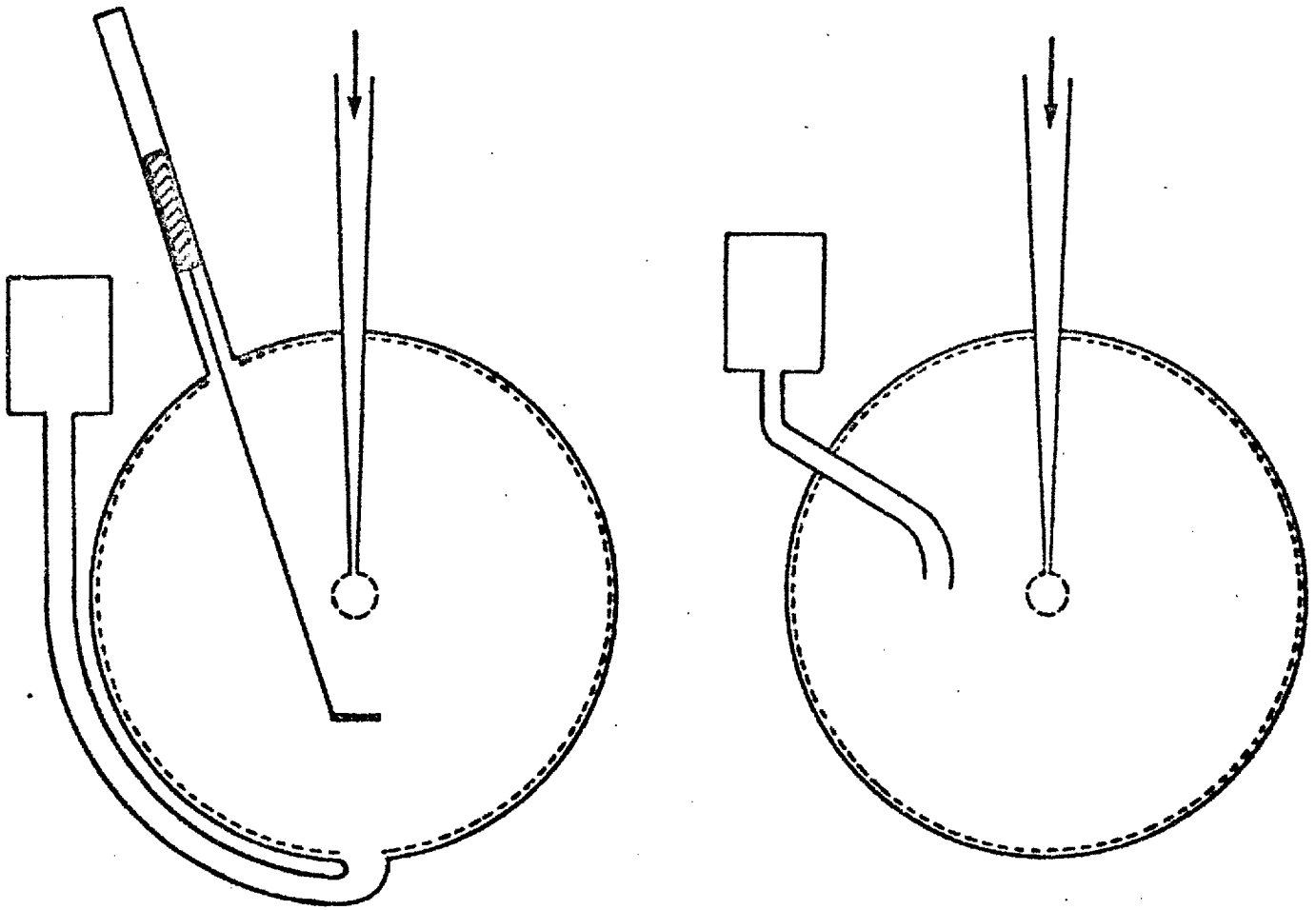

FIGURE 22. Alternative versions of the type III cell.

Table 1

Pressure rises recorded during adsorption of hydrogen on palladium at 78°K.

Mode of entry of gas	Pressure rise (torr)	Gauge used	Total number of H_2 molecules adsorbed $x10^{-16}$
C	ca. 6 $x10^{-12}$	MS	1.4
C	$6.4x10^{-12}$	IG	2.3
D	$6.4x10^{-11}$	IG	3.1
D	$6.0x10^{-11}$	MS	3.9
D	$7.2x10^{-11}$	IG	4.7
C	$8.0x10^{-12}$	IG	6.1
C	$1.2x10^{-11}$	IG	6.2
D	$9.6x10^{-11}$	MS	7.0
C	$1.8x10^{-11}$	MS	7.6

C - entry via capillary, D - entry via diffuser, IG - ionization gauge, MS - mass spectrometer.

former. This discrepancy is explained if 0.11% of the molecules entering the cell via the diffuser reach the gauge side-arm without colliding with the film. This problem could be avoided by resiting the side-arm as in figure 22a, or by using a somewhat different

arrangement, as in figure 22b. These cells would be superior to the capillary cell because the incoming molecules would be uniformly distributed over the surface of the film and molecular beaming effects would be eliminated. A cell similar to that shown in figure 22b has been used by R.E. Clausing (1961), the only important difference being that his reaction vessel was cubical instead of the ideal spherical shape.

To a good approximation sticking probabilities can still be calculated for gas entry via the capillary by using equation (13). The lowest pressure rise recorded in table 1 is 6.4×10^{-12} torr. This gives a sticking probability of 0.993 and thus confirms the accuracy of the values calculated for the types I and II cells. Even allowing for a factor of two between the recorded and ideal pressures because of molecular beaming effects etc., the sticking probability can still be placed between close limits, i.e. $0.986 < s < 0.997$.

10. COMPARISON OF CALCULATED AND EXPERIMENTAL VALUES OF β

To test the accuracy of equation (11) for calculating β, a number of cells were constructed, each with two ionization gauges attached to the reaction vessel. The entrance to one of these was via a small

hole as in the type II cell; the other had an unrestricted opening and the tubulation was of different dimensions for each cell. The pressures registered by the two gauges were recorded during adsorption of hydrogen on palladium at 78°K. Since the sticking probability is effectively one for this system at low coverages almost all the molecules that enter the gauge compartment come direct from the gas inlet and the ratio of the two pressures is also the ratio of the molecular beaming coefficients. As $\beta = 1$ for the side-arm with the small orifice, the value for the unrestricted side-arm is readily obtained. Experimental and calculated values of β are compared in table 2. The agreement between the two is good except for the first set of results where the larger error probably arises because the bend in the tubulation was not sufficiently sharp and resulted in a lack of precision in the value of L.

Table 2

A comparison of calculated and experimental values of β

Dimensions of side-arm (cm)		Molecular beaming coefficient β	
r	L	Experimental	calculated
1.70	5.4	1.08	1.14
1.70	7.0	1.25	1.24
0.60	5.0	2.19	2.25
0.725	14.5	2.79	2.80

Radius of spherical cell = 6.4 cm in all cases.

11. CORRECTIONS FOR DESORPTION

It was mentioned earlier that the sticking probability can have fundamental significance only when it is defined in terms of the actual rate of adsorption. Although the latter is equal to the measured rate of uptake of gas when the adsorbed layer is strongly bound, this is no longer so once the rate of desorption has become appreciable, and corrections must then be applied to the equations used previously in calculating s.

The onset of an appreciable rate of desorption from the adsorbed layer can always be detected by closing off the gas supply; if desorption is insignificant the

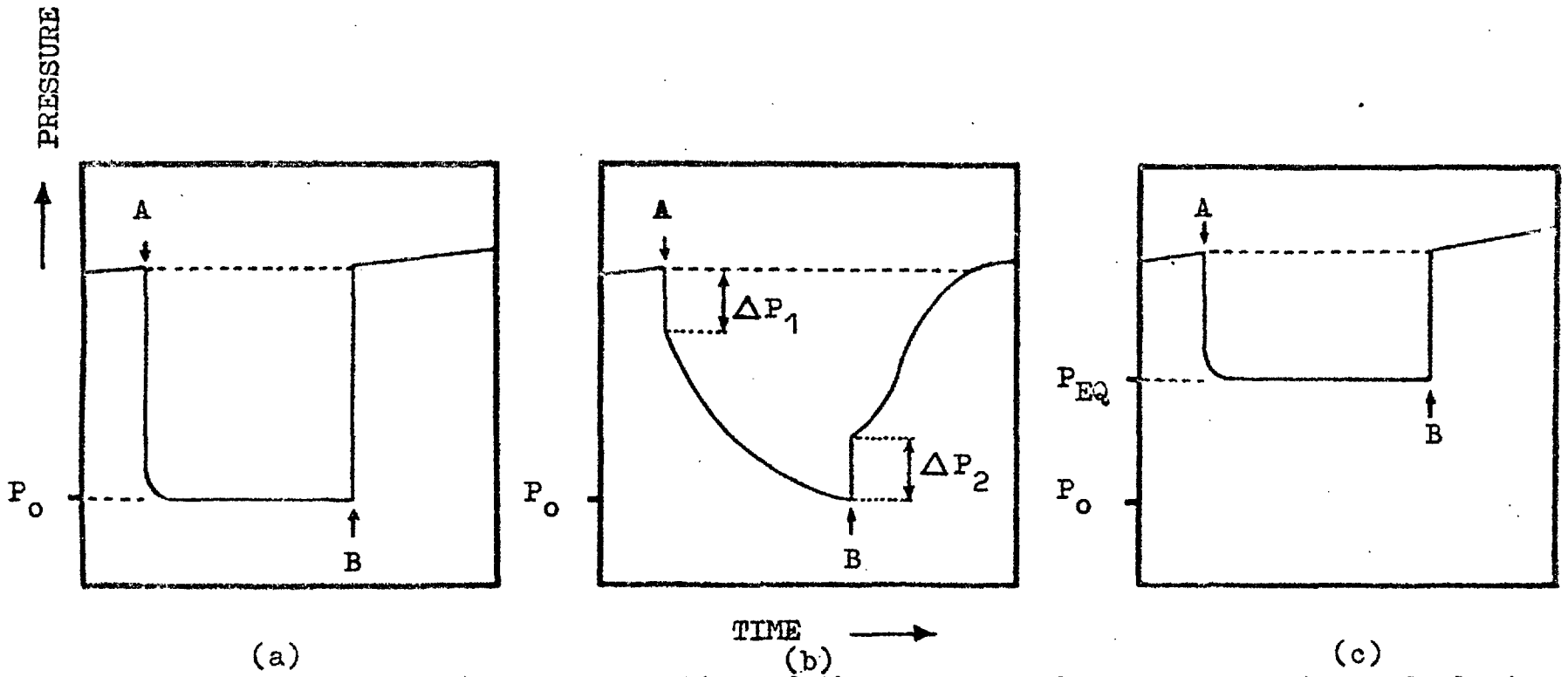

FIGURE 23. Diagrammatic representation of the pressure changes on opening and closing the gas supply to the film. A - gas supply opened, B - gas supply closed, P_o - 'background' pressure in vacuum system, P_{EQ} - equilibrium pressure.

pressure falls extremely rapidly to its background value, as shown in figure 23a but if significant desorption is occurring one of two types of behaviour may be observed:

(a) The pressure falls rapidly at first and then more slowly until it eventually reaches the background value (figure 23b).

(b) The pressure falls rapidly to P_{eq}, the equilibrium pressure above the adsorbed layer, and then remains constant (figure 23c).

The first type of behaviour is found at low temperatures when the adsorbed layer is immobile and the more accessible regions of the film have become saturated. The slow decrease in pressure is associated with a redistribution of adsorbate from the more accessible to the less accessible areas of the film (Hayward, Taylor and Tompkins, 1966). The true value of the sticking probability can be calculated approximately from the instantaneous pressure changes, ΔP_1, ΔP_2, which occur on stopping and restarting the gas supply. These pressure changes are measurable, however, only when they are comparable in magnitude with the total pressure P attained during gas flow.

The second type of behaviour is observed when the adsorbate is uniformly distributed over the surface of

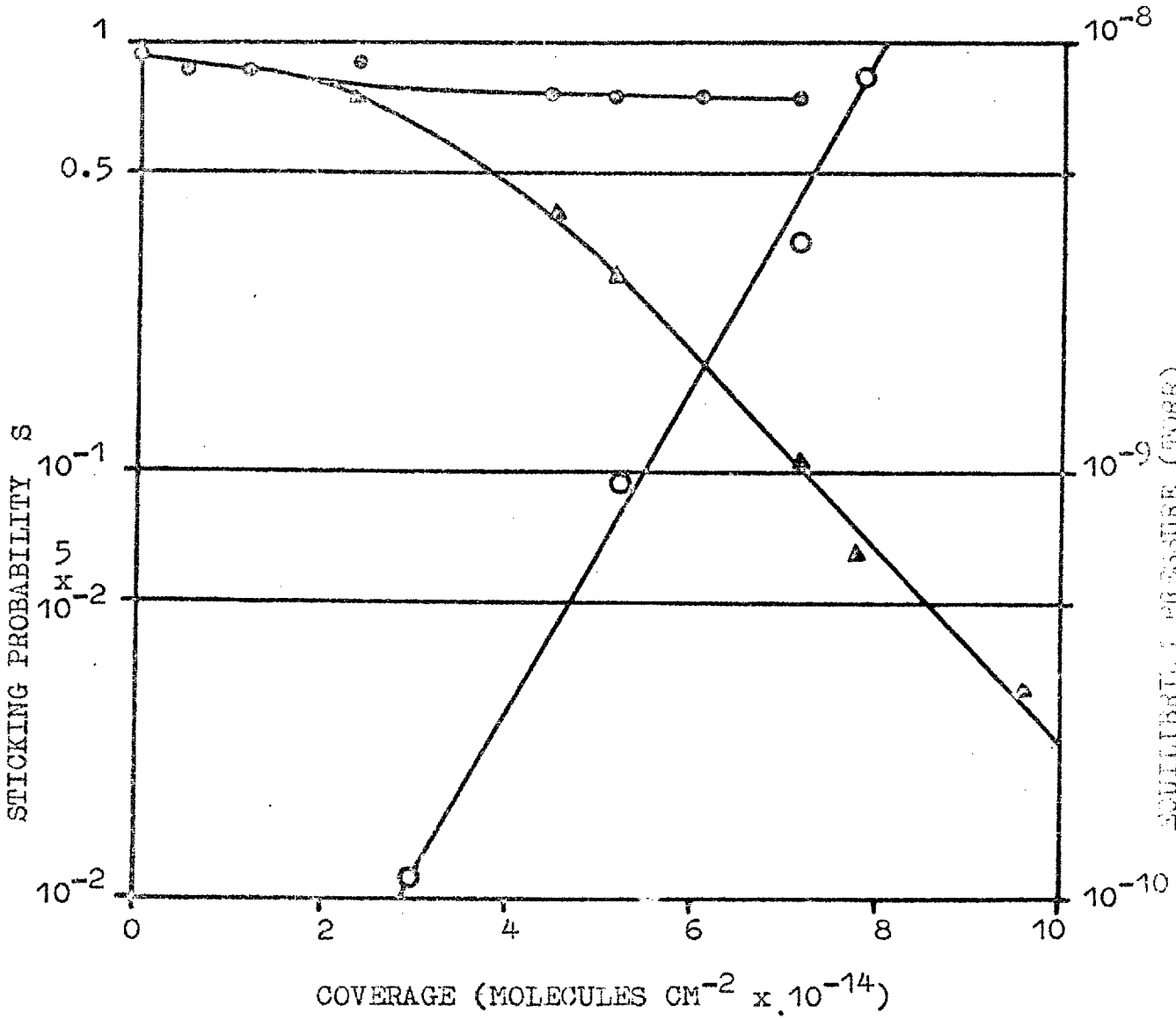

FIGURE 24. Sticking probability against coverage for hydrogen on palladium at 300°K, ● - S corrected for desorption, ▲ - S uncorrected for desorption, O - equilibrium pressure.

the film and is therefore most commonly found when the adsorbed layer is mobile. At equilibrium the rate at which molecules are adsorbed from the ambient gas is $sP_{eq}AZ$, and this is equal to the corresponding rate of desorption. Thus, when there is a net uptake of n_A molecules sec^{-1}, the total rate of adsorption from the ambient gas is $(n_A + sP_{eq}AZ)$. If this is used, rather than n_A, in equation (2) we have

$$s = \frac{n_A + sP_{eq}AZ}{ZAP},$$

and on rearranging

$$s = \frac{n_A}{ZA(P-P_{eq})}, \qquad (15)$$

Thus the true sticking probability can be obtained by substituting $(P-P_{eq})$ for P in the original equation, and this applies equally well for the more complicated expressions for s.

The effect of this correction on the plot of sticking probability against surface coverage for hydrogen on palladium at room temperature is shown in figure 24. It can be seen that the sharp drop in the apparent value of sticking probability at a coverage of 3×10^{14} molecules cm^{-2} geometric area is entirely due to a rapidly increasing equilibrium pressure above the

Run	T_F^oK	S^o	Coverage for an equilibrium pressure of 10^{-5} torr at 300°K (N_{300}) (molecules/cm^2 geom.)	Coverage for an equilibrium pressure of 10^{-5} torr at 78°K (N_{78}) (molecules/cm^2 geom.)	N_{78}/N_{300}	RF $N_{78}/7.5 \times 10^{14}$
2.12.64	195°	0.75	-	-	-	-
7.1.65	195°	0.75	-	*7.62×10^{15}	-	-

Table (a) - HYDROGEN - MOLYBDENUM - SINTERED FILMS

* - using a tungsten filament in the ionization gauge

\+ - uptake at 195°K - ratio is wrt 300°K and 195°K uptake

/ - a coverage at 78°K is estimated if necessary as 1.36 x uptake for 10^{-5} torr at 300°K

T_F^oK - temperature of film at initial addition of gas

S^o - sticking probability at zero coverage

RF - roughness factor of film.

Run	S^o	Coverage	RF
10.8.65	0.915	1.88×10^{16}	25
31.10.65	0.855	-	-
23.11.65	0.890	2.07×10^{16}	27.6

Table (b) - HYDROGEN - MOLYBDENUM - UNSINTERED FILMS

Coverage for an equilibrium pressure of 10^{-5} torr

Run	$T_F^{\circ}K$	S°	at $300^{\circ}K(N_{300})$ (molecules/cm^2 geom.)	at $78^{\circ}K(N_{78})$ (molecules/cm^2 geom.)	N_{78}/N_{300}	RF $N_{78}/7.5 \times 10^{14}$
12.6.63[H]	300°	0.65	5.84×10^{15}	-	-	10.6
18.6.63[H]	273°	0.81	4.75×10^{15}	-	-	8.6
21.6.63[H]	300°	0.68	5.61×10^{15}	-	-	10.2
24.3.64	300°	0.73	6.80×10^{15}	8.90×10^{15}	1.31	10.8
22.10.64	300°	0.62	-	-	-	-
22.10.64	78°	0.70	-	-	-	-
28.10.64	300°	0.73	7.45×10^{15}	1.04×10^{16}	1.40	13.7
5.3.64	300°	0.60	-	-	-	-
	78°	0.65	-	-	-	-
6.3.64	300°	0.58	3.04×10^{15}	4.20×10^{15}	1.38	5.6
15.11.65	300°	0.74	7.14×10^{15}	$^{+}8.21 \times 10^{15}$	$^{+}1.15$	11.0
9.4.64	78°	0.73	-	6.00×10^{15}	-	8.0
14.4.64	78°	0.85	-	-	-	-
18.1.65	78°	0.73	-	7.50×10^{15}	-	10.0
21.1.65	78°	-	-	9.00×10^{15}	-	12.0
11.3.65	78°	0.63	-	-	-	-
17.3.65	78°	0.75	-	-	-	-
28.5.65	78°	0.75	-	-	-	-

adsorbed hydrogen layer and that the drop disappears when the correction is applied.

RESULTS AND DISCUSSION

12. HYDROGEN ON MOLYBDENUM

12.1. The uptake of gas by molybdenum films

During evaporation of films of molybdenum the walls of the reaction vessel were either uncooled, in which case the temperature rose to around 100°C, or were held at 78°K by immersing in a bath of liquid nitrogen. The sintered films i.e. those deposited with the substrate around 100°C, had a markedly smaller gas uptake than the unsintered films - those deposited and maintained at 78°K. Tables (a) and (b) list, together with other data, the gas uptakes on various films at 300 or 78°K when the equilibrium pressures had reached 10^{-5}torr. The total gas uptake has been given in various ways in the literature, Beeck (1945) and Brennan and Hayes (1964) amongst others have shown that with films the uptake of gas in moles is directly proportional to the weight of film deposited and subsequently report 'coverage' in terms of moles of gas per unit weight of adsorbent. The practice in this work has been to follow that used for low area adsorbents and express the uptake in terms of molecules per unit area of adsorbent - the latter

term referring with films to the geometric area occupied by the film. To estimate the roughness of the films, i.e. the ratio of the true surface area to the geometric area, it is necessary to assume a value for the number of adsorption sites per unit area of true surface. Brennan et al. (1964) take a value of 1.315 x 10^{15} and Anderson and Baker (1961) 1.215 x 10^{15} for this factor for tungsten surfaces. Since in this work the surface coverage is not of prime interest it was decided to take a value 1.50 x 10^{15} sites per cm^2 of true surface for all the metals studied - this coincides with that normally accepted for a nickel surface. With this value it is seen that the gas uptake corresponds to roughness factors of about 10 and 25 times respectively for sintered and unsintered films assuming that each hydrogen molecule occupies two sites.

The ratios of uptake at 78°K and 300°K on the same film are also included in table (a). There is good agreement with values of 1.31 (Brennan et al, 1964), 1.21 (Trapnell, 1951), 1.28 (Anderson, 1961) and 1.34 (Hickmott, 1960) for tungsten surfaces. The literature values are for evaporated films with the exception of that of Hickmott which is for a tungsten filament. A single value of 1.15 was obtained for the ratio of

uptake at 195°K and 300°K - this agrees with a value of 1.20 obtained from Hickmott's data for a tungsten filament.

12.2 The sticking probability of zero coverage

The values of sticking probability near zero coverage are included in tables (a) and (b). It is seen that the values for sintered films are centred around 0.7 and are virtually independent of temperature between 78°K and 300°K. The values for unsintered films are somewhat higher - $\sim$ 0.89 - this is expected since it has been shown that there is a greater uptake and correspondingly greater roughness with these films thus enhancing the probability of multiple collisions. The sticking probabilities may be compared with those found by Pasternak and Wiesendanger (1961) for hydrogen on a molybdenum ribbon. These workers found values of 0.35 independent of temperature between 225°K and 400°K. Values for tungsten wires of 0.3 (Eisinger 1958), 0.1 (Hickmott 1960), 0.24 (Redhead 1962) and 0.32 (Rigby 1965) have been obtained at room temperature or below and are in all cases virtually independent of temperature in the range studied. Hunt, Damm and Popp (1961) have measured the pumping speed of a molybdenum film and conclude that the sticking probabilities for both

hydrogen and deuterium are around 0.5. However, this work is unable to give an accurate value within very large limits due to inherent defects in the design of the reaction system. Accepting the values obtained using filaments and assuming the same type of physical structure for films enables an estimate of the number of multiple collisions experienced at the film surface to be made. For values of 0.35 for a plane surface and 0.7 for a sintered film it is easily shown that about 2.8 collisions per reflected molecule are made while for an unsintered film around 4.7 collisions are required.

To enable the temperature dependence of sticking probability to be studied in more detail several runs were performed in which values on a single film near zero coverage were obtained at both 78°K and 300°K. The results show that the low temperature value is about 8% higher. It is probably unwise to attempt to correlate this with an activation energy since some artefact connected with gas temperature may be responsible.

Attempts were made to relate variations in initial sticking probability to a variety of experimental parameters including vacua during deposition and ionization gauge operating conditions. These were in general unsuccessful - the only reasonably substantiated

effect was a reduction in the value for rather thin films (roughness factors around 5).

12.3. The sticking probability as a function of surface coverage.

As pointed out previously great stress was placed in the whole of this work on the behaviour of the reacting system when the gas flow to the adsorbent was interrupted. At room temperature it was found that the adsorbed layer was at equilibrium at all times since the observed pressure changes at the flow interruptions were abrupt, and the calculated sticking probabilities both prior and subsequent to the interruption were equal. The coverage corresponded to an area many times that of the underlying substrate and there appears no doubt that gas is distributed by surface diffusion to the inner surface. A similar situation is observed at 195°K for about three quarters of the total gas uptake but after this point the slow pressure changes on closure of the supply indicate non-uniformity in the gas distribution on the film. The process by which the gas which is concentrated on the outer more accessible regions is redistributed will be discussed fully at a later stage.

At 78°K only about 8 x 10^{14} molecules per cm^2 of geometric surface can be added to the film before slow

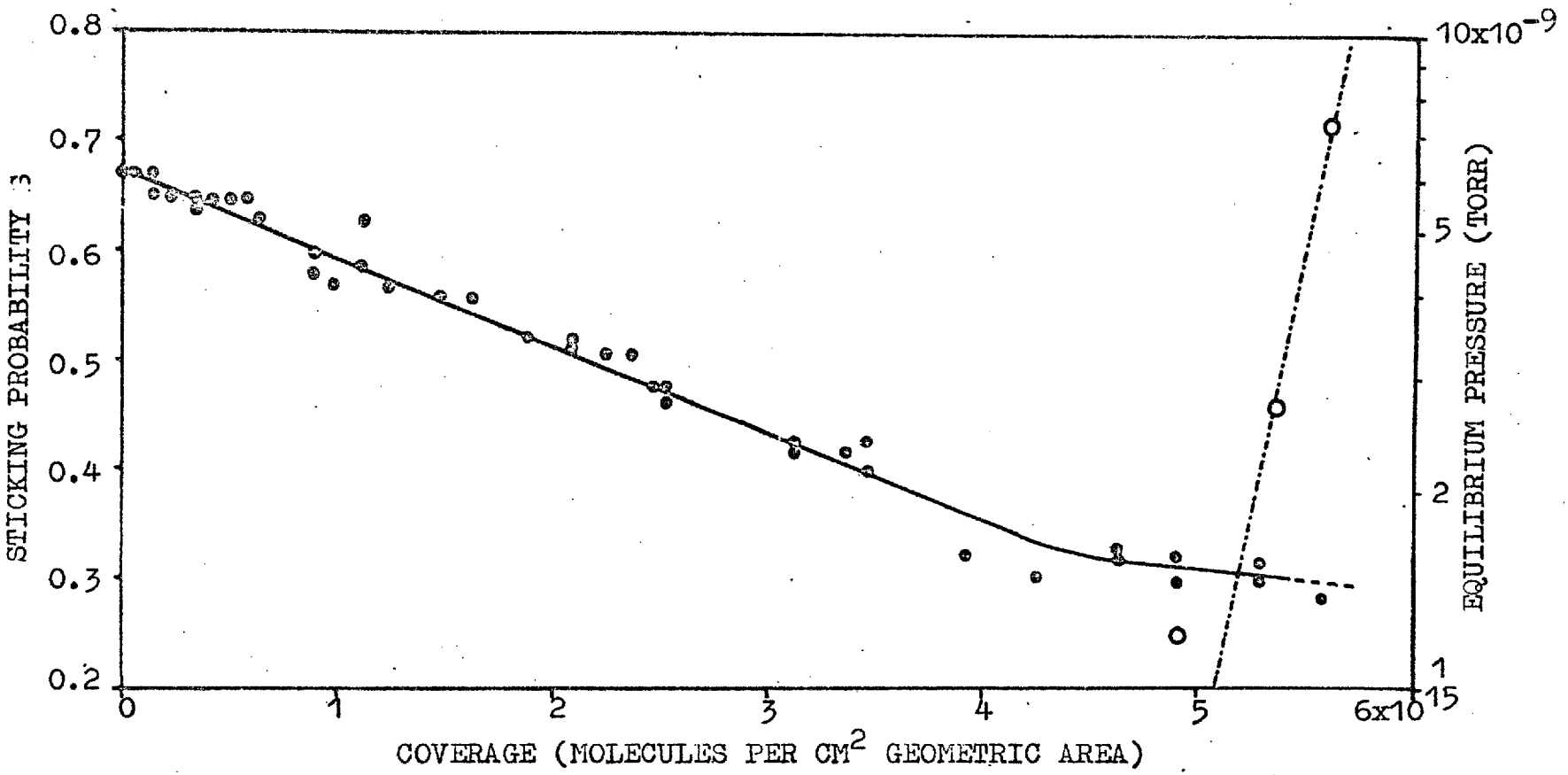

FIGURE 25. Sticking probability against coverage at 300°K.

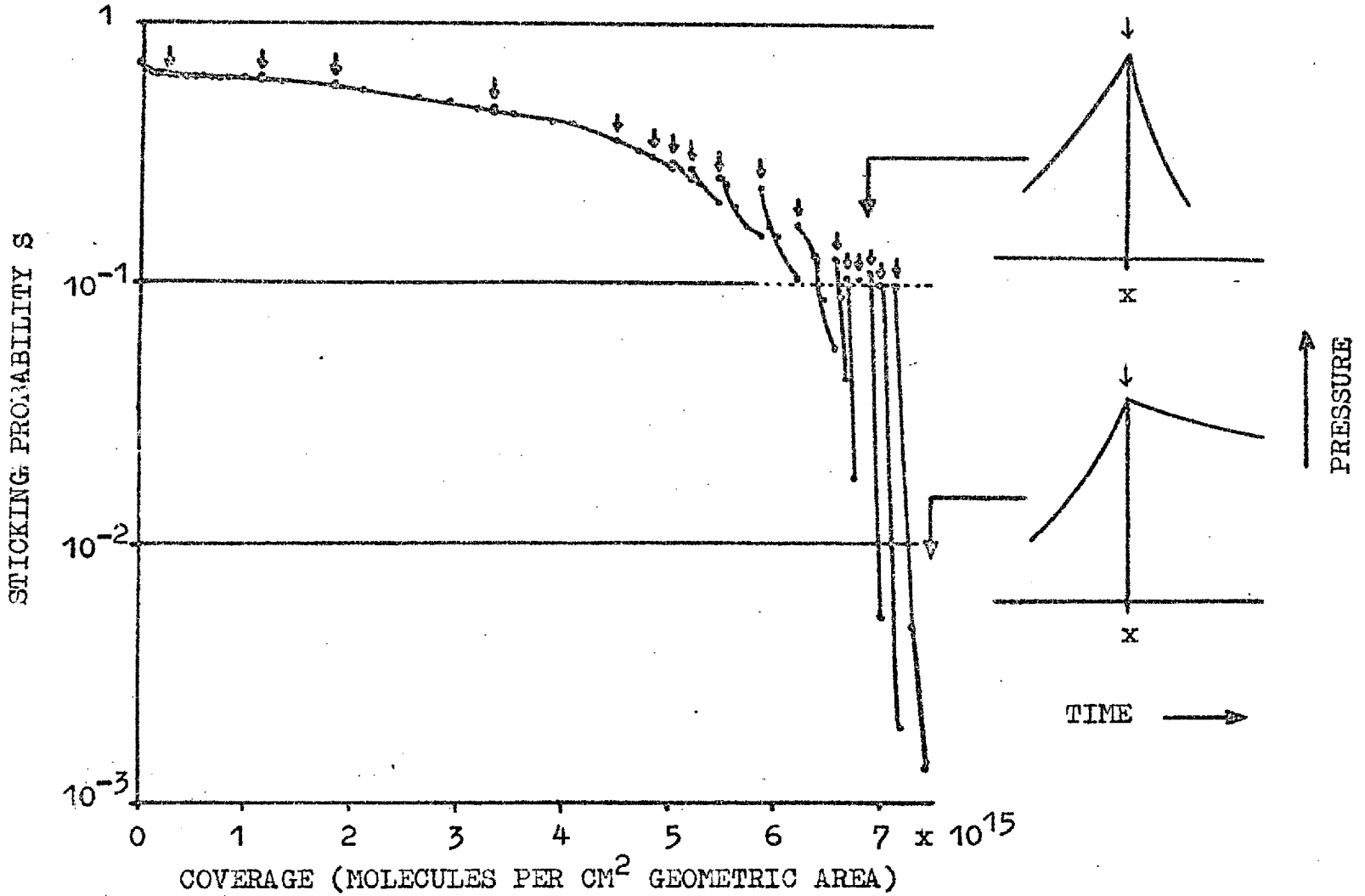

FIGURE 26. Sticking probability against coverage at 195°K. (Pressure time profiles at gas supply closure (x) are shown on R.H.S.)

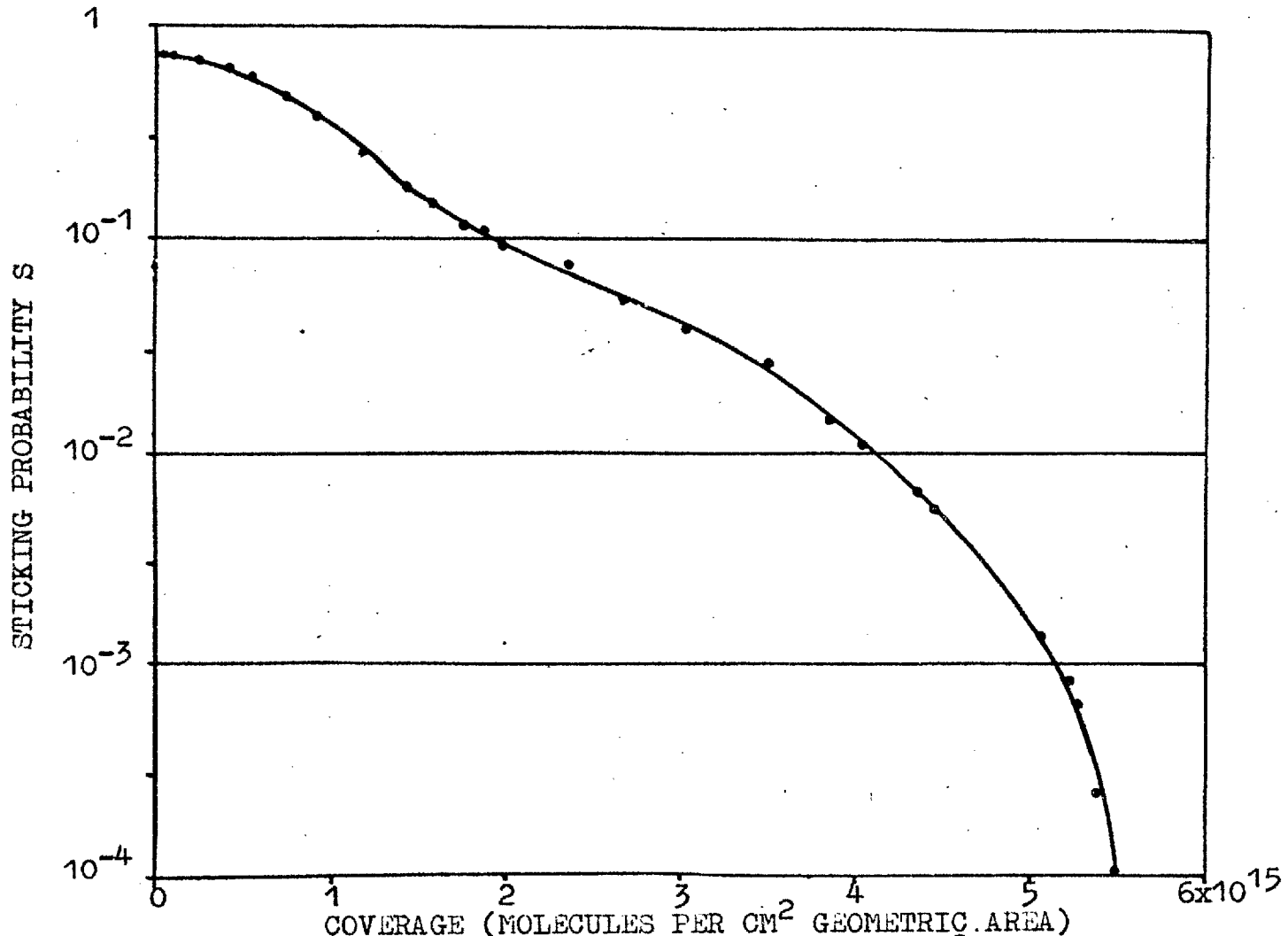

FIGURE 27. Sticking probability against coverage at 78°K.

redistributions are in evidence. These tend to complicate the variation of sticking probability with surface coverage and since a full description of the redistribution is to follow it was decided to report in this section the results of a run at 78°K in which there was no interruption of gas flow. Figures 25, 26 and 27 show typical behaviour at the three temperatures.

It may be noted from these curves that at no temperature is the sticking probability independent of surface coverage. The more slowly varying sticking probabilities at 300°K and 195°K are expected since the concentration of molecules on the outer surface is reduced by surface migration. As will be seen subsequently the values of sticking probability at 78°K displayed on figure 27 relate, after the initial coverage region, to the kinetics of gas phase diffusion into the porous structure of the film and are not of fundamental significance. In contrast those at 300°K and 195°K refer to adsorption on the outer surface followed by a rapid surface diffusion and, after correction for desorption, they give a true variation of S with coverage.

The absence of a region of constant sticking probability is in direct contrast to that reported for flash filament experiments by Eisinger, Pasternak and

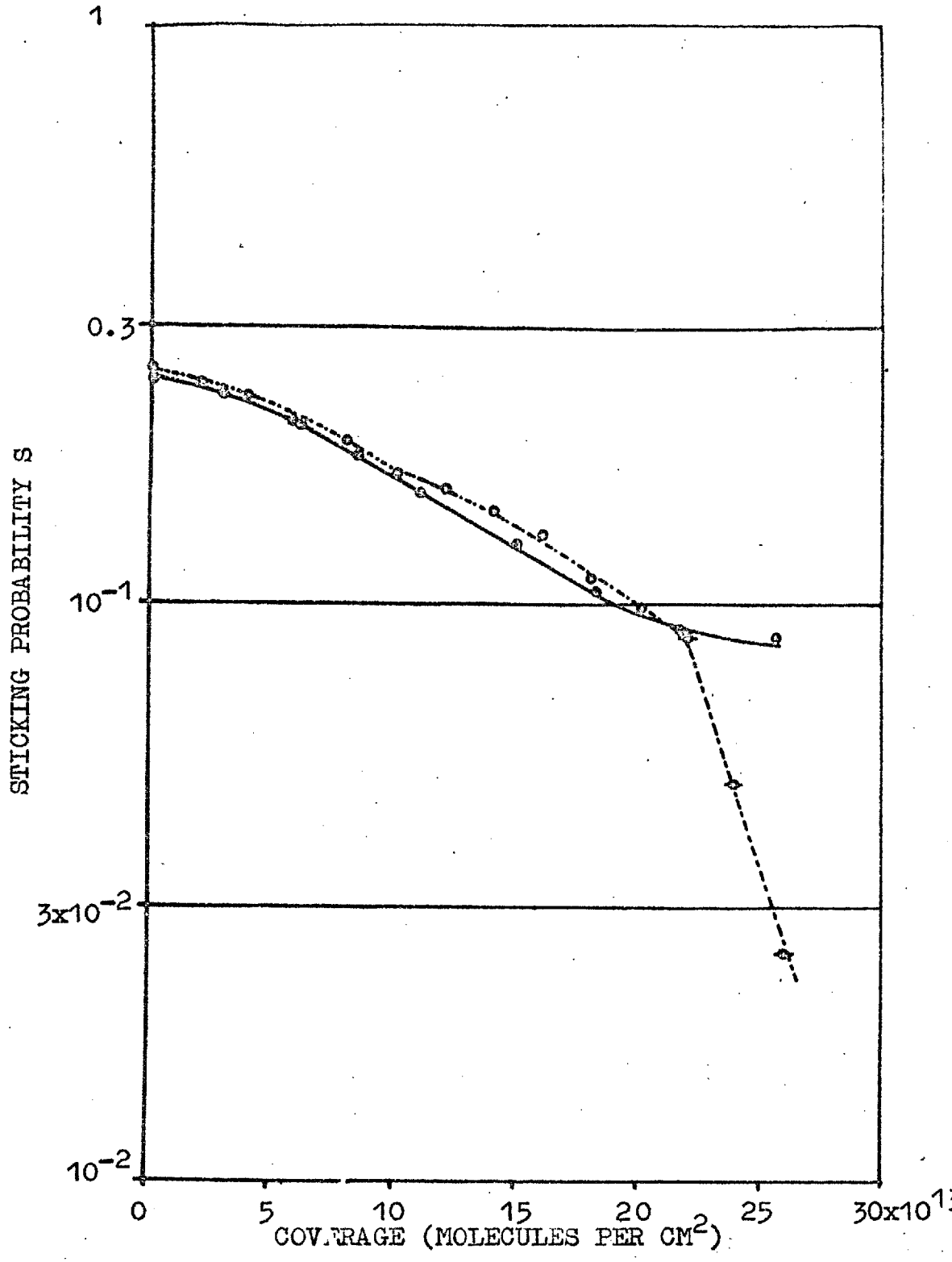

FIGURE 28. Sticking probability versus coverage for a molybdenum filament. ● - with continuous pumping thro' D1., O without pumping, ⊖ values uncorrected for desorption.

Redhead, who also observe a much sharper downward trend once a certain critical coverage is reached. To attempt to clarify this point it was decided to perform a flow type sticking probability experiment using a molybdenum filament as adsorbent. This was carefully cleaned by high temperature heating in ultra-high vacuum but great care was taken to avoid deposition of film. The gas was flowed to the adsorbent for short periods and from the results the curve displayed in figure 28 was constructed. Since the existence of an equilibrium pressure was readily detected on closure of the gas supply the points refer to a true sticking probability. To illustrate the dangers of methods which ignore equilibrium pressures the unfilled circles refer to values which are calculated from the total pressure above the adsorbent when desorption is occurring. It can be seen that the true variation of sticking probability with coverage is similar to that observed with evaporated films and even assuming that the outgassing procedure has not given a completely clean surface there is no doubt concerning the general shape. The latter results enable the sharp cut-off in sticking probability found in flash filament experiments to be ascribed to an (undetected) onset of desorption from the adsorbed layer.

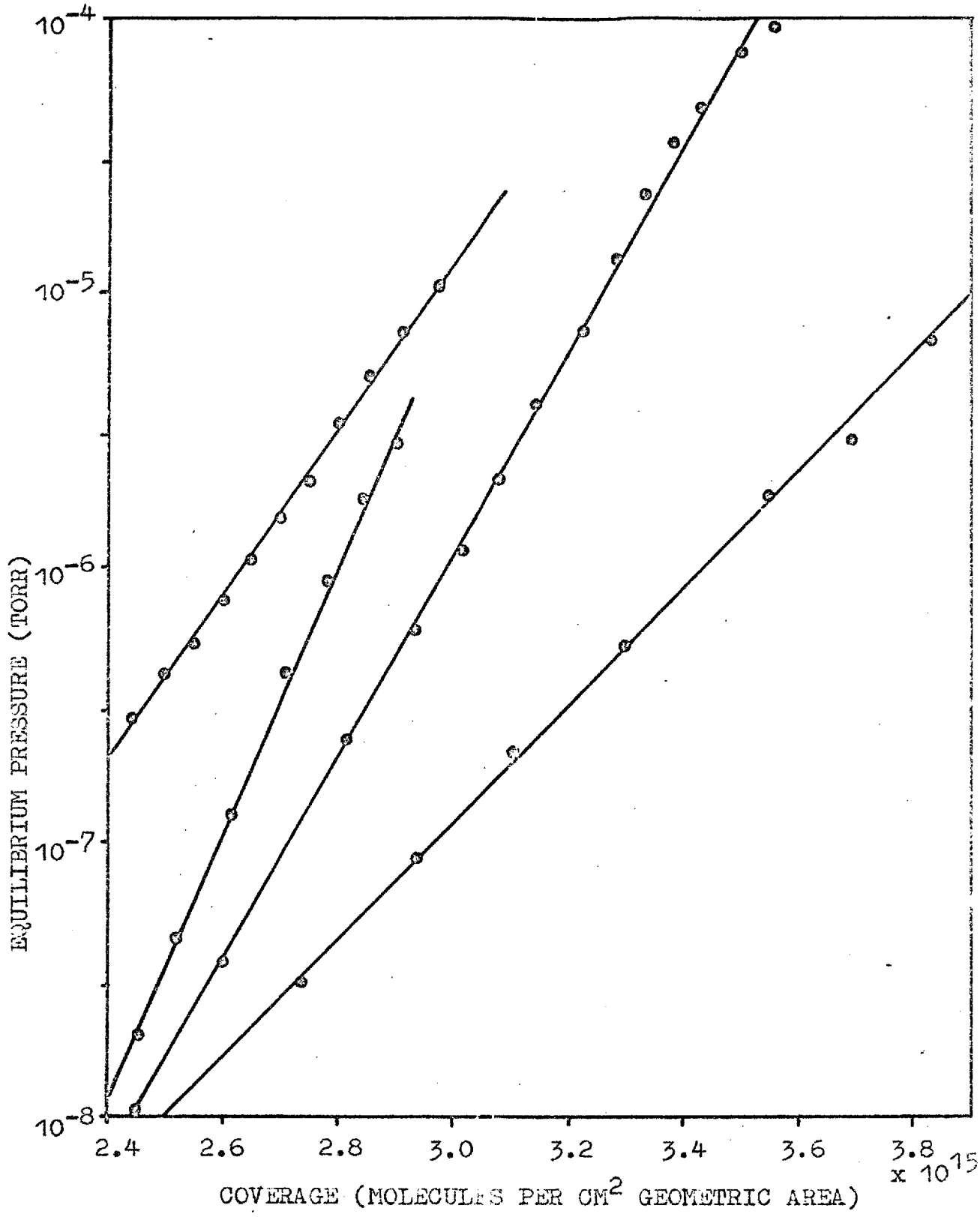

FIGURE 29. Temkin isotherms at 300°K.

12.4. The equilibrium properties of the adsorbed layers.

Before proceeding with a consideration of the various redistribution processes which are found to occur it is convenient to assemble data obtained from studies of the variation of the equilibrium pressure with surface coverage and temperature.

At room temperature the kinetic data indicates a highly mobile adsorbed layer and this is confirmed by the time-independent nature of pressures observed above the adsorbed layer near saturation. The onset of appreciable desorption is, as previously indicated, detected by the failure of the hydrogen pressure in the reaction vessel to return to background on closure of the gas supply. It has been seen that the sticking probability remains high even when appreciable desorption occurs thus indicating that adsorption and desorption are very rapid processes and the attainment of equilibrium thus virtually instantaneous. The high sticking probability has the further effect of causing the reaction vessel pressure to be sensibly equal to the equilibrium pressure over a wide range of the latter. Many isotherms have been constructed at 300°K and these without exception are found to obey the Temkin equation - logarithm of pressure linear with the amount adsorbed. Figure 29 displays several typical results. Adherence

to the Temkin equation indicates a heat of adsorption falling linearly with uptake in the range considered. It may be shown that if the isotherm is expressed as

$\alpha N = \ell nP + k$

N - coverage in molecules per cm^2 geometric area

P - equilibrium pressure (torr)

α, k - constants at a fixed temperature.

then the rate of change of the heat of adsorption with coverage N is given by αRT (R - gas constant, T - absolute temperature).

For a comparison of the slopes of isotherms for different films to have any significance it is necessary to express the coverage in terms of molecules adsorbed per cm^2 of true surface area - values of the slope α' computed in this way are given in the following table:

REFERENCE	ROUGHNESS FACTOR+	TEMPERATURE (^oK)	α' per molecule per cm^2 true area
7.6.63*	9.4	300	6.76×10^{-14}
18.6.63*	8.25	273	7.15×10^{-14}
6.3.65	5.30	303	8.05×10^{-14}
15.11.65	12.90	300	5.50×10^{-14}
28.10.65	12.80	300	8.15×10^{-14}
15.11.65	13.00	300	5.50×10^{-14}

* obtained using tungsten filament ionization gauges

+ calculated from the uptake at 78^oK for 10^{-5} torr equilibrium pressure.

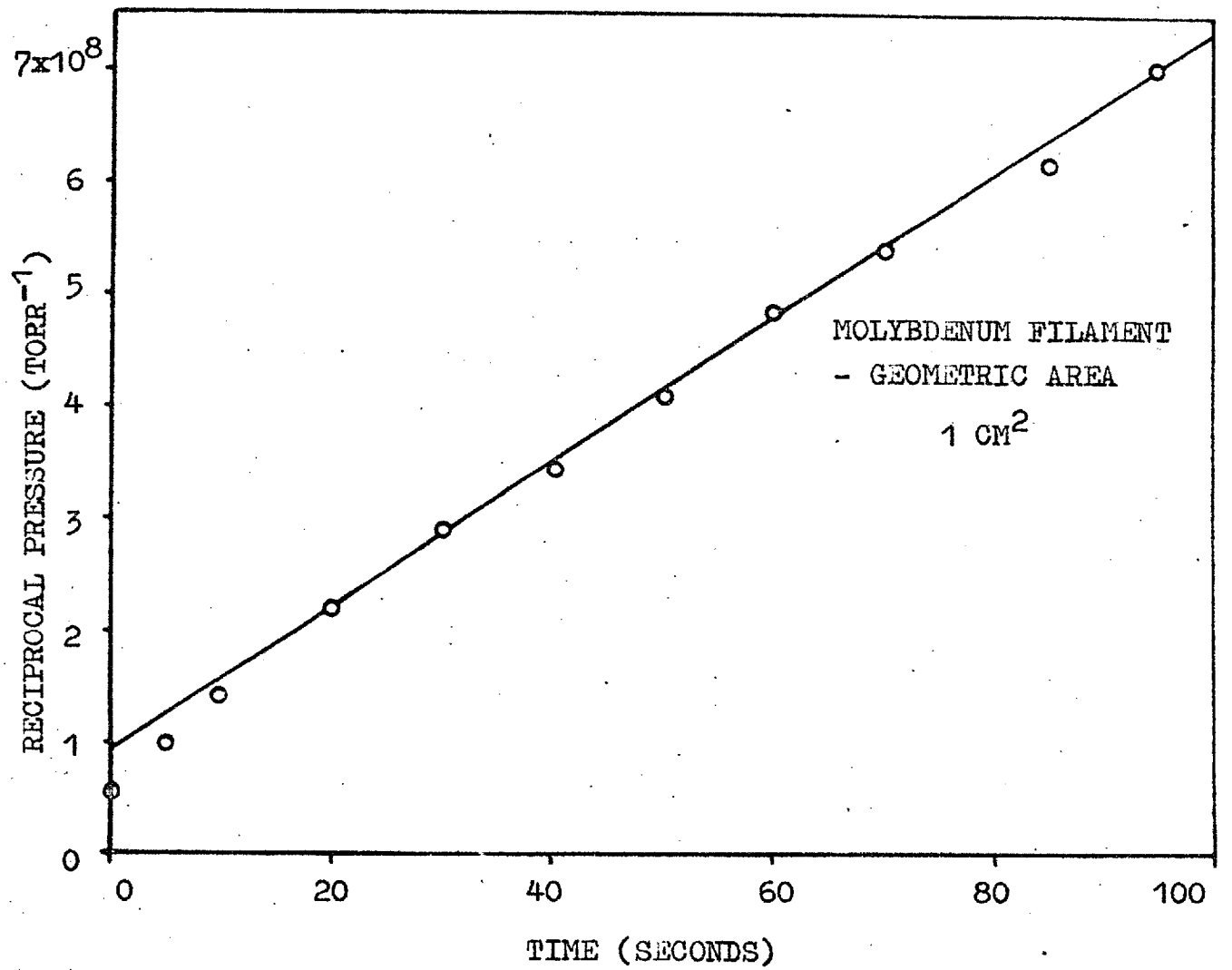

FIGURE 30. Variation in (equilibrium pressure)$^{-1}$ at 300°K on pumping through a conductance of 10^{20} molecules per torr per sec.

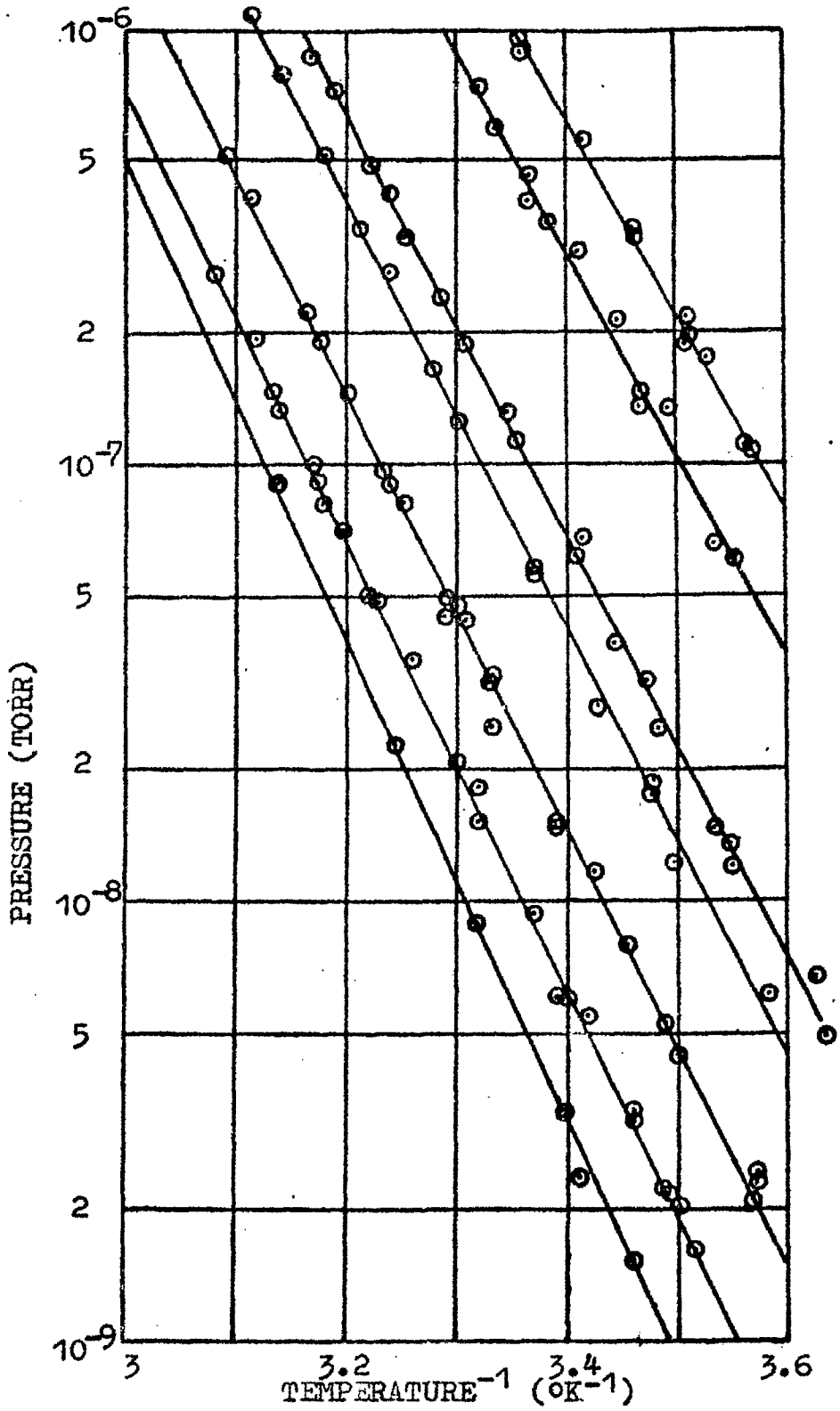

FIGURE 31. Isosteres for the hydrogen molybdenum system.

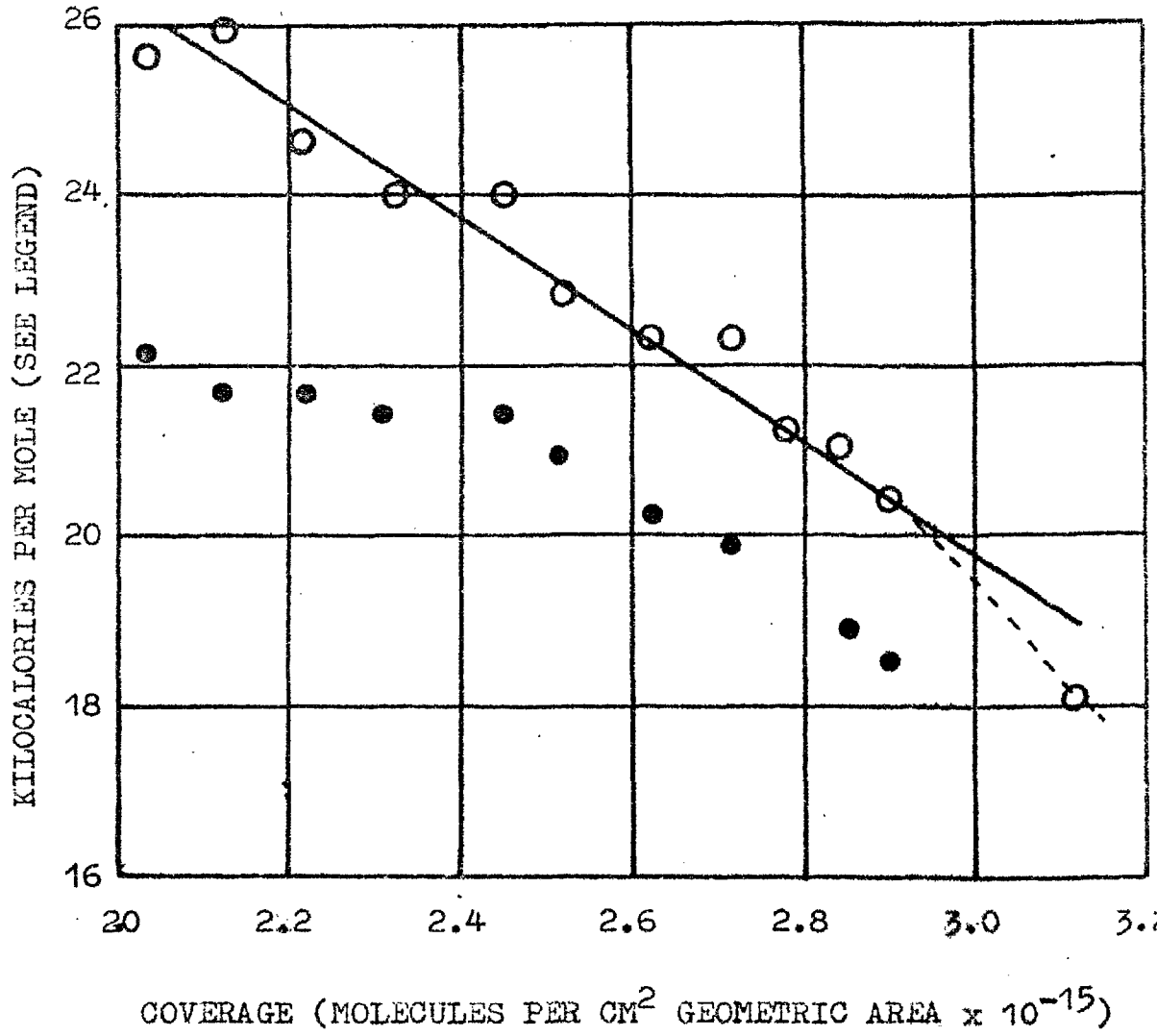

FIGURE 32. The isosteric heat of adsorption (open circles, negative sign) and the free energy of activation of the transition complex (filled circles, positive sign) versus coverage.

Table (c) The slopes of isotherms for hydrogen on molybdenum around 300°K

To obtain a value for the slope of the isotherm for hydrogen on a molybdenum filament the following novel experiment was performed. The filament was cleaned as previously indicated and saturated with gas to an equilibrium pressure of some 2×10^{-8} torr at 300°K. The gas was then steadily pumped off through a fixed known conductance. It is easily shown that if the Temkin equation is obeyed and if the rate of pumping is proportional to the reaction vessel pressure then the reciprocal of pressure increases linearly with time. The slope of such a plot (shown in figure 30) is the product of α' and the conductance. For the curve shown the conductance was 10^{20} molecules per torr per second and α' is thus 6.4×10^{-14} per molecule per cm^2 in excellent agreement with the film values. This is also in agreement with a value of 6×10^{-14} obtained for hydrogen on a tungsten filament by Hickmott (1960).

The variation of equilibrium pressure with temperature at a fixed surface coverage has been studied in the region of room temperature for a single film. Figure 31 displays the experimental isosteres and figure 32 the heats of adsorption obtained from the isosteres by the application of the Clausius-Clapeyron equation.

The isosteric heats are seen to fall linearly with amount adsorbed over the coverage range and the slope of the curve gives an α' value of 6.7×10^{-14} per molecule per cm^2 true surface in good agreement with that obtained from the slopes of the isotherms. Heats of adsorption for hydrogen on tungsten films at $300^{\circ}K$ have been obtained calorimetrically by Brennan and Hayes (1964). These workers display a somewhat sigmoidal heat curve at this temperature with an initial value of around 42 kilocals per mole compared with (assuming a linear extrapolation) a value of 40 k cals in this work. It is interesting to note that a value for α' of 5×10^{-14} per molecule per cm^2 of true surface may be obtained from the curve of Brennan at half coverage, with correspondingly higher values towards saturation as the heat curve bends off. Hickmott (1960) has obtained heats from desorption data and also from isosteres for the hydrogen tungsten system, finding that the heat falls nearly linearly over a wide coverage range. The slope of the heat curve of Hickmott gives an α' of 3.7×10^{-14} per molecule per cm^2 of true surface in apparent disagreement with the slope of his isotherm at $298^{\circ}K$.

Since the sticking probability can still be reliably obtained in the region where the equilibrium pressure is small it is possible to perform a

calculation using absolute reaction rate theory to obtain the difference in free energy $\Delta G^{\ddagger}$ between the adsorbed state and the surface transition complex preceding desorption. Thus, equating the rates of adsorption and desorption per cm^2 for an isolated system.

$$S.P.Z = \frac{n^2}{n_s} \cdot \nu \cdot \exp. - \frac{\Delta G^{\ddagger}}{RT}$$

where S - sticking probability

P - equilibrium pressure

Z - Hertz-Knudsen factor

n - number of molecules per cm^2 of true surface

n_s - number of adsorption sites per cm^2 of true surface.

ν - a frequency factor - taken as 10^{13} per sec.

The values of $\Delta G^{\ddagger}$ obtained by substituting the experimental values of S, P and n in the above equation are given on figure 32 ($\Delta G^{\ddagger}$ has of course a positive magnitude). If one assumes that $\Delta H^{\ddagger} = -\Delta H_{ADS.}$ i.e. that the activation energy for adsorption is negligible then the entropy of activation $\Delta S^{\ddagger}$ may be calculated from

$$\Delta G^{\ddagger} = \Delta H^{\ddagger} - T\Delta S^{\ddagger}$$

$\Delta S^{\ddagger}$ lies in the region +5 to +8 calories per mole per degree; this is about the entropy change expected for 2 degrees of vibrational freedom in the adsorbed state

becoming two degrees of translational freedom in the transition complex. That mobility of the adsorbed layer over the surface may not contribute appreciably to the entropy does not necessarily indicate immobility but merely that the atoms execute many vibrations at each site between each hop to a new site.

The differential entropy of adsorption $\bar{S}_\theta$ can be obtained from the expression

$$\bar{S}_\theta = Sg - R\ell nP - \frac{\Delta H_{ADS}}{RT}$$

where Sg - integral molar entropy of the gas at one atomosphere.

P - the equilibrium pressure in atmospheres.

ΔH_{ADS} - the isosteric heat of adsorption.

Values of $\bar{S}_\theta$ have been calculated from the above and are found to be around 5 - 6 calories per degree per mole. Unfortunately the integral entropies of adsorption cannot be determined at room temperature since both ΔH_{ADS} and P are required as continuous functions from zero coverage. The treatment given by Sweett and Rideal (1960) to data for the hydrogen-nickel system cannot, therefore, be repeated here. Trapnell (1951) obtained an $\bar{S}_\theta$ of 5 calories per degree per mole for the hydrogen-tungsten system around room temperature.

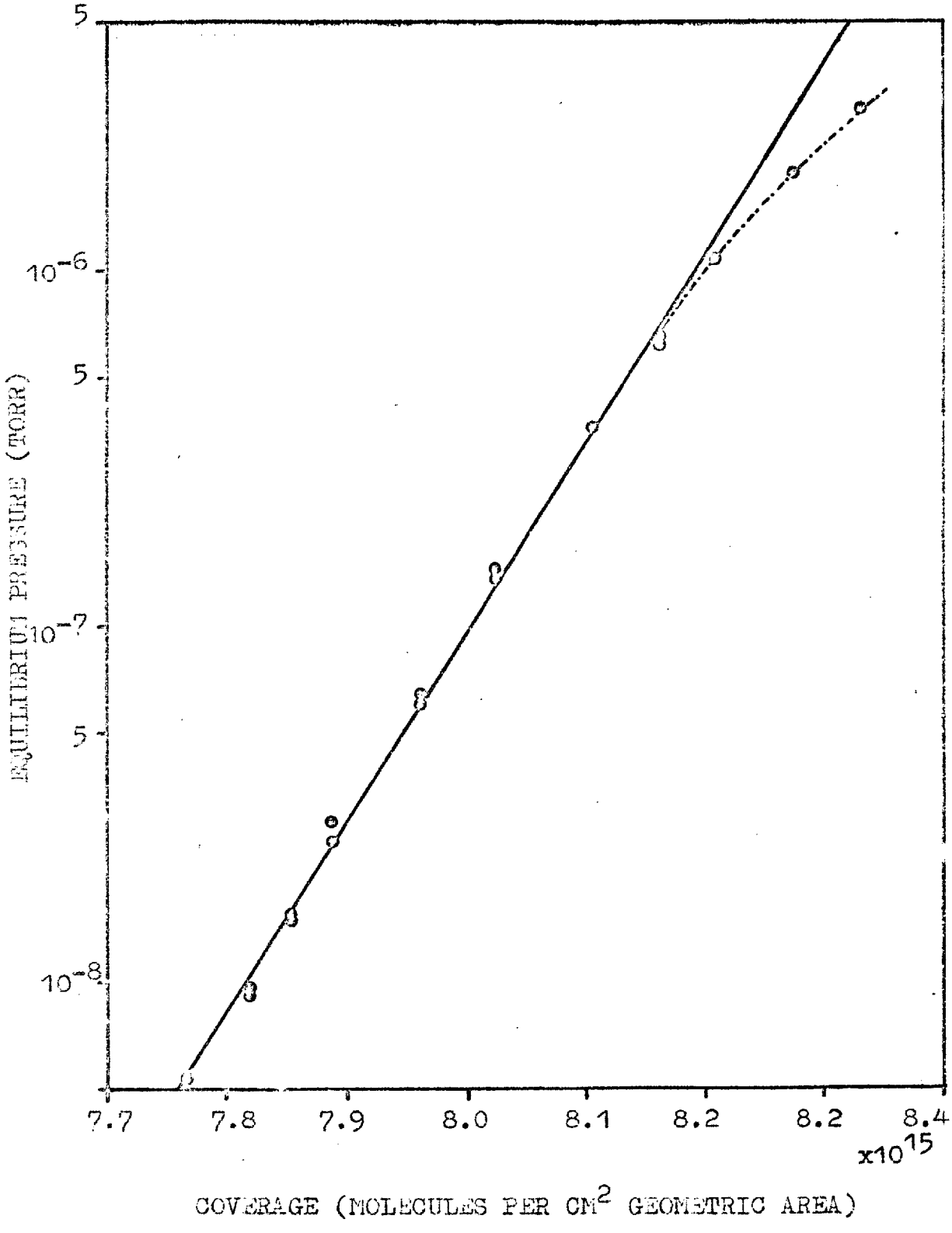

FIGURE 33. Temkin isotherm at 195°K.

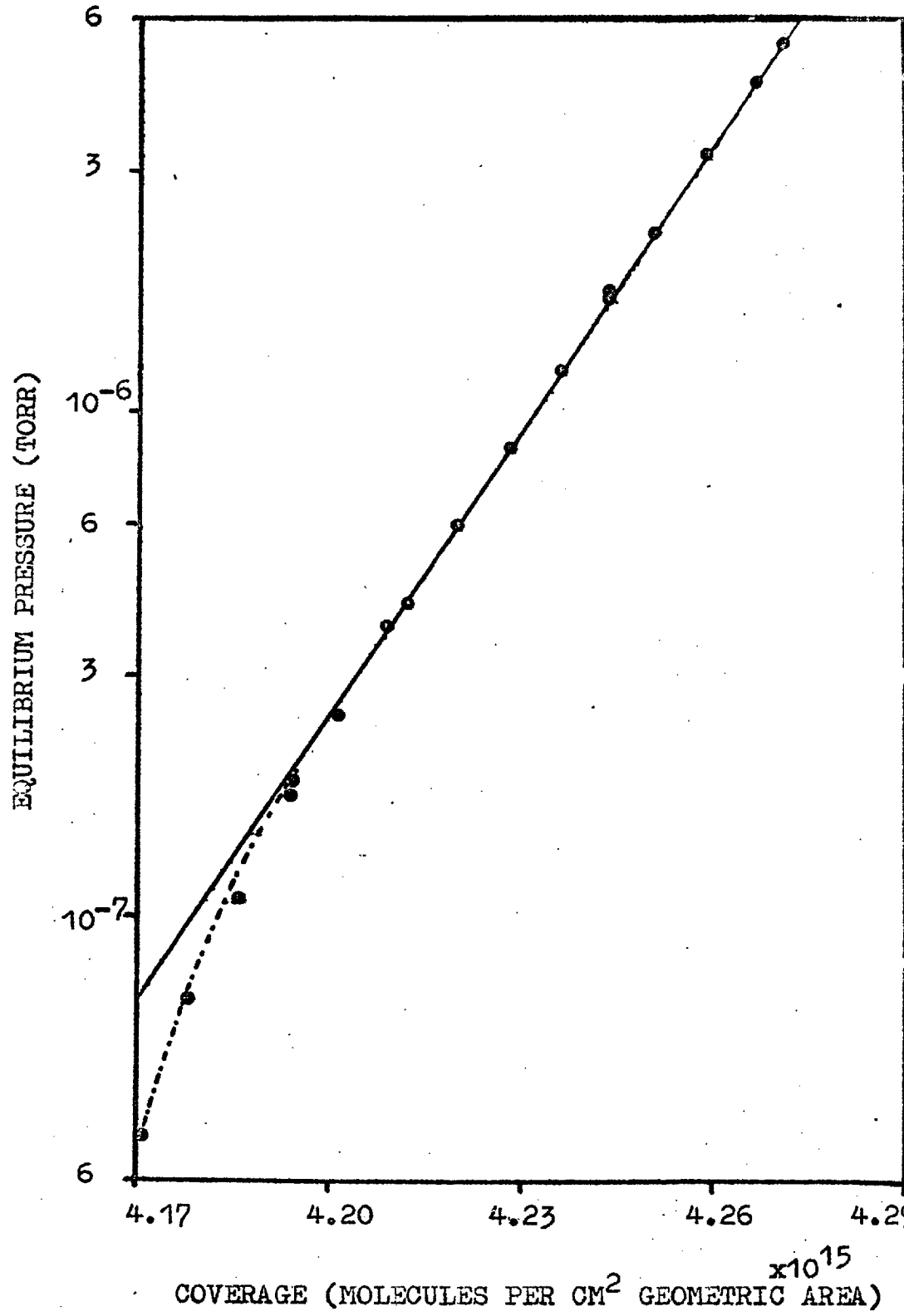

FIGURE 34. Temkin isotherm at 78°K.

Isotherms similar in form to that at room temperature have been obtained at 195°K and 78°K. Figures 33 and 34 display typical results at the two temperatures and show adherence to the Temkin equation. It was difficult, particularly at 78°K, to obtain a reasonable measure of equilibrium pressure since slow drifts went on apparently ad infinitum. These could be reduced by cycling the isolated system between 78°K and some higher temperature preferably approaching 200°K. The effect of the drifts could also be overcome to some extent by calculating α' values of individual additions of gas rather than attempting to construct a complete isotherm. The following table gives α' values at 195°K and 78°K. The values obtained in the run 21.1.65 refer to individual doses of gas and correspond to increasingly greater equilibrium pressures as the table is descended. It is to be noted that the values of α' so obtained approach those from isotherms only at the higher coverages indicating a closer approximation to equilibrium in this range.

The velocities of desorption vary approximately exponentially with the heat of desorption and thus with the heat of adsorption if the activation energy for adsorption is negligible. For an adsorbed layer in which the heat of adsorption falls markedly with

REFERENCE	TEMPERATURE °K	ROUGHNESS FACTOR	α' per molecule per cm^2 of true area
7.1.65	195°K	11.8	1.96×10^{-13}
15.11.65	195°K	13.0	1.61×10^{-13}
6.3.65	78°K	5.3	2.36×10^{-13}
2.4.65	78°K	9.3	2.24×10^{-13}
23.1.65	78°K	12.3	2.06×10^{-13}
21.1.65*	78°K	12.5	2.62 2.93 2.69 2.30 $\times 10^{-13}$ 2.58 2.36 2.26 2.00

Table (d) Values of α' at 195°K and 78°K

coverage the situation corresponds to full occupation of the low energy sites down to those corresponding to the differential heat of adsorption at the particular coverage, and virtually no occupation of higher energy sites. The equilibrium with the gas phase is maintained mainly by desorption from sites at the boundary of occupation. Absolute rate calculations indicate that to maintain an equilibrium pressure of 10^{-8} torr with a

sticking probability of 10^{-1} the heats of adsorption (and desorption) are around 20, 14 and 5 kilocalories per mole at 300°K, 195°K and 78°K respectively. If the heat of adsorption were linear with coverage over this range then the product α' T from the isotherms should be constant. Inspection of the values in the various tables indicates that there is good agreement at 78°K and 300°K but, surprisingly, not at 195°K. The trend of α' at 195°K indicates a more steeply sloping heat versus coverage curve in the region of 14 kilocalories per mole than that found around 20 and 5 kilocalories per mole. The data of Hickmott (1960) extends apparently linearly between 30 and 14 kilocalories but examination of his isotherm at 78°K indicates that there must be an abrupt change at heats less than 14 kilocalories otherwise the extrapolated value of the heat of adsorption at the saturation coverage at 78°K would give an impossibly low rate of desorption. The isosteric heat data of Trapnell (1951) for the hydrogen tungsten system does show a small inflexion in the region of 15 kilocalories; unfortunately, the results in our work were not extended to this region although there does appear to be a departure from linearity of the heat curve at 18 kilocalories per mole (see figure 32).

In terms of the occupation of energy sites the

Temkin equation and a linearly falling heat of adsorption correspond to an equal distribution of sites in any energy interval within the range covered. The results at 195°K may thus be couched in terms of a low density of states with heats around 15 kilocalories, but adherence to the Temkin equation indicates that the density does not vary significantly within two or three kilocalories of this value. The isotherm does, however, depart from linearity at around 10^{-5} torr and the changing slope indicates an approach to the density of states indicated at 78°K. Likewise, the departure from linearity of the isotherm at 78°K and 10^{-7} torr indicates a decreasing density of states with increasing heat. However, the latter may be due to a failure to approach equilibrium.

The calorimetric heat data obtained by Brennan and Hayes (1964) for hydrogen adsorption on tungsten films at 78°K applies to a non-equilibrium state as complete immobility of the strongly adsorbed layer is indicated. The results of these workers are considered in the next sections which are mainly concerned with the slow redistribution processes which occur at 78°K and also at 195°K.

12.5 The slow redistribution processes at 78°K

As indicated in a previous section only about

8×10^{14} molecules per cm^2 geometric area can be added to the film at 78°K before the pressure fails to return rapidly to the background value on closure of the gas supply. Above this coverage the pressure may take many seconds or minutes to approach the background even though the sticking probability is high and on resumption of gas flow some 10^{13} molecules per cm^2 must be added to reattain the pressure existing prior to the interruption. The pressure time curves observed are displayed in figure 23 (b). The decay at closure may appear when P is high to be different in form but this is merely because the sharp pressure change ΔP_1 is small compared with the total reaction vessel pressure. The behaviour is interpreted as due to molecules becoming immobilised on the outer surface of the film which are thus saturated after about 8×10^{14} molecules per cm^2 have been added. On closure of the supply the pressure falls to a pseudo-equilibrium value which is maintained by desorption from the film. The decay of the pseudo-equilibrium pressure is a direct indication of the redistribution of gas to the inner surface, thus reducing the outer surface concentration. The sticking probability of fundamental significance can, as seen previously, be calculated only from the sharp pressure changes; that calculated from the total pressure has no significance when a pseudo-equilibrium pressure is present except to indicate the

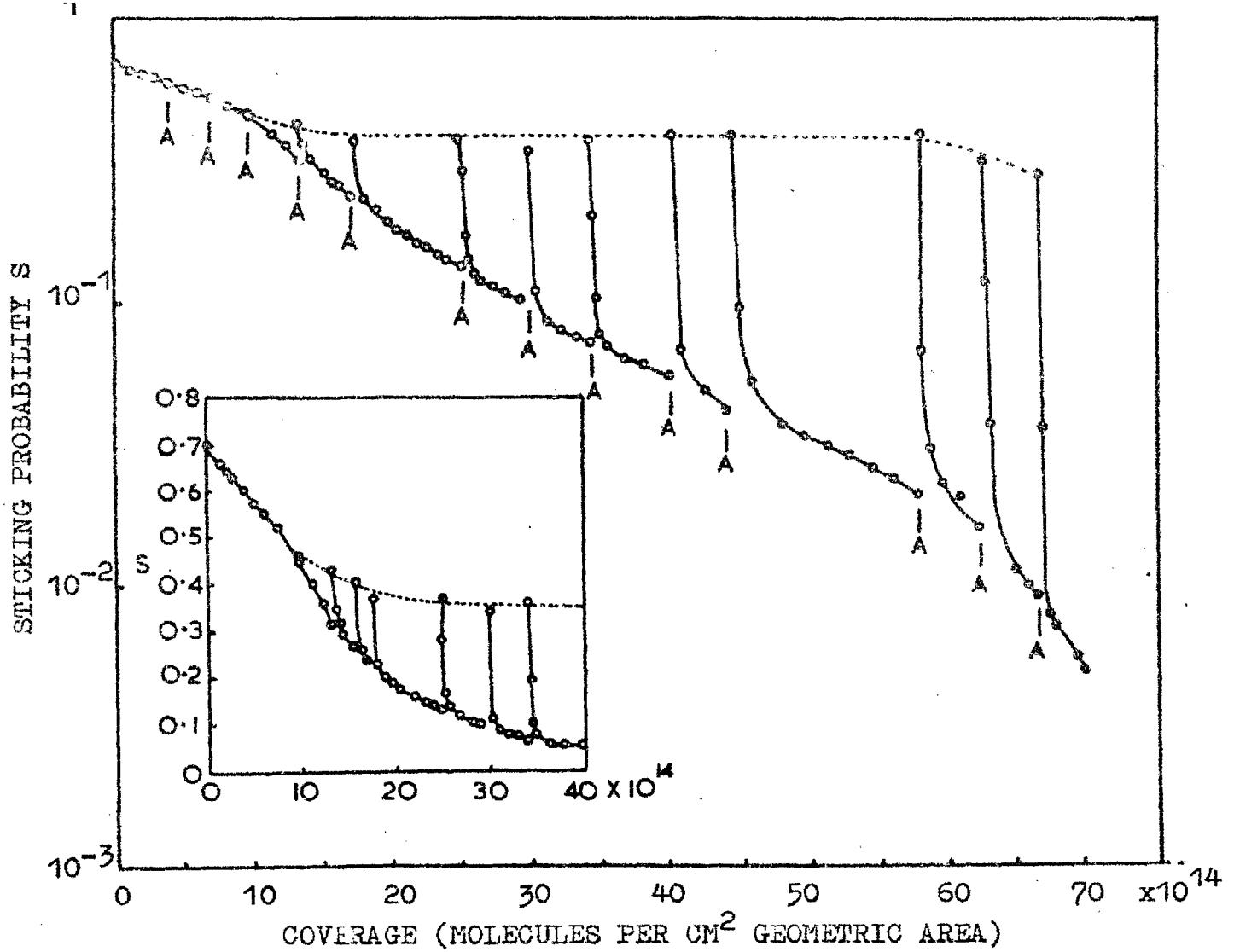

FIGURE 35. The variation of sticking probability with coverage at 78°K. The gas supply was closed for about 20 minutes at the points marked A

overall kinetics. Figure 35 shows a typical sticking probability curve at 78°K, the gas supply was interrupted for about 20 minutes at the points marked A. The upper dotted line refers to sticking probabilities calculated from the sharp pressure changes on reopening the supply - these can, of course, be observed only when the pseudo-equilibrium pressure is comparable with or smaller than the sharp change. The constancy of the sticking probability on reopening the supply is expected since, in many cases, the redistribution proceeded until identical pseudo-equilibrium pressures existed and adsorption thus took place on virtually identical surfaces. Also it has been seen that at room temperature the sticking probability does not alter abruptly with increasing desorption and this appears from the results to be true also at 78°K. From the slope of the Temkin isotherms at 78°K it can be deduced that the outer surface concentration of gas increases only slowly during gas addition and the sticking probabilities lying on the lower curve refer to the overall kinetics of passage of gas to the inner surface of the film, until true saturation is approached.

The kinetics of the redistribution process can be obtained from the rate of decay of the pseudo-equilibrium pressure in an isolated system. For hydrogen

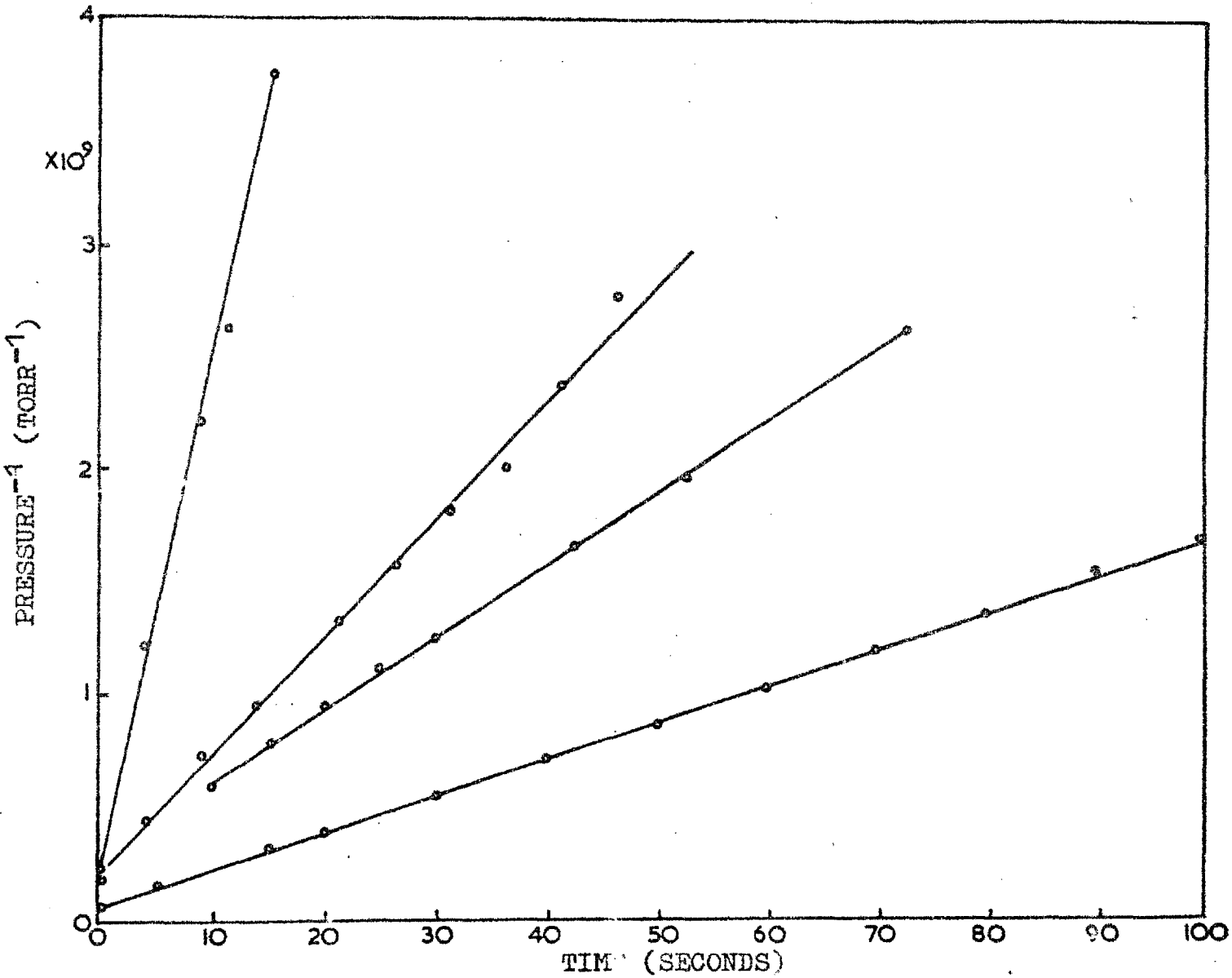

FIGURE 36. Reciprocal pressure versus time after closure of the gas supply.

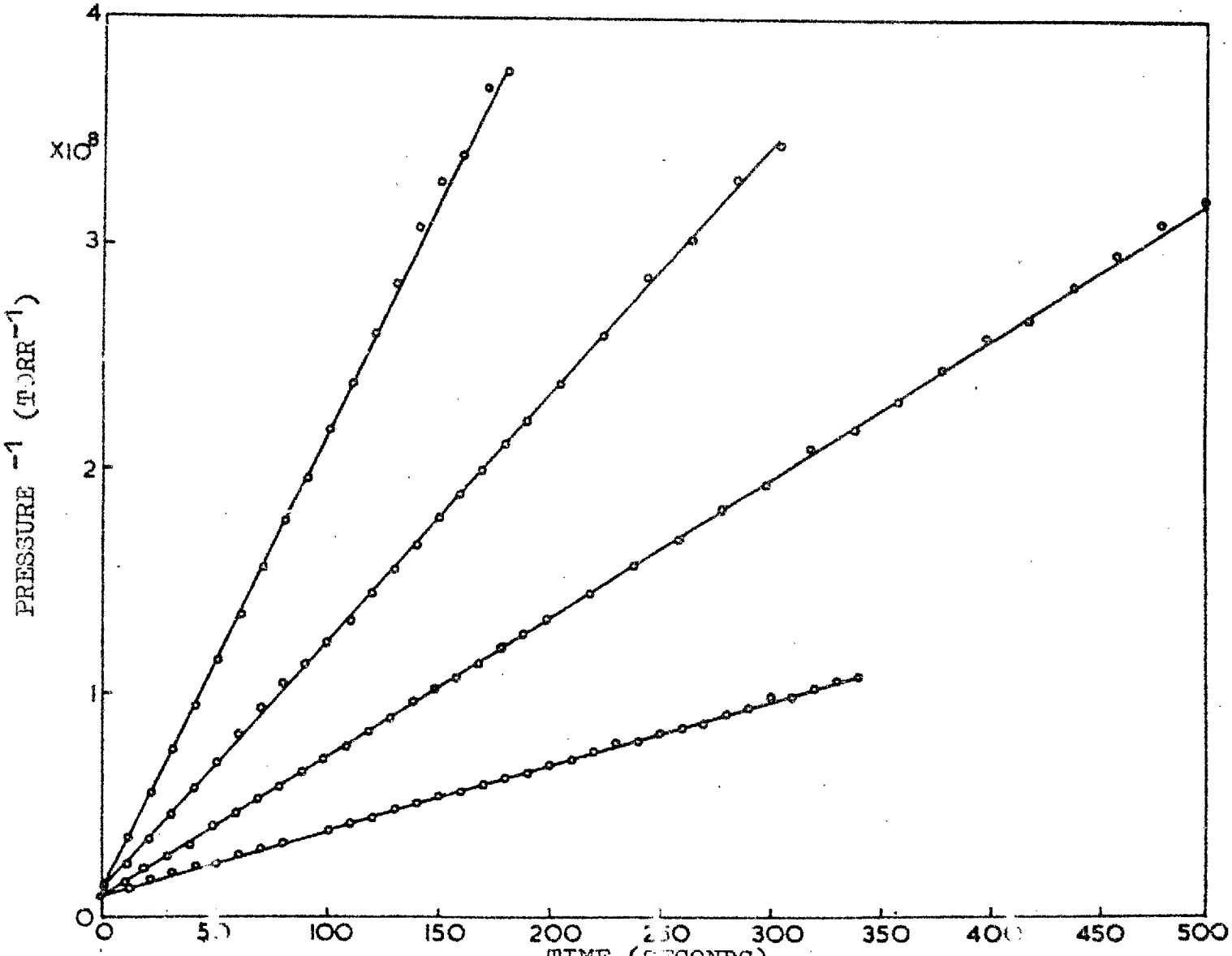

FIGURE 37. Reciprocal pressure versus time after closure of the gas supply.

on molybdenum films at 78°K the reciprocal of pressure varied linearly with time both near the onset of the slow process, when the pressure decay is fairly rapid, and also when the film is nearing saturation and the process may take upwards of twenty minutes to approach the background. The results, for the same run as displayed in figure 35, are given in figures 36 and 37. Such a relationship can be obtained from a variety of models of the redistribution process which all assume that the Temkin equation applies to the layer at saturation. A simple case, probably applicable near the onset of redistribution, assumes that only the most exposed parts of the outer surface are at saturation and that on closing off the gas supply there is a net transport to regions of the outer surface not at saturation. A second, and similarly derived case, assumes that the net transport is via a Knudsen type diffusion and that the whole of the layer at saturation is in pseudo-equilibrium with the pressure in the void of the reaction vessel. (The latter restriction is removed in a subsequent, more sophisticated derivation).

Thus using symbols previously defined:-

$$\alpha N = nP + k \quad \text{- The Temkin Equation}$$

Hence $$-\frac{dN}{dt} = \frac{1}{P}\frac{dP}{dt}$$

For Knudsen diffusion down pores $\frac{dN}{dt} = MP$ (M is the effective pumping conductance of the unsaturated regions in molecules per cm^2 per sec. per torr or since M may be

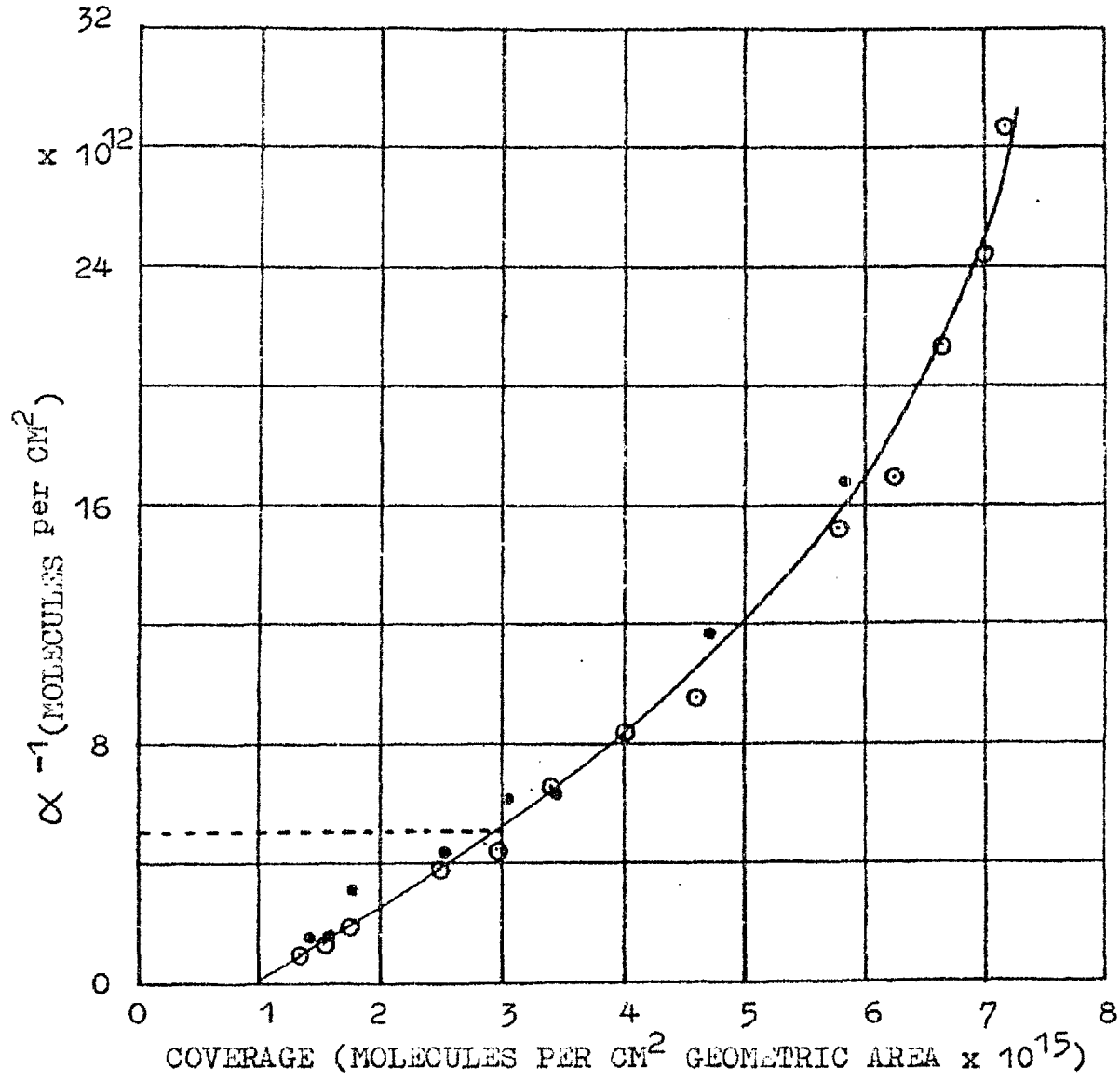

FIGURE 38. α^{-1} versus coverage.

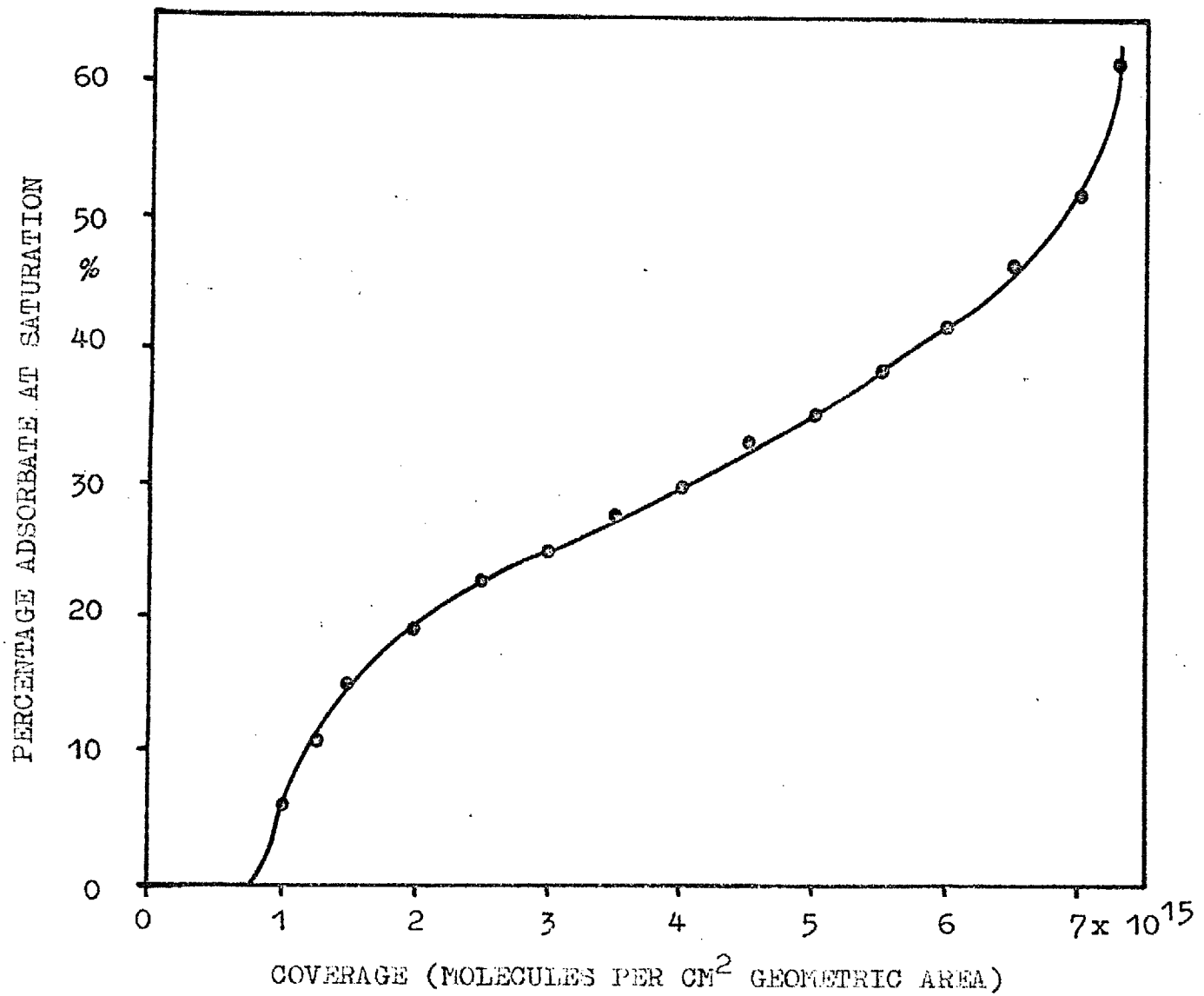

FIGURE 39. The percentage of adsorbate at saturation as a function of surface coverage.

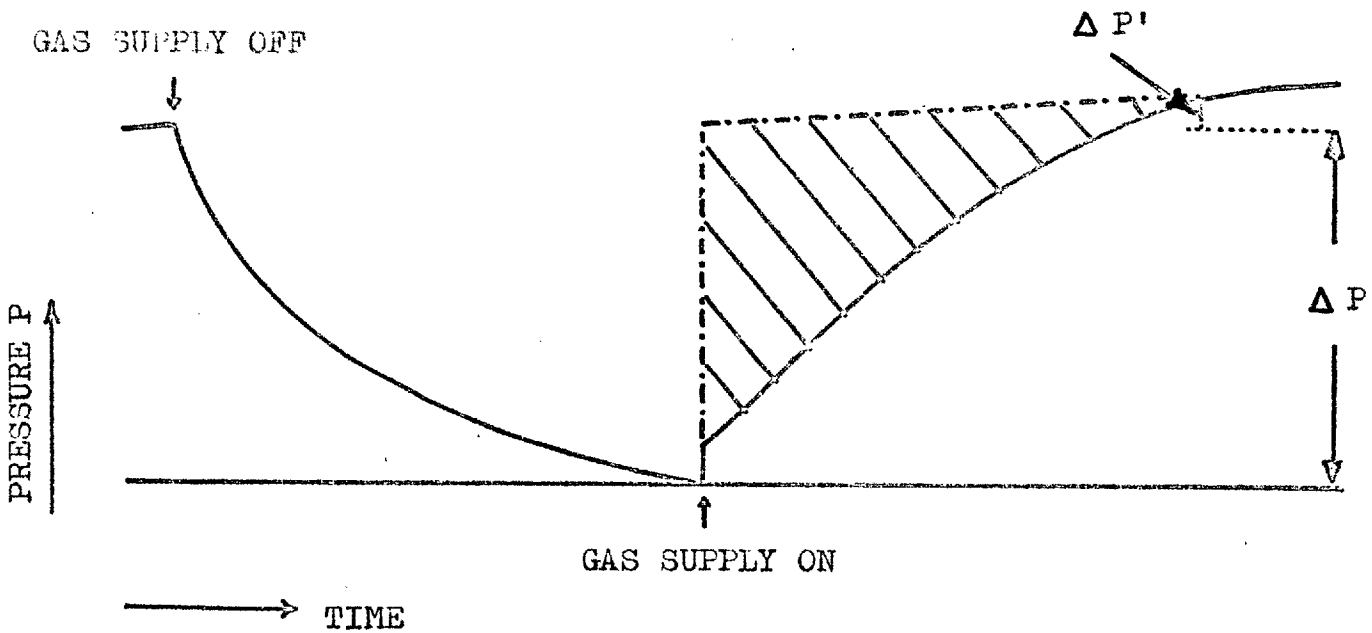

FIGURE 40. The pressure-time profiles created by an interruption in gas supply to the film. ----- pressure-time curve on reopening supply if gas were adsorbed solely on the 'inner' surface of the film. $\Delta P'$ correction for rate of adsorption exceeding that of desorption.

expected to be constant over a small coverage range it may be replaced by SZ where S is the sticking probability measured from the total reaction vessel pressure prior to closure of the supply.

Thus, we have, on substituting for $\left(\frac{dn}{dt}\right)$

$$\alpha SZP = -\frac{1}{P}\left(\frac{dP}{dt}\right)$$

or $$\frac{1}{P} - \frac{1}{P^o} = (\alpha SZ)t$$ where P^o is the pressure at zero time.

i.e. the required relationship.

From the slopes of the reciprocal pressure against time curves and the measurements of S a range of values of α can be obtained. Remembering that α and N refer to molecules per cm^2 geometric area it is seen that α^{-1} is proportional to the area of true surface per cm^2 of geometric area on which the adsorbate is at equilibrium with the gas phase. If it is assumed that the Temkin isotherms obtained near true saturation have equivalent values then the absolute extent of the adsorbate at saturation can be determined. Figure 38 records the values (unfilled circles) of α^{-1} against coverage for run 18.1.65 and figure 39 the percentage of adsorbate at saturation assuming the above treatment to be substantially correct. Values of α^{-1} can also be obtained from the pressure time profile on reopening the supply in the following way (referring to figure 40). If, on restarting the gas supply, adsorption occurred

only on the inner surface of the film then the pressure-time curve would follow the dotted line. The true pressure-time curve lies below the latter but the amount going to the inner surface should still be $\int_0^t$ S.Z.P. dt

where S is the sticking probability calculated when the reaction vessel pressure varies only slowly with time and thus refers only to the overall kinetics of the redistribution. The product of the cross-hatched area and S.Z. thus refers to the number of molecules entering the outer surface per cm^2 geometric area and this number raises the pseudo-equilibrium pressure by ΔP. α is then obtained by applying the Temkin equation; α^{-1} values so obtained are shown (in figure 38) to be in excellent agreement with those obtained from the reciprocal pressure-time curves.

The result of extrapolating the α^{-1}/coverage curve back to the coverage axis is interesting since it indicates that about 10^{15} molecules per cm^2 geometric area must be added to the film before any part of the surface is at saturation - this is in accord with the knowledge that around 7×10^{14} molecules must be added per cm^2 of plane surface to achieve saturation. This figure should be compared with the 3×10^{15} molecules per cm^2 geometric area which must be added before the film as a whole is at

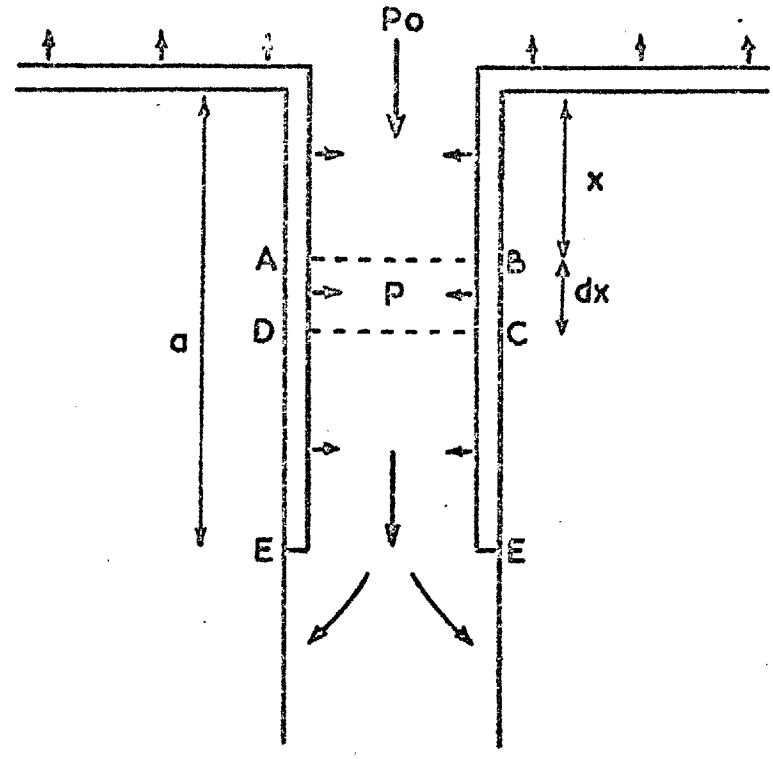

FIGURE 41. Diagrammatic representation of the redistribution down a single pore.

saturation. As complete saturation is approached the pressure rises steeply with further gas addition and the kinetic treatment given earlier must be corrected for this effect. At very high coverages α^{-1} approaches a constant value equivalent to that found for the Temkin isotherm.

The reciprocal pressure function can also be obtained from a more sophisticated model which treats the film as a series of pores of uniform cross section. Again the saturated areas of film are assumed at all times to be in equilibrium with the gas phase above them but pressure gradients are allowed for in the porous structure.

The situation is shown diagrammatically in figure 41. The saturated layer, each element of which is in equilibrium with the gas phase above it, covers the outer surface and extends down the pore to the point E. The equilibrium, as before, obeys the Temkin equation -

$$\alpha' N = f n P + k \qquad (1)$$

noting that α' and N apply to true surface area.

Differentially with respect to time

$$\alpha' \frac{\partial N}{\partial t} = \frac{\partial f nP}{\partial t} \qquad (2)$$

This equation applies providing $\left(\frac{\partial N}{\partial t}\right)$ is small compared

with the rates of adsorption and desorption i.e. the pseudo-equilibrium is maintained.

From Fick's first law of diffusion the net flow across the line AB is given by

$$\left(\frac{\partial N_G}{\partial t}\right)_x = - AD \left(\frac{\partial P}{\partial x}\right)_x \qquad (3)$$

where $\left(\frac{\partial N_G}{\partial t}\right)_x$ is the total number of molecules flowing across AB per second, A is the cross-sectional area of the pore and D is the diffusion coefficient, assumed constant.

Similarly for the flux across the line CD

$$\left(\frac{\partial N_G}{\partial t}\right)_{x+dx} = -AD \left(\frac{\partial P}{\partial x}\right)_{x+dx} \qquad (4)$$

The total rate of desorption from the saturated walls of element ABCD is

$$-\left(\frac{\partial N_A}{\partial t}\right) L.dx.$$ where L is the circumference of the pore. Using equation (2)

$$\text{rate of desorption} = - \frac{L}{\alpha'} \left(\frac{\partial \ell n\ P}{\partial t}\right) \partial x \qquad (5)$$

The equivalent of Fick's second law may be obtained by considering mass balance in the element ABCD. The rate of change of the number of gas phase molecules due to changes in pressure may be neglected since it is very small compared with the rate of flow and the rate of

desorption from the walls. Therefore

$$\left(\frac{\partial N_G}{\partial t}\right)_{x+dx} - \left(\frac{\partial N_G}{\partial t}\right)_x = -\frac{L}{\alpha'}\left(\frac{\partial \ell n\ P}{\partial t}\right) dx \qquad (6)$$

or, substituting equation (3) and (4) and rearranging

$$\left(\frac{\partial^2 P}{\partial x^2}\right) = \frac{L}{\alpha' AD}\left(\frac{\partial \ell n\ P}{\partial t}\right) \qquad (7)$$

A solution of this equation, applicable to the present problem, is

$$P = \frac{L}{2\alpha' AD}\ \frac{(a^2 - bx - x^2)}{(t + c)} \qquad (8)$$

where a, b and c are constants which are determined by the particular boundary conditions imposed on the model.

The pressure that is measured is P_o, the value at $x = 0$

$$P_o = \frac{La^2}{2\alpha' AD}\ \frac{1}{t+c} \qquad (9)$$

i.e. a linear relationship between the reciprocal pressure and time.

Returning to (8), the following relationships are derived for a and b.

(a) At $t = \infty$ $P = 0$

(b) At $x = \ell$ (ℓ is the length of saturated pore)

$P \rightarrow 0$

$t \neq \infty$

therefore $a^2 - b\ell - \ell^2 = 0$

or $$\underline{a^2 = \ell(\ell + b)} \qquad (10)$$

The diffusion coefficient D may be expressed in terms of r by considering the flow down a pore under steady state conditions. The saturated column of adsorbed gas may be considered inert under these conditions provided the boundary ℓ moves only slowly with time. The required equation for flow down a tube of length ℓ and radius r is, providing $\ell >> r$,

rate of flow in molecules per second =

$$\frac{8}{3}\pi r^2 \cdot \frac{r}{\ell} Z(P_o - P_1) \qquad (11)$$

where P_o and P_1 are the pressures at the ends of the tube.

In our problem P_1 is assumed zero thus

$$-\pi r^2 D \left(\frac{\partial P}{\partial x}\right) = \frac{8}{3}\pi \frac{r^3}{\ell} Z P_o \qquad (12)$$

and since there is a constant pressure gradient in the tube

$$-\left(\frac{\partial P}{\partial x}\right) = \frac{P_o}{\ell} \qquad (13)$$

and

$$D = \frac{8}{3} r Z \qquad (14)$$

remembering that end corrections have been ignored. This allows (2) to be written as

$$P = \frac{3}{8\alpha' r^2 Z}\left(a^2 - \frac{bx - x^2}{(t + c)}\right) \qquad (15)$$

and the slope of reciprocal pressure (at x = 0) against time becomes

$$\frac{8\alpha' r^2 Z}{3a^2} \qquad (16)$$

If each individual pore is considered to have an area E of external surface associated with it then b may be related to E as follows. During a redistribution the net amount of gas desorbed from E passes down the single pore. If the pressure is uniform over the area E and equal to P_o then

$$(\text{net flux down pore})\ x = 0 = -\frac{dN_E}{dt} = -\frac{E}{\alpha}\frac{d\eta}{dt} P_o \qquad (17)$$

Differentiating (15) with respect to x gives

$$\left(\frac{\partial P}{\partial x}\right)_{x = 0} = -\frac{3b}{8\alpha' r^2 Z} \cdot \frac{1}{(t+c)}$$

and using this equation together with (17) the flux down the pore at x = 0 is

$$-\left(\frac{dN_E}{dt}\right) = \frac{\pi b r}{\alpha' (t+c)} \qquad (18)$$

Thus using (17) and (18)

$$E \frac{d\ln P_o}{dt} = \frac{-\pi br}{(t + c)}$$

and hence

$$P_o^{-\frac{E}{\pi br}} = K(t + c) \quad (K - \text{integration constant}) \tag{19}$$

To satisfy the original equations $E = \pi br$ and the nature of the constant b is demonstrated. The relationship between pressure and time in terms of the physical dimensions of the model is thus

$$P = \frac{3}{8\alpha' r^2 Z} \quad \frac{[b(b + \frac{E}{\pi r}) - \left(\frac{E}{\pi r}\right)x - x^2]}{(t + c)} \tag{20}$$

The model is capable of further development by, for example, treatment as a system of short capillaries or as a system of pores of various dimensions. It will suffice here, however, to have indicated how the experimentally observed kinetics may arise.

The form of the kinetics of the slow processes indicates a gas phase process by which the interior surface is covered. Although the interpretation is contrary to that given here, the calorimetric heat data for hydrogen on tungsten films of Brennan and Hayes (1964) is in agreement with that expected for a gas phase process. These workers found an almost constant heat of adsorption at 90°K over the whole coverage range. The

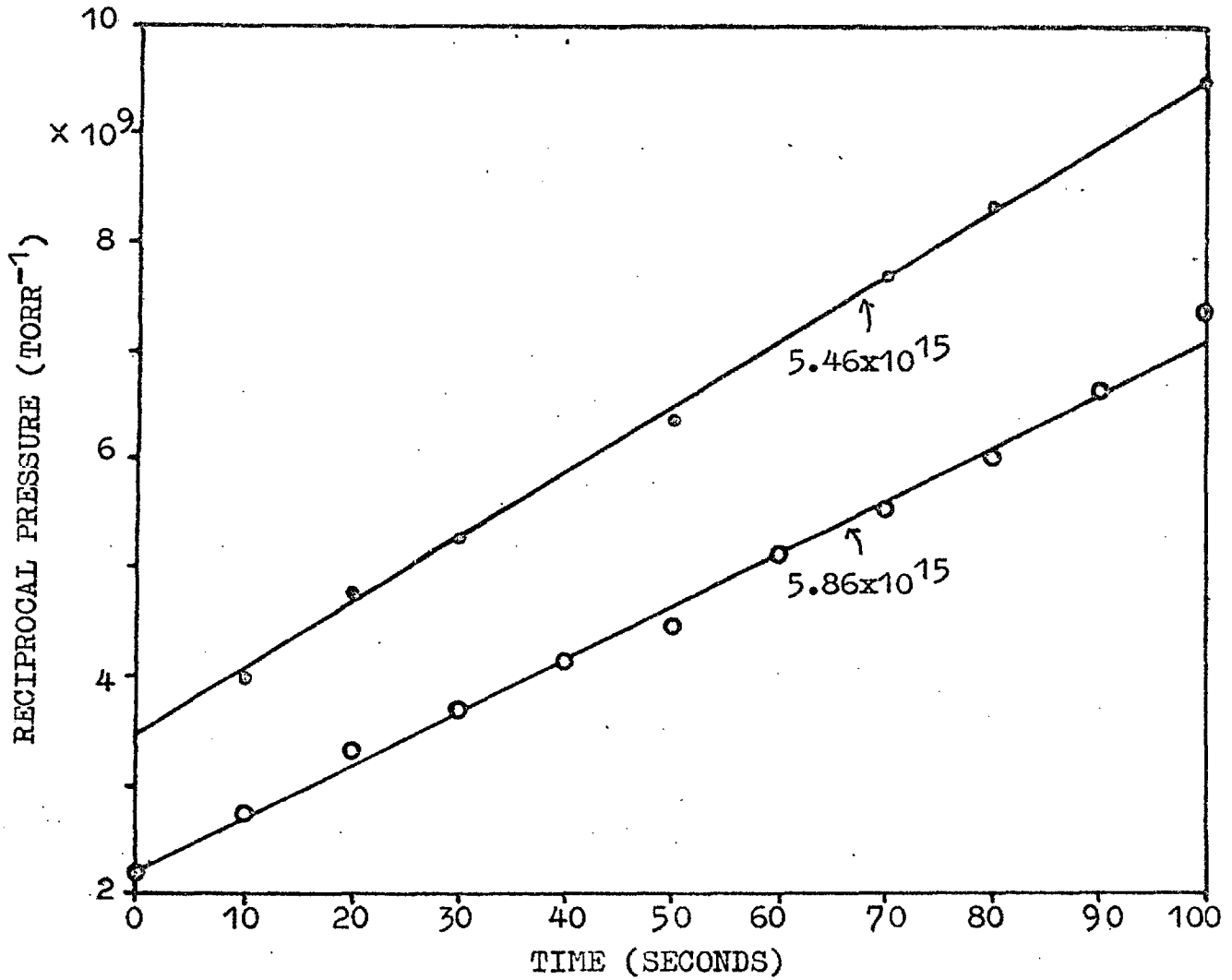

FIGURE 42. Reciproc l pressure ersus time at 195°K.
(Figures on graph re er to coverage in molecules per
CM^2 geo etric area.

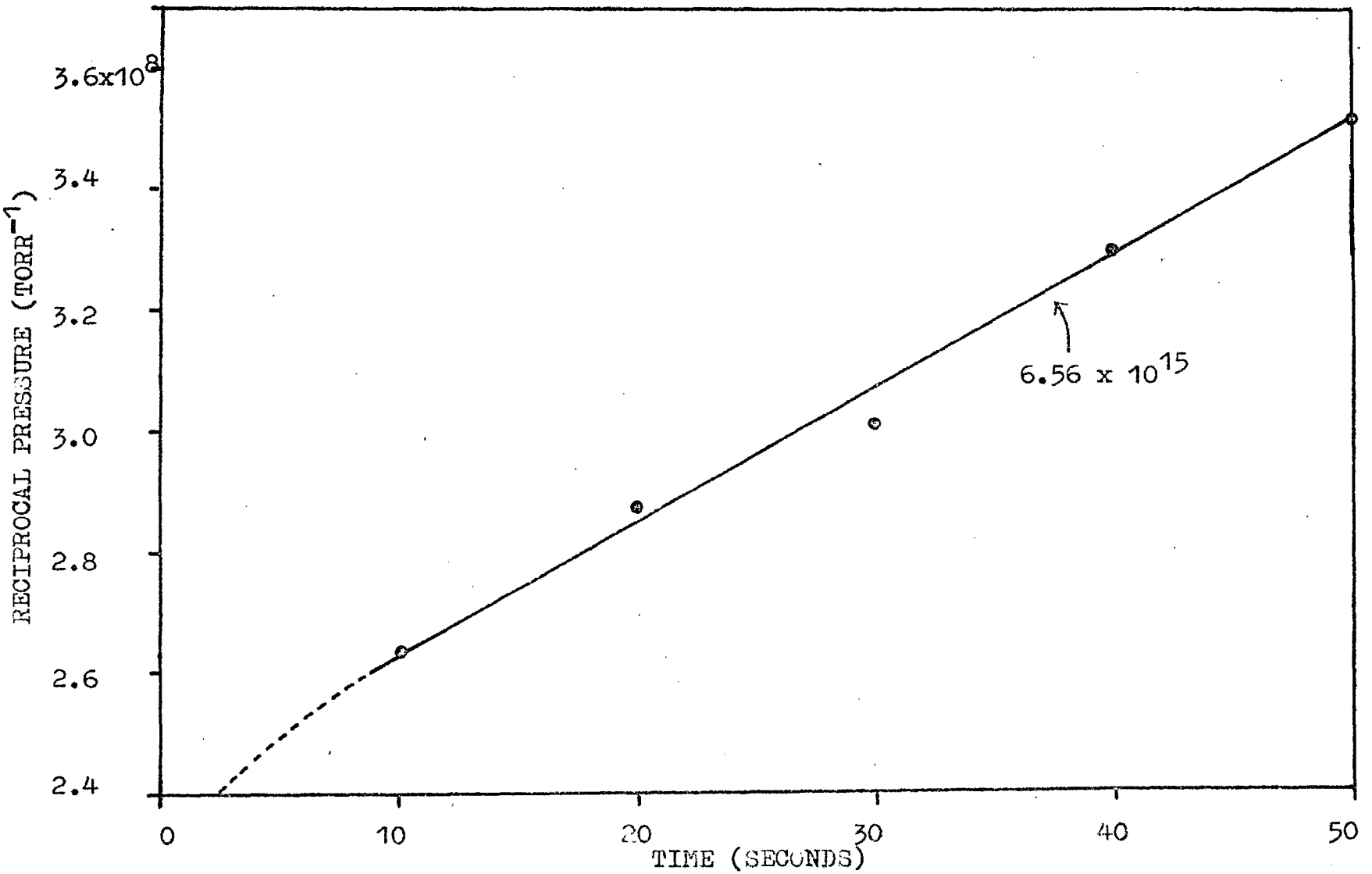

FIGURE 42. Reciprocal pressure versus time at 195°K.

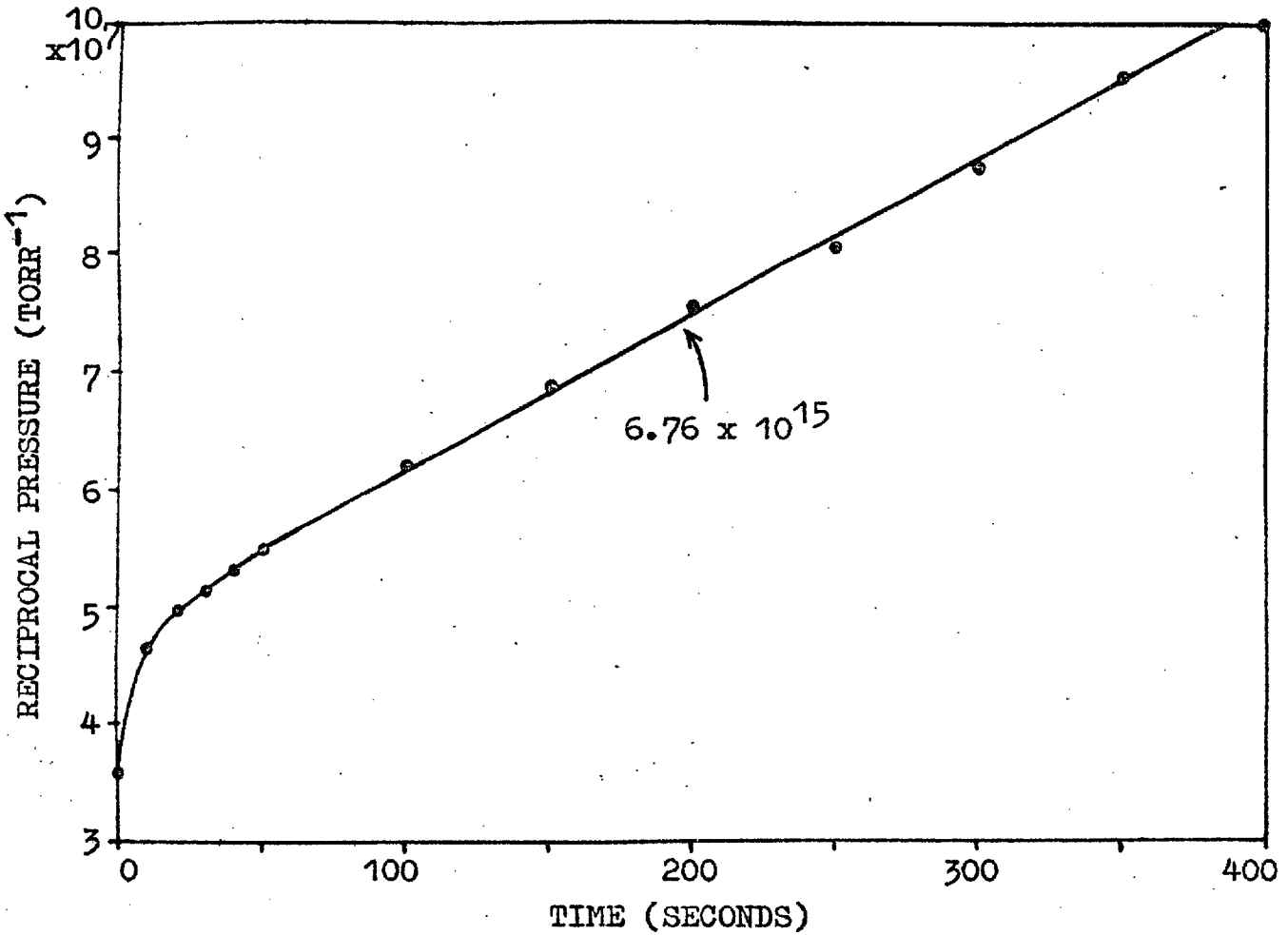

FIGURE 42. Reciprocal pressure versus time at 195°K.

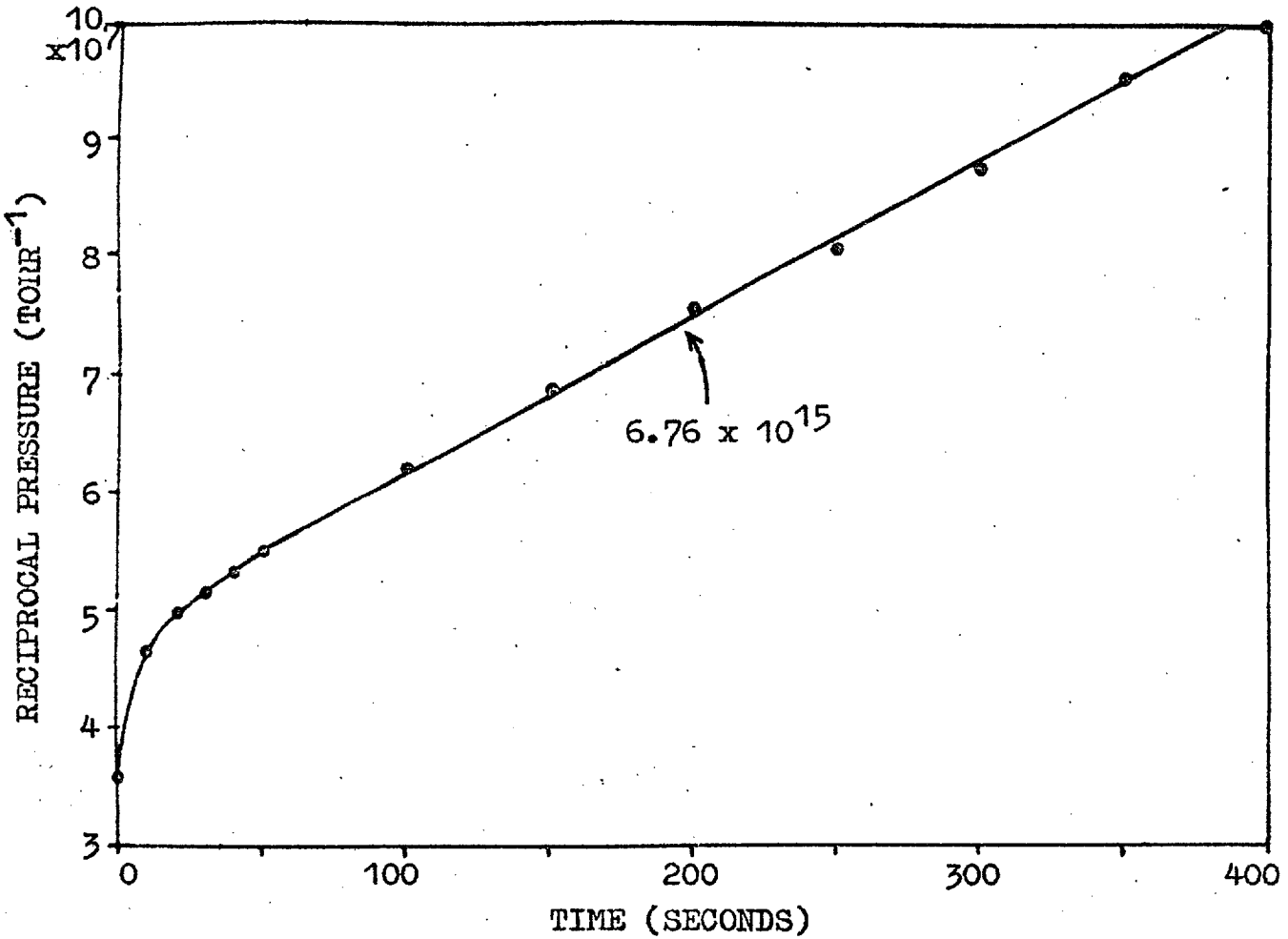

FIGURE 42. Reciprocal pressure versus time at 195°K.

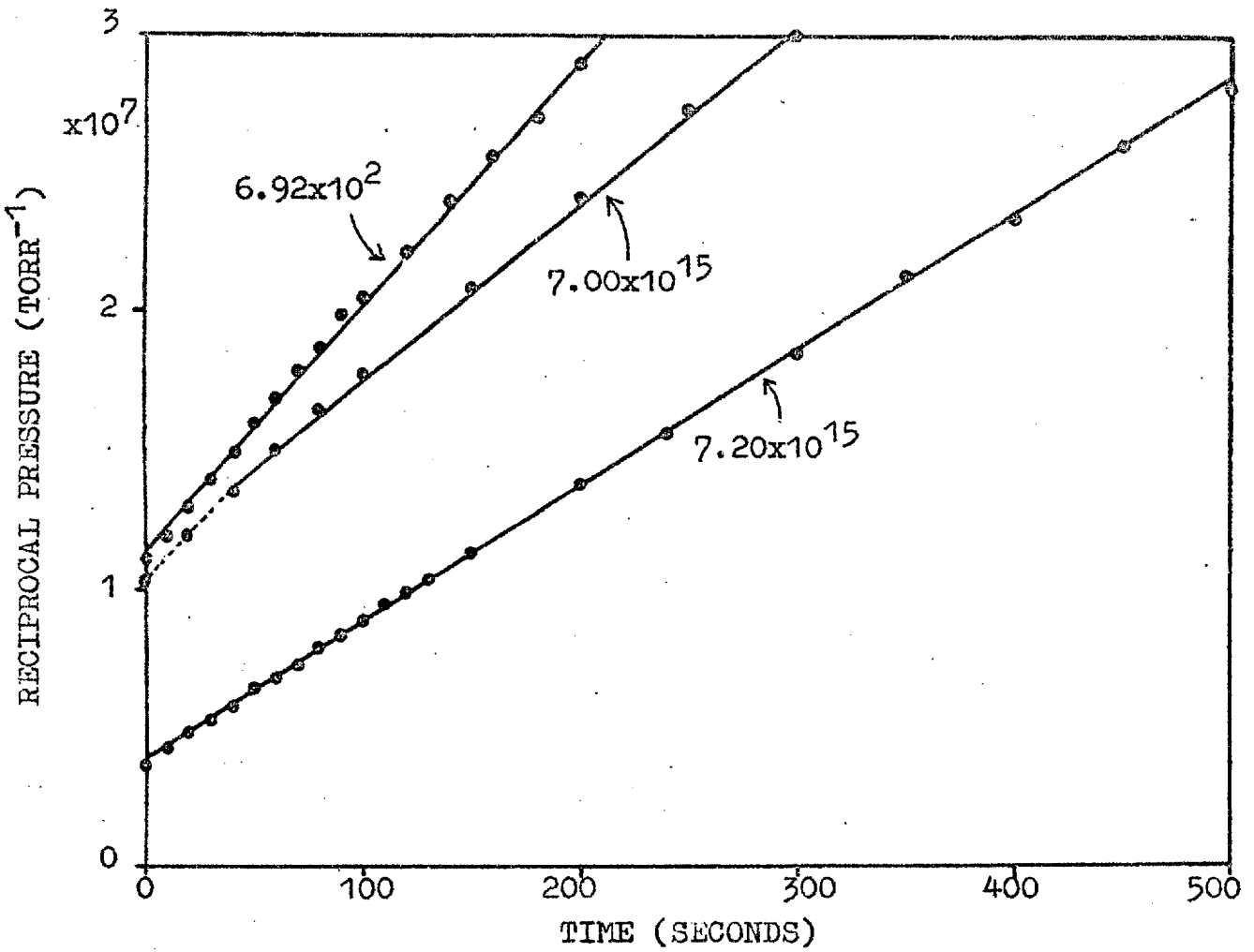

FIGURE 42. Reciprocal pressure versus time at 195°K.

magnitude of this heat is almost equal to the integral value at 300°K, where the layer is highly mobile, suggesting that a fresh increment of clean surface is covered by each addition of gas. In the next section results are presented which demonstrate the existence of of a weakly bound adsorbed state thus confirming the results of Hickmott and others. The state, however, is not sufficiently stable to be capable of transporting gas to the inner surface of the film by a surface migration process since desorption is observed after only 7×10^{14} molecules per cm^2 geometric area of gas is adsorbed at 78°K.

12.6 The slow redistribution at 195°K

Molybdenum films at 195°K behave in a similar way to those at 300°K up to about three quarters of the total uptake i.e. the adsorbed layer is highly mobile and gas freely redistributes to the inner surface. However, above this coverage the adsorbed layer apparently loses this mobility and slow redistributions of gas are observed in the same manner as described at 78°K. The form of the kinetics is found to be identical to that at 78°K viz. the reciprocal pressure falls linearly with time after closure of the gas supply, and the process is thus probably one of gas phase diffusion. Figure 42 displays such curves for a single run - the slopes varying by a

factor of 10^3, as seen in the following table. This run is also used in figure 26. (run reference 1.7.65)

Slope of P^{-1}/time $torr^{-1}$ sec^{-1}	Coverage in molecules/cm^2 geom.
6.1×10^7	54.6×10^{14}
4.8×10^7	58.6
8.2×10^6	62.1
2.1×10^6	65.8
9.3×10^5	66.6
1.3×10^5	67.6
7.1×10^4	69.2
6.15×10^4	70.0
5.00×10^4	72.0

Table (e) The slopes of the reciprocal pressure against time curves.

The coverage range over which the redistribution occurs is, of course, much more restricted than at 78°K but the behaviour generally appears similar with the exception that the curves do seem to deviate from linearity near zero time. This deviation is, for plots at the lower pressures, more apparent than real since it is probably associated with the response time of the

pressure display system to the sharp pressure drop preceding the slow redistribution. The sticking probability calculated from the sharp pressure changes on opening and closing the gas supply follow a similar pattern to those observed at 78°K having a constant region and an indication of a fall as true saturation is approached. Figure 26 displays such values of sticking probability against coverage, again for run (7.1.65). It may be noted that the magnitude of the sticking probability in the constant region is lower than that found at 78°K. This is in general agreement with other results which, as will be seen, show that at non-zero coverages the sticking probability for a given surface condition always increases towards 78°K.

12.7 Desorption spectra of hydrogen on molybdenum films

In order to attempt to substantiate the proposed mechanism for the slow redistribution processes a series of experiments were conducted to obtain the pressure temperature relationship during warming of a partially saturated film. These 'desorption spectra' were normally obtained by admitting a known quantity of hydrogen to a film maintained at 78°K and then warming the film slowly towards some desired temperature and monitoring both the temperature (by thermocouples attached to the reaction vessel walls) and the pressure in the reaction vessel.

The process was normally repeated with further doses of gas until the film was saturated.

As with flash desorption experiments using filament adsorbents the system may be isolated or pumped during the desorption. The latter is normally preferred as the resolution is enhanced and furthermore with filaments readsorption can be minimised by a sufficiently fast pumping system. With high area evaporated metal films an enormous pumping speed would be required to reduce readsorption significantly and this together with an experimentally restricted maximum rate of temperature rise precludes any investigation of a non-equilibrium system. The situation with films thus corresponds during a desorption spectrum to near equilibrium between the gas phase and the regions of the film most accessible to the gas phase; if the temperature is sufficiently high and the adsorbed layer highly mobile then the equilibrium may extend to the whole surface. As will be seen subsequently, the high net rate of pumping required to resolve a spectrum was, in the case of unsaturated films, supplied by the film itself in which case it was immaterial whether the reaction vessel was open to the pumps or not. Near saturation very large pressure changes occurred and the system had to be pumped to give adequate resolution and even then the pressure could not

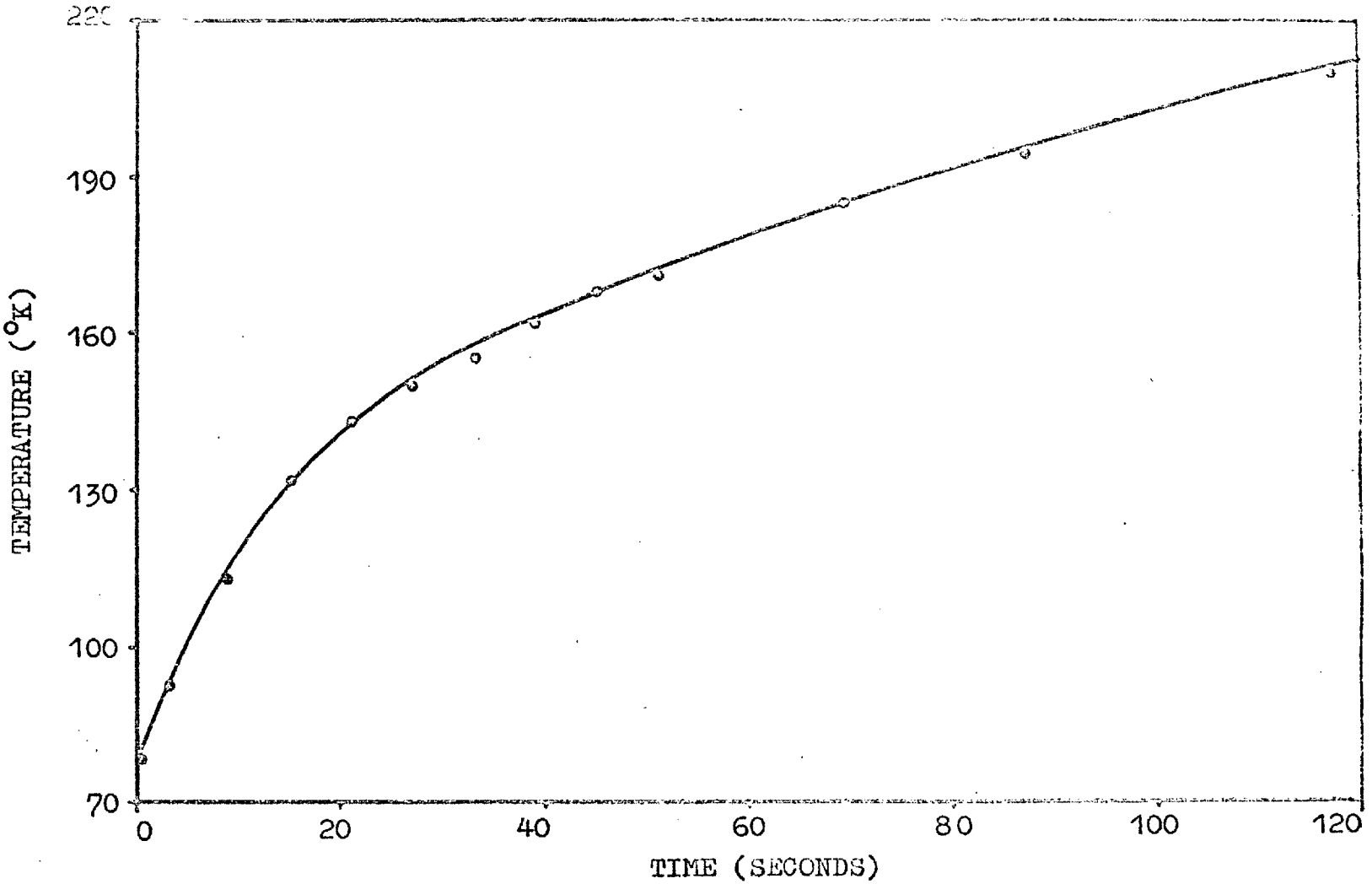

FIGURE 43. Temperature-time profile after removal of liquid nitrogen bath from around the unlagged reaction vessel.

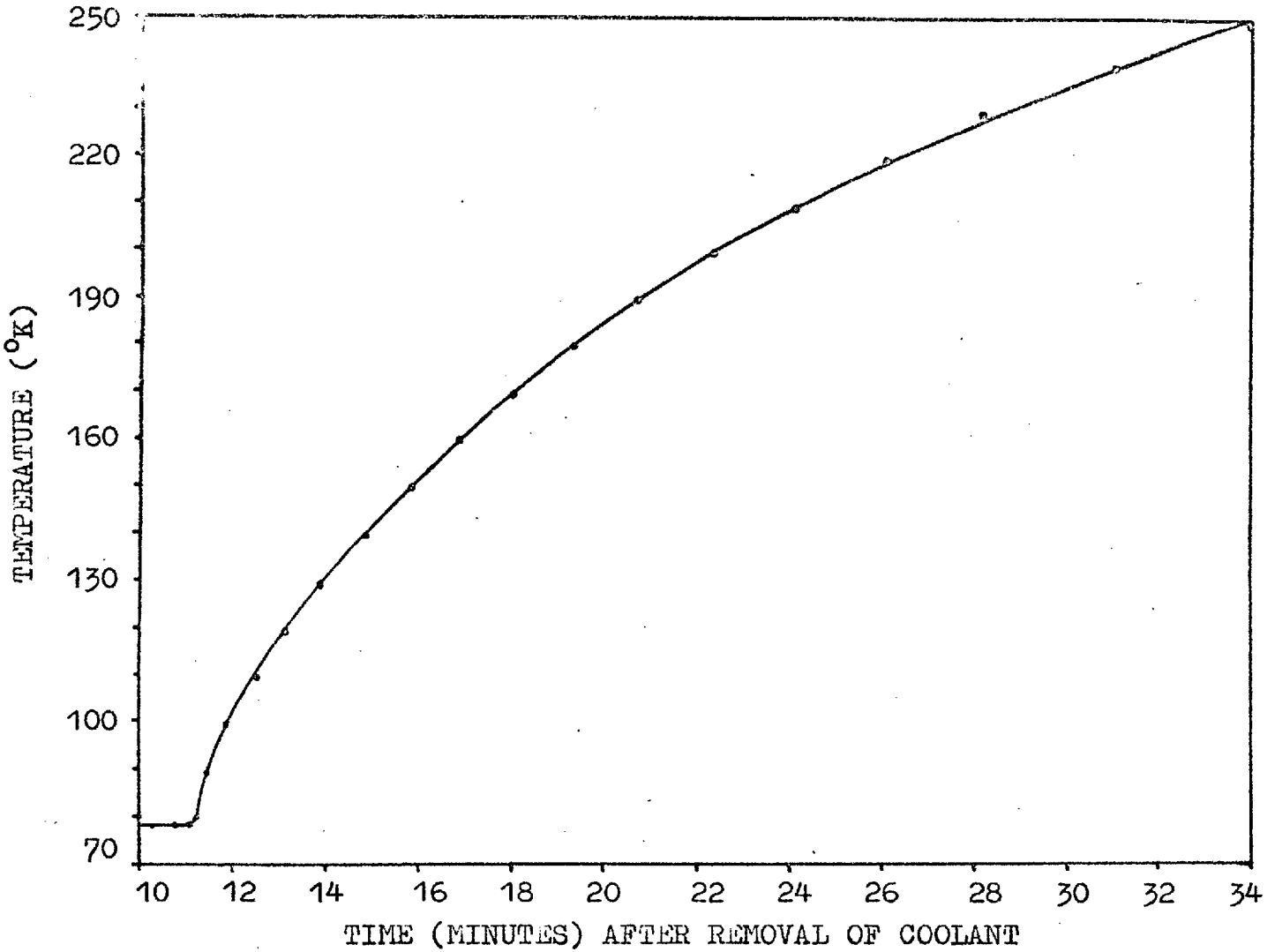

FIGURE 44. Temperature-time profile after removal of liquid nitrogen bath from around unlagged reaction vessel.

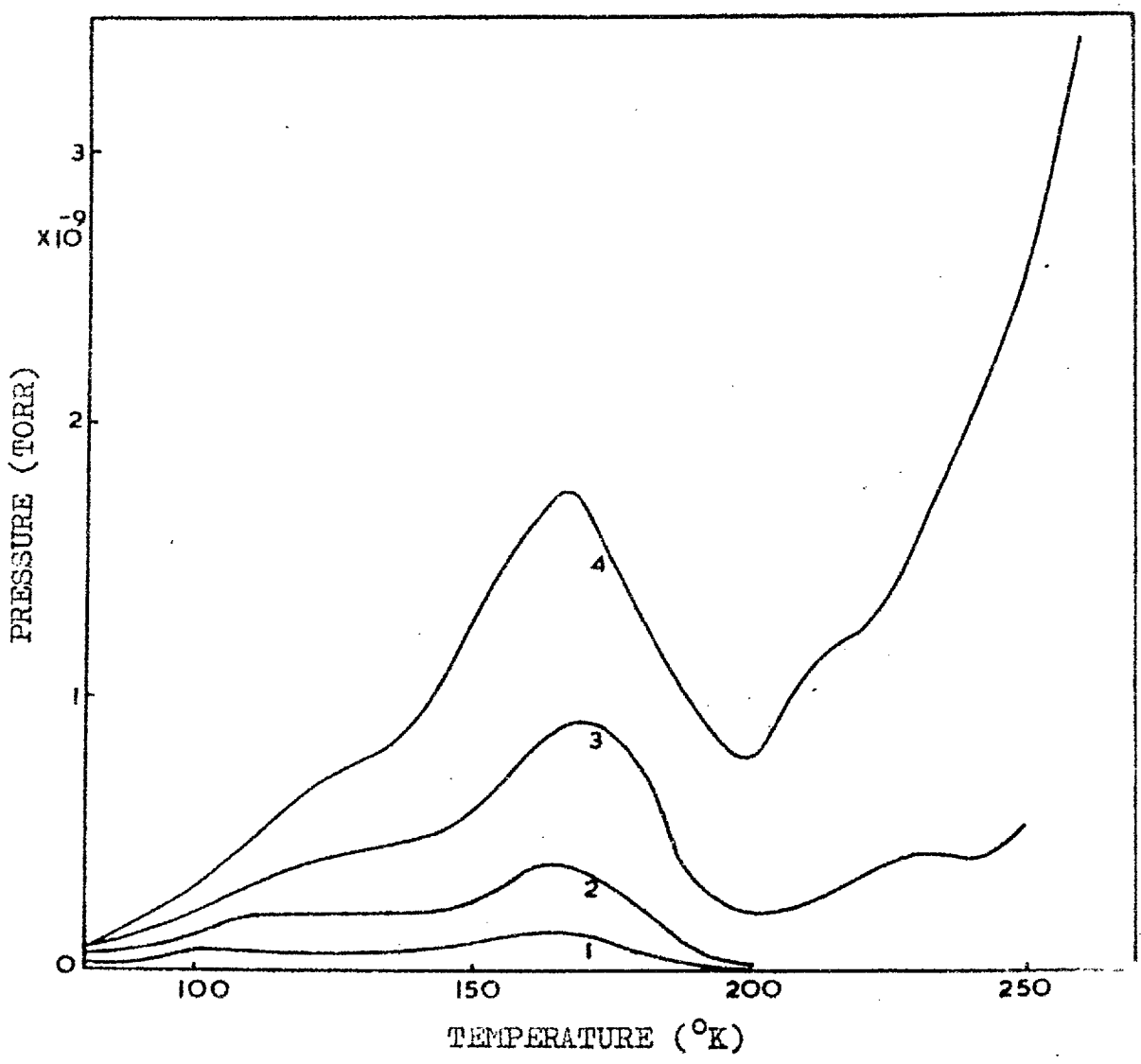

FIGURE 45. Desorption spectra between 78 and 300°K for a single molybdenum film. Numbers refer to desorptions at successively higher coverages.

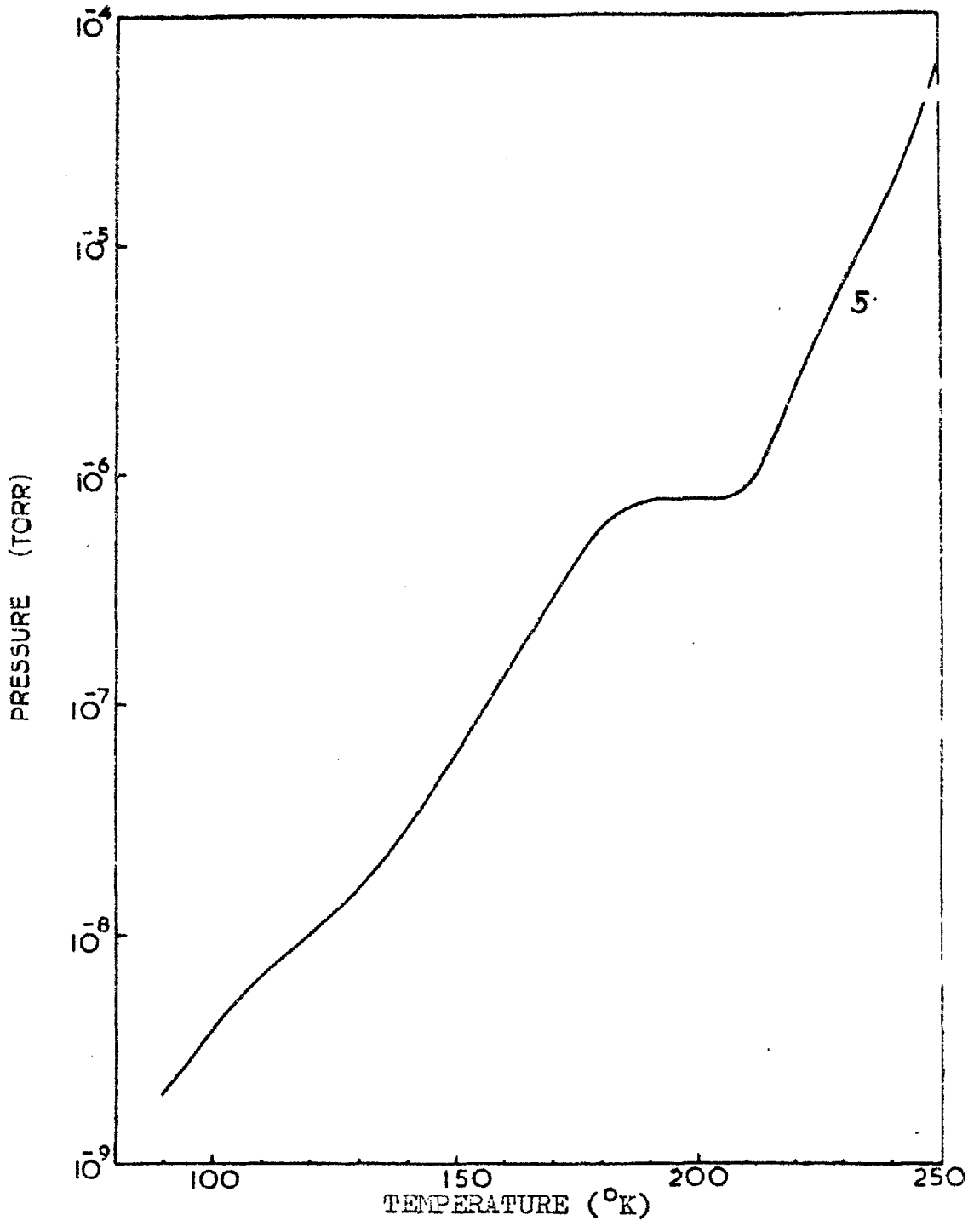

FIGURE 46. Desorption spectrum with film isolated from the pumps. Desorption from the same film as Figure 45.

be maintained much below 10^{-6} torr during the desorption.

Two rates of warm up were used - one corresponding to the natural rate of warm up of the unlagged reaction vessel after removal of the liquid nitrogen bath and a slower warm up with the reaction vessel lagged with asbestos string. Even with the latter method it was very difficult to maintain a uniform temperature over the whole of the reaction vessel wall but by manipulation of the lagging the variation could be reduced to about 15°K. The lagging gave one great advantage - the temperature of the reaction vessel did not start to increase for about fifteen minutes after removal of the nitrogen bath and this allowed ample time for the electronics to 'settle down'. Figures 43 and 44 display temperature time profiles at the two rates of warm up. Figures 45 and 46 show several desorption spectra at increasingly higher total uptakes of gas. Table (f) is constructed from desorption data obtained in the following way. A quantity of gas, Δn, was added to a film held at 78°K and then the film was warmed to 300°K whence equilibration over the whole film surface occurred (see figures 37 and 38 for spectra). The total uptake at this point, n_T, is related to the outer surface concentration via the roughness factor R and the outer surface concentration, n, after recooling the film

to 78°K and adding a further quantity Δn is thus

$\frac{n_T}{R} + \Delta n.$

n_T total H_2 adsorbed (molecules per cm^2)	Δn H_2 increment at 78°K (molecules per cm^2)	n H_2 concn. in outer layer (molecules per cm^2)	Number of desorption spectrum (see Figures 37 and 38)
4.57×10^{14}	4.57×10^{14}	4.57×10^{14}	No desorption
9.21	4.64	5.21	"
13.44	4.23	5.38	"
18.62	5.18	6.86	1
23.45	4.83	7.16	2
27.83	4.38	7.32	3
32.07	4.24	7.72	4
45.57	13.50	-	5

Table (f) The onset of desorption

Below n = 6.8×10^{14} molecules per cm^2 of geometric area no desorption is observed on raising the temperature of the film. This has been substantiated in experiments using about 10 films - no desorption is detected before approximately 6.5×10^{14} molecules per cm^2 have been

added to a clean film. It will be remembered that the onset of the slow redistributions, the kinetics of which have been previously discussed, occurred at about 7.5 x 10^{14} molecules per cm^2 geometric area; the discrepancy in the coverages at which the two phenomena are first observed arises because of differences in the amounts of weakly held hydrogen which can be detected by the two methods.

In desorptions 1 to 4 the film was pumped for most of the time but periodic isolation from the pumps had no detectable effect - due, as previously indicated, to the high pumping rate of the film swamping that of the exhaust port. In desorption 5 the film was approaching saturation and, in this particular case, the system was isolated.

Pressure peaks or shoulders can be observed in figures 45 and 46 at 130, 170 and 220°K. The drop in pressure between 170°K and 200°K observed in figure 45 is attributed to the onset of mobility in this region. This results in weakly held hydrogen, present at 78°K in the outer concentrated layer of the film, migrating by surface diffusion to strongly adsorbing sites on the inner surface of the film thus reducing the gas phase pressure above the adsorbed layer. This hydrogen would in the absence of such migration, have desorbed at

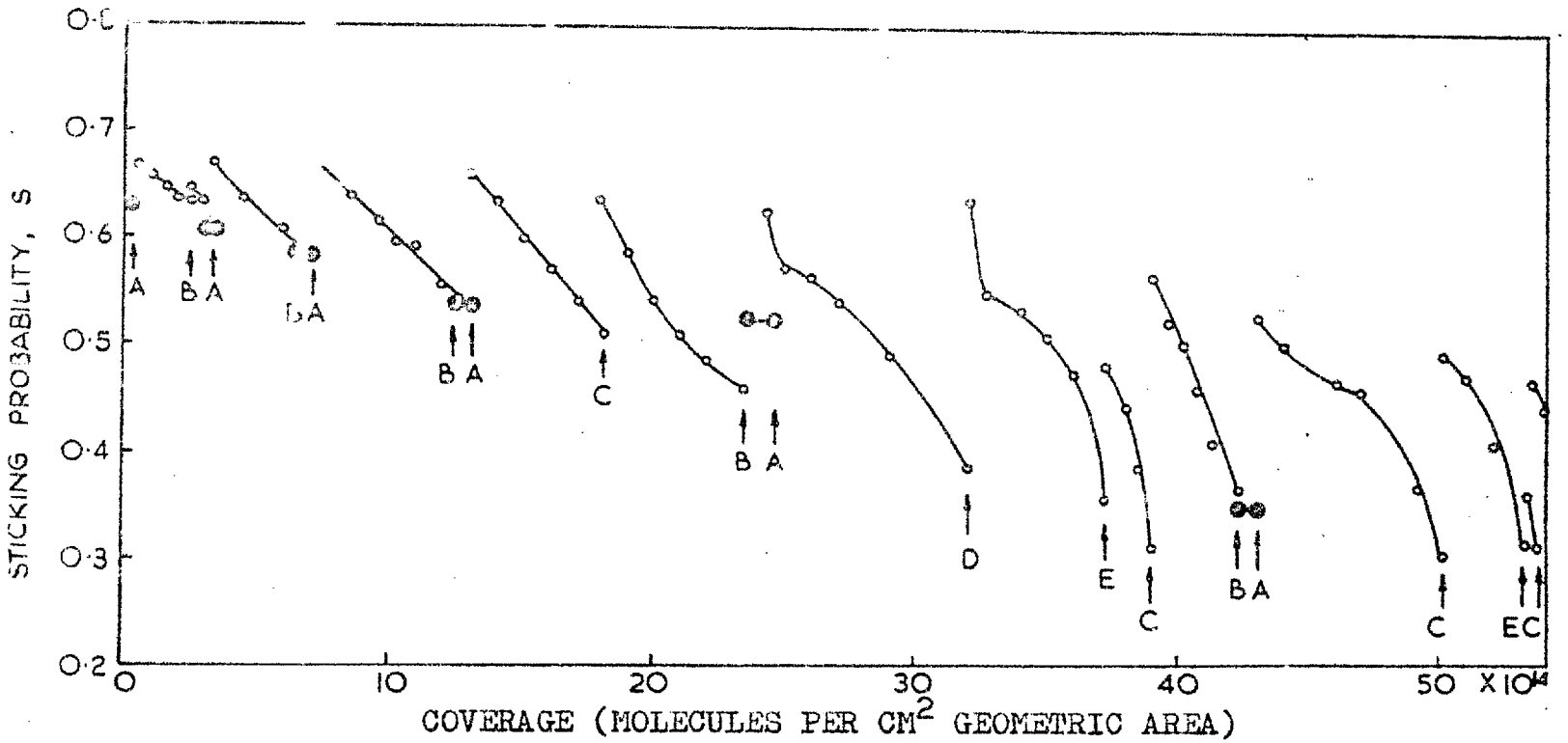

FIGURE 47. The effect of redistribution on sticking probability. Open circles, sticking probabilities measured at 78°K; filled circles, sticking probabilities measured at 300°K; A, cooled to 78°K; B, warmed to 300°K; C, warmed to 190°K and recooled; D, warmed to 200°K and recooled; E, warmed to 170°K and recooled.

temperatures greater than 170°K. Thus, on this basis, the pressure maximum observed at 170°K does not indicate the existence of a separate adsorbed phase because the pressure time profile does not reflect the variation of population density with bond energy at this point.

The onset of mobility around 170°K was demonstrated in the following experiment (reference 5.3.65). Desorption data were obtained as before except that the cooling bath was replaced around the reaction vessel at various stages during the desorption procedure. After each temperature cycle the sticking probability was measured at 78°K, and in some cases room temperature measurements were also made. Figure 47 displays the sticking probability curve constructed from the data, the letters A to E refer to the highest temperature reached during the desorption (see key). The sticking probability at 78°K always increases after warming of the film to temperatures greater than 170°K due to a redistribution of hydrogen to the inner surface of the film. The number of molecules which have to be added after a desorption to return the sticking probability to its value just prior to the previous closure of the supply is a measure of the extent of the redistribution process. However, the

redistribution is partly via the gas phase and partly by the surface. The contribution of the former ΔN_G can be calculated approximately from the pressure time profile of the desorption if it is assumed that the sticking probability remains constant. (It is hoped that the use of the term sticking probability in the above does not generate any ambiguity; that referred to is calculated from the total reaction vessel pressure) The contribution of surface diffusion ΔN_S is obtained by subtracting ΔN_G from the total amount N redistributed. N is calculated as the number required to reattain the value of sticking probability existing at 78°K prior to the previous warm up. The figures in table (g) are calculated in this way for the same run as displayed in figure 39. Examination of the values in the table indicates that at 170°K only a small amount of redistribution occurs by surface migration whereas at 200°K this process is nearly complete.

However, an examination of desorption no 3 in figure 45 indicates that equilibration is not entirely complete even at temperatures somewhat in excess of 200°K since although the coverage is below that required for saturation at 300°K desorption is still occurring at 230°K. If equilibration were complete at 200°K only the low energy sites would be covered

N total number of hydrogen molecules adsorbed (molecules per cm^2 geom.)	ΔN_G number of molecules redistributed via the gas phase (molecules per cm^2 geom)	ΔN_S number of molecules redistributed by surface diffusion (molecules per cm^2 geom)	Highest temp. reached during a desorption ^oK
18.18×10^{14}	0.042×10^{14}	2.7×10^{14}	190
23.64	0.12	6.0	300
31.92	0.29	4.2	200
37.23	0.32	0.9	170
39.03	0.97	3.0	190
42.25	0.65	6.0	300
50.04	0.94	2.0	190
53.41	0.47	0.5	170
54.82	2.3	2.0	190

Table (g) The relative contributions of gas phase diffusion and surface migration in redistribution.

above this temperature and desorption would not occur until the film reached the saturation temperature. In desorption no 4 saturation appears to be achieved above about 240°K as the pressure is rising steeply. In

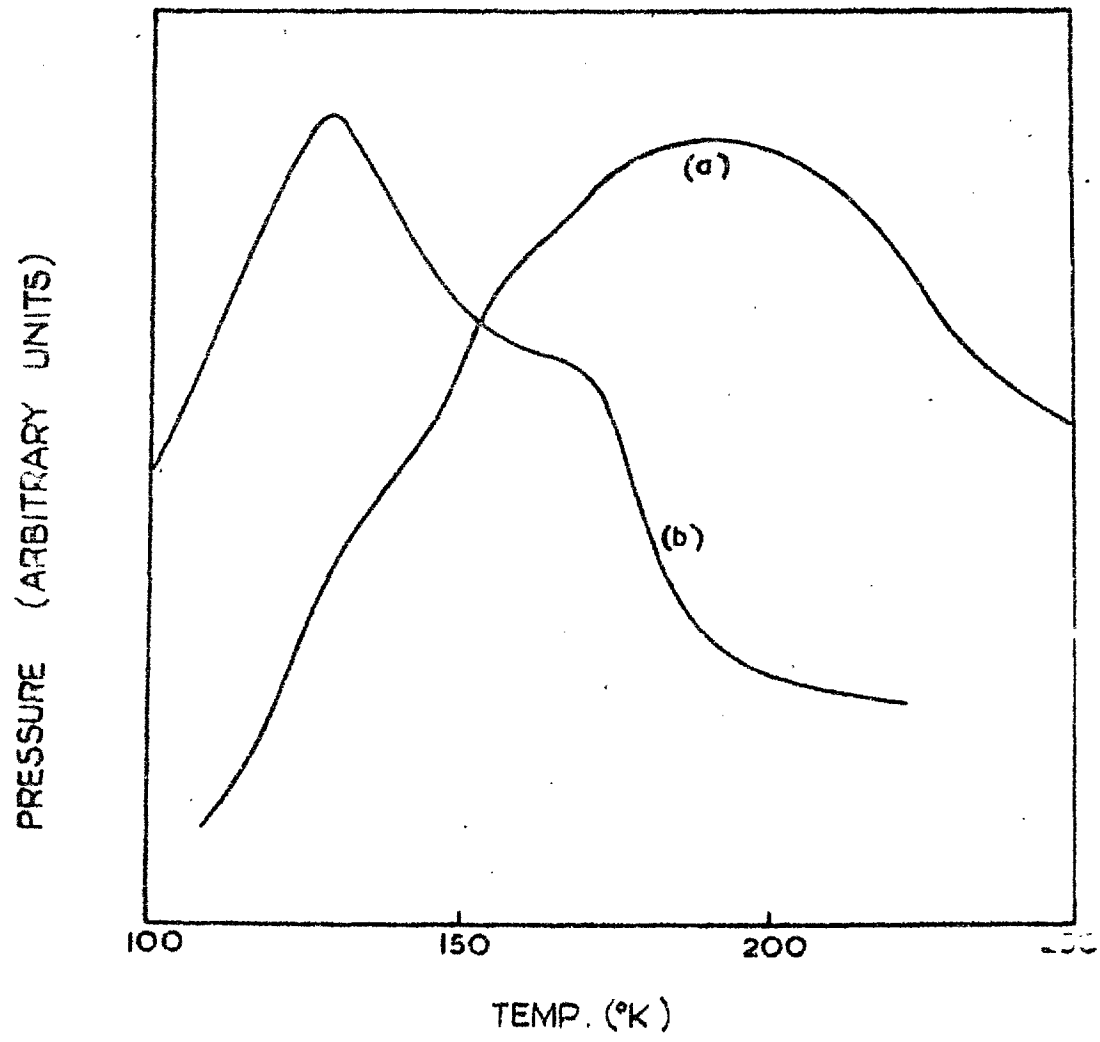

FIGURE 48. Desorption spectra for two films.
(a) cell lagged, adsorbed layer equilibrated;
(b) cell unlagged, adsorbed layer not equilibrated. Both desorptions were carried out with continuous pumping.

desorption no 5, figure 46 the film is near saturation at 78°K and is apparently in pseudo-equilibrium between 140°K and 170°K, above which the adsorbed layer commences to rearrange. As the system is isolated in this desorption the last part of the pressure temperature profile should correspond to an isostere if equilibration is complete. This is not so below about 250°K, but above this temperature isosteres were successfully constructed and gave heats of around 17 k cals per mole between 250°K and 270°K.

The rearrangement of the adsorbed layer around 170°K was further investigated. Figure 48 shows the desorption spectra of two films which had been effectively saturated with gas at 78°K. Part of the difference in the two spectra is due to the fact that in (a) an attempt was made to equilibrate the adsorbed layer by cycling the temperature between 78°K and 220°K whereas in (b) the film was saturated at 300°K and the remainder of the hydrogen added with the film maintained at 78°K. The sharp pressure decrease at 170°K in (b) is again attributed to a rearrangement within the adsorbed layer so that more hydrogen is accommodated on the surface.

However, figure 48 (and to some extent figures 45 and 46) is somewhat misleading because the rate of

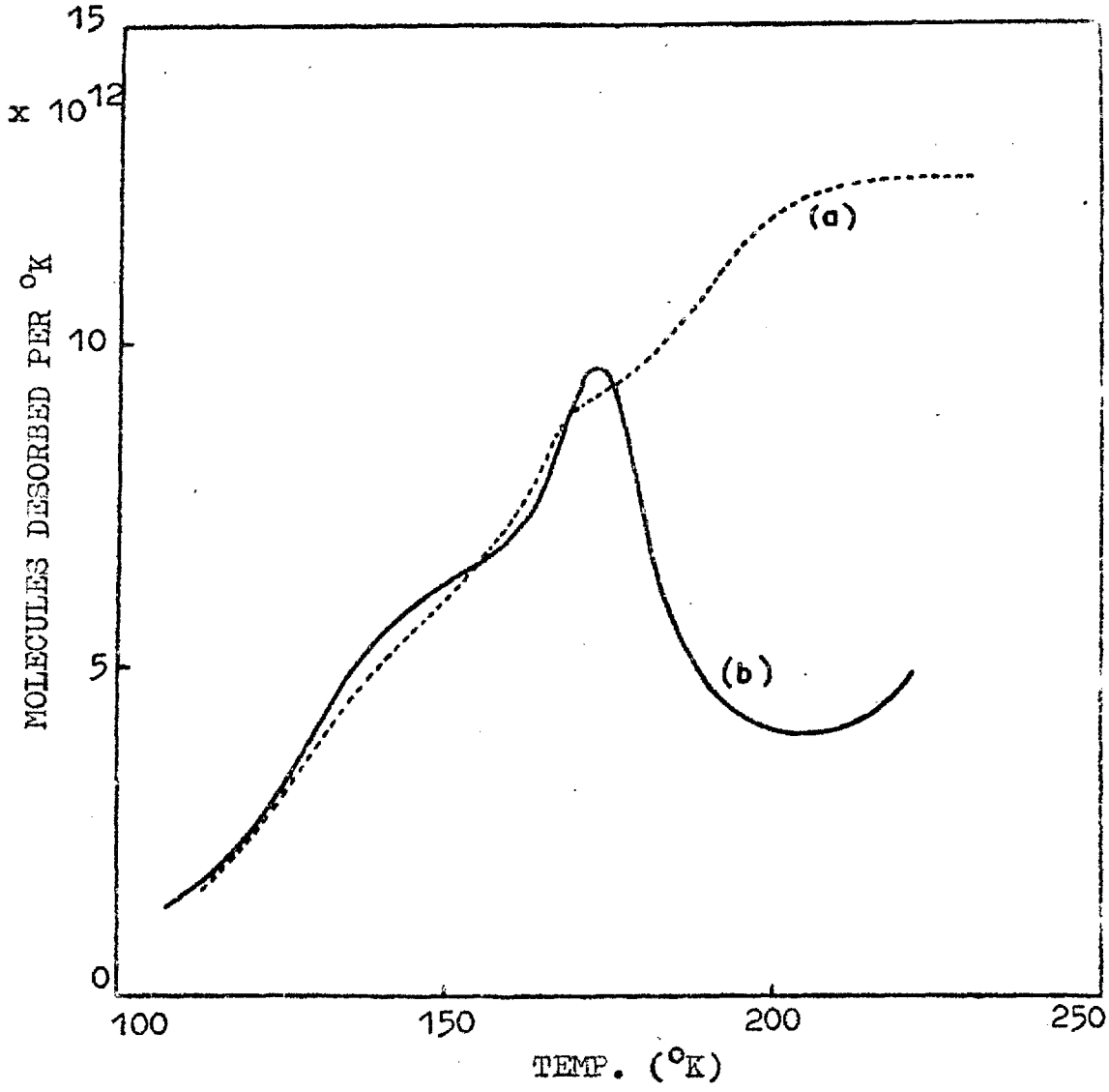

FIGURE 49. Number of molecules desorbed per °K against temperature. (a) and (b) refer to the same desorptions as in Fig. 48.

temperature rise is continuously decreasing and the number of molecules pumped in any particular temperature interval is not proportional to the area under the pressure time curve. If the number of molecules desorbed per cm^2 per ^oK is plotted (instead of the instantaneous pressure) then the shape of the curves is considerably altered - figure 49 is such a treatment of figure 48. This is especially true at the highest temperatures where the rate of temperature rise tends to zero and since the system is being pumped the pressure must also tend to zero irrespective of the population distribution of the various binding energies.

12.8. The number of low temperature states of adsorption

In flash desorption studies it has been common practice to identify each shoulder or maximum in the pressure time profile during desorption with a separate state of adsorption. Each state of adsorption is supposed to reflect a discrete population density within a range of binding energies and for its existence to be substantiated the effects discussed in the previous section must be eliminated. In particular it has been seen that a rearrangement of the adsorbed layer around 170^oK to 190^oK causes a fall in pressure which is not a reflection of a falling population distribution with

binding energy and should not therefore be considered as a separate adsorbed state without additional evidence.

The present investigation of the hydrogen molybdenum system indicates, at most, two weakly bound states of adsorption in the low temperature region: one desorbing below about 150°K and another around 220°K, although the latter is doubtful since it was not observed in all runs. Two studies of the adsorption of hydrogen on molybdenum filaments or ribbons have been made and unfortunately neither provides information on binding states desorbing below 200°K. Pasternak and Wiesendanger (1960) find evidence for two states of adsorption when desorbing from 225°K. However, these workers used tungsten filament gauges and since the system contained no means of identification of chemical species it is possible that carbon monoxide is responsible for one of the observed states (Hickmott 1960; Moore and Unterwald 1964). However, valid comparison can probably be made with the hydrogen tungsten system which has been more extensively studied. Hickmott (1960) found for this system two states of adsorption; one designated α desorbing below 195°K and a second designated β desorbing above this temperature. More recently Ricca, Medana and Saini

(1965) have obtained desorption spectra for hydrogen adsorbed on a tungsten sheet that show six pressure peaks designated γ_1, γ_2, α_1, α_2, β_1, and β_2 in order of increasing temperature of desorption, the γ peaks being identified with Hickmott's α phase. However, the differentiation of the adsorption states into α and β phases may be artificial due to the fact that the desorption was carried out in two stages - 78°K to 300°K and 300°K to 600°K. No such differentiation was found in this region by Hickmott (1960) or Moore and Unterwald (1965) who desorbed in a single flash.

In neither the work of Ricca nor Hickmott was an attempt made to equilibrate the adsorbed layer at 78°K by cycling the temperature during adsorption, although Ricca saturated the surface at 300°K before cooling to 78°K in some experiments. It is relevant, therefore, to compare the desorption spectra obtained by these workers with curve (b) in figures 48 and 49 rather than with curve (a). This suggests that the differentiation of the α and β phase of Hickmott and the γ_2 and α_2 phases of Ricca is due to a rearrangement of the adsorbed layer in the region of 170°K which enables gas to migrate to the more strongly adsorbing sites which are created. However, the

equilibrium data from this work and also in that of Hickmott does indicate a change in the slope of the heat curve below about 15 kilocalories per mole and there is thus probably good evidence for one low temperature state of hydrogen on molybdenum or tungsten, this state may be identified with the α phase of Hickmott and the γ_1 phase of Ricca et al. The field emission results of Rootsaert, van Reijen and Sachtler (1962) indicate the existence of many adsorption complexes in the hydrogen-platimum and hydrogen-tungsten systems. This is not necessarily against the conclusions drawn here but merely indicates that the heats of adsorption of the complexes are not sharply defined but overlap each other and vary with coverage such that they cannot be resolved during a desorption.

The nature of the low temperature state in the hydrogen molybdenum or hydrogen tungsten system is still a matter of conjecture. This state is responsible for the slow redistribution process at 78°K after closure of the gas supply and is first observed after about 6.5×10^{14} molecules per cm^2 geometric area have been adsorbed on the film maintained at 78°K. However, if the film were first saturated with gas at 300°K it was found that the weakly held state could be detected after much smaller additions of gas at 78°K. This

behaviour suggests that the weakly held layer can exist only above a layer of the strongly held β state. There is little doubt that the β phase is an atomic layer and one possibility is that the α phase is molecular and held over single vacancies in the atomic layer. This would be in line with the observations of Hickmott (1960) that the concentration of the phase was proportional to the ambient pressure of hydrogen suggesting molecular adsorption and that the majority of the α phase was formed after the β phase was nearly complete suggesting a layer of α on top of the β phase. It also explains why the low temperature state is reduced if the surface is first equilibrated at 300°K as observed in this work and also in that of Ricca et al. One further point worthy of consideration is the reason for the desorption when surface migration is negligible. The immobility at 78°K occurs over the whole coverage range and can be explained by an activation energy of migration of the adsorbed species. At 195°K there is the interesting situation of immobility setting in at high coverage. Whether or not the immobility is in a second layer of gas over a still mobile strongly held state is not clear from the results, it is hoped with a series of experiments using isotopic mixtures to resolve the situation.

13 HYDROGEN ON NICKEL

13.1 The uptake

As with the other metals, films of nickel were deposited on a substrate held either at 78°K or near room temperature. The uptake for the unsintered films indicates a roughness factor around 10 to 15 i.e. around that of 'sintered' molybdenum films. The sintered films were relatively smooth with roughness factors of 1 to 2.

For films saturated at 300°K (i.e. $P_{EQ} \sim 10^{-5}$torr) there was an additional uptake at 78°K of 30 to 50%. This contrasts with the results of Brennan and Hayes (1964) which indicate equal uptakes at 90°K and 273°K. There is no indication given in the latter paper as to how the result was obtained. If the uptakes were measured with the film at a constant temperature then the 'low' uptake at 90°K is expected since it has been shown that there is always an additional uptake at low temperatures if the adsorbed layer is equilibrated by warming to say 200°K.

13.2 The sticking probability

The initial sticking probability for unsintered films is around 0.6 and that for sintered films around 0.38. Again, there is no discernible temperature

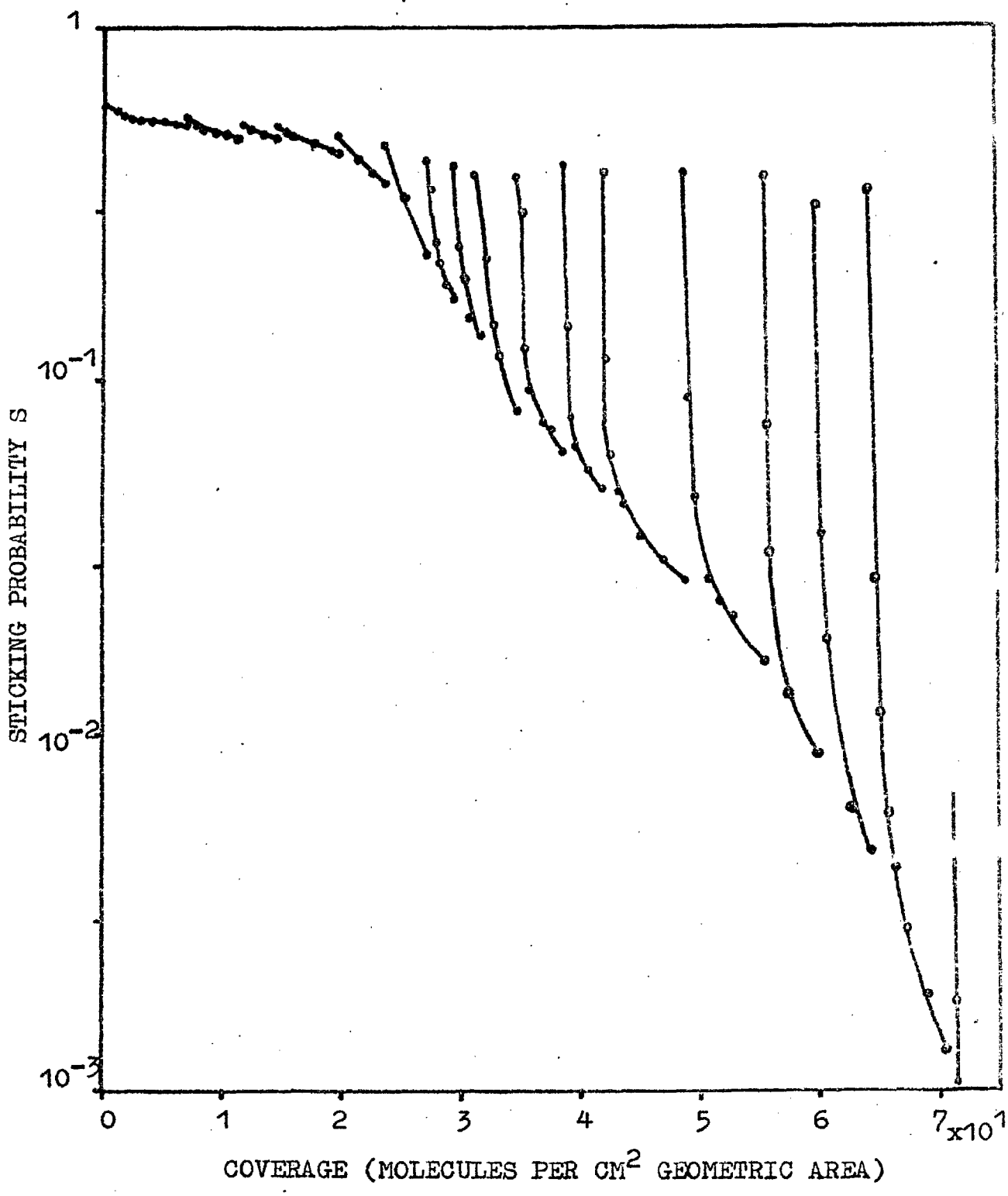

FIGURE 50. S versus coverage at 78°K - unsintered film.

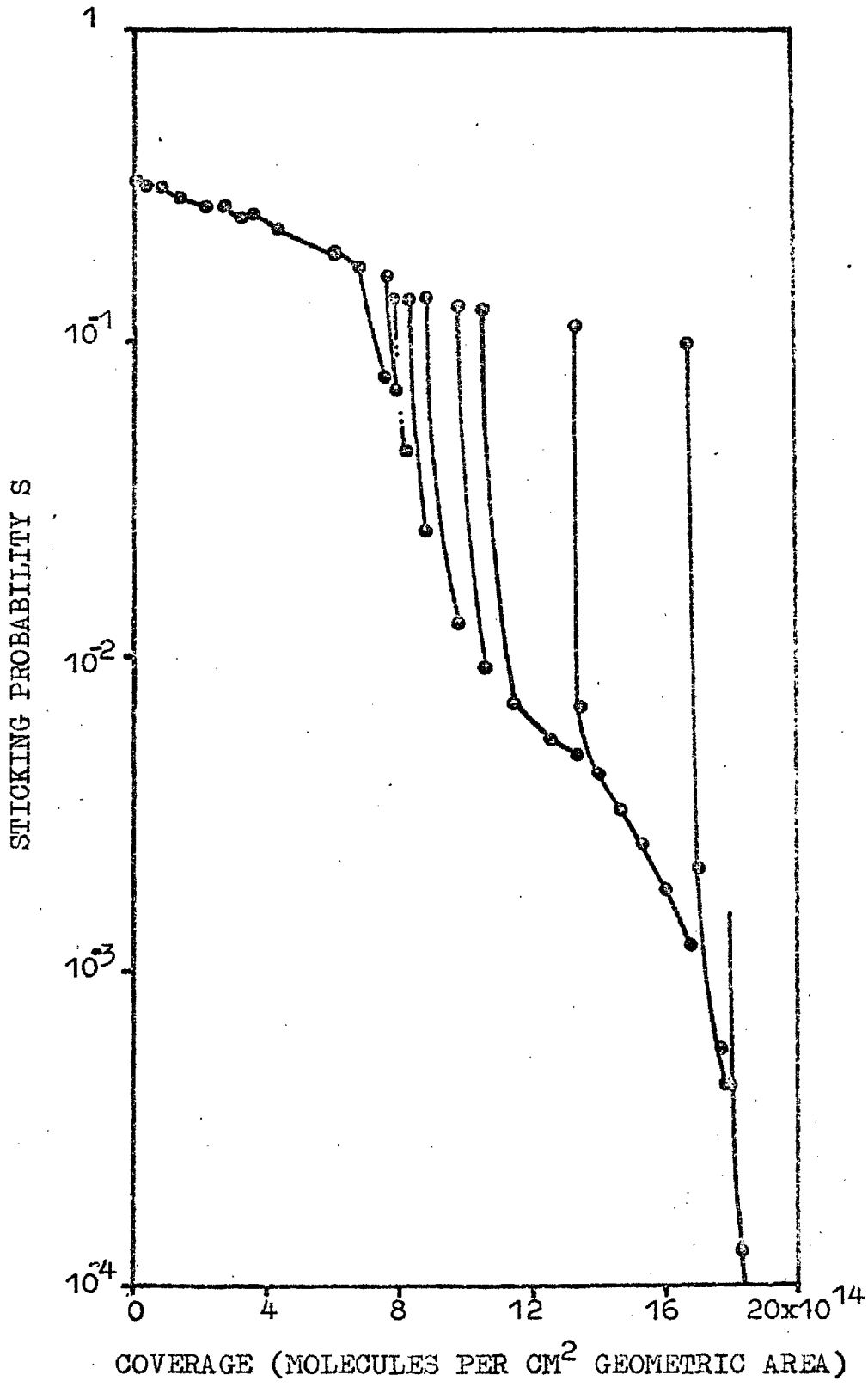

FIGURE 51. S versus coverage at 78°K - sintered film.

dependence of the initial sticking probability in the range 78°K to 300°K for sintered films and no pressure dependence within the range experimentally obtainable. Unfortunately, with nickel, no experiment was performed in which gas was added to a single film held at both 78°K and 300°K in the initial coverage region.

The shapes of the sticking probability against coverage curve at 78°K for both unsintered and sintered films of nickel were similar to those for molybdenum films held at 78°K except that, with the unsintered nickel films, the slow process is not appreciable until a coverage of about 15 - 20 x 10^{14} molecules per cm^2 of geometric area is reached. With the sintered nickel the slow process is evident at 6 - 8 x 10^{14} molecules per cm^2 i.e. at a similar point to molybdenum at 78°K. Figures 50 and 51 display typical curves for runs in which interruptions of gas flow were made during adsorption at 78°K.

At 300°k runs were performed only with films deposited around room temperature and, with the low internal area, mobility of the adsorbed layer cannot be predicted solely from the sticking probability curve. However, when equilibrium pressures become measurable they are relatively independent of time thus indicating

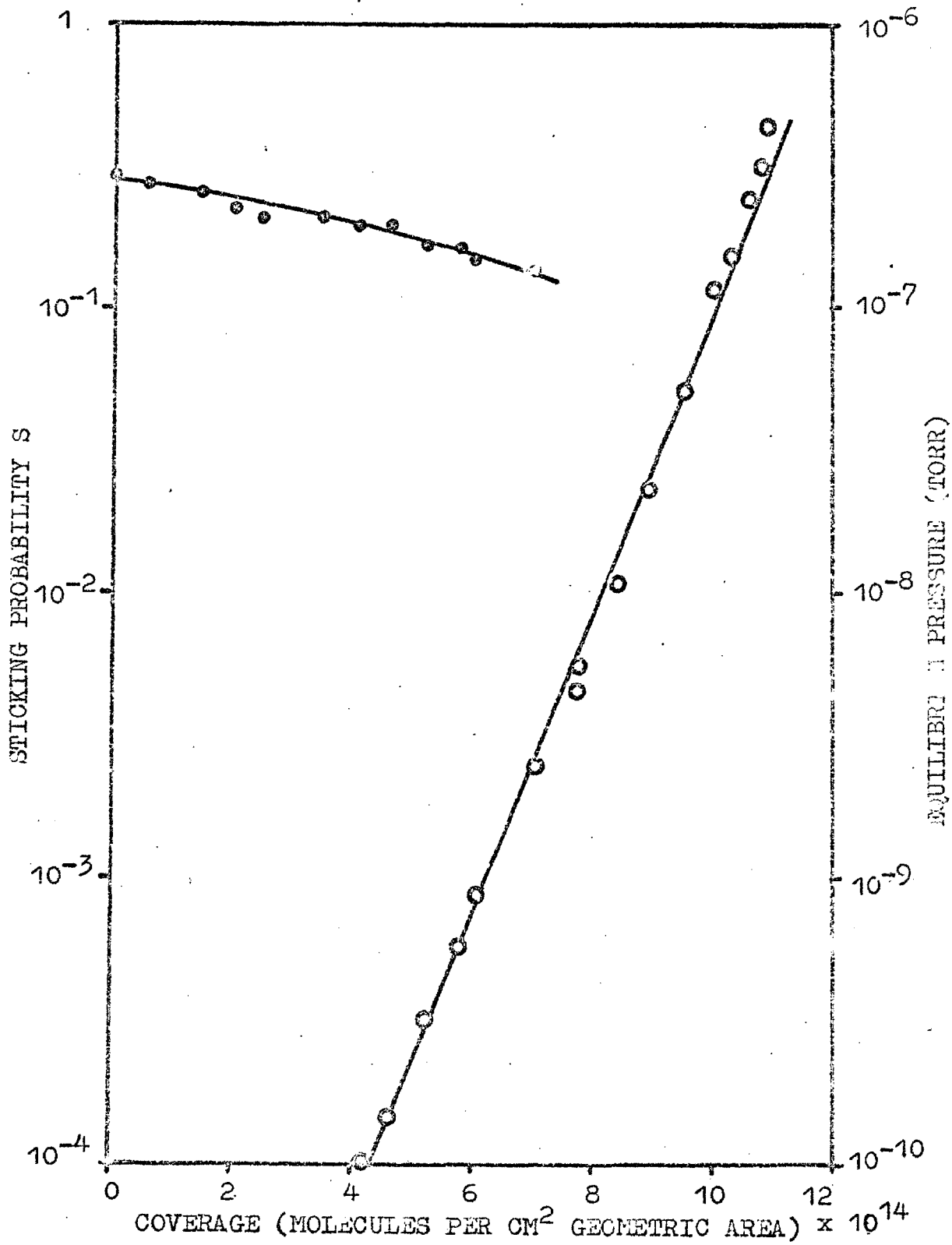

FIGURE 52. S versus coverage at 300°K.

a surface equilibrium. Isotherms constructed from the equilibrium pressure data are again Temkin in form, with slopes at 300°K around 2 x 10^{-14} per molecule per cm^2 of true surface area. This is lower than found for molybdenum at 300°K (6 x 10^{-14} in the same units) and is in line with the less steeply falling heats of adsorption for the hydrogen nickel system at 300°K obtained by Brennan and Hayes (1964), Rideal and Sweett (1960) and others. The heat curves of Rideal and also of Wahba and Kemball (1953) have a slope in the 15 kilocalorie region equivalent to an α' value (see page 135) a little higher than that obtained from the isotherms. Figure 52 displays a typical sticking probability curve at 300°K together with an isotherm as saturation is approached.

13.3 The slow process at 78°K

The similarity of the sticking probability curves at 78°K of hydrogen on nickel and molybdenum has been seen in the previous section. With the unsintered films (figure 50) of nickel the sticking probability values obtained from the sharp pressure changes on restarting the gas supply lie around 0.42 over a very wide coverage range; this is almost the same as that obtained for sintered films of molybdenum held at 78°K (0.40). The onset of the slow process, as detected

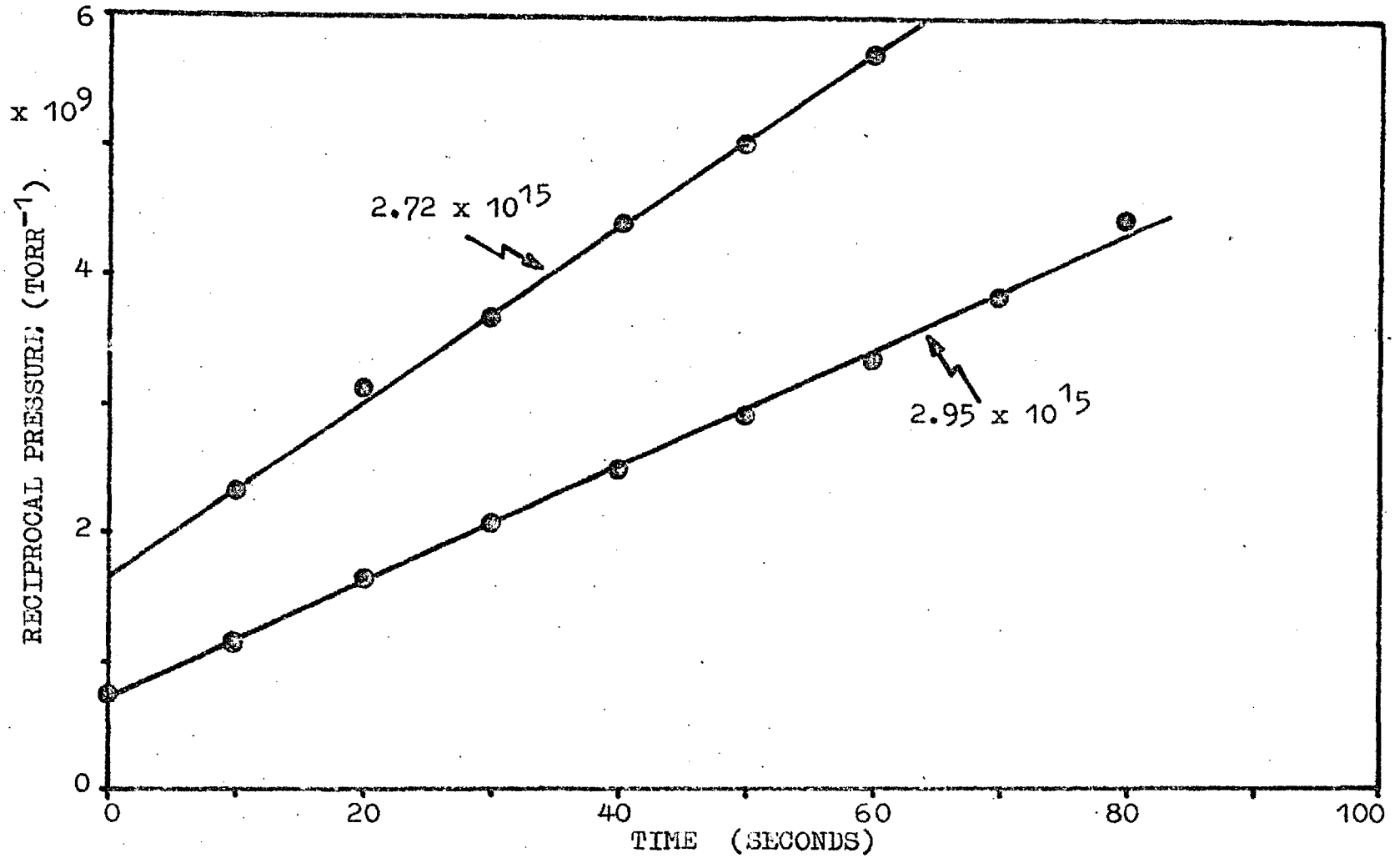

FIGURE 53(a). Reciprocal pressure versus time at 78°K - unsintered film. (Coverages in molecules per CM^2 geometric area are indicated.)

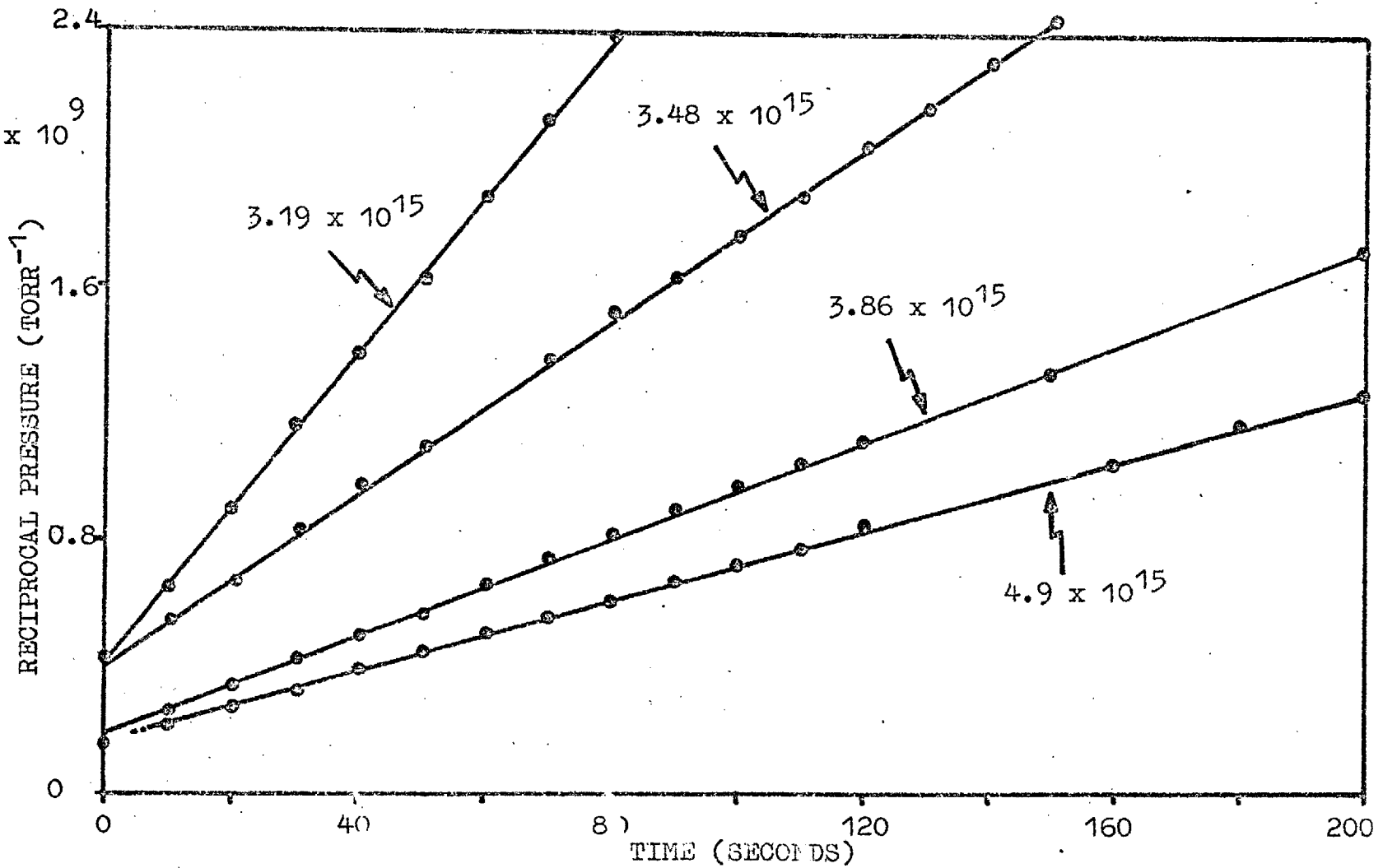

FIGURE 53(b). Reciprocal pressure versus time at 78°K - unsintered film.

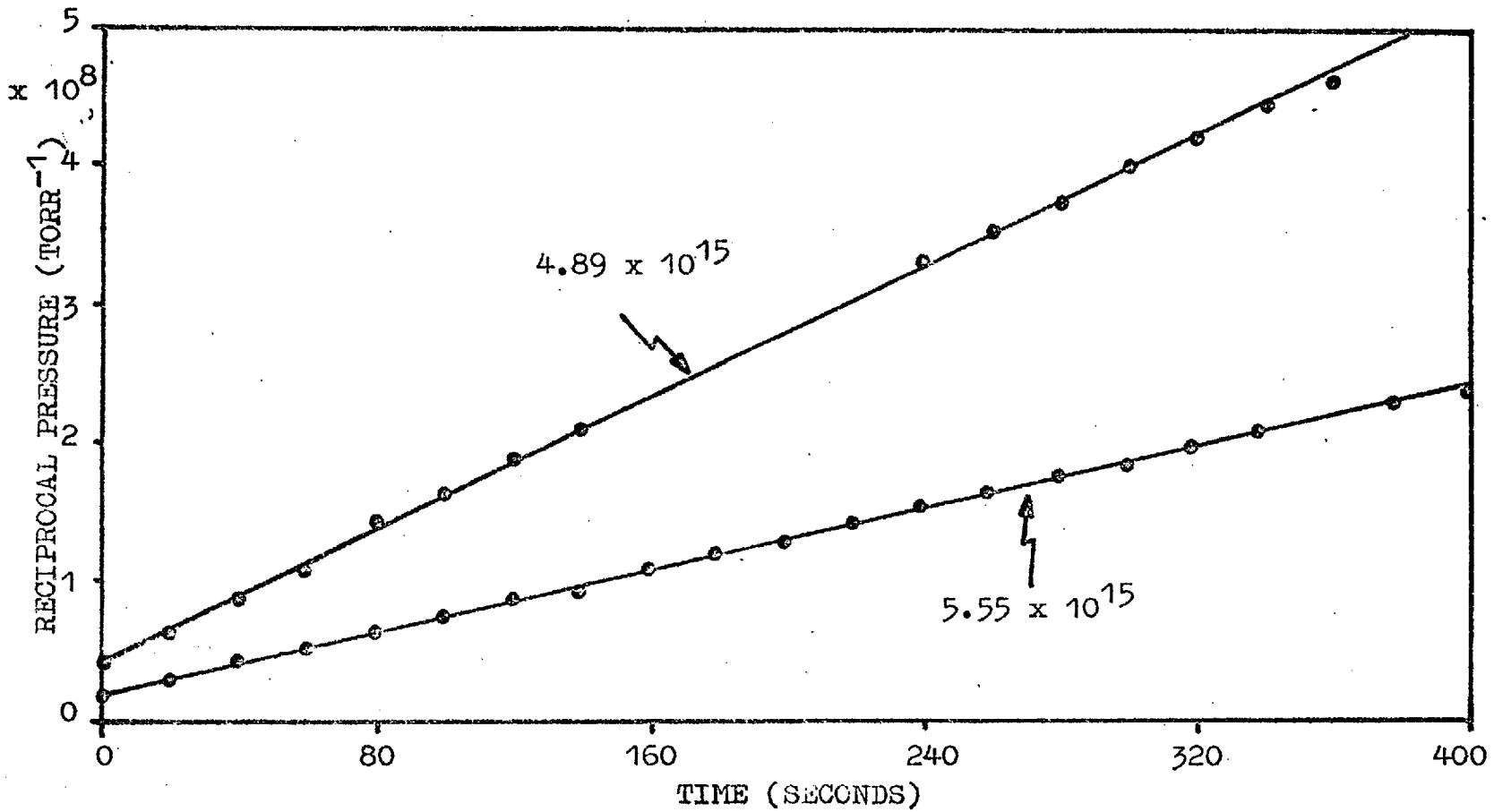

FIGURE 54(a). Reciprocal pressure versus time at 78°K - unsintered film.

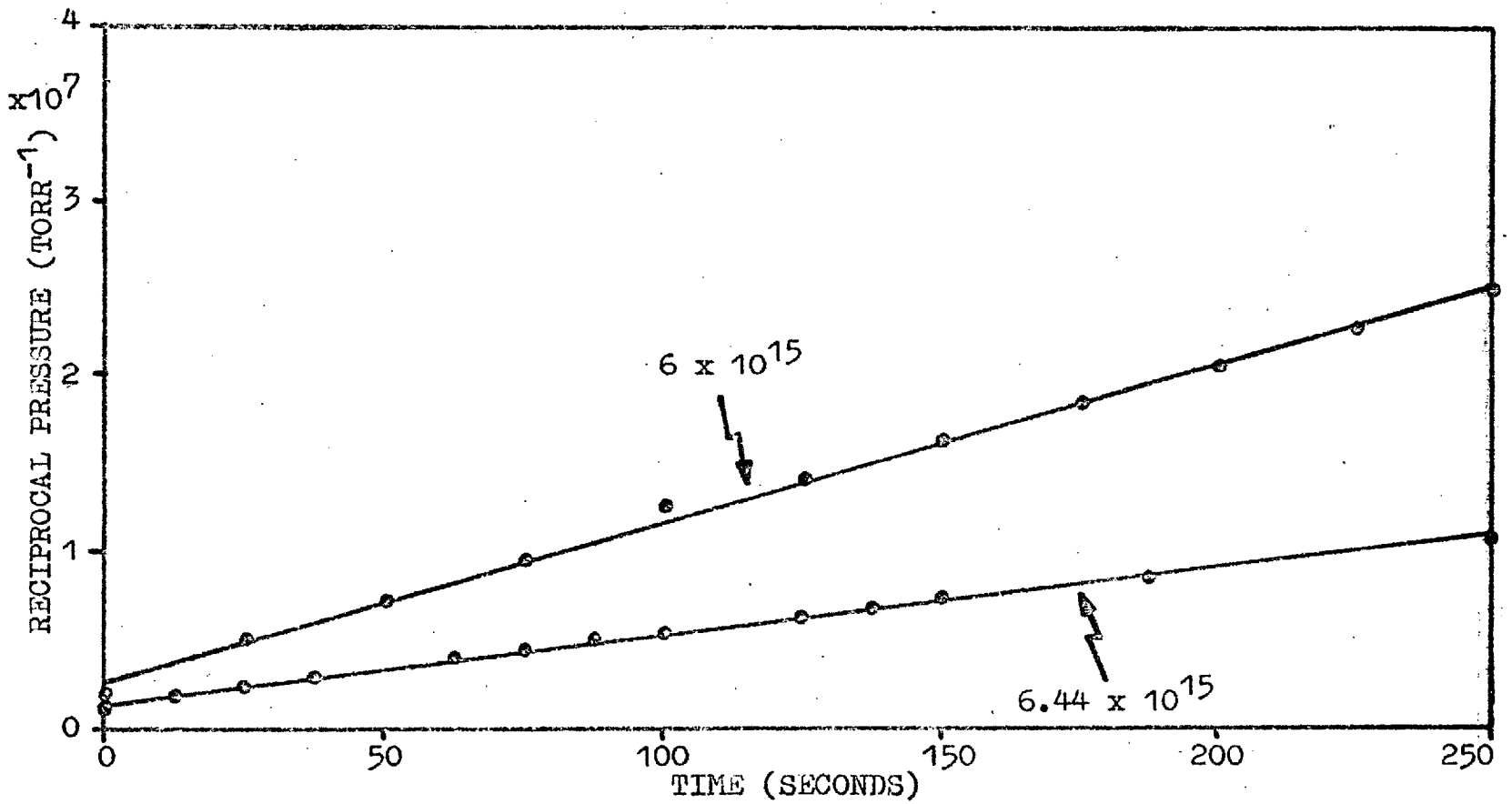

FIGURE 54(b) Reciprocal pressure versus time at 78°K - unsintered film.

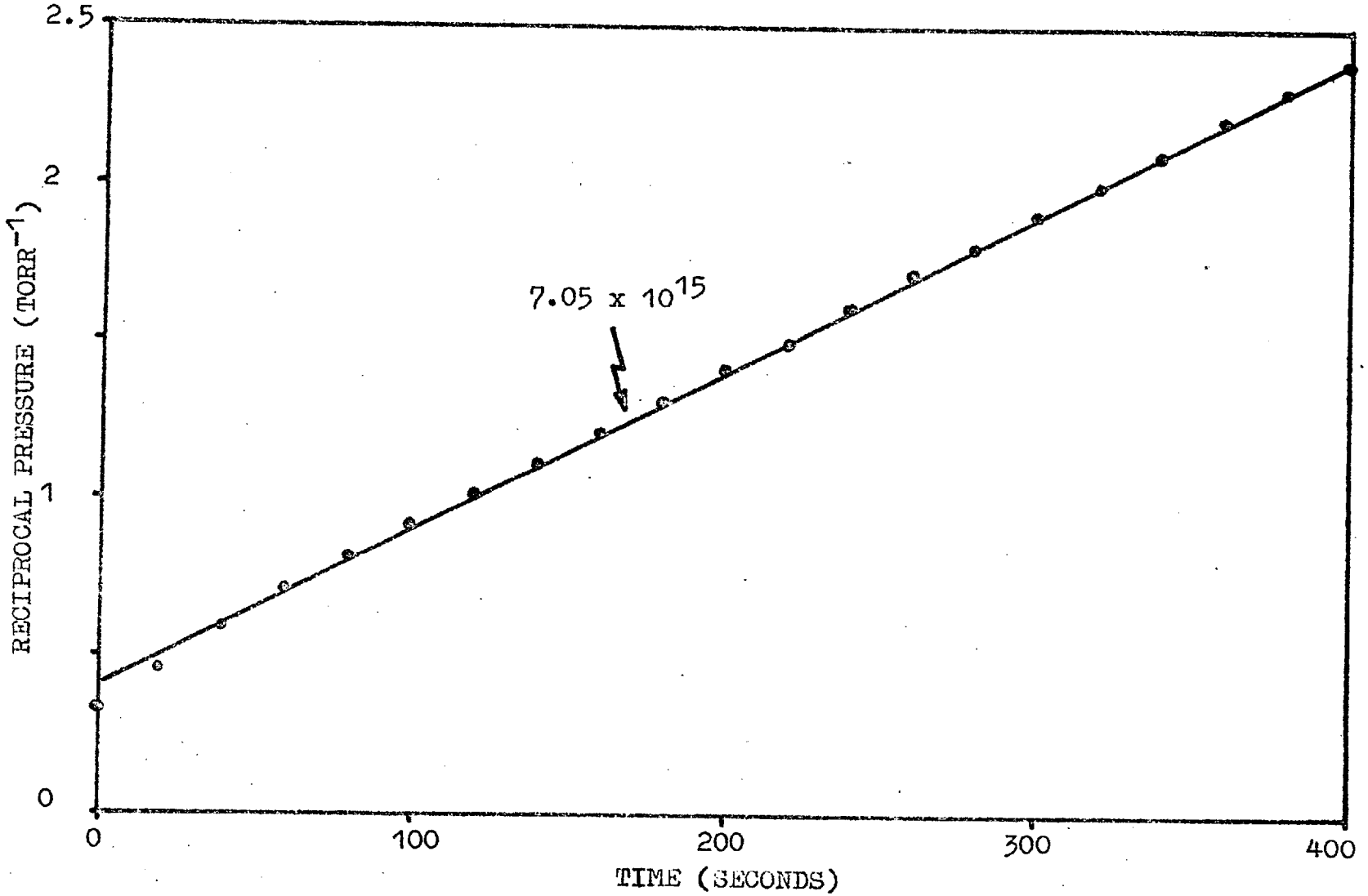

FIGURE 55. Reciprocal pressure versus time at 78°K - unsintered film.

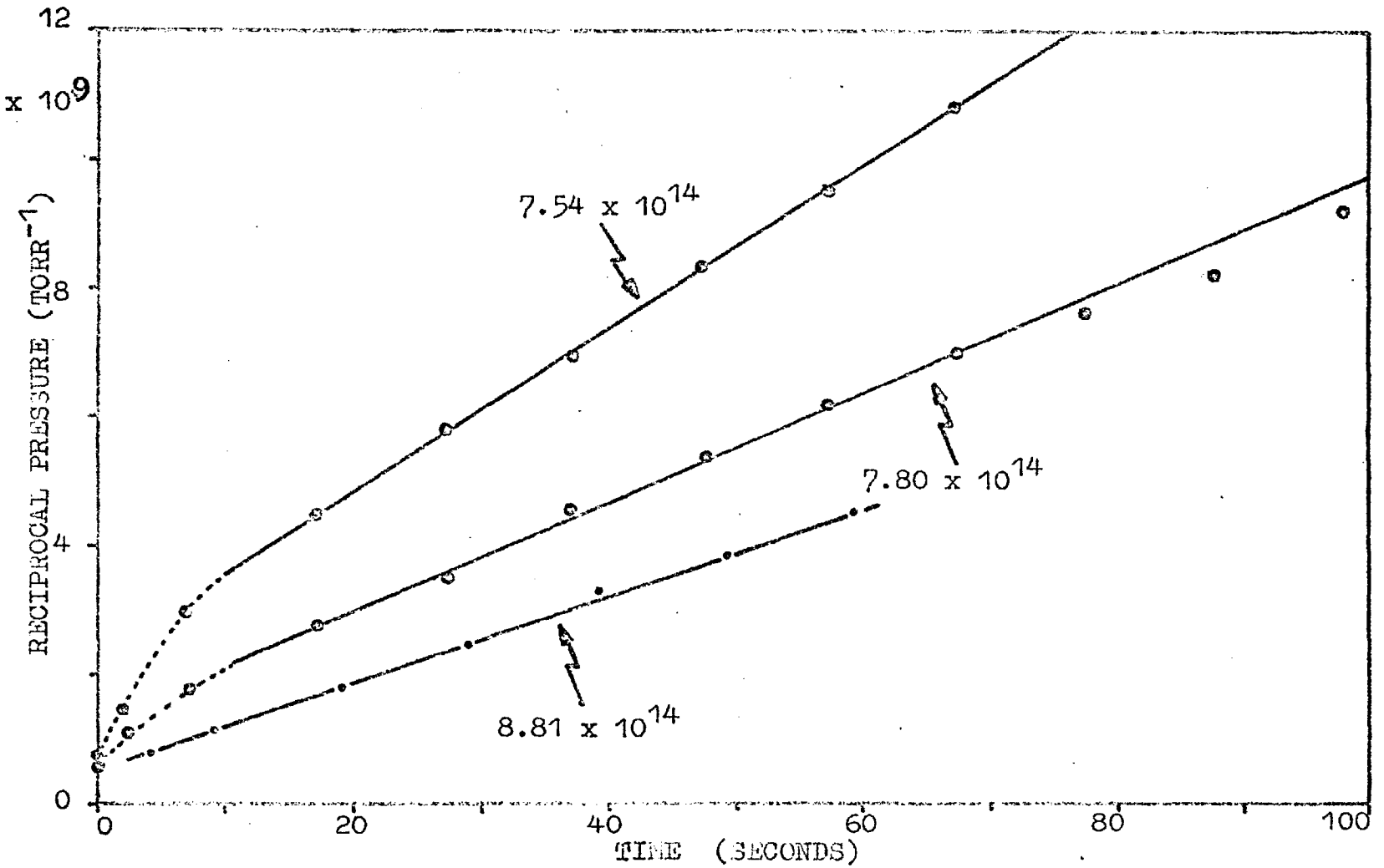

FIGURE 56. Reciprocal pressure versus time at 78°K - sintered film.

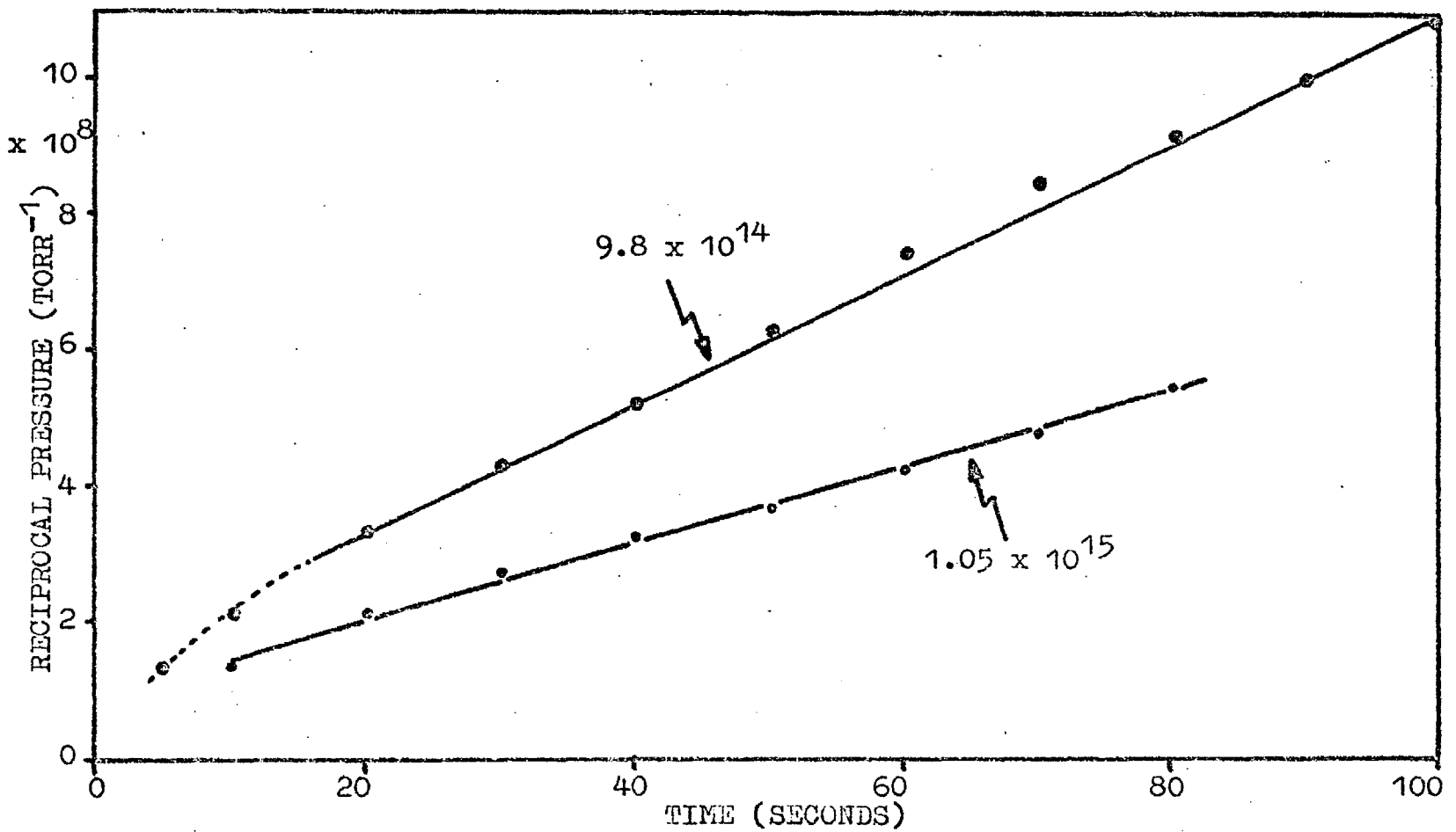

FIGURE 57. Reciprocal pressure versus time at 78°K - sintered film.

from the pressure time curves after closure of the gas supply, occurs around 7 x 10^{14} molecules per cm^2 geometric area for the sintered films but not until at least 15 x 10^{14} molecules per cm^2 for those unsintered. However, the recovery time of the sticking probability during isolation of the system occurs at about 10 x 10^{14} molecules in the case of unsintered nickel films (see figure 50) indicating the presence of a slow redistribution at this point.

The kinetics of the slow redistributions is similar in form to that observed for molybdenum i.e. the reciprocal pressure rises linearly with time after closure of the gas supply. Figures 53, 54 and 55 display a series of curves for an unsintered film (ref. 25.7.65) and figures 56 and 57 for a sintered film (ref. 24.6.64), the gas addition in each case being with the film held at 78°K. The slopes of the reciprocal pressure against time curves vary, for both types of film, over the same range as found for molybdenum i.e. 10^8 to 10^5 $torr^{-1}$ per second. The number of observations for sintered films is necessarily restricted by the low proportion of internal surface. The treatment applied to the molybdenum results to give α^{-1} values (see page160)is not repeated here - the

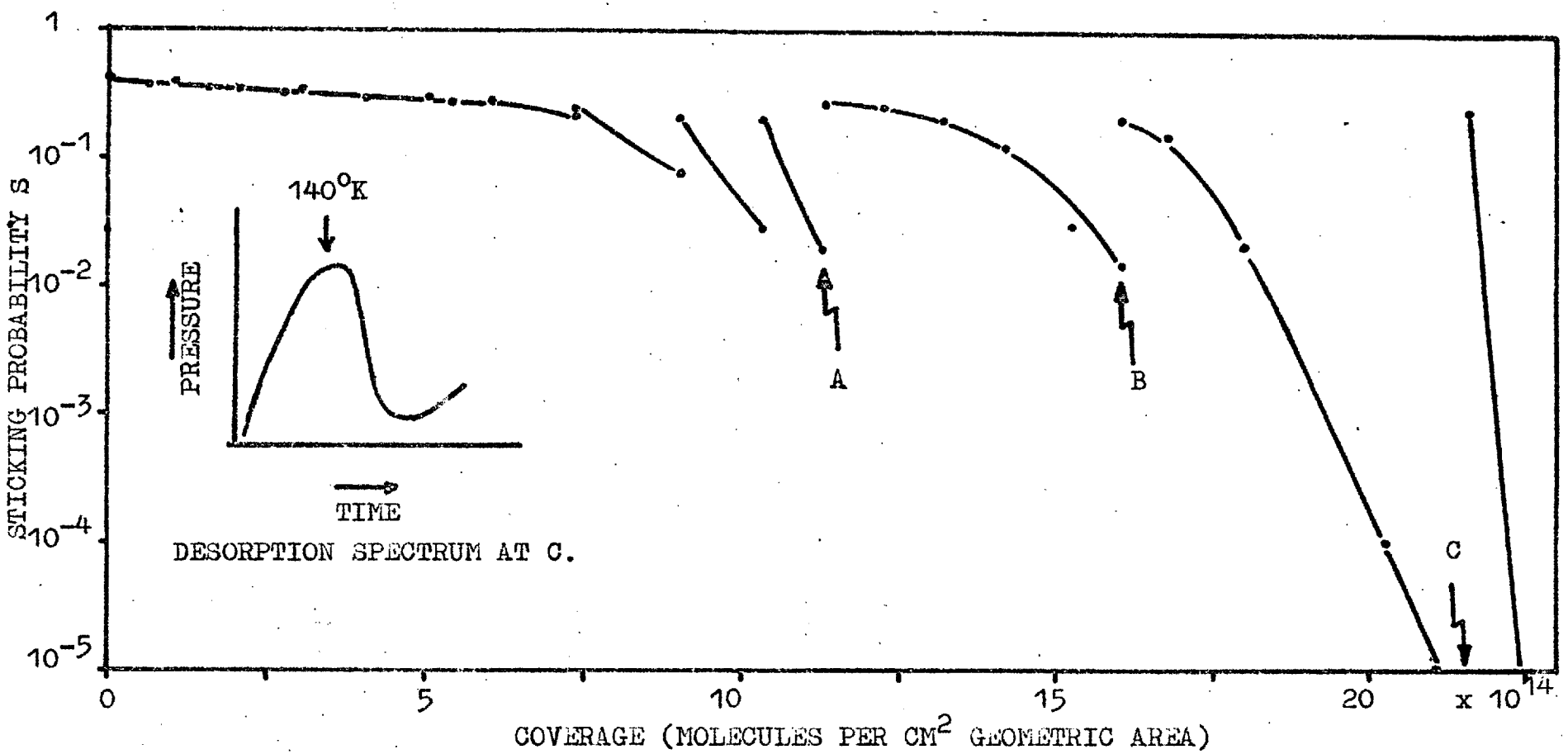

FIGURE 58. S versus coverage at 78°K - sintered film.
The film was warmed to 300°K at A, B and C.

general features being entirely similar to molybdenum at 78°K.

The rearrangements in the adsorbed layer observed in the desorption experiments with molybdenum are seen with nickel. This is exemplified by the results displayed in figure 58. At a coverage of 21.5×10^{14} molecules per cm^2 of geometric area the film is effectively saturated at 78°K i.e. the gas reservoir and reaction vessel pressures are nearly equal. On warming to around 200°K and recooling to 78°K there is an additional uptake of 10^{14} molecules per cm^2 (the film had been previously warmed and recooled at the indicated stages). The desorption spectrum accompanying the warm up at 21.5×10^{14} molecules per cm^2 is shown in the inset indicating that the rearrangement occurs with nickel at about 140°K in contrast to 170°K with molybdenum. The mobility of the adsorbed layer at 300°K is indicated by the lack of slow redistributions after closure of gas supply; this agrees with the results of Wortman, Gomer and Lundy (1957) who observed mobility of the adsorbed layer of hydrogen on nickel above about 240°K in the field emission microscope. The activation energy for surface diffusion has been calculated incorrectly by Gomer, from the Arrhenius plot shown in his figure 19 and

should be 14 kilocalories. This is now in marked disagreement with the value of 8.8 kilocalories obtained by Gomer from a direct observation of the rate of diffusion of hydrogen on nickel assuming a random walk process. From the latter value it can be shown that the hydrogen atoms would migrate a distance of 10Å in 100 secs at 130°K and a distance of 1000Å at 240°K in a similar time interval. This would indicate that the rearrangements observed at 130°K are relatively short range processes i.e. around 10 hops required per adatom to generate an appreciable number of extra sites in the adsorbed layer.

14 HYDROGEN ON TITANIUM

14.1. The uptake

As with the other metals studied, films of titanium were thrown either onto an uncooled cell wall (in which case the temperature of deposition was around 70°C) or onto the cell wall held at 78°K. The roughness factors of the films could not be estimated directly from the uptake of hydrogen molecules as absorption into the bulk metal occurred throughout the temperature range investigated but could be calculated for sintered films indirectly from experiments

involving gas additions to a single film held at both 78°K and 300°K (see later). The results of the latter experiments suggest a roughness of about 5 for the sintered films.

At 195°K and 300°K the absorption process occurs rapidly ($S > 10^{-5}$) to a hydride composition between TiH and TiH_2, in agreement with Wedler et al (1966) who found compositions of $TiH_{1.5}$ to TiH_2 and Della Porta et al (1966) whose final composition was around $TiH_{0.9}$. At 78°K the measurable absorption was greatly reduced and the determination of stoichiometry was complicated by the presence of an evaporator filament at a somewhat higher temperature than the film. Assuming that the evaporator filament behaves in a similar way to a film held at 300°K it may be shown that for zero absorption on the film at 78°K the recorded pressures will indicate a sticking coefficient (calculated for the film) of about 10^{-5}. Thus measurements in this region must be viewed with suspicion! It was found in fact in several runs that there was an apparent flattening out of S in the 10^{-5} range thus supporting the proposed behaviour. The uptakes up to this point for sintered films indicate stoichiometries of $TiH_{0.03}$ to $TiH_{0.07}$ and this is taken to be the limit of measurable absorption at 78°K. These values agree with

Della Porta who finds absorption at 78°K to $TiH_{0.04}$. Unsintered films appear to absorb to a higher hydrogen composition, e.g. run reference 3.3.65, absorbed to about $TiH_{0.2}$ before S fell to 10^{-5}. This is not solely a surface effect as a roughness factor of about 35 would be required to accommodate the extra gas, assuming a concentration in the bulk as for a sintered film. It will be seen subsequently that if attempts are made to sinter films thrown at 78°K the resulting surface does not even approximate to that of a film deposited near room temperature. The large difference in S values at 300°K for films thrown at high temperature (~70°C) and those thrown at 78°K and subsequently sintered to 50°C cannot be explained in terms of enhancement by multiple collisions (see table on page 220).

14.2. The sticking probability at zero coverage

Initial values of sticking probability were somewhat less reproducible in this system than for others studied and there was evidence of a variation with temperature in the range 78°K to 300°K. This variation was observed by adding small doses of gas to sintered films held successively at 300 and 78°K. The results are summarised in the following table together with initial S values on a number of other sintered films.

Reference	S_o 78°K	S_o 300°K	S_o 78°K/S_o 300°K
24.9.64	0.28	0.18	1.55
28.9.64	0.34	0.26	1.30
22.6.64	0.36	-	-
17.6.64	0.26	-	-
16.12.64	0.38	-	-
16.6.64	-	0.22	-
1.3.63*	0.38	-	-

* W filament gauge

For unsintered films the initial sticking probability is higher (0.61), this may again be due to an enhancement by multiple collisions with the rougher film structure (but see later). Clausing (1961) reports values of 0.25 and 9×10^{-2} for hydrogen on unsintered and sintered titanium films at 78°K thus agreeing in degree of enhancement of sticking probability. Holland et al (1965), however, report values of 0.25 and 10^{-2} for the two types of film - the very low value of the latter is almost certainly an artefact introduced by performing experiments in a reaction vessel containing underlying films from previous runs.

The temperature dependence of initial sticking probability has been observed by Holland et al (1965)

who for sintered films find a ratio of 2.3 between S_o^{78} and $S_o^{300°K}$. However, the sticking probability falls much more rapidly with coverage for the titanium system than for others studied and thus a smaller degree of precoverage (i.e. during film deposition) is required to produce a given deviation in the initial value measured. In support of this it may be noted that large quantities of hydrogen are evolved during outgassing of many metals. Also in this work it was found that flushing the system with hydrogen prior to film deposition gave rise to very low values of S_o ($< 10^{-1}$) although the final stage of film deposition was in a vacuum of around 5×10^{-10} torr (for example in run ref. 14.12.64). The extent of precoverage necessary to explain the variation of S_o may be obtained by extrapolating the sticking probability curves of runs 24.9.64 and 28.9.64 back to where $S_o^{78°K}$ equals $S_o^{300°K}$. Values of precoverage of 5×10^{14} and 2×10^{14} molecules per cm^2 geometric area respectively are indicated. The mobility of hydrogen throughout the titanium lattice certainly indicates that this gas is not trapped in the film during evaporation of sintered films and may migrate to the surface during or subsequent to deposition. For a partial pressure of 5×10^{-10} torr of hydrogen above the film and a S_o of 0.3 only around 1000 secs are requried to give the evaluated magnitude of

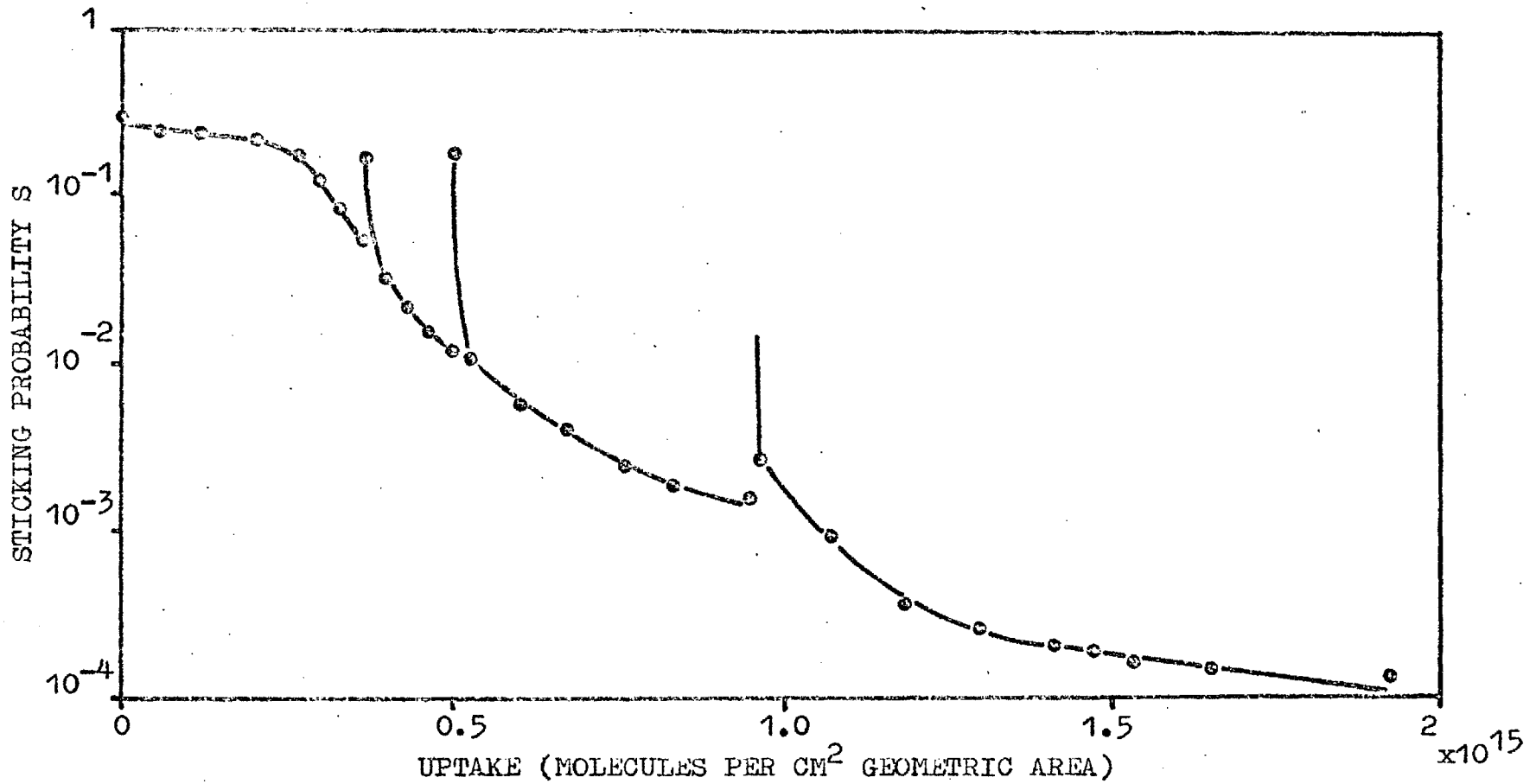

FIGURE 59(a). S versus uptake at 78°K - sintered film.

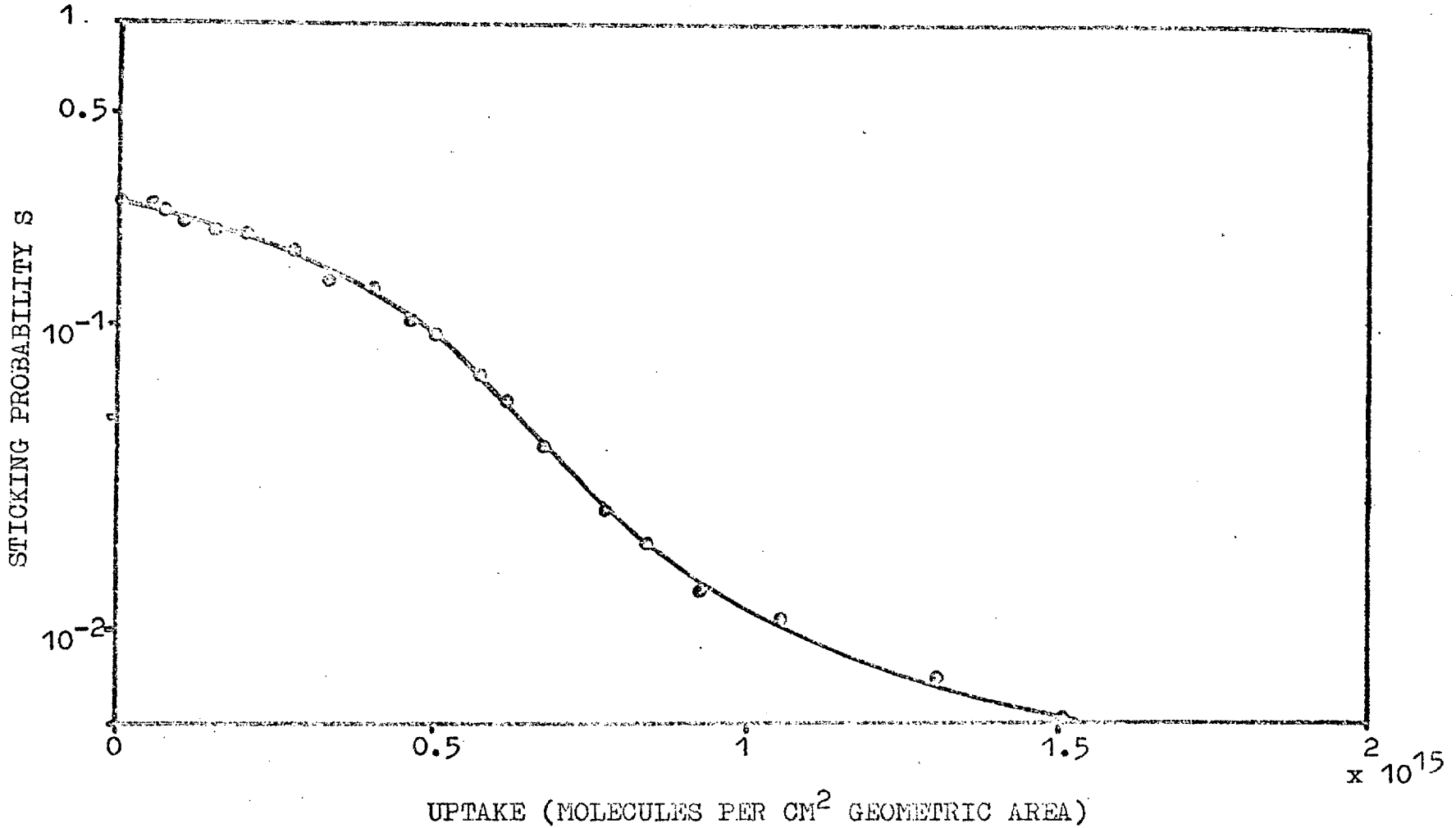

FIGURE 59(b). S versus uptake at 300°K.

precoverage!

14.3 The sticking probability as a function of coverage

The adsorption region

As mentioned in the previous section the sticking probability of hydrogen on titanium falls more rapidly with coverage than in the other systems studied. At 300°K and 195°K a decrease of about two orders of magnitude in S is observed after an addition of 10 to 15 x 10^{14} molecules per cm^2 geometric area i.e. after 2 - 3 x 10^{14} molecules per cm^2 of true area; at 78°K a similar fall occurs after the addition of 5 - 7 x 10^{14} molecules per cm^2 geometric area of film. The onset of a slow redistribution at 78°K occurs near the point of saturation of the outer surface if complete immobility is assumed - for titanium - hydrogen this is at around 3 x 10^{14} molecules per cm^2 (3.4, 3.0, 2.6 and 2.7 x 10^{14} in 4 separate experiments on sintered films) in contrast to 7 x 10^{14} molecules per cm^2 for molybdenum and nickel films. Figure 59 exemplifies typical initial regions of adsorption using sintered films at 78°K and 300°K.

Mobility of the adsorbed layer at 195°K and 300°K is demonstrated by the lack of time dependence of

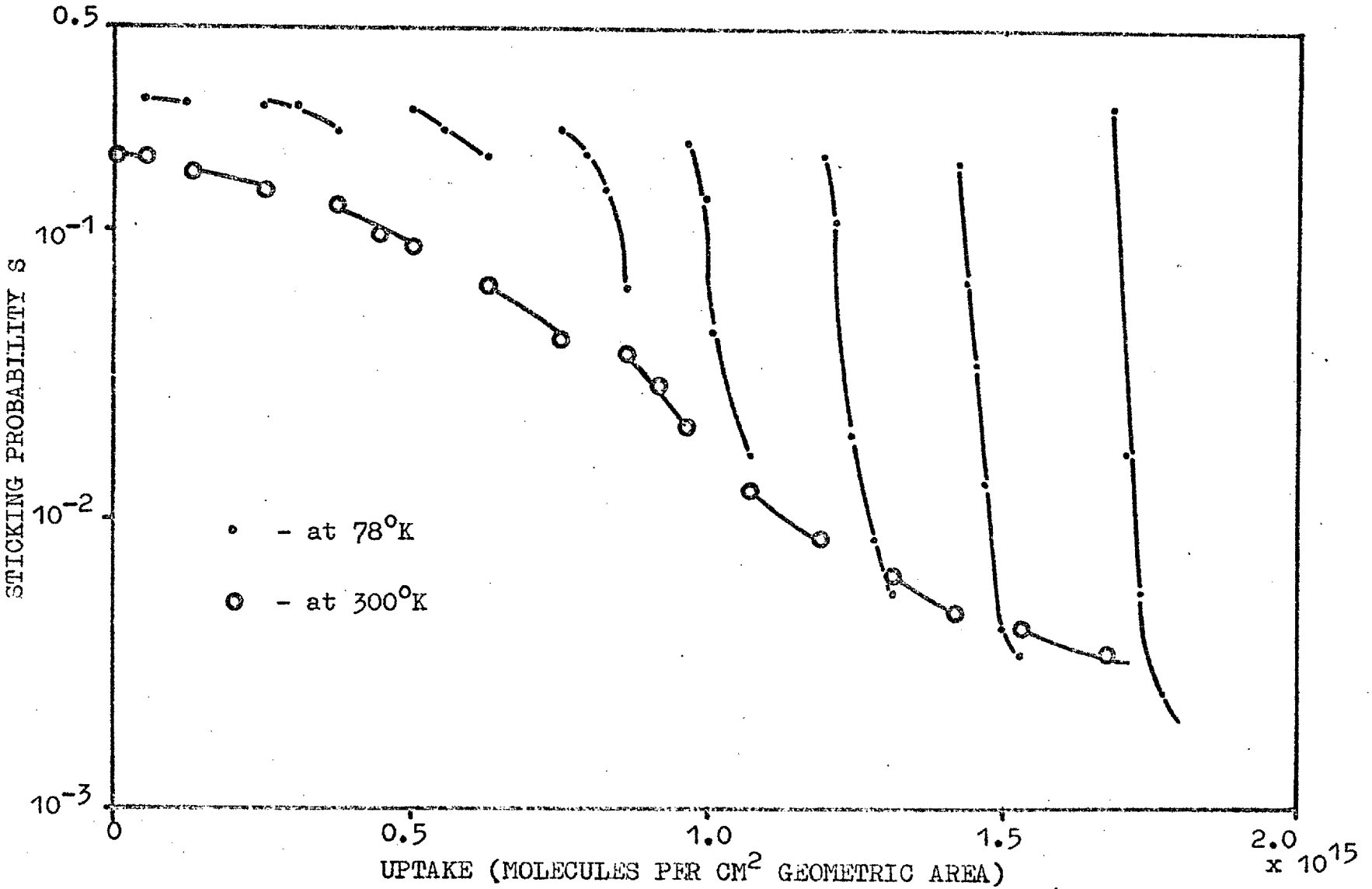

FIGURE 60. S versus uptake - film alternately at 78°K and 300°K.

sticking probability before and after long interruptions in gas flow to the film and also by behaviour observed during experiments in which increments of gas are admitted with the film held alternately at 300 and 78°K. Figure 60 illustrates the results of such an experiment. It is observed that the two sticking probabilities decrease in the same way and that the onset of a very sharp drop in S is not observed at 78°K until a total of 10 x 10^{14} molecules per cm^2 have been added. This is a much higher coverage than that for the sharp decrease in S when gas is added to a film held throughout at 78°K and thus supports the concept of mobility at 300°K. It is possible to reconstruct the sticking probability curve at 78°K of figure 60 in terms of true surface coverage - the result is a similar fall in S with coverage to that observed in runs solely at the low temperature.

Unsintered films at 78°K show a more gradual decline in S with coverage but the slow redistribution is observed at nearly the same coverage (e.g. run 3.8.65 - at 5.0 x 10^{14} molecules per cm^2 geometric area). This demonstrates lack of appreciable mobility at 78°K.

The absorption region

At 300 and 195°K S is independent of uptake over a

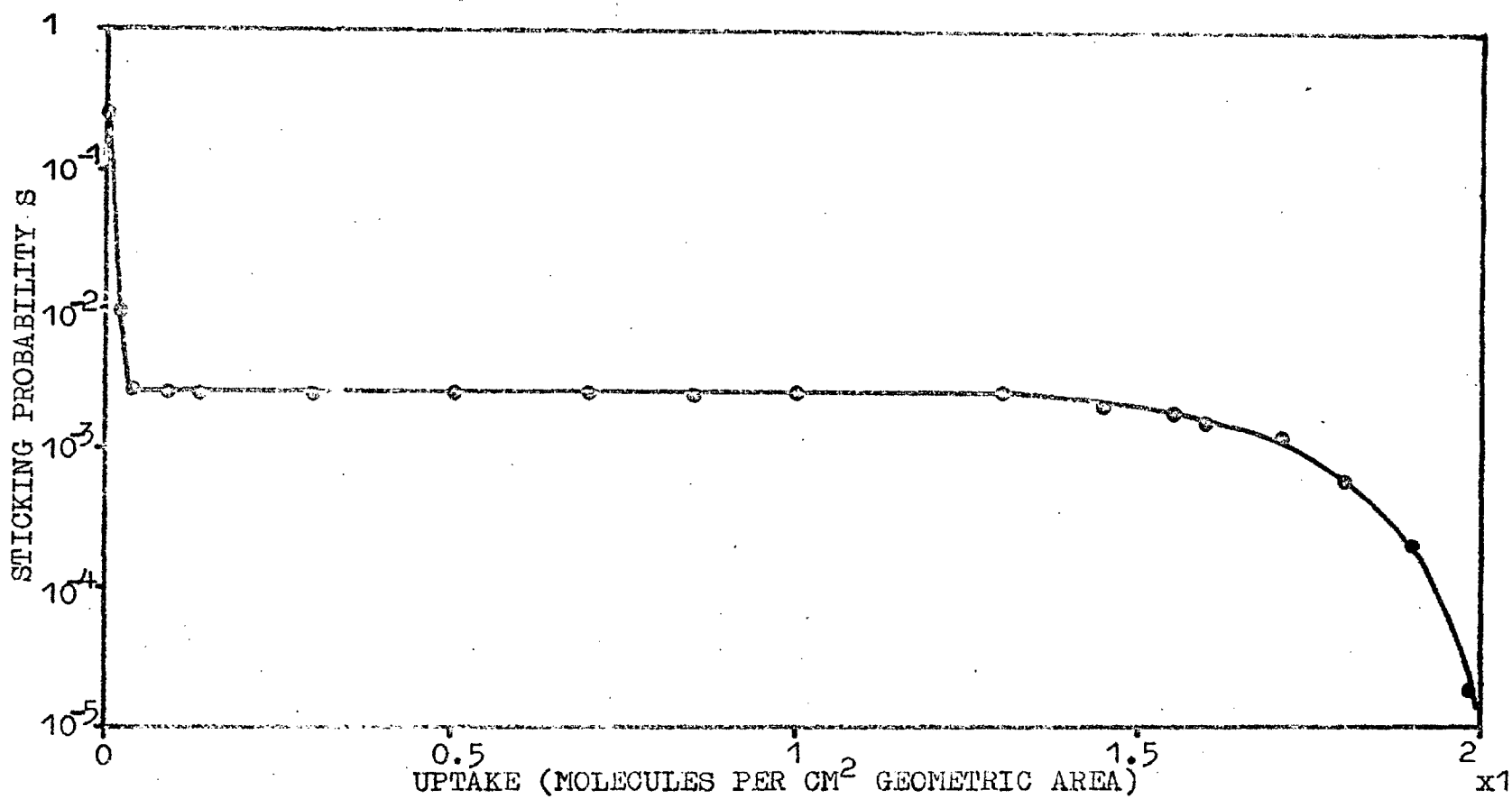

FIGURE 61(a). S versus uptake at 300°K.

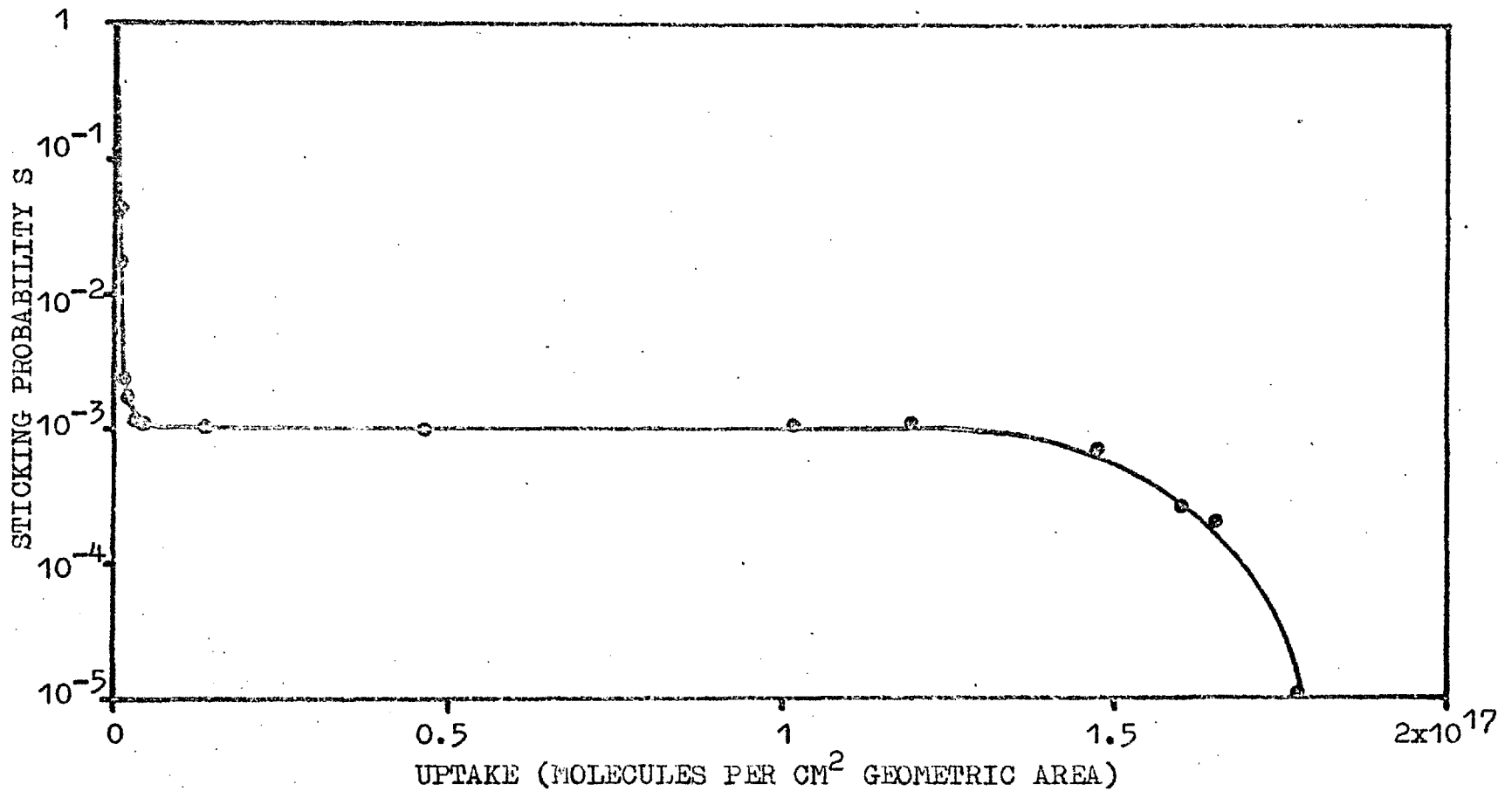

FIGURE 61(b). S versus uptake at 195°K.

wide range; typical results are displayed in figure 61. To characterise the curves of S against uptake the following are defined; S_c - the S in the uptake independent region, θ_1 and θ_2 - the uptakes defining the boundaries of the constant S region and θ_3 - the total uptake (all in molecules per cm^2 geometric area). The results for a number of films are given in the table below. Except where otherwise stated the temperature is 300°K.

PART A

Run	θ_1	θ_2	θ_3
20.2.63+			
11.2.63+	2×10^{15}		
26.9.63	2.3×10^{15}		
16.6.64	1.4×10^{15}	17×10^{16}	24×10^{16}
24.9.64	1.5×10^{15}		
28.9.64	1.5×10^{15}		
29.7.65	-	7.5×10^{16}	12×10^{16}
3.8.65¥		8.0×10^{16}	12×10^{16}
14.12.64ø	1.2×10^{15}	13.0×10^{16}	18×10^{16}

Run	S_c	θ_1/θ_3	θ_2/θ_3	Hydride
20.2.63+	4.0×10^{-3}			
11.2.63+	6.0×10^{-3}			
26.9.63	4.0×10^{-3}			
16.6.64	3.4×10^{-3}	5.9×10^{-3}	0.71	
24.9.64	4.0×10^{-3}			
28.9.64	4.0×10^{-3}			
29.7.65	3.5×10^{-3}			$T_1H_{1.1}$
3.8.65¥	1.6×10^{-2}			$T_1H_{1.2}$
14.12.64ø	1.3×10^{-3}	6.6×10^{-3}	0.72	$T_1H_{1.3}$

Table - Data for various runs at 300 and 195°K

+ - W filament gauges

⁂ - film thrown at 78°K and sintered to 50°C after addition of 2.5×10^{16} molecules cm^{-2}.

ø - Sintered film, gas added to film at 195°K.

The results at 195°K and 300°K differ in the magnitude of S_c and also in that there is a dependence of S on flow rate in the final stages of the absorption at the lower temperature. Thus at 300°K the sticking probability was found to be independent of flow rates in the range 2×10^{11} to 1×10^{13} molecules per second per cm^2 geometric area up to at least 90% of the final uptake whereas at 195°K such independence was found only to 50% of the final uptake. At the latter temperature there was also evidence of a small recovery of sticking probability after a period of gas supply interruption at uptakes higher than 50%.

One attractive proposal is that in the regions where S is constant and independent of flow rate there exists a virtually constant surface condition during the absorption. This is substantiated by the results displayed in figure 60 in which gas is added to a film held alternately at 300 and 78°K. Inspection reveals that, after each addition of gas at 300°K within the

range of uptake where S is constant, the results at 78°K follow a given pattern both in the initial magnitude of the sticking probability and, at a fixed flow rate, in the variation of S with additional uptake.

It is well known from isosteric heat data and from calorimetric measurements that the heat of adsorption falls with increase of uptake. The results of Wedler and Strothenk (1966) confirm that such a situation exists for hydrogen adsorption on titanium at both 78°K and 300°K up to uptakes of about 10^{15} molecules per cm^2 geometric area. At 300°K the latter workers find a heat constant at about 27 kilocalories per mole for the absorption region between $TiH_{0.05}$ and $TiH_{1.8}$ thus giving a heat curve remarkably similar in form to the sticking probability curve presented here. The initial adsorption is accompanied by falls in both heat of adsorption and sticking probability. The surface state is, however, favoured thermodynamically only while its free energy is below that of the adsorbed state. It is proposed that in the uptake region where S is both constant and independent of flow rate the situation is as follows. From the point at which absorption becomes the favoured process, a constant surface will be maintained until the absorption

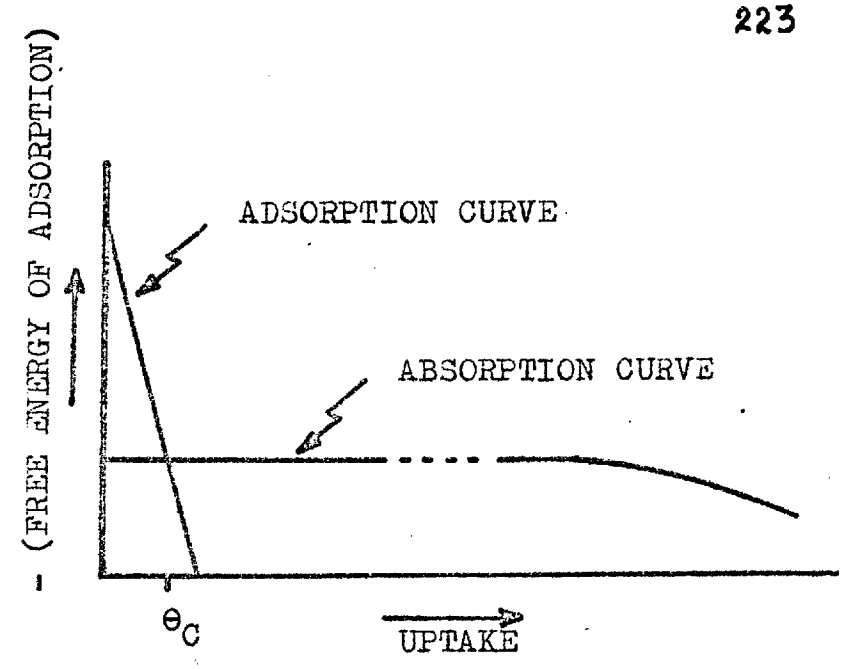

FIGURE 62(a).

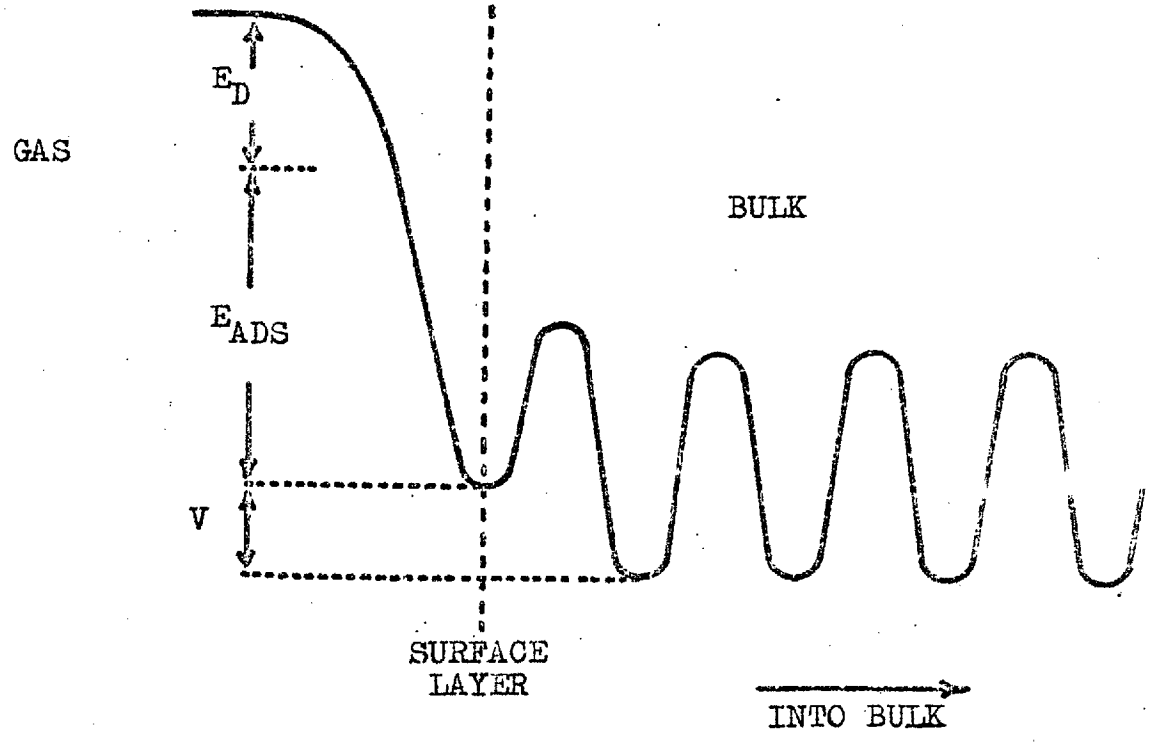

FIGURE 62(b). The potential energy barriers to absorption of hydrogen atoms in titanium

E_D - dissociation energy of hydrogen molecules

E_{ADS} - adsorption energy for H_2 molecules

V - difference of adsorption and absorption energies for H_2 molecules.

heat falls, in which case the surface coverage will increase such that the adsorption and absorption free energies are maintained equal. Unfortunately, the heat curves of Wedler display large variations in the compositions at which the absorption heat falls and this prevents a close correlation between the latter behaviour and the composition at which S decreases.

The proposed energetics of the system are displayed in figures 62 (a) and (b). Figure (a) shows the intersection of the two heat curves at θ_c - for uptakes higher than θ_c absorption occurs via surface sites of lower energy than those in the bulk metal. The rate of vacation of the latter sites is known from the independence of S on flow rate and from the absence of slow redistribution processes to be rapid compared with the uptake rates used. The heat curve for adsorption is known to fall steeply near θ_c since on adding gas at 78°K to a film which had previously absorbed at 300°K there is an immediate sharp fall in S and an accompanying slow redistribution. The titanium system is thus unusual in having a low density of energy sites between about 27 kilocalories per mole (accepting Wedler's value for the heat of absorption) and 5 kilocalories per mole (where desorption at 78°K becomes appreciable). The results of Wedler at 77°K

(Strothenk Ph.D thesis 1965) do not indicate a scarcity of energy sites in this interval - about 2×10^{14} molecules per cm^2 being adsorbed. It is suggested that the dosewise addition of gas in the calorimetric measurements enables appreciable absorption to occur, thus reducing the sensitivity of the heat to changes in density of surface states. Figure 62 (b) gives the suggested reaction path.

At 78°K the absorption process is thought to be diffusion controlled, S decreasing with uptake and becoming flow rate dependent. This behaviour suggests that the bulk site to bulk site activation energy is rate controlling (see figure 62 (b)) since if the latter were not the case S would, at 78°K, be expected to vary with flow rate but to be relatively independent of total uptake. This is further discussed in 14.5

14.4 The final stages of absorption

At 300°K and 195°K S has been shown to decrease after about 70% of the final uptake has been reached. On approaching saturation at these temperatures pseudo-equilibrium pressures are observed which slowly decay but with titanium sticking probabilities can still be measured even when pressures as high as 10^{-4} torr are present. This behaviour is unique among the results presented here - in all other systems S remains high

on approaching saturation and the sharp pressure changes necessary for calculations become 'lost' in the total reaction vessel pressure.

Typical results at 300°K (e.g. run ref. 16.6.64) shows an equilibrium pressure of 10^{-7}torr at about 96% of the total uptake (the latter defined as that for 10^{-5}torr). Construction of an isotherm is difficult because of slow drifts - the rough indication is that the Temkin is obeyed with a slope around ten times that for a non-absorbing metal. For example run 16.6.64 yielded α(molecules^{-1} cm^2 geometric area) = 5×10^{-16} for an 'isotherm' extending between 10^{-7} and 10^{-5}torr. In the same run it was possible to measure S up to 100% saturation (as defined above) - the value obtained ($\sim 10^{-5}$) is by far the lowest for any system studied.

The final stages of absorption at 78°K are discussed in the next section.

14.5 The kinetics of redistribution at 78°K

On sintered films of titanium a slow redistribution of gas from the outer surface is first observed at a coverage of $2 - 3 \times 10^{14}$ molecules per cm^2 of geometric area i.e. at some 30 - 40% of the coverage at which the phenomenon becomes observable on films of molybdenum and nickel. For the adsorbate

which is in pseudo-equilibrium with the gas phase the heat of adsorption must be around 5 kilocalories per mole thus stressing the rapid fall in heat in the initial uptake. The low heat when only one site in three is occupied by a hydrogen adatom could indicate that repulsions between adatoms are much stronger with titanium i.e. that an induced heterogeneity exists. However, it seems more likely that the surface itself is heterogeneous in a kinetic sense having regions of high sticking probability balanced by regions of very low sticking probability. Thus, on this model, the slow redistribution process is first observed when the 'active' regions on the most exposed parts of the film surface approach saturation.

The enhancement of the coverage on the exposed 'active' regions above that experimentally measured (per unit geometric area of film) may be obtained as follows.

The coverage (n) per cm^2 of 'exposed' active region at time t_n is given by

$$n = Z\int_0^{t_n} SP\,dt \qquad \text{.....(1)}$$

where S is the true sticking probability of the active regions and P is the pressure. At any time t

the experimentally determined sticking probability S' is related to the rate of adsorption n_A per unit geometric area of film by the expression

$$S' = \frac{n_A}{ZP} \qquad \text{.....(2)}$$

P being the ambient pressure

Substituting for P in equation (1) gives

$$n = Z\int_0^{tn} \frac{S}{S'} \cdot \frac{n_A}{Z}\, dt \qquad \text{.....(3)}$$

Now the experimental coverage n' at t_n is simply $n_A.t_n$ molecules per cm^2 geometric area (assuming n_A has been held constant) and thus -

$$\frac{n}{n'} = \frac{1}{t_n}\int_0^{t_n} \left(\frac{S}{S'}\right) \qquad \text{.....(4)}$$

To a good approximation $\left(\frac{S}{S'}\right)$ may be assumed constant in the initial stages of an experiment. Therefore if S is assumed to be unity and S' is taken as 0.3 then the enhancement $\frac{n}{n'}$ is around 3.3. Thus the slow redistribution is at around 10^{15} molecules per cm^2 of active region i.e. when there is approximately one adatom per surface site.

The kinetics of redistribution at $78^{\circ}K$ at coverages less than 7×10^{14} molecules per cm^2 geometric area follow a similar pattern to that

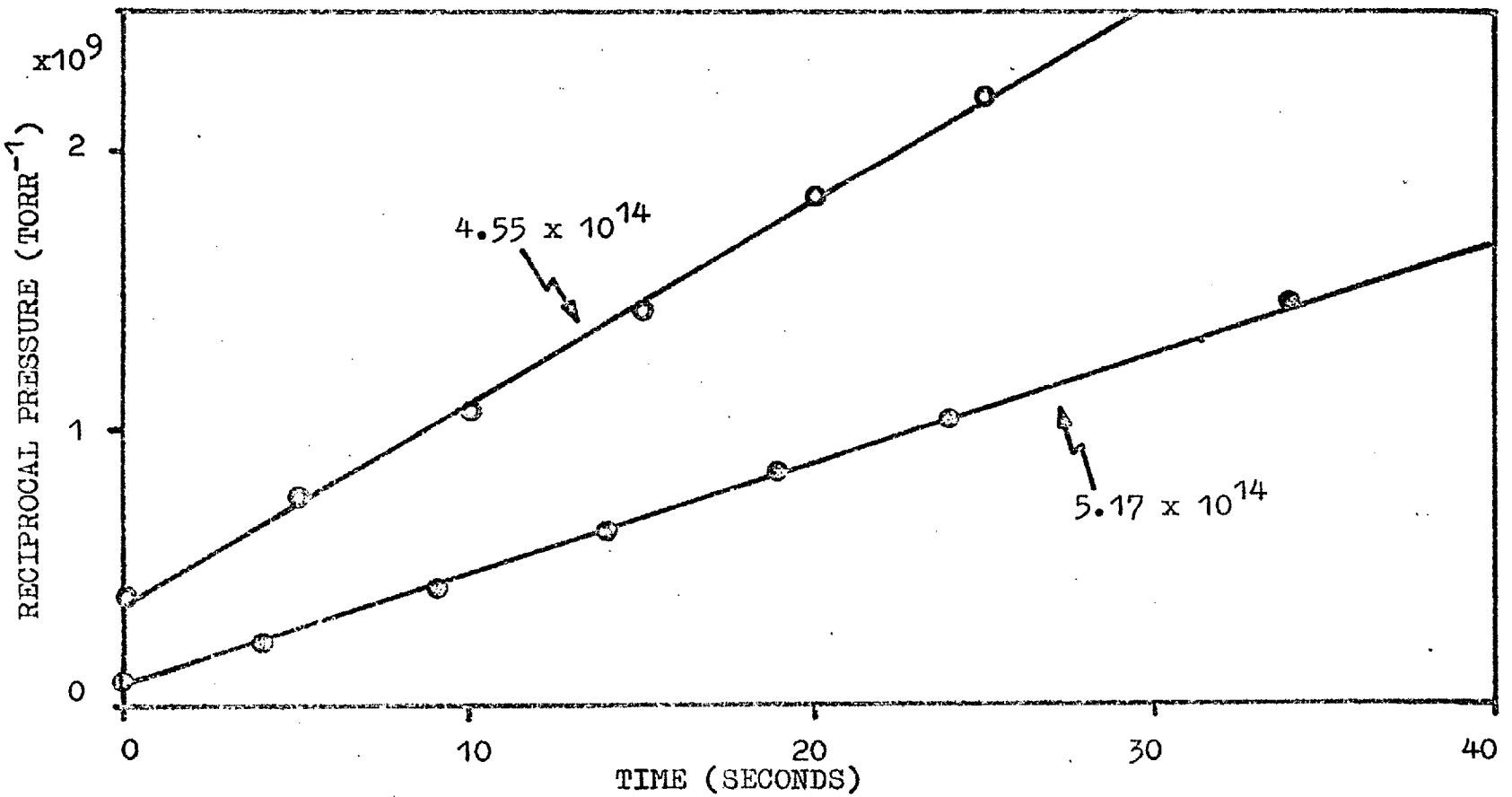

FIGURE 63(a). Reciprocal pressure versus time at 78°K. (The uptake in molecules per CM^2 geometric is indicated on the graph.)

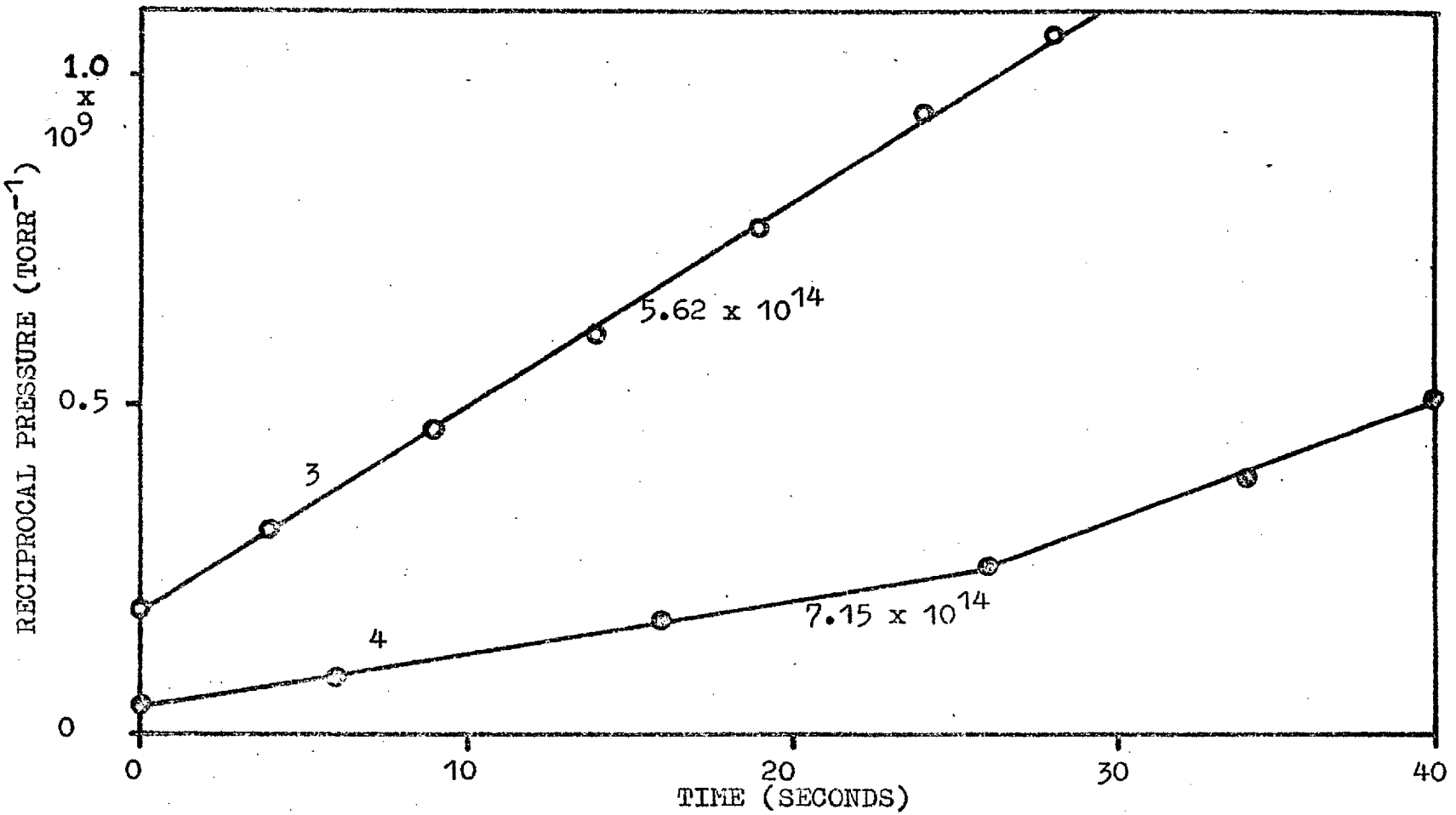

FIGURE 63(b). Reciprocal pr ssure versus time at 78°K.

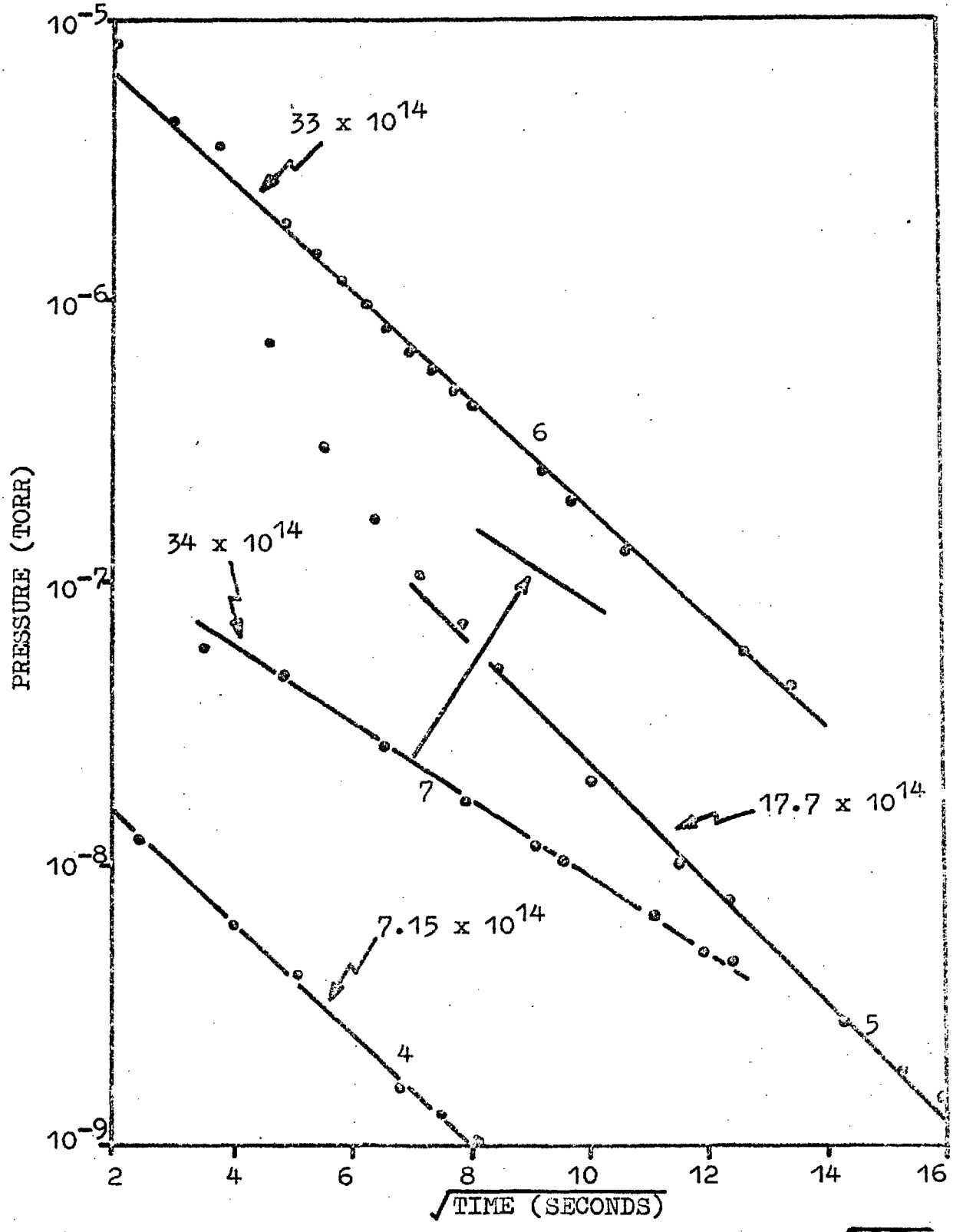

FIGURE 64. Logarithmic display of pressure versus $\sqrt{\text{time}}$ at 78°K (zero time is at gas supply closure).

observed on films of molybdenum and nickel viz reciprocal pressure varies linearly with time after closure of the gas supply. Figure 63 displays four such curves in the coverage range 4.5 to 7.2 x 10^{14} molecules per cm^2 geometric area (run 17.6.64). The slopes of the curves are approximately the same as observed initially with films of molybdenum and nickel i.e. 10^8 to 10^7 torr $^{-1}$ per second.

At coverages higher than 7 x 10^{14} molecules per cm^2 the reciprocal pressure - time relationship becomes non-linear as exemplified by curve 4 on figure 63 and the kinetics are represented by the expression $\ell n \frac{P^o}{P} = k t^{\frac{1}{2}}$ where P^o, P are the pressures at zero time (i.e. at gas supply closure) and time t respectively. Figure 64 displays several such curves (also for run 17.6.64) including the results shown previously as reciprocal pressure versus time on curve 4 figure 63. The constant k decreases from about 0.5 to 0.3 in the coverage range investigated and is relatively independent of the flow rate to the film prior to supply closure. As mentioned earlier, isotherms for a true gas - surface equilibrium cannot be constructed for the hydrogen-titanium system because of the effects of absorption. However, if Temkin type behaviour is assumed then the kinetics of

the '$t^{\frac{1}{2}}$' diffusion may be represented by the expression $(N^{o} - N) = k' t^{\frac{1}{2}}$ where N^{o}, N are the concentration in the Temkin layer at zero time and time t respectively and k' is a constant which includes k and the Temkin constant. This form of the kinetics suggests a random walk diffusion process and it was hoped that a simple physical model could be devised to fit the experimental results.

One difficulty is that, when the surface is not uniformly covered, there is a gas phase diffusion competing with the '$t^{\frac{1}{2}}$' process. However, transport via the gas phase decreases more rapidly with falling pressure and will only influence the second process during the initial stages of pressure decay. A second, and more serious, difficulty arises from the form of the experimental kinetics. During the latter stages of a pressure decay (i.e. when $\ell n P$ is linear with $t^{\frac{1}{2}}$) an estimate of the rate of transport of gas may be made if a reasonable value of the Temkin constant is assumed (say $\sim 10^{-13}$ per molecule per cm^{2}). This rate is not negligible compared with the flow rate to the cell and a concentration gradient must be expected to exist within the system at the time of closure of the gas supply. Thus the true time zero of the diffusion process (i.e. when the concentration gradient is zero along the distance axis) should be prior to

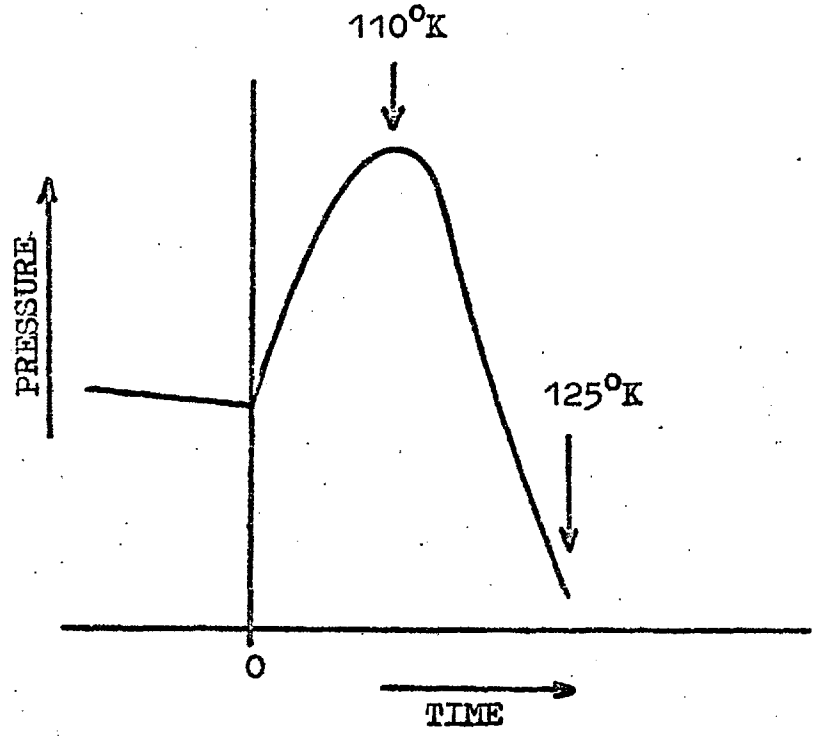

FIGURE 65. Desorption spectrum on warming a film previously saturated at 78°K. (Reaction vessel unlagged, liquid nitrogen bath removed at zero time.)

the time of closure of the gas supply - such a correction is found to be unnecessary to 'fit' the experimental results to a straight line!

Studies in the field emission microscope have shown a general immobility of hydrogen adatoms at 78°K on a range of metals and it will be assumed that such a situation exists on titanium i.e. that the '$t^{\frac{1}{2}}$' process is in fact bulk phase diffusion. This correlates with the observation of uptakes at 78°K which are too large to be solely on the surface and also with the very rapid diffusion processes observed at high temperatures (195°K, 300°K). The temperature at which the diffusion becomes rapid compared with the time scale of the experiment has been estimated from the 'desorption spectra' of films which had been previously saturated at 78°K. Figure 65 displays one such spectrum - the rapid fall in pressure between 110 and 125°K is most probably due to the onset of a rapid bulk phase diffusion which cannot, therefore, have an activation energy exceeding about 7 kilo-calories per mole.

Any simple process in which the amount diffused after time t is proportional to $t^{\frac{1}{2}}$ may be expected to involve a constant concentration at or just within the surface (see "Mathematics of Diffusion" by J. Crank,

pages 35 - 36) and also a constant concentration within the solid at zero time. The latter condition has been mentioned above and does not appear to be fulfilled. It is still interesting, however, to consider how the first condition (constant concentration of diffusing species near the surface) is or could be maintained. It has been mentioned previously (section 14.3) that the bulk site to bulk site activation energy is probably rate controlling since the measured sticking probability is a function of both the flow rate to the film and the total uptake. If the activation energy for passage of gas from surface to a subsurface layer is lower than for bulk diffusion then the subsurface may be maintained nearly full while gas lost by diffusion can be replaced from the surface.

14.6 Phase equilibria in the hydrogen-titanium system

No mention has been made in previous sections of the various phase equilibria which exist in the hydrogen-titanium system since these were not essential to the general arguments put forward. However, rates of diffusion of hydrogen through the various phases have been measured and some considerations are pertinent to a more general discussion.

It is well established [see for example M. Hansen,

Constitution of Binary Alloys, (McGraw-Hill Book Company, Inc., New York, 1958)] that the hydrogen-titanium system exhibits three distinct phases - α , β and γ. The α phase is essentially a solid solution of hydrogen in the hexagonal close packed metal lattice; it is not known whether the preferred sites have tetrahedral or octahedral symmetry. Below about 600°K the γ phase develops in equilibrium with the α phase at overall compositions greater than about 5 atomic % hydrogen at 300°K and at progressively lower compositions as the temperature is decreased. The γ phase has a face centred cubic structure with a minimum hydrogen composition of around $TiH_{0.7}$ at 300°K. Progressive filling of vacancies in the γ phase gives a final composition of around $TiH_{1.98}$. At temperatures higher than 600°K a body centred β phase may exist either alone or in equilibrium with α or the γ phase.

Rates of diffusion of hydrogen have been measured in all three phases by a variety of techniques. Stalinski, Coogan and Gutowsky (1961) have used proton magnetic resonance techniques on a powder sample held between 78°K and 400°K and obtain activation energies for diffusion in the γ phase of 9.4 $\pm$ 0.5 kilocalories per gm atom at composition $TiH_{1.607}$ and 10.4 $\pm$ 0.5 kilocalories per gm atom at $TiH_{1.93}$. An analysis of their results indicates the possibility of a linear

increase in the activation energy with hydrogen composition. Using a similar experimental technique Spalthoff (1962) obtained an activation energy for diffusion of hydrogen of about 6 kilocalories per gm atom in the γ phase at composition $T_1H_{1.98}$ within the temperature range 420 to 570°K. Coogan and Gutowsky (1962) have further treated the diffusion of hydrogen in the γ phase in terms of a simple electrostatic model and conclude that migration is between tetrahedral vacancies in the lattice, with an octahedral site as the 'saddle point' along the (curved) diffusion path. (It is interesting to note that the concept of a partially positively ionized hydrogen atom within the lattice although used by Coogan and others is not universally accepted - Gibb (1962) considers a hydride model to be more appropriate and accounts for the rapid hydrogen diffusion within the lattice by proposing a quasi-tautomeric structure of the transition state).

Rates of diffusion of hydrogen in α and β phases have been obtained using transport techniques. Wasilewski and Kehl (1954) found at 'high temperatures' values of 12.4 and 6.44 kilocalories per gm atom for α and β phases respectively using samples of relatively low hydrogen composition.

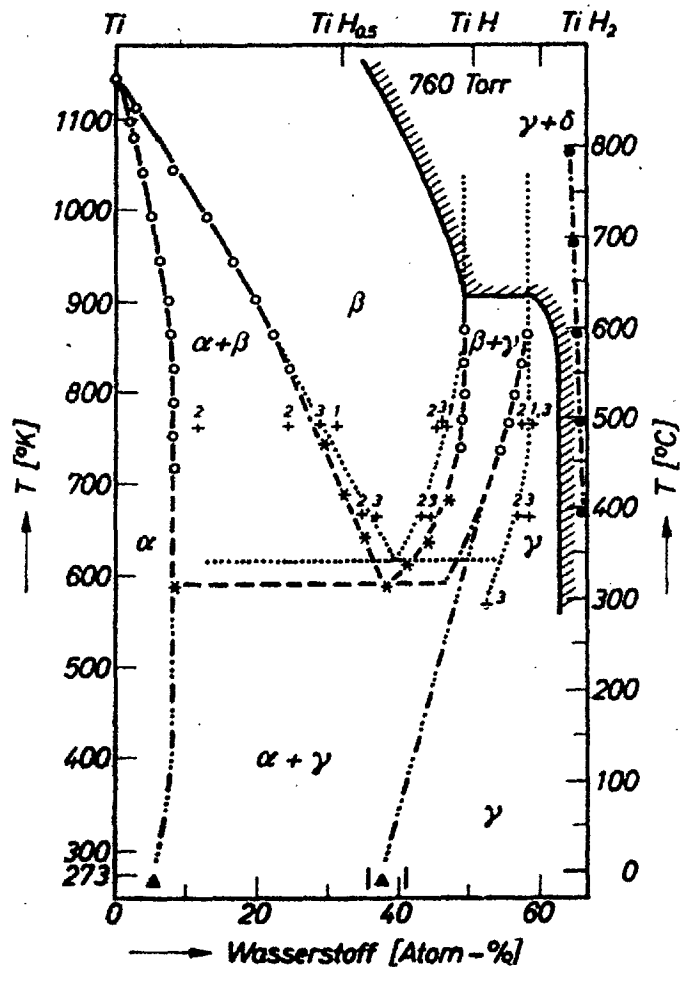

Abb. 7. Zustandsdiagramme des Systems Titan-Wasserstoff —o—o— McQuillan[12] (experimentell), —*—*— McQuillan (extrapoliert), ·····+·····+····· Haag und Shipko[9] (1 = H_2—Ti-Folie; 2 = H_2—Ti-Pulver; 3 = D_2—Ti-Folie), —·—·● —·—●—·— Gibb[11], ——·—▲—·—▲—·—— eigene Messungen

It was proposed in an earlier section that the region of near constant sticking probability at 300°K and 195°K was due to a constant surface condition - it now remains to reconcile this with the concept of a steady conversion of α to γ phase with increasing hydrogen composition. There is one feature of the phase diagram which readily correlates with details of the S versus uptake curve - namely the point of onset of a decrease in S and that of the final disappearance of α phase. Both are observed at a composition around $TiH_{0.7}$ at 300°K (see the table of θ_2 values in section 14.3 and the phase diagram of Wedler and Strothenk (1966) reproduced here for convenient reference). This is some evidence that the 'normal' phase diagram applies to film absorbents since the falling absorption heat with composition in the pure γ phase region will be reflected, on the basis of the proposals in 14.3, in an increase in adsorbate concentration and thus in a lowering of S. In the two phase region one possibility is that the γ phase nucleates readily near the surface and further uptake occurs via diffusion through this layer. Reference to values of θ_1 in section 14.3, however, shows that the region of constant S is reached at uptakes equivalent to a few 'monolayers' of gas - the lattice distension over such a large area may be insufficient to create

nucleation. (It is worthwhile noting that the nucleation of a second phase within a phase of smaller lattice constants is inhibited by the distension produced - this concept has been utilized by Everett and Nordon (1960) and Scholtus and Keith Hall (1963) to explain hysteresis in the α-β transformation of the hydrogen-palladium system. This influence will be lower near a surface and for the small crystallites of which the film is composed.) If γ phase exists near the surface in the manner described then there is still difficulty in explaining why the concentration in the adsorbed layer is not a function of the duration of gas flow interruptions since the two phases would not be in thermodynamic equilibrium nor (judging from measured activation energies) near a steady (i.e. time independent) state.

A second and stronger proposal is that the α and γ phases are near true equilibrium both during and subsequent to gas uptake. This is expected by virtue of the low activation energies for diffusion giving high mobility at 300°K and 195°K. (An activation energy of 10 kilocalories per gm atom gives around 10^6 hops per atom per second at 300°K and about 10^2 hops per second at 195°K.) Thus we have the situation in which each phase is in equilibrium with essentially similar surface phases i.e. the adsorbate composition is fixed

while α and β phases co-exist.

At 78°K it has been shown (section 14.5) that under the conditions of high surface cleanliness the sorption is probably diffusion controlled. Unfortunately transport methods have not been refined to eliminate surface contamination at low temperatures and there is the possibility that the surface to subsurface stage is modified by adsorbed 'foreign' species such that it becomes rate controlling. This view is in line with the results of Silberg and Bachman (1958) for the hydrogen-palladium system which showed that passage of hydrogen through the membrane was a sensitive function of surface area but was relatively independent of membrane thickness.

Presumably in the low temperature region the α and β phases still coexist but since mobility of hydrogen atoms is greatly reduced there may not be even an approach to equilibrium. Thus the activation energies in the individual phases are critical in determining both the sorption rate during gas uptake and also the redistribution process observed after closure of the gas supply. It is hoped that a comprehensive model of diffusion into a two phase system can be devised to eliminate the various anomalies in the form of the redistribution kinetics which have previously been discussed in section 14.5

15. HYDROGEN ON TANTALUM

15.1 The uptake

All films of tantalum were deposited with the substrate at around 100°C i.e. they were somewhat sintered. The weight of the deposits varied widely due to 'premature' burning out of the filament during evaporation. Several attempts were made to estimate film weight from the weight loss of the filament; these failed because of the extreme brittleness of the tantalum filament after film deposition.

Hydrogen was absorbed into tantalum films at 78, 90 and 300°K. The low temperature behaviour was similar to titanium in that the apparent sticking probability was very low ($\sim 10^{-5}$) during the latter stages of absorption. At room temperature the system was unique in that absorption (as evidenced by slow but continuous drifts in the pseudo-equilibrium pressure above the film) was appreciable only at relatively high pressures ($>10^{-6}$ torr). Films required from 2-10 x 10^{16} molecules per cm^2 geometric area to approach saturation. (The latter term refers to a 'pseudo-equilibrium' pressure of about 10^{-3} torr; the reason for this choice will become apparent in later sections). The only data available for hydrogen adsorption/absorption on tantalum films is due to Beeck (1950)

who used calorimetric techniques to measure the heats of adsorption and absorption. Beeck, in presenting his data, refers to absorption of 860 x 10^{18} for attainment of equilibrium pressure of 1.3 torr at 300°K but unfortunately fails to give the weight of the film. (Beeck's data cannot refer to 100 mg of film in this instance as this is equivalent to a hydride composition of TaH_5). Further reference will be made to the above work when dealing with absorption at room temperature. The weights of film deposited in our experiments were probably in the range 10 to 30 mg. This would indicate a stoichiometry approaching that of the bulk hydride TaH.

15.2 The sticking probability at zero coverage

Run	S_o	T_{Film} (°K)
22.4.64	0.42	300
27.4.64	0.44	90
20.4.64	0.42	300
7.10.64	0.44	300
	0.47	90
5.6.64	0.48	78

The table includes the values of initial sticking probability (S_o) for several experiments at 78, 90 and 300°K. In run (7.10.64) about 3.5 x 10^{13} molecules per

cm^2 geometric area were adsorbed at 300°K before cooling to the lower temperature. As with other metals S_o was independent of flow rate within the range studied i.e. about 2×10^{11} to 3×10^{12} molecules per cm^2 per second. In view of the high melting point of tantalum (3000°K) the film surface is expected to be very rough and S thus enhanced by 'multiple collisions'. For molybdenum it was assumed that the sticking probabilities were 0.35 and 0.7 over plane and rough surfaces respectively. If the same probability of a multiple collision is assumed for tantalum then the sticking probability over a plane surface is about 0.12 - 0.13. If α is the probability that a molecule, having collided with the rough film surface and been reflected, will collide with it again rather than reach the void of the reaction vessel then it is readily shown that

$$S_F = \frac{S_T}{1 - \alpha + \alpha S_T}$$ where S_T and S_F are the sticking probabilities over plane and film surfaces. This expression was used to calculate the above data.

15.3 The sticking probability as a function of coverage

15.3.1. The 'adsorption' region.

At 300°K the sticking probability falls with

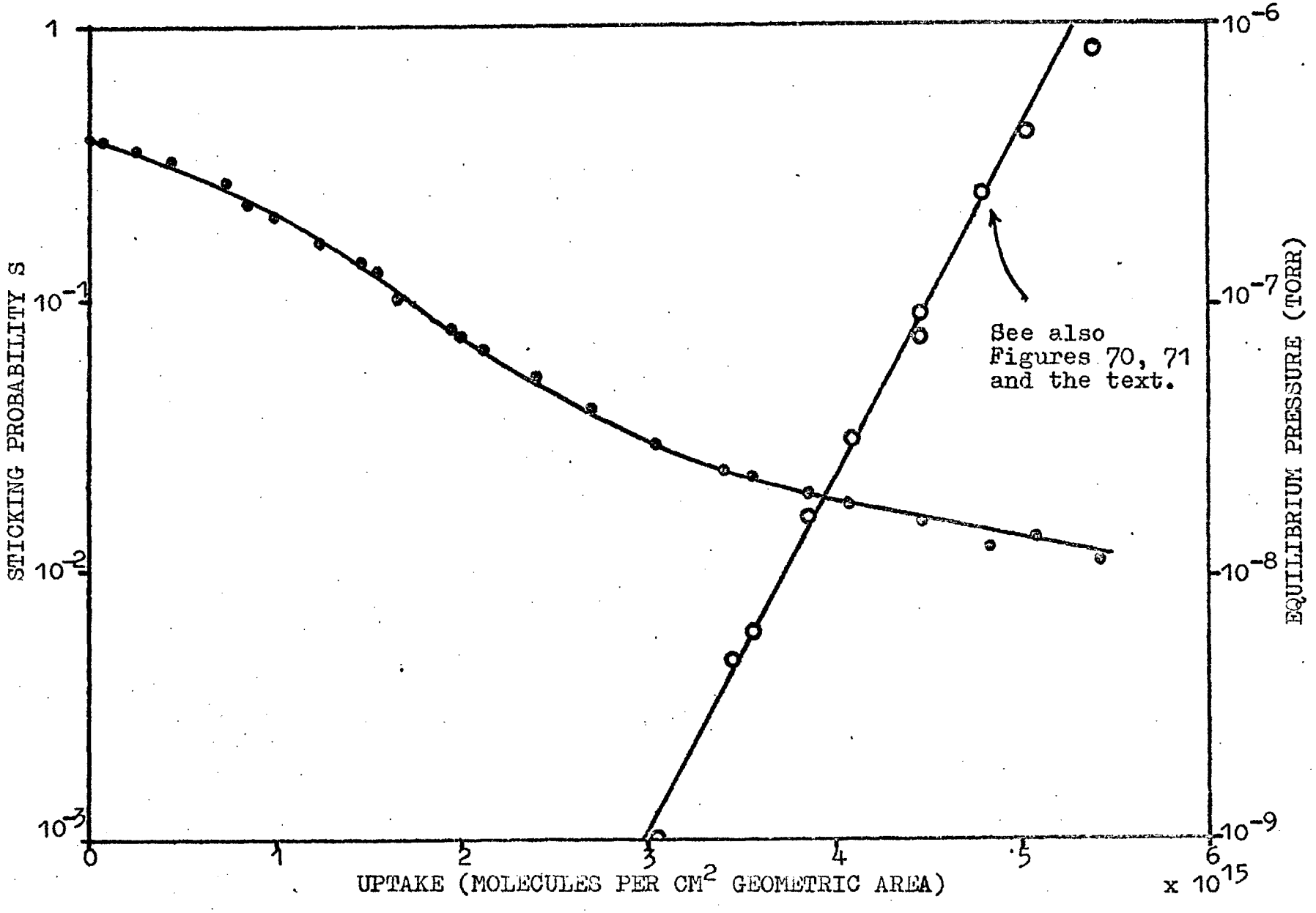

FIGURE 66. S versus uptake at 300°K.

increasing coverage until at $S \sim 3 \times 10^{-2}$ equilibrium pressures become measurable ($>10^{-10}$ torr). This contrasts with films of molybdenum, nickel and palladium at 300°K on which S falls to around 0.32, 0.26 and 0.8 respectively at a similar equilibrium pressure. Figure 66 displays a typical curve at 300°K. It may be noted that, as with the other metals mentioned above, there is a flattening off of the true sticking probability (i.e. that calculated from the sharp changes in pressure at interruptions of gas flow) at coverages where equilibrium pressures are readily observed. In the case of tantalum, S is comparatively low in this region and the phenomenon is most readily observed. Thus, in one experiment at 300°K (3.6.64) it was possible by using a high flow rate (4×10^{13} moleculesper sec.) to measure a true sticking probability at equilibrium pressures of about 10^{-4} torr. The value obtained at a coverage of 1.5×10^{16} molecules per cm^2 geometric area was around 1×10^{-2} thus demonstrating near constancy of S over a wide range (see figure 68) and also a virtual independence of S on flow rate to the film.

At 78, 90°K the sticking probability curves in the initial region are similar to those of Mo, Ni and Ti. The values obtained from ΔP_2 (figure 23) lie

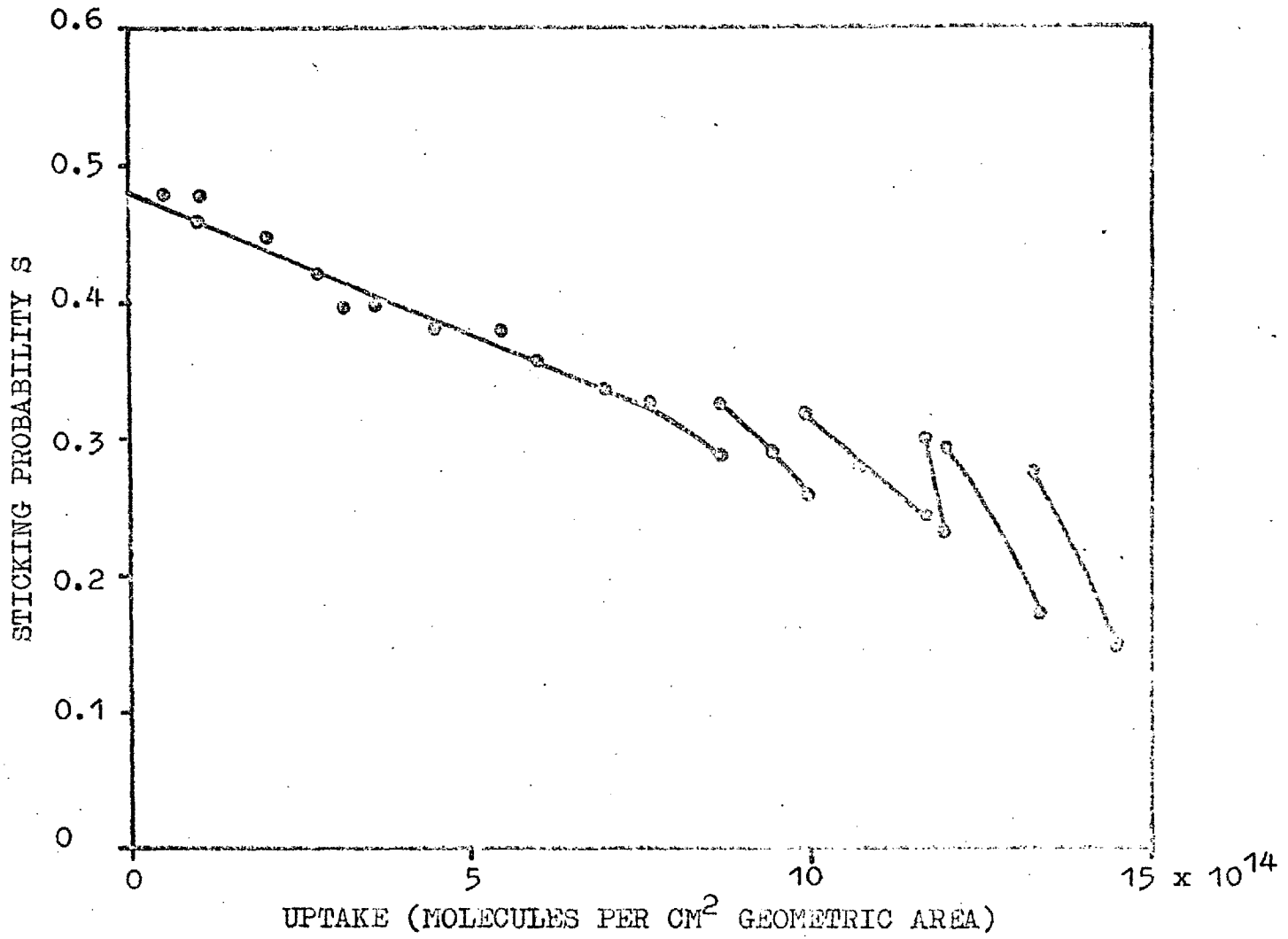

FIGURE 67. S versus uptake at 78°K.

around 0.26 up to coverages of about 4 x 10^{15} molecules per cm^2 geometric area. Figure 67 illustrates the variation of S with coverage during the initial stage of adsorption at 78°K.

In several experiments the films were warmed to 300°K after gas additions at 78 or 90°K and on recooling to the low temperature the initial sticking probability was around 0.34 and independent of coverage up to at least 18 x 10^{15} molecules per cm^2 geometric area (see for example the results displayed in figure 75).

Slow redistributions are observed on closing off the gas supply at coverages greater than about 9 x 10^{14} molecules per cm^2 geometric area. As with other metals, the onset of redistribution may be observed with greater sensitivity from the recovery of S during gas flow interruptions.

15.3.2. The 'adsorption' region.

At 300°K the observed pseudo-equilibrium pressures are relatively independent of time e.g. the drift is around 10^{-2}% per second at 10^{-8} torr; at higher pressures the drift is more marked - around 1% per second at pressures greater than 10^{-5} torr. At a flow rate of 2 x 10^{13} molecules per cm^2 and a temperature of 300°K the pseudo-equilibrium pressure becomes

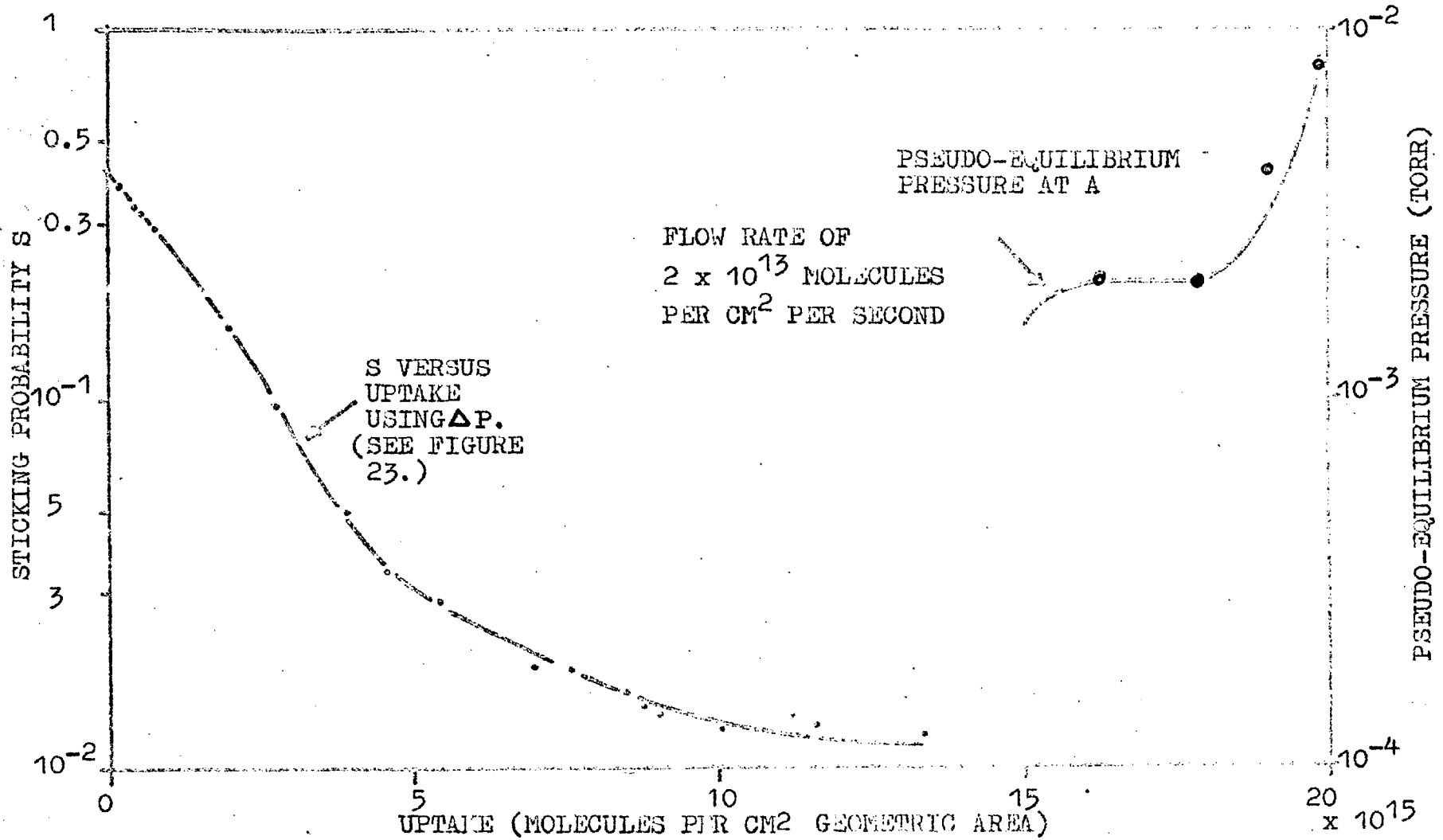

FIGURE 68. Adsorption and at orption at 30(°K.

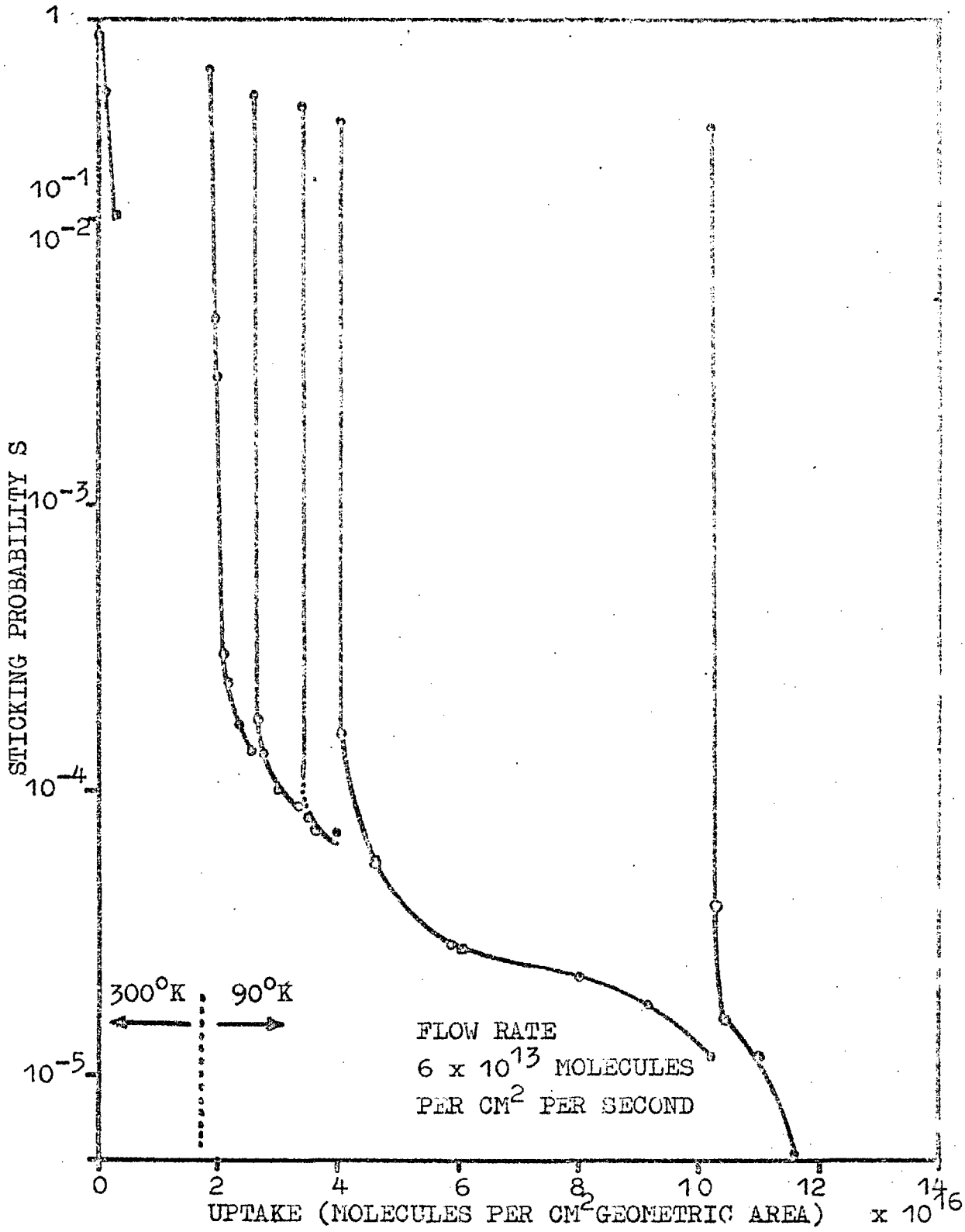

FIGURE 69. Absorption at 90°K.

nearly constant at about 2 x 10^{-3} torr - all gas entering the reaction vessel is now being absorbed. Figure 68 illustrates one attempt to saturate a film at 300°K.

The results of Beeck (1950) are very pertinent to this section since, from his data, it is possible to deduce the onset of the absorption process at 300°K. Beeck observes a heat of adsorption falling from about 39 kilocalories per mole to 14 kilocalories per mole after which point the heat curve changes slope as absorption proceeds. This agrees with the data reported here in that absorption is appreciable only in the region where measurable equilibrium pressures exist i.e. where the heat is about 16 kilocalories or below at 300°K.

At 78 and 90°K the absorption occurs with a low apparent sticking probability; figure 69 shows a typical curve at 90°K. As at room temperature the sticking probability calculated from the sharp pressure changes is almost independent of both uptake and the flow rate to the film. The latter was varied by a factor of 40 in one experiment (22.4.64), S was essentially constant up to at least 80% of the total uptake. In contrast the sticking probabilities calculated from the total reaction vessel pressure are

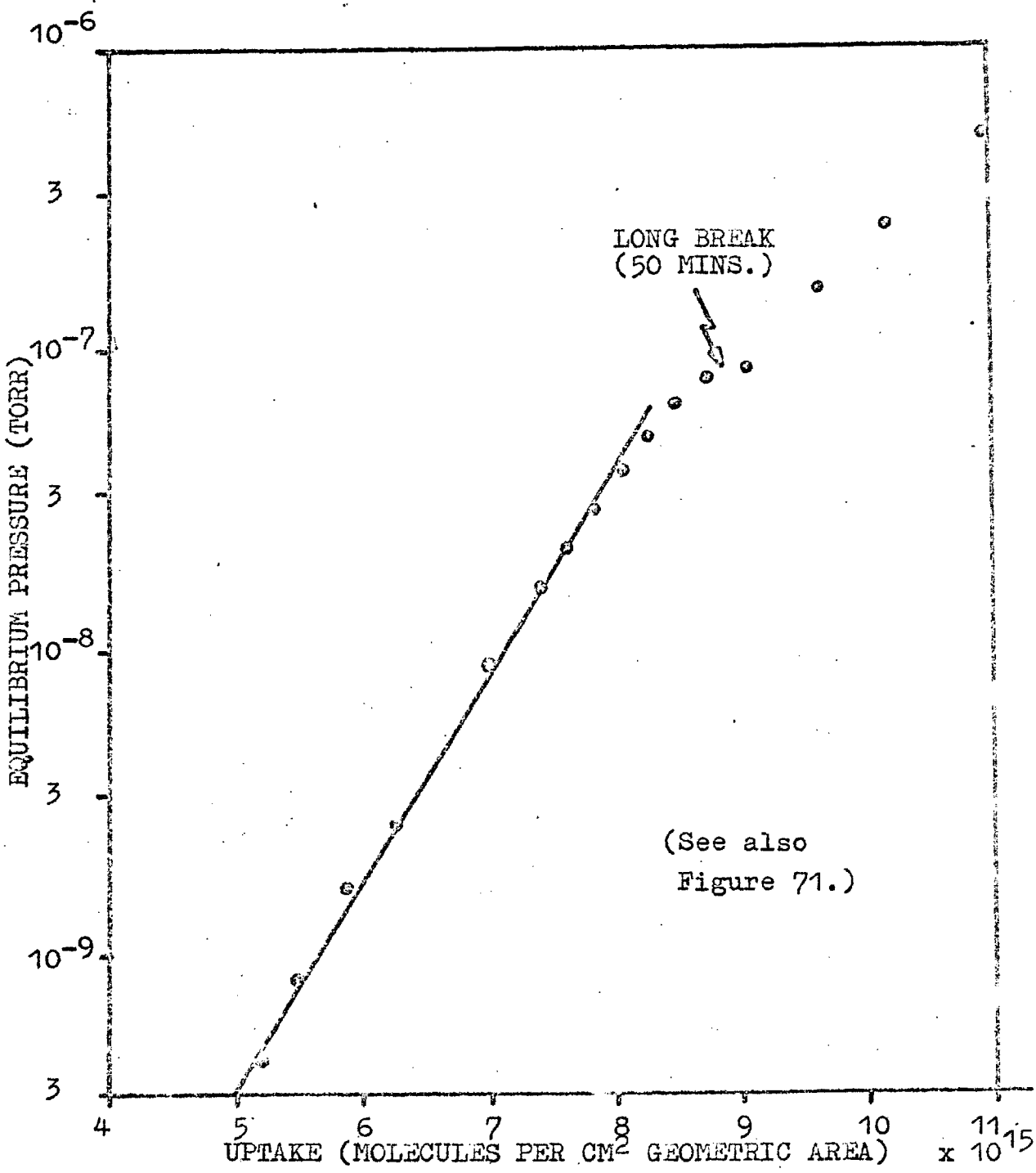

FIGURE 70. Display of equilibrium pressure data at 300°K as a Temkin isotherm.

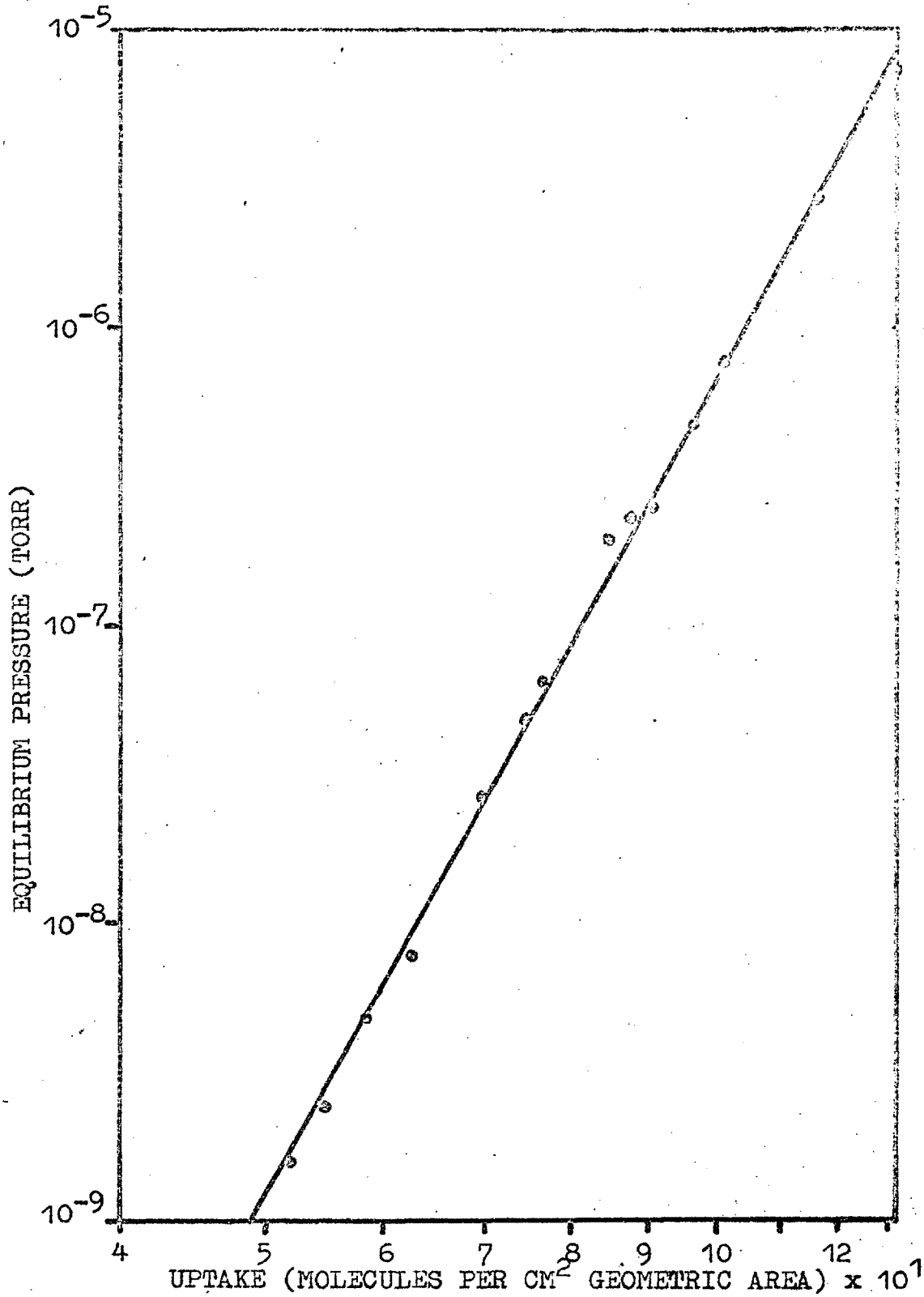

FIGURE 71. A Freundlich isotherm at 300°K. (Same data as Figure 70.)

not independent of flow rate. For the last mentioned experiment an approximate relationship was $P_1 = (CP_2)^{0.69}$ (P_1 - gas reservoir pressure, P_2 reaction vessel pressure, C - a constant) at coverages between 4 and 6 x 10^{16} molecules per cm^2 geometric area for a variation in P_1 of 30 times.

15.4 Redistribution processes.

At 300°K the Temkin equation is not obeyed even approximately except in the limited range 10^{-9} to 10^{-7} torr the decreasing slope of the isotherm is at least in part due to removal of surface gas by absorption. Attempts were made to correct for the effects of absorption but although the isotherm approached the Temkin form there was still some curvature. The same data as displayed in figure 70 was replotted as logarithm uptake versus logarithm pressure (figure 71). A straight line was obtained without recourse to any disposable parameter - the indicated relationship being N (molecules per cm^2 per geometric area) = $10^{16.55}$. $P^{0.1}$ (P, the equilibrium pressure in torr). This has the empirical form of a Freundlich isotherm; to demonstrate adherence to the non-empirical form requires measurements over a range of temperatures and is thus not possible from the results presented here. Unfortunately, the decays in equilibrium pressure

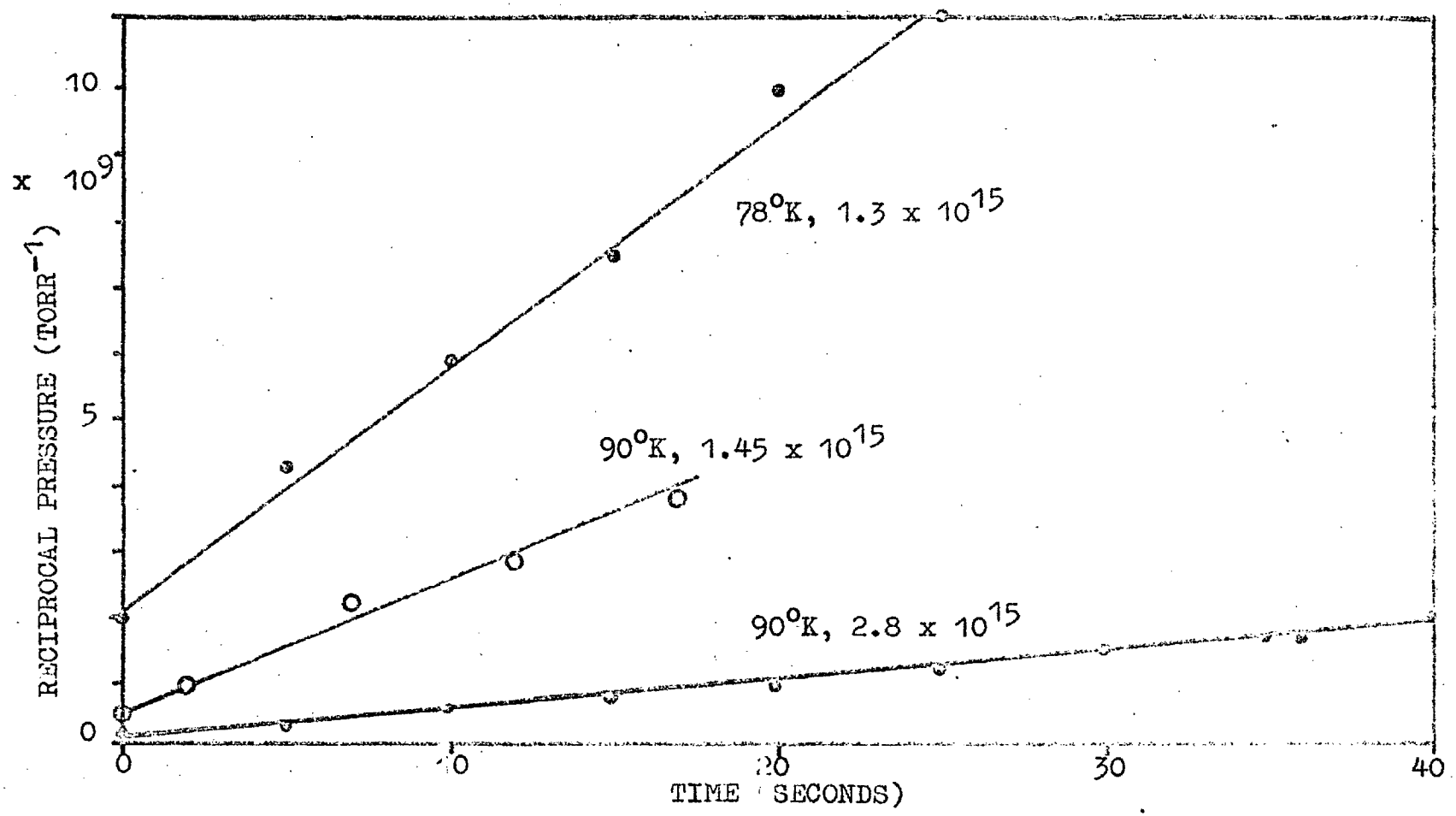

FIGURE 72. Reciprocal pr sure versus time t 78, 90°K

at 300°K were too slow to be conveniently studied over a large pressure range. Such results as were obtained suggest kinetics of the form logarithm of pressure linear with the square root of time i.e. as found for titanium (and tantalum) at 78°K.

At 78°K and 90°K slow redistributions are detected at coverages in excess of about 8 x 10^{14} molecules per cm^2 geometric area from the recovery of S during gas flow interruptions. The pressure decays after gas supply closure are too rapid to be quantitatively observed until around 1.4 x 10^{15} molecules per cm^2 have been added i.e. as for molybdenum films at 78°K. With titanium at 78°K it was demonstrated that the reciprocal pressure versus time relationship held over a small coverage range. This is also observed with tantalum at both 78°K and 90°K; three such curves are displayed in figure 72 for coverages between 1.3 and 2.8 x 10^{15} molecules per cm^2 geometric area. The gradients of the curves are virtually identical to those observed at similar coverages on films of molybdenum at 78°K. If it is supposed that the Temkin equation does not hold at 78°K then the kinetics of a gas phase diffusion might be expected to have a radically different form. However, Hayward, King and Tomkins (1967) have shown, using a similar argument to that used here for

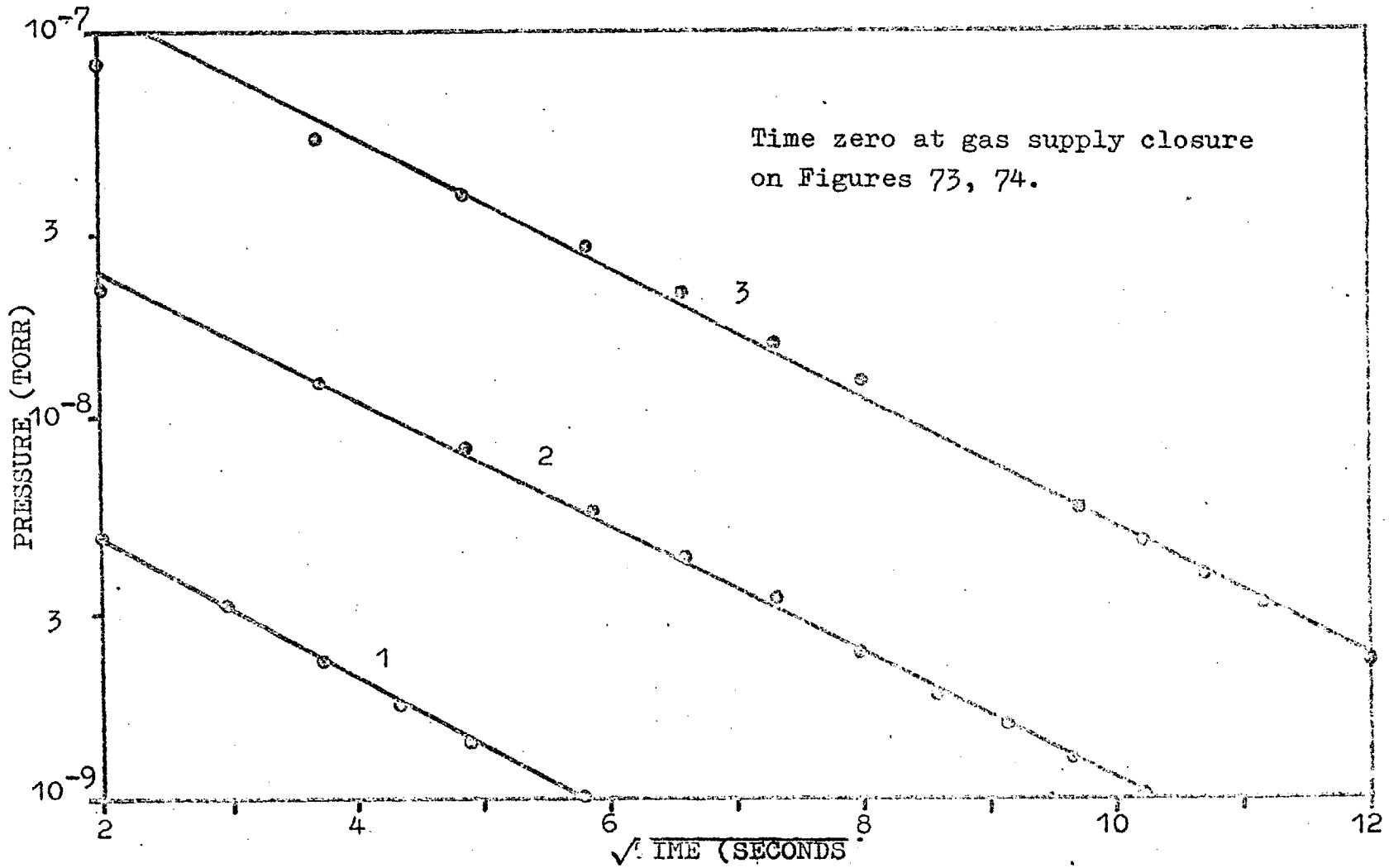

FIGURE 73(a). Logarithmi display of pressure versus $\sqrt{\text{time}}$ at 78°K.

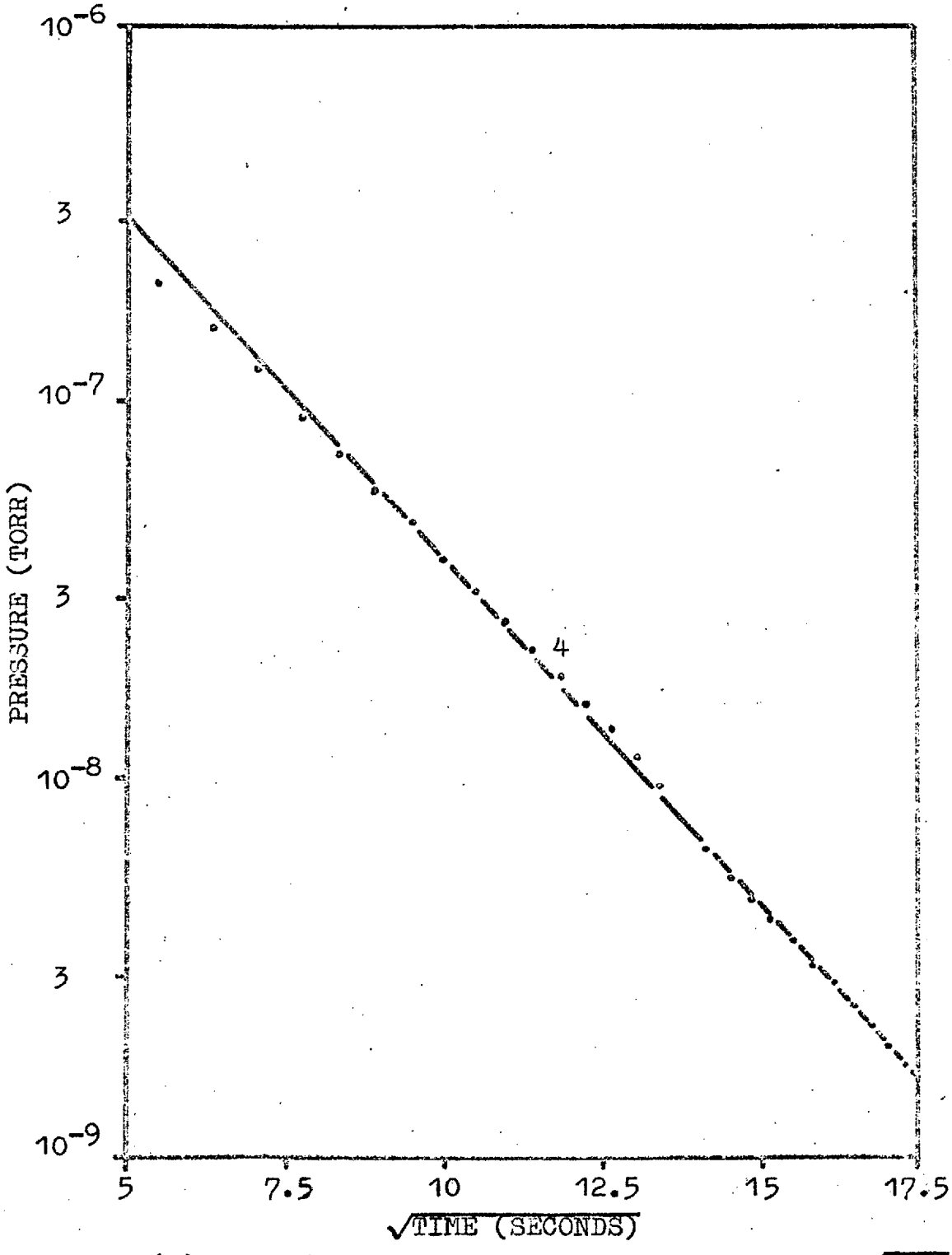

FIGURE 73(b). Logarithmic display of pressure versus $\sqrt{\text{time}}$ at 78°K.

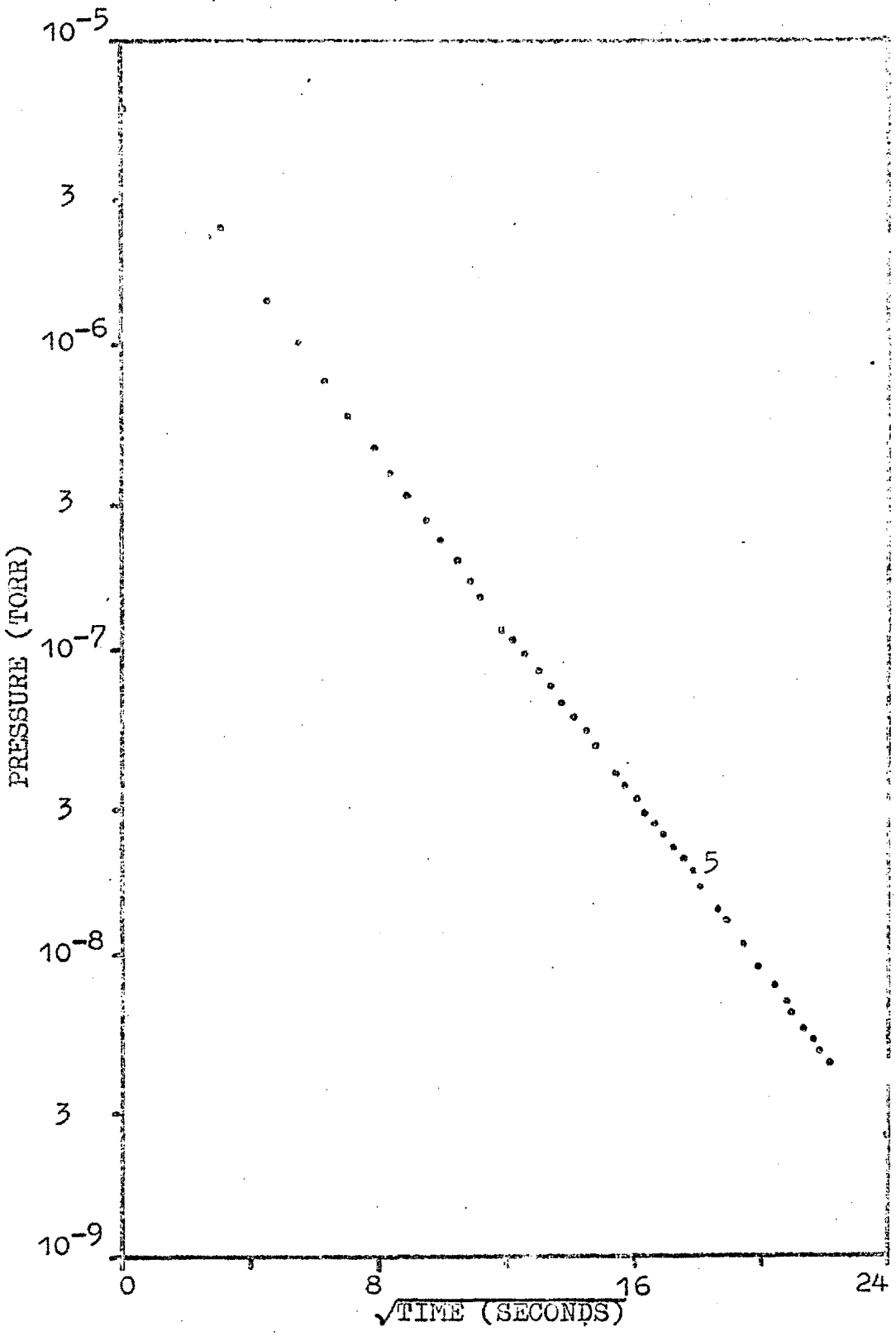

FIGURE 74. Logarithmic display of pressure versus $\sqrt{\text{time}}$ at 78°K.

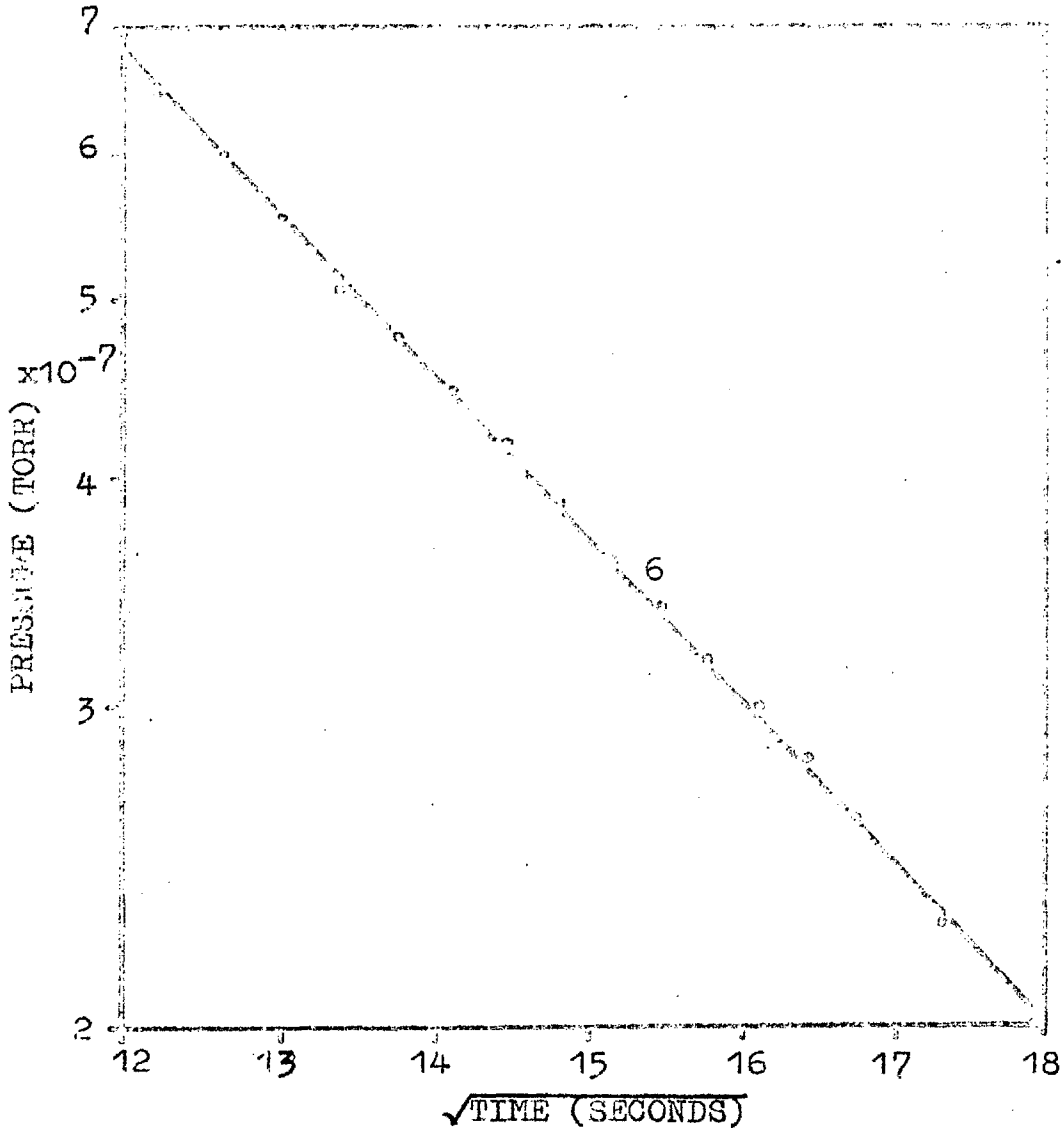

FIGURE 73(c). Logarithmic display of pressure versus $\sqrt{\text{time}}$ at 78°K

molybdenum, that, for a Freundlich type isotherm, the gas phase diffusion obeys the expression $P^{\frac{1-n}{n}} = K(t+t_o)$ where n is related to the coverage N and the pressure P by the expression $N = CP^{\frac{1}{n}}$ (C, a constant). At 300°K n is around 10 and assuming that the non-empirical forms of the Freundlich equations extend between 300°K and 78, 90°K then n is around 38 at the low temperatures. Thus the kinetics of redistribution will still be virtually 'reciprocal' in form!

At higher coverages at the low temperatures the pressure decay after closure of the gas supply follows the relationship logarithm pressure linear with the square root of time. Unfortunately the KNICK pico-ammeters were used for some me surements at this time and there was a non-linearity introduced on changing the current range thus giving a sharp break in the experimental curves. Figure 73 displays several results at 78°K and figure 74 a single result at 78°K (using the EKCO vibrating reed electrometer) which was linear over four orders of magnitude change in pressure. The gradients of the curves and the gas uptakes are included in the following tables (run 28.5.64).

The gradient is thus similar in magnitude to that observed with titanium at 78°K.

Gradient ($Sec^{\frac{1}{2}}$ per 2.7 change in P)	Uptake (molecules per cm^2 geom. area)
0.45	70.9×10^{14}
0.40	73.4
0.35	73.95
0.38	77.0
0.274	86.4
0.21	437

At 90°K the kinetics are similar in form but with gradients a few times larger than at 78°K. Unfortunately, no comparisons were made at the two temperatures using a single film.

The discussion given in section 14.5 applies here since again no t_o parameter is required to improve the linearity of the '$t^{\frac{1}{2}}$' curves. In formulating the kinetics as 'number diffused proportional to square root of time' there is the tacit assumption that the Temkin equation holds at the low temperature. This, particularly with tantalum, involves the not unreasonable assumption that the shape of the heat curve is different in form at high and low temperatures.

15.5 Desorption spectra

Desorption spectra were obtained with tantalum by rapidly warming films which had been previously

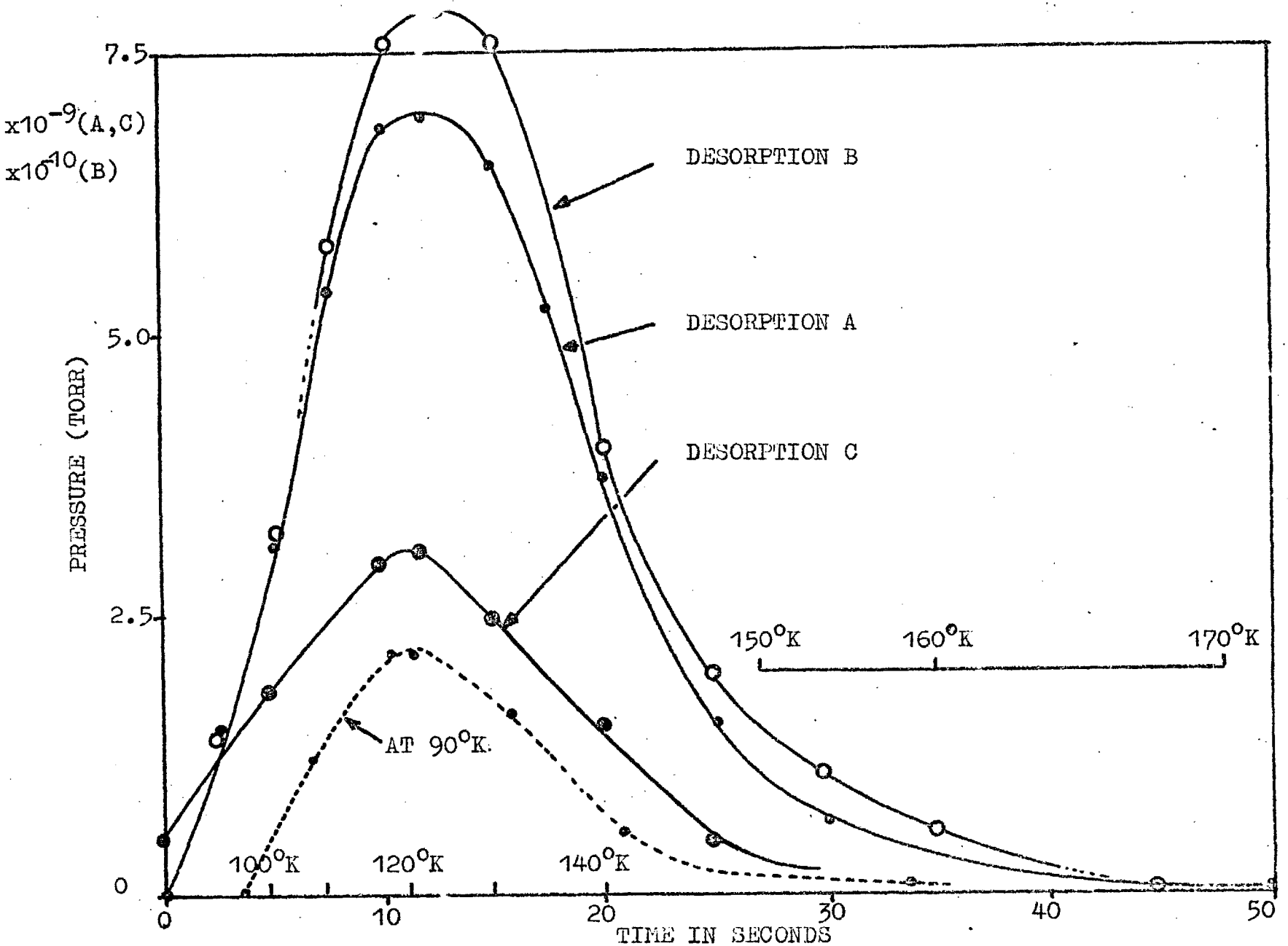

FIGURE 74. Desorption spec ra (see text and Figure 75).

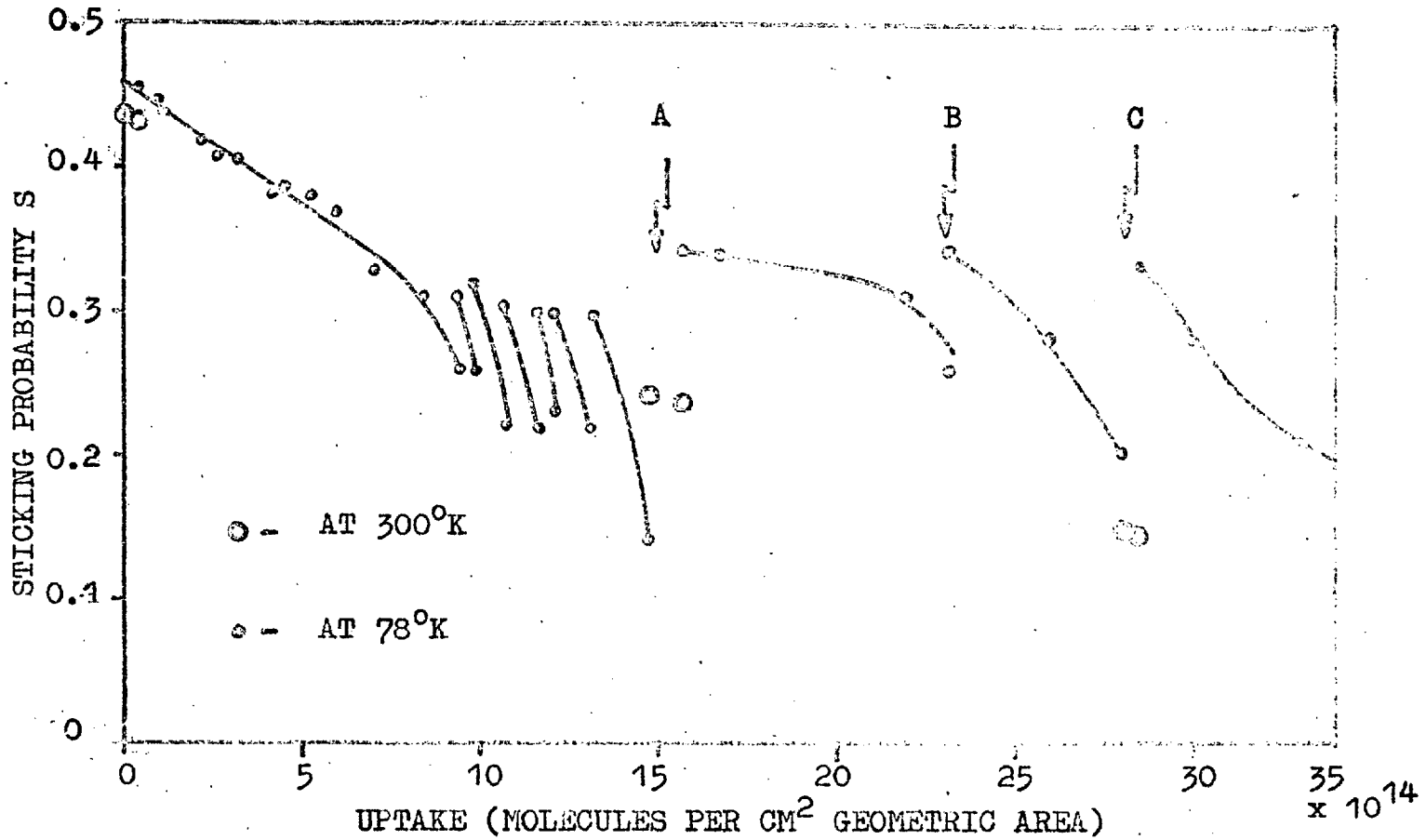

FIGURE 75. S versus uptake at 78, 300°K. A, B and C refer to the uptakes at which the desorption spectra displayed in Figure 74 were obtained.

partially saturated at 78° or 90°K; the temperature - time profile used was similar to that displayed in figure 43. The results are very similar to titanium-hydrogen spectra viz a rapid fall in pressure at temperatures above 110 - 120°K. Figure 74 displays three such spectra starting at 78°K and a single spectrum for an initial temperature of 90°K. The time axis of the latter has been displaced to make the temperatures coincident at about 110°K - there is excellent agreement in the temperatures at which the pressure rapidly decreases. The results at 78°K are for a single film to which gas was added at both low and high temperatures. Figure 75 illustrates the 'history' of the film prior and subsequent to the various desorptions. The number of molecules desorbed can be approximately calculated in the manner previously described in section 12.7. About 3×10^{13}, 3×10^{12} and 1×10^{13} molecules per cm^2 geometric area are desorbed in spectra A, B and C respe tively thus indicating that only a small fraction of the redistribution is via the gas phase. The numbers of molecules desorbed are approximately proportional to the amount of the preceeding uptake for which $S<0.31$ i.e. when the gas phase is in pseudo-equilibrium with the surface. This indicates that the amount desorbed is proportional to the total surface at 'virtual' saturation.

15.5 Phase equilibria in the hydrogen-tantalum system.

It has been seen that the phase equilibria in the hydrogen-titanium system are reasonably well understood; unfortunately the same cannot be said of the hydrogen-tantalum system. Waite, Wallace and Craig (1956) reported a tentative phase diagram for this system based on their own Xray and resistance measurements and on the heat capacity data of Kelly (1940). The heat capacity measurements were extended by Saba, Wallace, Sandmo and Craig (1961) but their other Xray data has not been published in detail. Stalinski (1954) obtained Xray data which conflicted with the proposals of Waite et al and it has been pointed out by Pedersen, Krogdahl and Stokkeland (1965) that Stalinski's results are consistent with α and β 'phases' differing only in the degree of distortion of a single cubic phase. It appears that the interpretation of Xray data might not be unique, which could be the reason for the large scatter in the reported values of the composition ranges at 300°K of the two phases (the α phase has been claimed to exist up to $TaH_{0.15}$, $TaH_{0.2}$, $TaH_{0.37}$ and $TaH_{0.5}$ in various investigations, likewise β phase has been reported at compositions greater than $TaH_{0.43}$, $TaH_{0.5}$ and $TaH_{0.6}$).

Rates of diffusion of hydrogen in the high temperature α 'phase' have been measured on powdered samples using proton magnetic resonance by Pedersen et al who obtained an activation energy of diffusion of 1.6 ± 0.4 kilocalories per gm atom between 200 and $400^{\circ}K$. The same workers obtain a value for a β_2 phase of 6.3 ± 0.6 kilocalories per gm atom which, as with the α phase, is apparently independent of composition. In contrast Pedersen et al find for the β phase at $TaH_{0.1}$? an activation energy of 3.7 ± 0.5 kilocalories per gm atom and an approximately linear decrease with composition to 2.6 ± 0.3 kilocalories at $TaH_{0.66}$. Spalthoff (1961) and Torrey (1958) find activation energies for diffusion of hydrogen of about 2.5 kilocalories per gm atom below $240^{\circ}K$, Torrey finds a value 5.8 kilocalories above $240^{\circ}K$.

Work presented in this thesis has indicated that the sorption of hydrogen into tantalum at 78, $90^{\circ}K$ was probably diffusion controlled at least during the redistribution process. This would indicate an activation energy for bulk diffusion of not less than about 5 kilocalories per gm atom i.e. considerably higher than most P.M.R measurements. Without further information it is not possible to decide whether the 'hydride' structure is basically different when gas uptake is at a low temperature (as in the sticking

probability experiments) to when there is prior formation at a high temperature.

16. HYDROGEN ON PALLADIUM

16.1 Stoichiometry and phase equilibria

The stoichiometry and the phase structure of the hydrogen-palladium system have been studied extensively by a wide variety of techniques. There is general agreement that two phases may exist at room temperature and below; the range of stability of these (α and β) phases has not been so clearly characterised. The α phase has been commonly regarded as a solid solution of hydrogen in the face-centred cubic palladium lattice with a maximum composition of about $PdH_{0.04}$ at 300°K. (see for example the neutron diffraction results of Worsham, Wilkinson and Shull, 1957). There is evidence, however, from resistance measurements (Lindsay and Pement, 1962) that a relatively long range order of hydrogen may exist in this phase. Above an overall composition of $PdH_{0.05}$ the β phase nucleates within the α phase - the minimum composition of the former is around $PdH_{0.5}$. The structure of the β phase has been recently determined by Worsham et al using neutron diffraction techniques, they conclude that in $PdH_{0.5}$ each face centred palladium atom is surrounded by four hydrogen atoms. The β phase

can take up additional hydrogen to an approximate composition $PdH_{0.7}$ (but see later). Formerly it was proposed that the zero paramagnetic susceptibility of the hydride $PdH_{0.6}$ was due to electrons from the hydrogen entering and filling the d band of the metal. Michel and Gallisot (1945) have shown conclusively that the effect is due solely to distension of the lattice. This, and other evidence, has caused Gibb (1962) to suggest that the weight of evidence favours a hydride model of the β phase. Gibb accounts for the high mobility of hydrogen within the lattice by proposing a quasi-tautomeric structure of the transition state for diffusion between lattice sites.

It has been previously mentioned that, generally, the limiting composition is found to be around $PdH_{0.7}$ irrespective of whether electrolysis or direct methods of formation are used. This is in good agreement with results obtained here during sticking probability measurements on sintered and unsintered films. The weights and overall compositions of various films are recorded in the following table - the latter stages of sorption are invariably at 78 or 90°K.

In contrast Suhrmann, Wedler and Schumicki (1959) obtained a maximum composition of $PdH_{1.5}$ at 78, 90 and 195°K using ultra-high vacuum evaporated films and Castellan, Hoare and Schuldiner (1958) obtained

RUN	FILM WEIGHT (mg)	HYDRIDE + COMPOSITION
22.1.64	47	$PdH_{0.68}$
¥28.1.64	60	$PdH_{0.7}$
5.8.65	31	$PdH_{0.46}$
12.8.65	36	$PdH_{0.50}$
27.8.65	29	$PdH_{0.60}$
¥10.11.65	53.4	$Pd_{0.66}$

¥ unsintered films, + for $S \sim 10^{-5}$ at 78°K or 90°K.

$PdH_{0.98}$ using an aqueous colloidal suspension of the metal. One possibility is that the metals so produced had a high concentration of defects which allowed additional uptake. The films of Suhrmann et al were deposited at 90°K and annealed at 373°K; it has been shown in this thesis that the surface structure (and presumably the bulk also) of films deposited in this way is entirely dissimilar to that obtained by deposition above 300°K.

Hysteresis has been observed in the α, β transformation e.g. Lambert and Gates (1925) obtained a typical 'loop' in their sorption/desorption isotherms. Gill spie and Galstaun (1936) claimed to have eliminated hysteresis by heat treating the sample to around 630°K between each addition or removal of hydrogen but their conclusions have been questioned by

Everett and Nordon (1960) who consider that there is no reversible transition between the two phases. The latter workers propose that the nucleation of the β phase can be arrested by lattice stress due to an abrupt increase in lattice parameter on forming β phase. The effect of the stress is expected to diminish with crystallite size thus offering an explanation of the data of Nace and Aston (1957) which indicated a low hysteresis effect in a sample of palladium black. The view of Everett and Nordon is in contrast to that of Nace and Aston who consider that, during desorption, β phase near the surface reverts to α phase thus explaining the abrupt drop in equilibrium (i.e. time independent) pressure. There will be further discussion of the hysteresis effect in a following section.

16.2. The sticking probability of zero coverage

The accurate measurement of sticking probabilities of hydrogen on palladium films near zero coverage has been extensively considered in previous sections. The results were presented for sintered films at 78°K and it was concluded that $0.99 < s < 0.998$. Results for unsintered films gave virtually identical values to the above - this is expected since the enhancement effect decreases to zero as the sticking probability approaches

unity. Unfortunately, data of a similar accuracy was not obtained at 300°K as only 'normal' flow methods were used. An analysis of results, however, indicates that values near unity are also obtained at room temperature.

It is of great interest to consider why the sticking probability approaches but does not quite attain a value of unity. The sintered films are undoubtedly relatively smooth in view of the low melting point of palladium (c.a. 1825°K)and the magnitude of s should nearly correspond to that for a smooth surface exposing a similar set of crystal planes. No sticking probability data has been previously reported for the hydrogen-palladium system; the discussion must therefore be confined to the results of the present work and to those obtained with certain other systems which also exhibit a value of s near unity. Before considering the theoretical interpretations of the results it is necessary to discuss one experimental artefact which could explain the departure of s from unity at zero coverage - namely 'precoverage' of the film prior to gas admission. It will be shown (in more detail) in the next section that s falls continuously with gas uptake and since s was very high the precaution was taken of only allowing

hydrogen into the gas reservoir just prior to its release to the film. The only possible source of appreciable hydrogen is thus the evaporation filament; this was made negligible by prolonged outgassing of the filament (run no 10 figure 20) such that there was virtually no pressure change after evaporation was completed - s was still less than unity!

The high initial sticking probability for the hydrogen-palladium system indicates that the energy accommodation and the adsorption are virtually independent of the crystal planes exposed to the gas. This is further substantiated by the similar values recorded for sintered and unsintered films. Apart from deposition of metal atoms or condensation phenomena (i.e. adsorption of atom or molecule on to its own lattice) the only reliable recorded values of s near unity are due to Bell and Gomer (1966) and King (1966) both for the carbon monoxide-tungsten system. Gomer and Bell considered that the gas temperature was an important factor in determining the magnitude of s. In contrast King finds no variation in s (from unity) with gas temperature within the range $78^{\circ}K$ - $300^{\circ}K$ for carbon monoxide adsorption on tungsten films at $78^{\circ}K$. Thus in the latter system energy accommodation is probably complete irrespective of the kinetic energy of the incident molecule.

There are three major possible reasons as to why s^o is not unity in the hydrogen-palladium system.

1) The non adsorbed molecules might be reflected at some particular crystal plane or defect which occupies about 0.5% of the exposed surface. This would not appear to explain the similarity in values of s using sintered and unsintered films unless by chance the latter exposed a similar proportion of reflecting surface. There may, however, have been a slight tendency towards LOWER s^o values with unsintered films - this, if substantiated, would suggest a crystal plane effect.

The 'non adsorbed' molecules might desorb from the surface after 2) only partial accommodation to the surface temperature or 3) after full accommodation but while still in some precursor state. The former would almost certainly make s^o a function of gas temperature while the latter would depend upon the temperature of the adsorbate. No evidence is available for either 2) or 3) on palladium but other evidence (e.g. King, 1966, Shade, 1964) suggests that 2) is unlikely. The situation with regards to 3) could be resolved by using the '(1-S)' methods of measuring the sticking probability to determine whether s^o is a function of surface temperature.

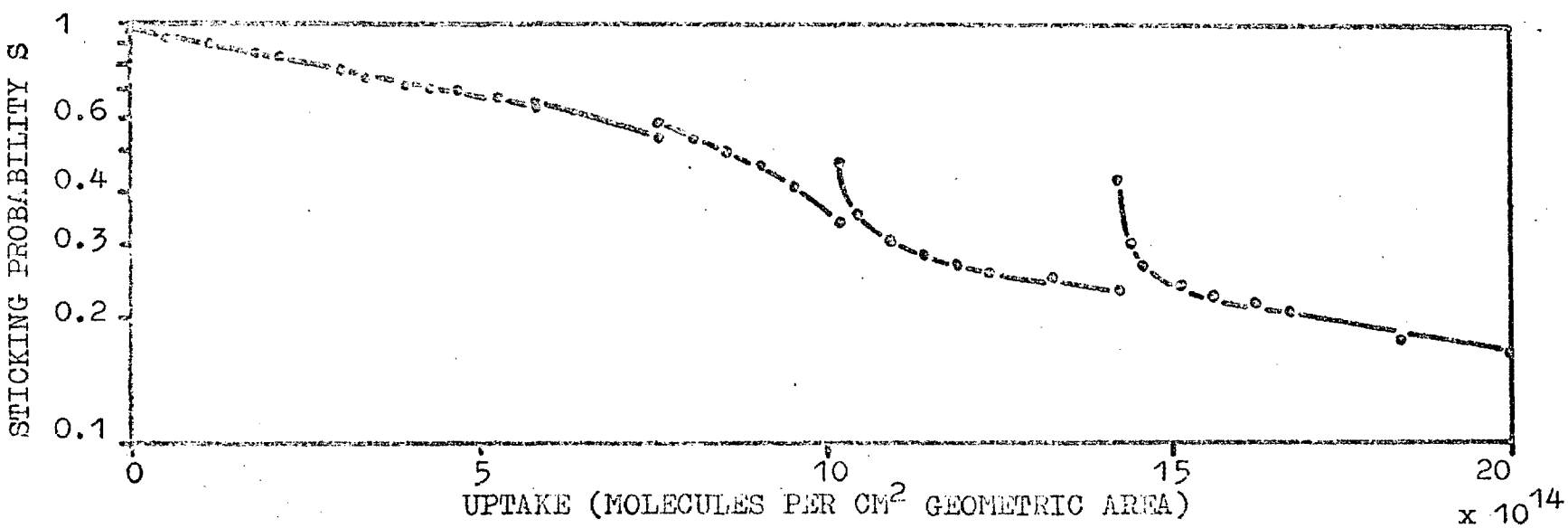

FIGURE 76. S versus uptake at 78°K - sintered film.

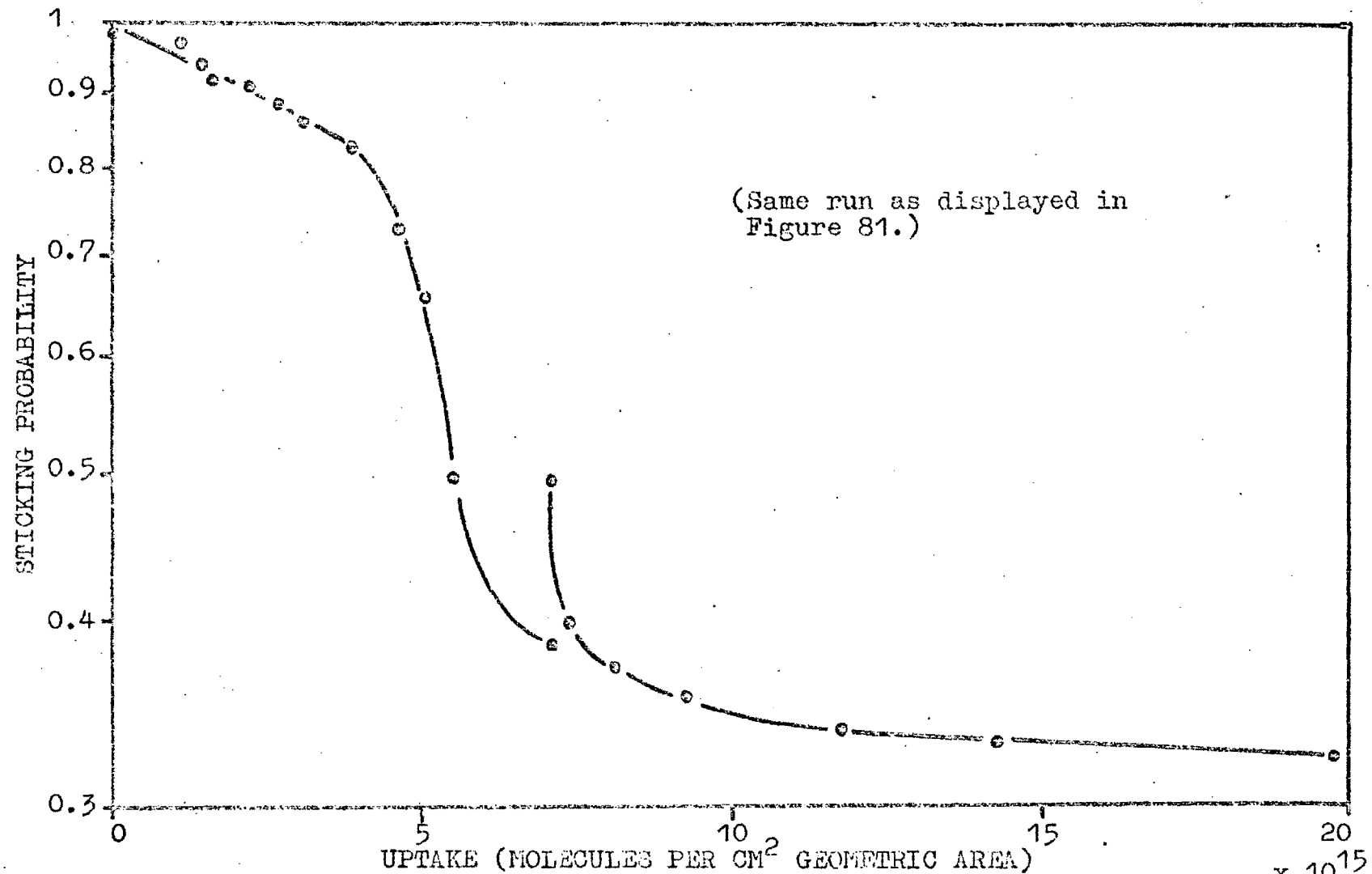

FIGURE 77. S versus uptake at 78°K - unsintered film.

16.3 The sticking probability as a function of uptake.

16.3.1 Adsorption and absorption at 78°K.

As with the other systems studied the sticking probability of hydrogen on palladium at 78°K falls continuously during the initial uptake - figures 76 and 77 display typical variations for sintered and unsintered films respectively. The onset of a redistribution process is detected at a coverage of $4 - 5 \times 10^{14}$ molecules per cm^2 geometric area by the recovery of s during interruptions in gas flow to the film; slow pressure decays after closure of the gas supply are observable at coverages greater than about 7.5×10^{14} molecules per cm^2. The kinetics of the redistribution processes are fully discussed in a subsequent section.

Sticking probabilities calculated from the 'sharp' pressure changes (i.e. ΔP_1, ΔP_2 in figure 23(b)) are invariably independent of flow rate at all stages of the sorption; this is NOT the case when the total hydrogen pressure is used at uptakes greater than about 2×10^{15} molecules per cm^2. (See also the results for titanium and tantalum.) Thus the absorption curves (s versus uptake) are relatively meaningless unless constructed from data referring to a fixed flow rate to the film. The effect of flow rate on the measured

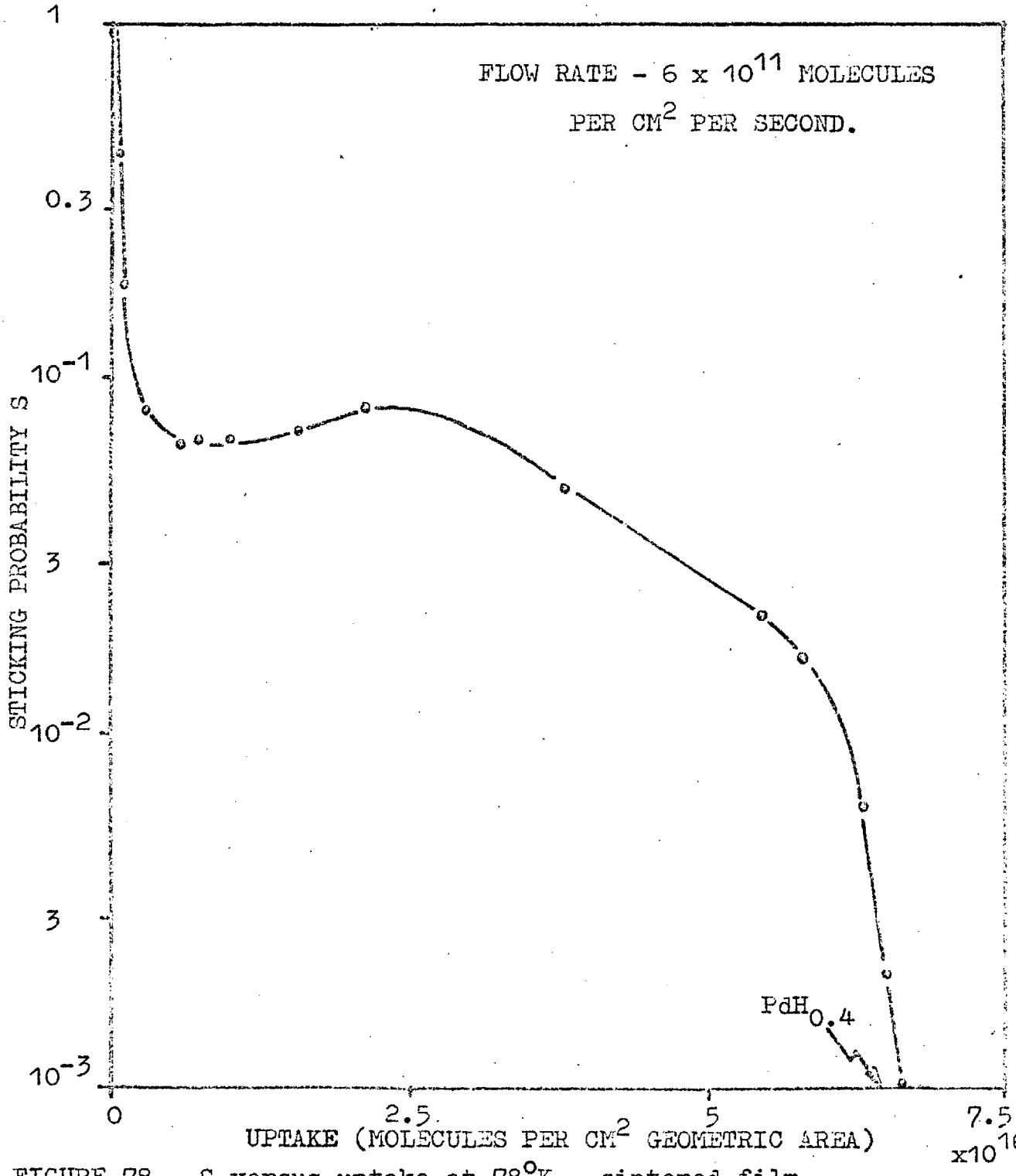

FIGURE 78. S versus uptake at 78°K - sintered film.

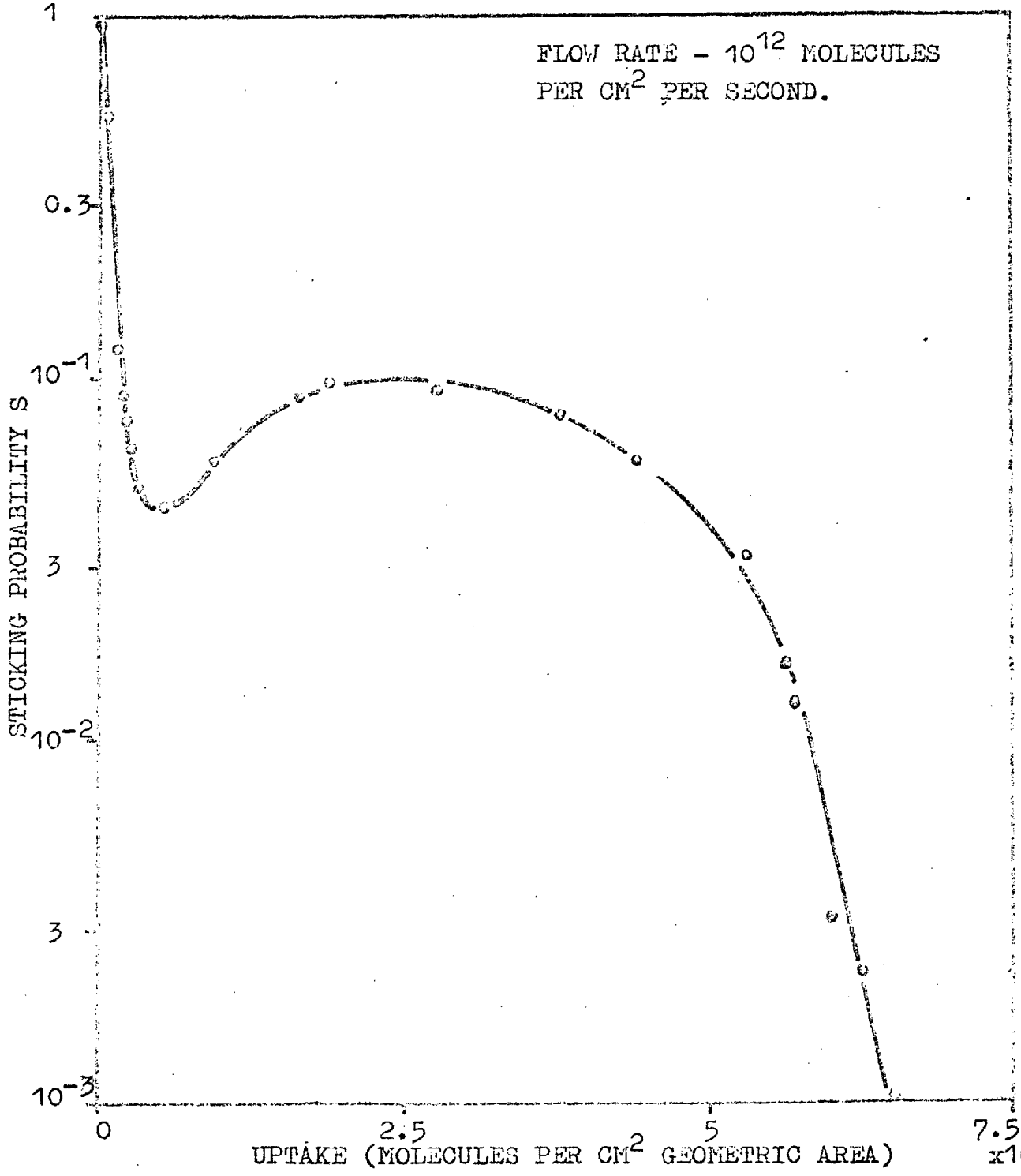

FIGURE 79. S versus uptake at 78°K - sintered film.

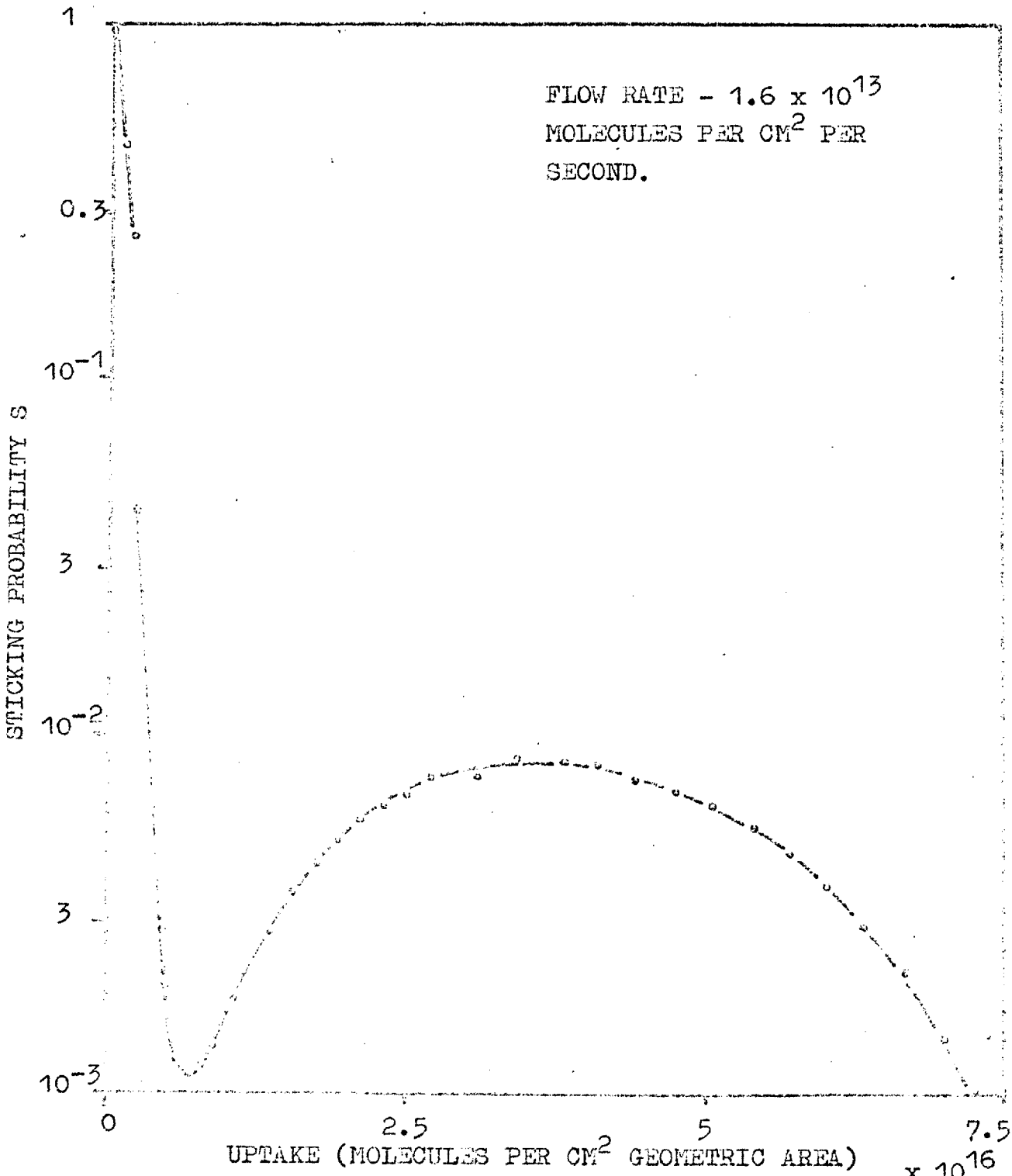

FIGURE 80. S versus uptake at 78°K - sintered film.

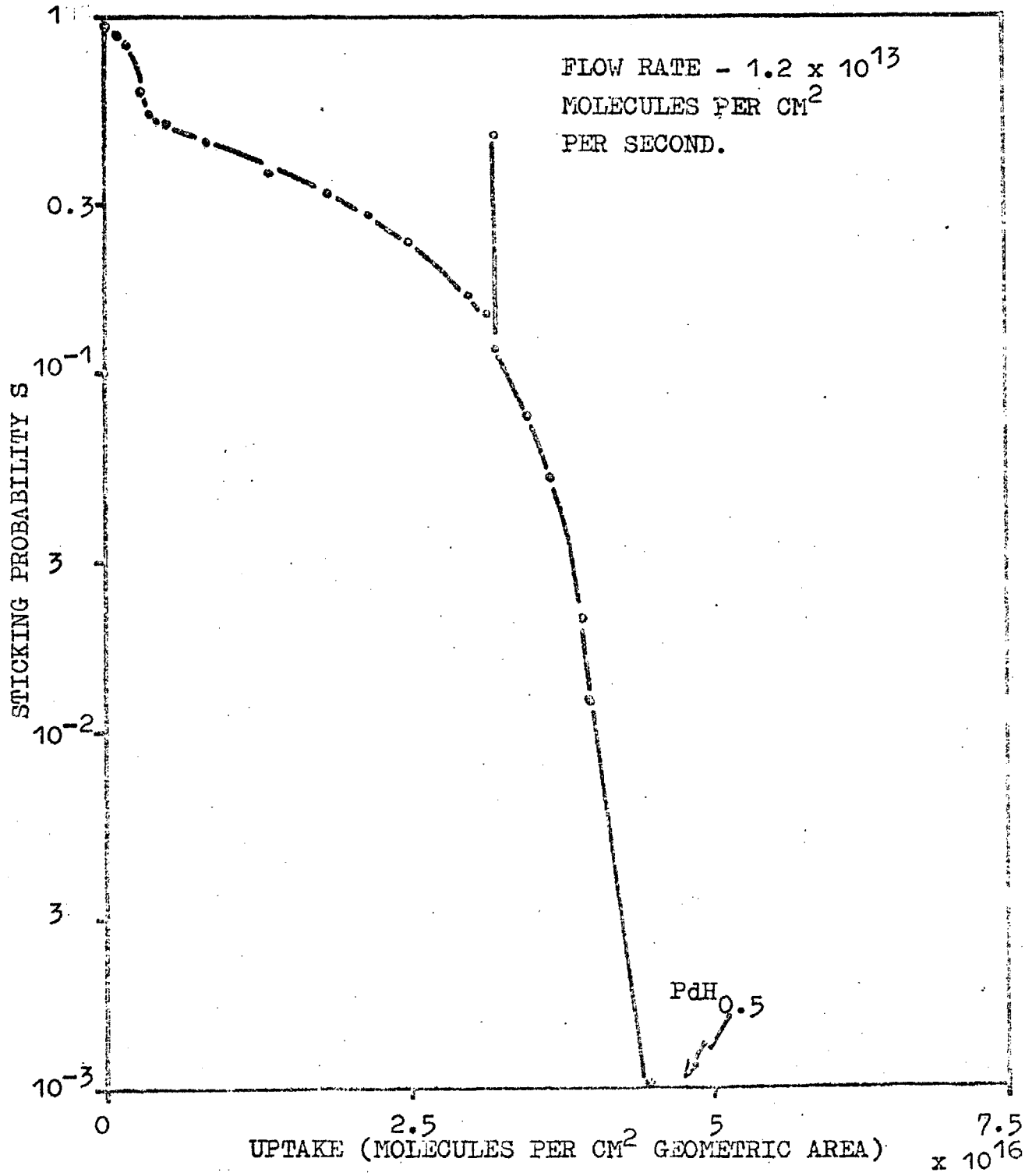

FIGURE 81. S versus uptake at 78°K - unsintered film.

pressure above the film is conveniently displayed as a log log function of the pressures P_2 and P_1 in the reaction vessel and gas reservoir. A linear relationship is obtained at a fixed uptake but the slope is a sensitive function of composition (see later). Such a family of curves enable, by interpolation, sorption curves to be constructed for a fixed rate of uptake - figures 78, 79, 80 display results for sintered films at various flow rates and figure 81 a single curve for an unsintered film. The results for sintered films are most interesting in that they possess well defined minima which increase in depth at the higher flow rates. Significantly, each minimum is at an overall composition within the range $PdH_{0.04}$ to $PdH_{0.06}$ i.e. at the maximum value for pure α phase (see section 16.1). It is suggested that the sorption curves to the base of the minima involve only the α phase and the remainder a mixture of α and β and ultimately pure β phase. Some evidence for this is as follows:-

1) The depth of the minimum increases with flow rate only in so far as shorter times are required for the sorption i.e. the magnitude of the sticking probability at the minimum is not predictable from the known pressure dependencies. Thus in one experiment using a sintered film the initial uptake took place

over a long period due to frequent interruptions of the gas supply and the use of low flow rates. There was subsequently little or no evidence for a minimum even though the flow rate used was almost identical to that in the sorption displayed in figure 80.

2) If a time dependent nucleation phenomenon exists then it should increase in rapidity with decrease of crystallite size since the distension effects inhibiting the growth of β phase will be diminished (see Everett and Nordon, 1960, and Scholtus and Keith Hall, 1963). Thus the sorption curves for unsintered films (e.g. see figure 81) show no evidence for a minimum at any point of the uptake.

Activation energies for diffusion of hydrogen within the lattice have been reported from the rate of passage of gas through metal membranes and from the rate of uptake of gas into palladium wires. The results are only of interest if the surfaces are contaminant free since otherwise the rate determining step may not be characteristic of the hydrogen palladium reaction. Thus Silberg and Bachman (1958) found that the diffusion through a membrane was dependent of surface area but independent of the thickness of the membrane thus suggesting a rate determining step at or near the metal gas interface.

Katz and Gulbransen (1960) have measured the activation energy for hydrogen diffusion through a palladium tube and have found a value of 5.6 kilocalories per gm atom in the temperature range 500 to 750°K. The latter value is presumably for the α phase palladium hydride Jewett and Makrides (1965) have observed that at 300°K the diffusion coefficient for the β phase hydride is a factor of 10 higher than that for the α phase. On this basis the activation energy for the β phase must be around 4.2 kilocalories at this temperature. Accepting these values for a bulk phase diffusion process there is therefore the situation at 78°K in which diffusion control exists only in the α phase - this agrees with the general features of the sorption curves for sintered films viz a strong dependence of s on uptake only at compositions less than $PdH_{0.05}$ (or where the saturation uptake is approached). This is particularly well exemplified in figures 78 and 79.

16.3.2. The Flow rate dependence of the reaction vessel pressure at 78°K

During the initial uptakes (<2 x 10^{15} molecules per cm^2 geometric area) the calculated sticking probabilities are independent of the flow rate to the film i.e. at a fixed uptake the reaction vessel pressure is directly proportional to the flow rate. At higher uptakes this proportionality disappears - S is 'pressure dependent'. This has been previously noted in both tantalum and titanium systems at 78°K but the elucidation of a definite relationship was difficult in these cases because 'S' fell rapidly with increasing uptake. With the hydrogen-palladium system at 78°K, S varies relatively slowly for compositions greater than about Pd $H_{0.05}$ and the relationship between reaction vessel pressure and flow rate is readily investigated. Results indicate that there is invariably a linear relationship between the logarithms of flow rate and cell pressure. Expressing the flow rate (i.e. the rate of gas uptake) in terms of the reaction vessel pressure P_2 and the gas reservoir pressure P_1 we have

flow rate = $F(P_1 - P_2)$ where F is the conductance of the tubulation between vessel and reservoir. The experimentally obtained relationship between P_1 and P_2

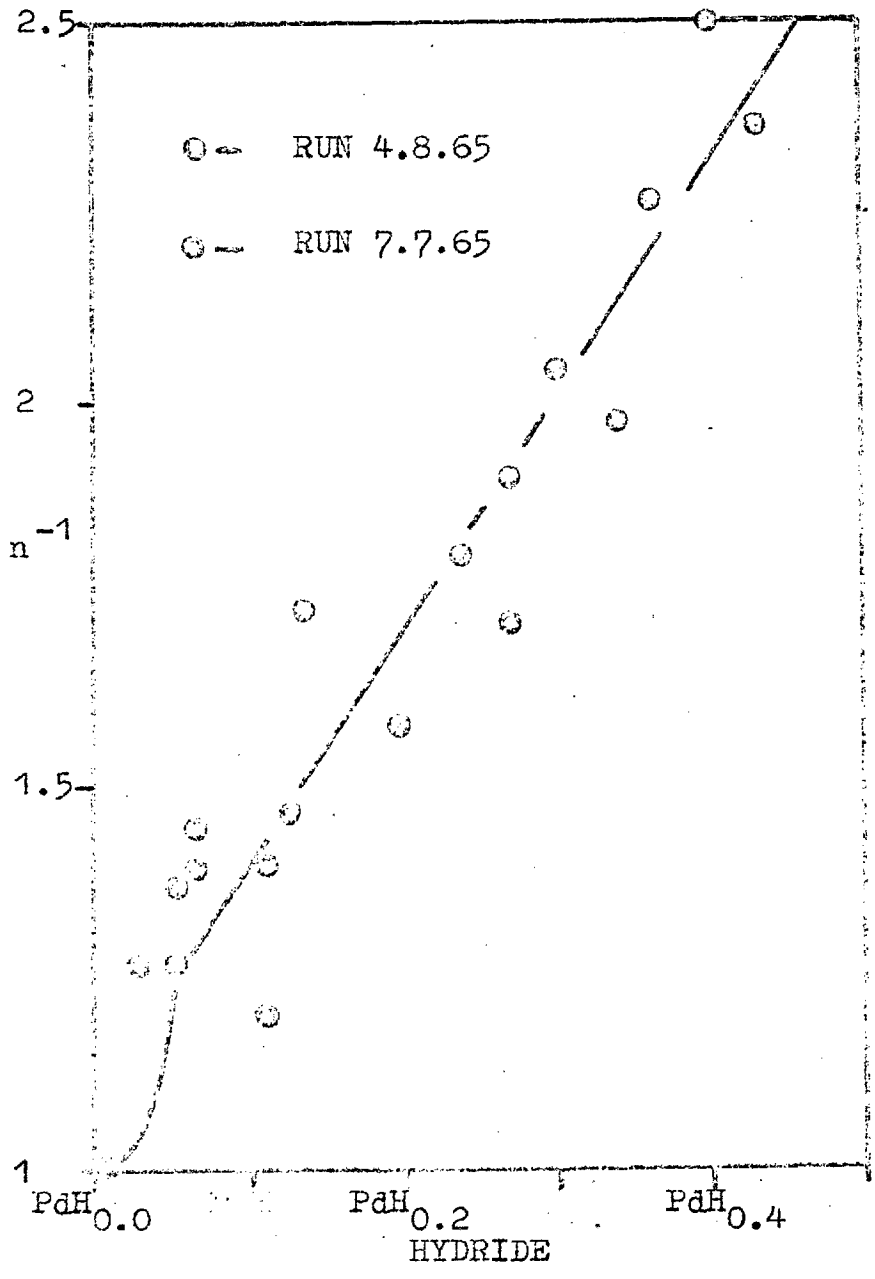

FIGURE 82. n^{-1} versus hydride composition at $78^{\circ}K$.

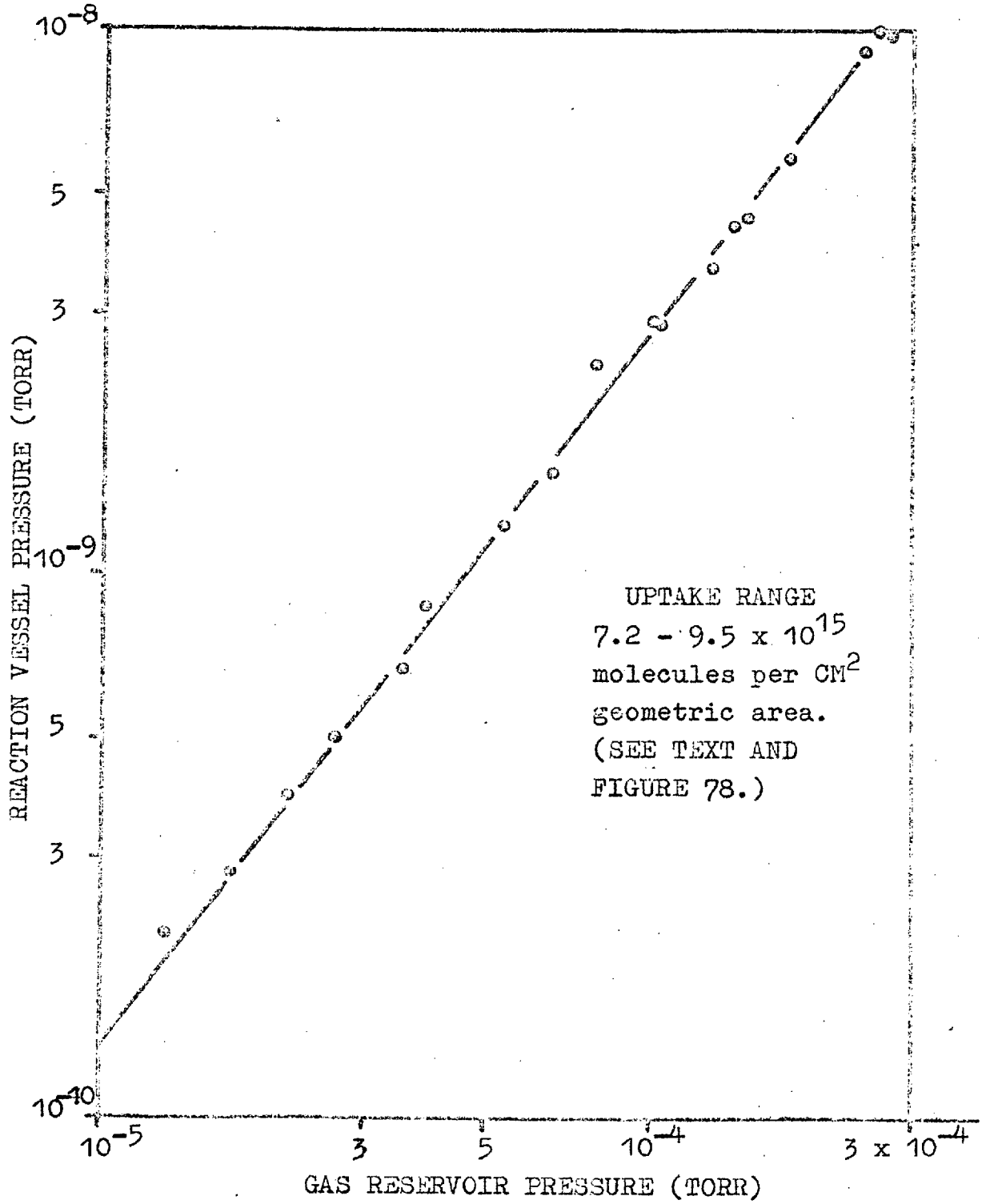

FIGURE 83. Log. log. plot of reaction vessel and reservoir pressures.

may be expressed as

$\log P_1 = n \log P_2 + n \log C$ (n, C are constants).

Thus since $P_1 >> P_2$

flow rate $= FP_1 = F(CP_2)^n$. Values of n have been calculated from two separate experiments both using sintered films - the results are displayed in figure 82 as a function of hydride composition. Figure 83 demonstrates the linearity of the relationship between P_1 and P_2 - this particular data was obtained near the minimum of the sorption curve displayed in figure 78. The values of n^{-1} vary approximately linearly with composition n falling to around 0.4 near the saturation uptake. It has been established by Katz and Gulbransen (1960) that at high temperatures (>500°K) the permeability of palladium to hydrogen is proportional to the square root of pressure. This has been taken as evidence that bulk diffusion is rate controlling since the '$P^{\frac{1}{2}}$' relationship is then readily derived if Sievert's Rule is assumed. The results of Silberg and Bachman (1958), however, indicate that such a situation does not exist since permeability was completely insensitive to membrane thickness. Likewise, in careful experiments on the degassing of nitrogen from niobium and tantalum wires at high temperatures (1400°K) Griffiths (1967) has shown conclusively that

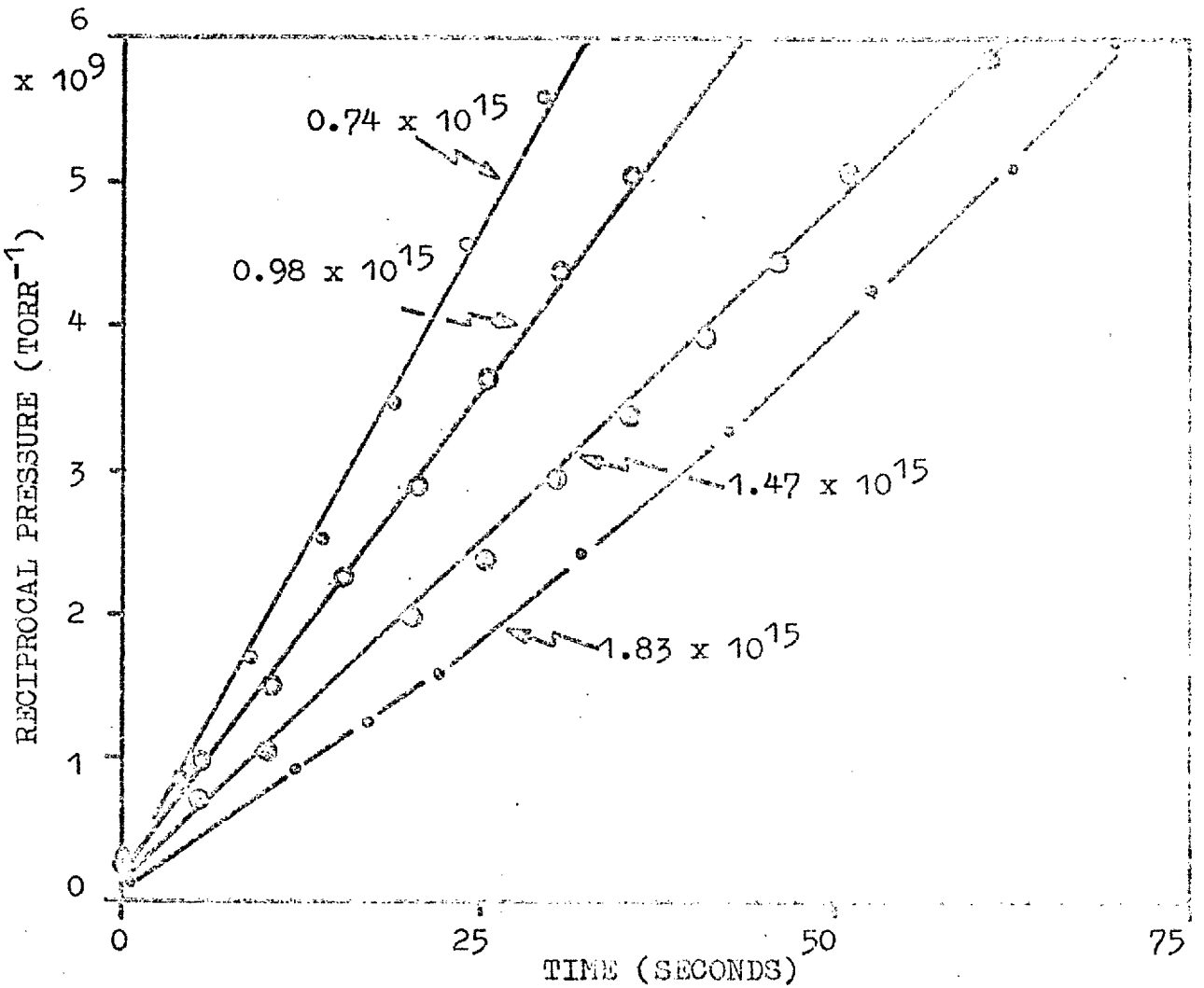

FIGURE 84. Reciprocal pressure versus time at 78°K. (Coverages in molecules per CM^2 geometric area are shown.)

the desorption of gas from the surface of the metal and not diffusion within the metal was rate controlling. This is, as previously mentioned, also in accord with general features of the variation of S with uptake at compositions greater than about $PdH_{0.05}$.

16.3.3 Slow redistribution processes at 78°K

On sintered films at uptakes between 0.7 and 1.8 x 10^{15} molecules per cm^2 geometric area the reciprocal of pressure varies linearly with time after closure of the gas supply. Figure 84 displays three such variations together with an example when the relationship is becoming non-linear (in this particular case at 1.83 x 10^{15} molecules per cm^2). Assuming adherence to the Temkin equation (see also section 15.4) the above relationship indicates that some parts of the surface become saturated with respect to the ambient gas pressure and, on closing the gas supply, there is a net transport to regions not at saturation. As shown previously the redistribution may be a process of diffusion down pores or merely a transport of gas between the exposed and less exposed parts of the outer surface, the two processes overlapping near the onset of the slow pressure decays. Both modes of redistribution have been treated in the sections on the hydrogen-molybdenum system. It is interesting to utilize the equation for transport between

regions of the outer surface to estimate the extent of the saturated region at the point when slow pressure decays are just observed. The slope of the reciprocal pressure versus time curve is given approximately by $A^{-1}\alpha' SZ$ where A is the fraction of the total surface at saturation, α' is the slope of the Temkin Isotherm i.e. $\alpha'[N(\text{molecules per cm}^2 \text{ true surface})] = \ell n \frac{P}{P^o}$, S is the sticking probability giving (from SZP) the net rate of transport of molecules and Z is the Hertz-Knudsen Collision Factor. Unfortunately α' cannot be measured at 78°K because of absorption and the difficulty in estimating the roughness factor of the film. As a (very) rough estimate it may be assumed that α' is proportional to $(T^oK)^{-1}$ between 300 and 78°K and that the roughness factor of the film is around 2.5. From results at 300°K (see later), α' is thus estimated at 78°K to be 10^{-13} per molecule per cm^2 true surface for 2.7 change in 'equilibrium' pressure. Substituting the highest value of the gradient of the reciprocal pressure versus time curves (2×10^8 $torr^{-1}$ per second) gives the relationship A^{-1}. $S = 0.7$ thus indicating (since $S \sim 0.19$) that $A \sim 0.25$ i.e. that one quarter of the total surface is at saturation at this point.

At uptakes higher than about 2.0×10^{15} molecules

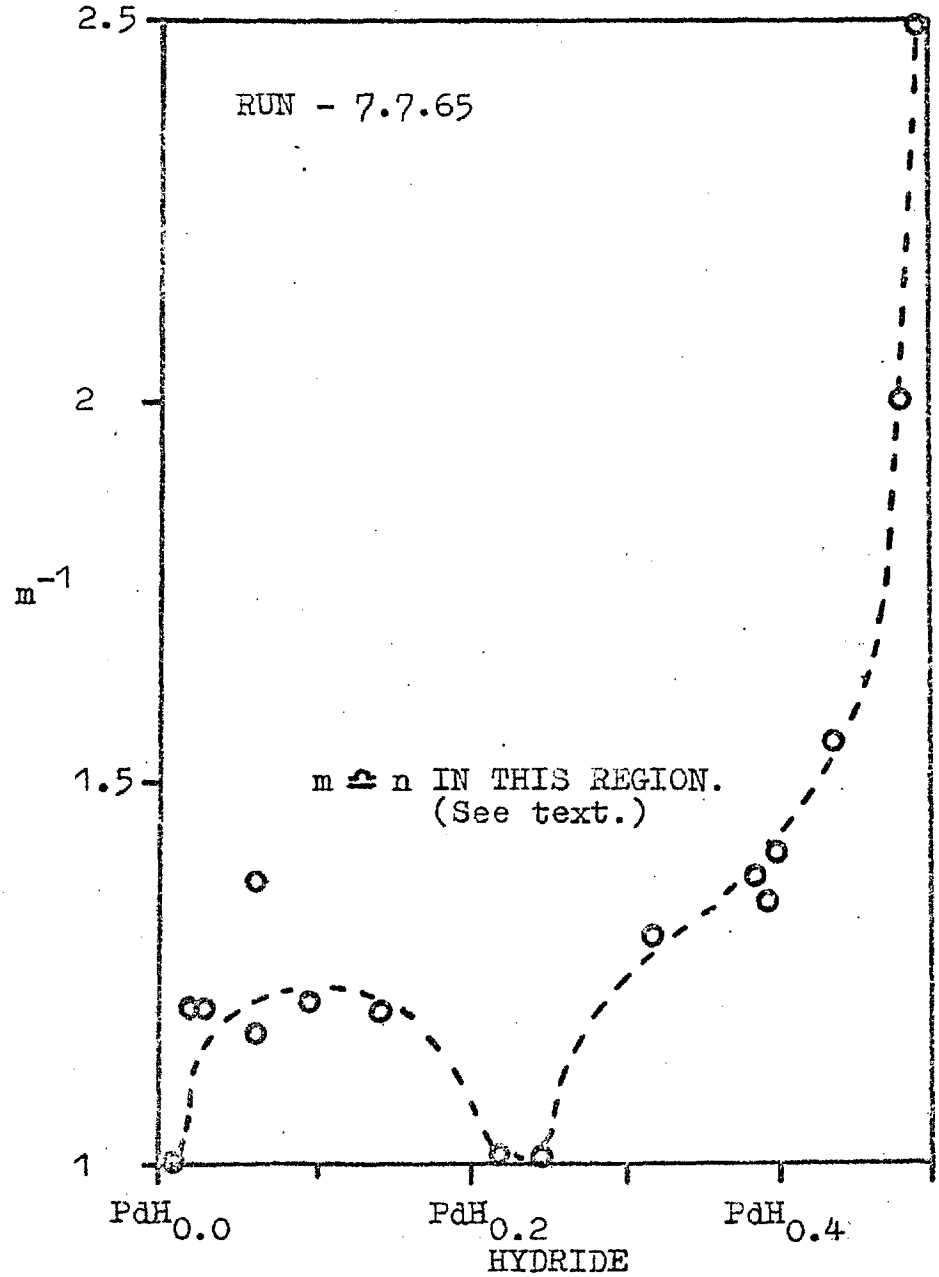

FIGURE 85. m^{-1} versus hydride composition at 78°K.

per cm^2 geometric area the kinetics of the pressure decays after closure of the gas supply do not follow any previously discussed relationship but instead are adequately described by the relationship

$$-m\,\ell n(\text{pressure}) = \ell n(\text{time} + \text{a constant}, t^o).$$

Values of m vary from unity (i.e. P^{-1} linear with time) at the low uptakes to 0.4 near saturation. Thus m varies over almost exactly the same range of magnitude as the parameter n discussed in section 16.3.2. but, as is demonstrated in figure 85, m^{-1} does not decrease linearly with increasing hydrogen uptake (see figure 82). The parameter t^o is usually in the range 3 - 7 seconds except near saturation where it rapidly increases to about one minute. No reasonable model has yet been devized to explain the kinetics of redistribution and the variations in n and m with hydride composition although in the regions where n and m are approximately equal it can be shown that the kinetics are consistent with an activation energy in the rate controlling step which is a constant fraction of that for desorption from the surface.

16.3.4. Adsorption at 300°K

The variation of sticking probability with coverage at 300°K has been displayed previously in

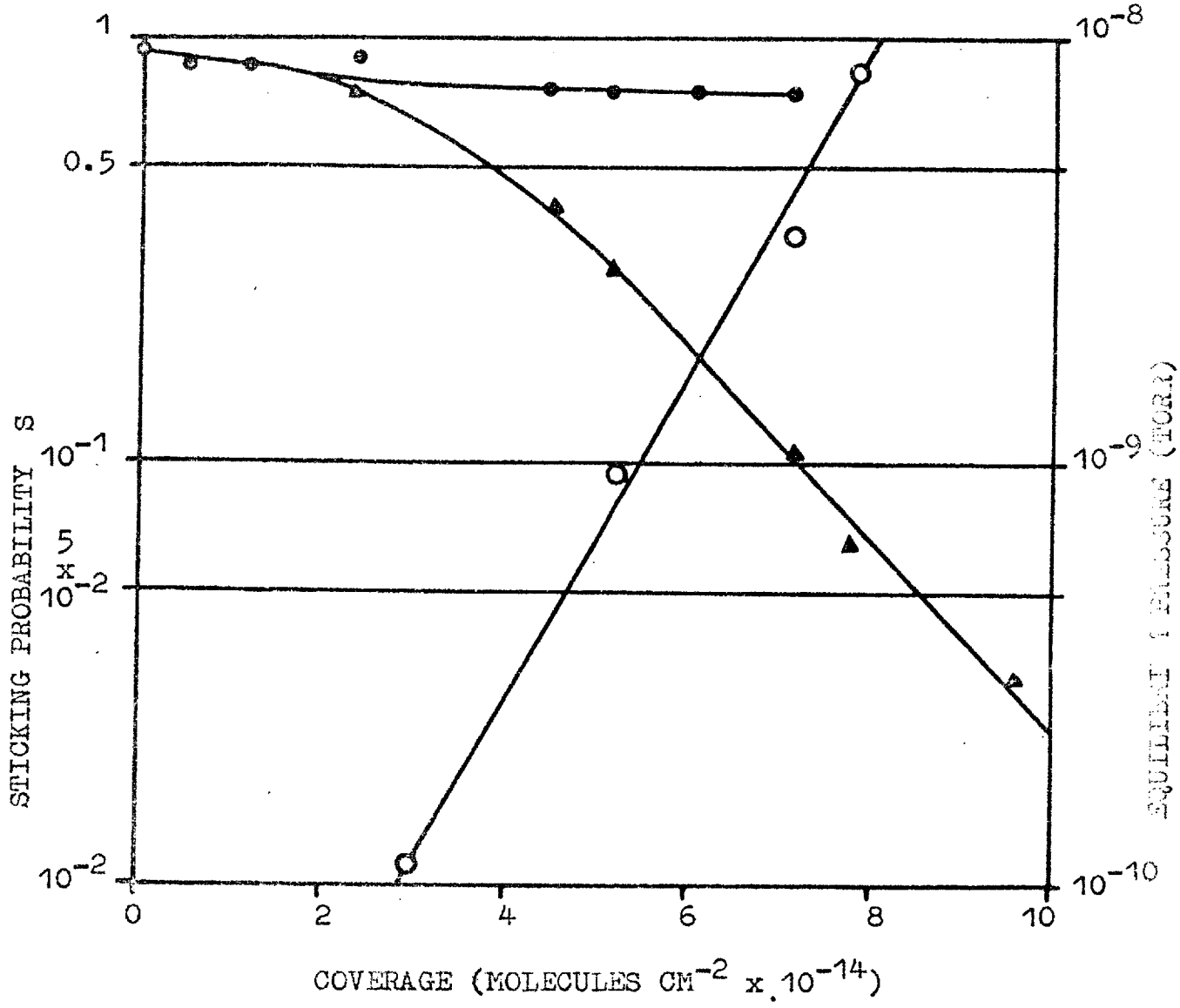

FIGURE 24. Sticking probability against coverage for hydrogen on palladium at 300°K, ● - S corrected for desorption, ▲ - S uncorrected for desorption, ○ - equilibrium pressure.

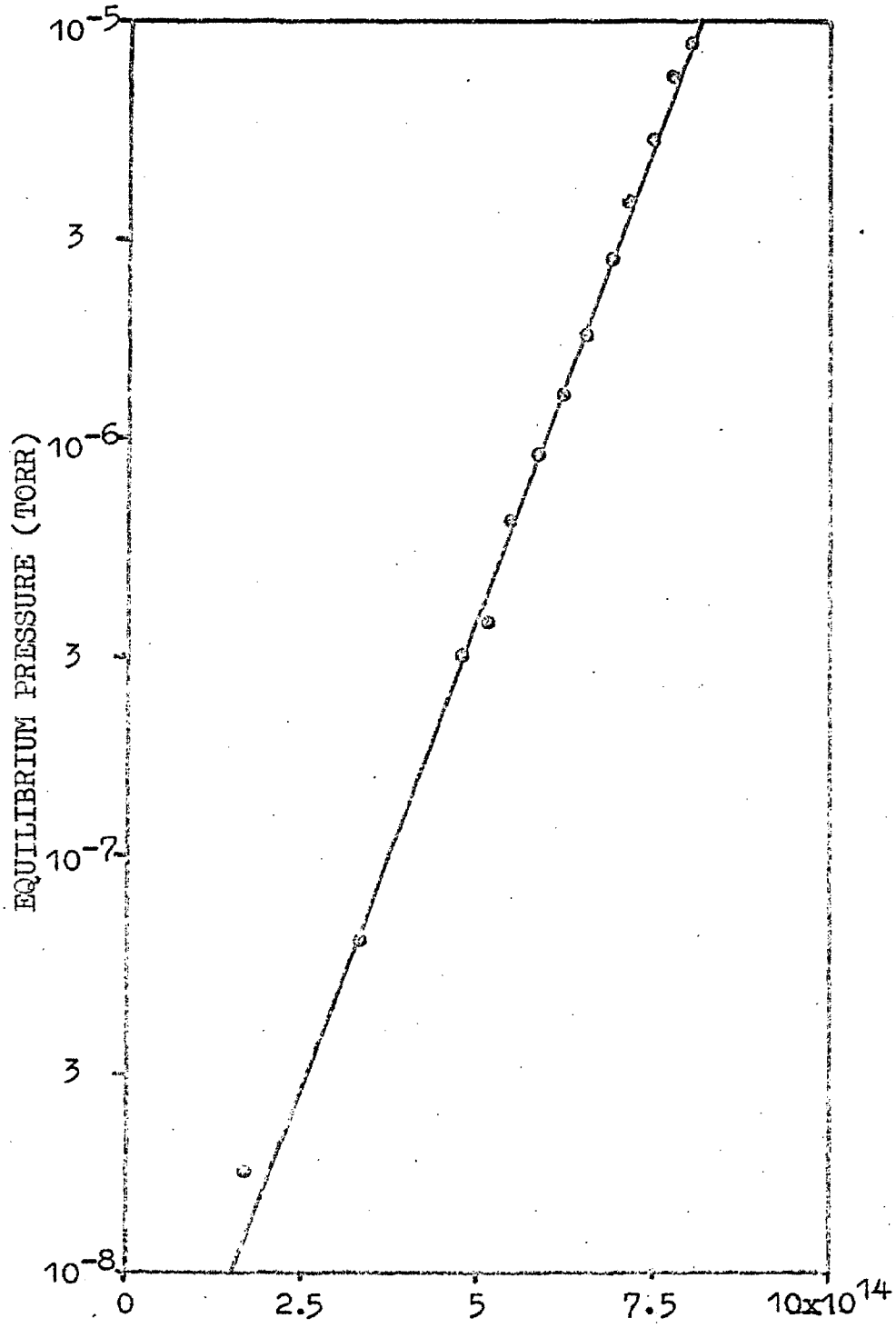

FIGURE 86. Temkin isotherm at 300°K.

figure 24; the figure is repeated here for easy reference. The general forms of S versus coverage curves at 300°K have been described in section 15.3.1. for the whole range of metals including palladium.

The isotherms at 300°K are Temkin in form with gradients around 10^{-14} per molecule per cm^2 geometric area (see also section 16.3.3.). Figure 86 displays a typical isotherm showing linearity over at least three orders of magnitude. There is no evidence of appreciable absorption at 300°K up to the highest equilibrium pressures reached (10^{-4}torr) showing that, unlike tantalum, the heat of absorption must be appreciably below about 16 kilocalories per mole. The results of Suhrmann, Wedler and Schumicki (1959) show that rapid absorption occurs at low pressure into palladium films held at 195°K thus setting a lower limit to the heat of absorption at around 12 kilocalories. These limits are confirmed by observations of absorption at temperatures greater than about 400°K when high pressures (>100 torr) are used.

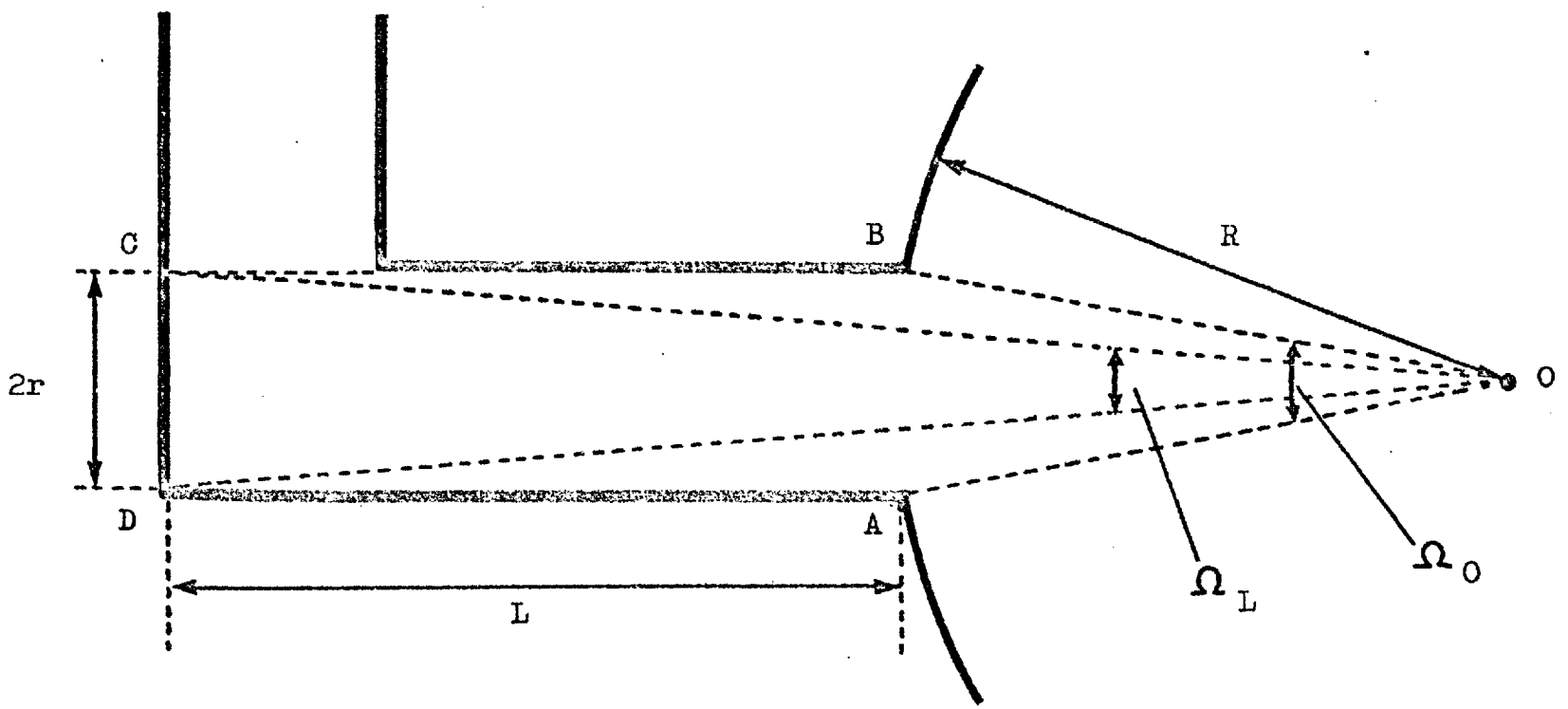

FIGURE 87. A section through the sidearm of the ionization gauge.

APPENDIX

Calculation of $\bar{\ell}$

Figure 87 shows a section through the side-arm of the ionization gauge. The situation is somewhat idealized in that the bend in the tubulation is shown as a sharp right angle, and the gas is considered to originate from a point source, whereas the diffuser sphere is about 1 cm in diameter.

The mean distance $\bar{\ell}$ that molecules travel along the gauge tubulation before colliding with the walls is $1/n\int_0^n \ell\,dn$, where n is the total number of molecules involved. This equation can equally well be given in terms of solid angles since the number of molecules emanating from the source per unit solid angle is constant. Thus

$$\bar{\ell} = \frac{1}{\Omega_0} \int_0^{\Omega_0} \ell\, d\Omega, \qquad (16)$$

where Ω_0 is the solid angle subtended at O by the cross-section of the tubulation at AB.

For $R > r$ and $\ell < L$, to a good approximation Ω is equal to $\pi r^2/(R+\ell)^2$ and $d\Omega = -2\pi r^2 d\ell/(R+\ell)^3$.

The maximum distance that molecules can penetrate before colliding with the wall is L. Thus the integration of equation (16) can be carried out in two parts:

$$\bar{\ell} = \frac{1}{\Omega_0}\int_0^L \frac{2\pi r^2 d\ell}{(R+\ell)^3} + L \int_0^{\Omega_L} d\Omega,$$

where Ω_L is the solid angle subtended at O by the cross-section of the tubulation at CD. On integrating, and substituting $\Omega_0 = \pi r^2/R^2$ and $\Omega_L = \pi r^2/(R+L)^2$ we obtain

$$\bar{\ell} = \frac{RL}{R+L}$$

References

Anderson,J.R., and Baker,B.G., 1962, J. Phys. Chem., 66, 482.

Archer,R.J., and Gobelli,G.W., 1965, J. Phys. Chem., Solids, 26, 343.

Bayard,R.T., and Alpert,D., 1950, Rev. Sci. Instrum., 21, 571.

Becker,J.A., and Hartman,C.D., 1953, J. Phys. Chem., 57, 153.

Becker,J.A., in Solid State Physics (eds. F.Seitz and D.Turnbull), 7, 379, New York; Academic Press, 1958.

Beeck, O., 1945, Rev. Mod. Phys., 17, 61.

Beeck, O., 1950, Disc. Faraday Soc., 8, 118.

Bell,R.A., and Gomer,R., 1966, J. Chem. Phys., 44, 1065.

Bloomer,R.N., 1957, Brit. J. Appl. Phys., 8, 40.

Brennan,D., and Fletcher,P.C., 1960, Trans. Faraday Soc., 56, 1662.

Brennan,D., and Hayes,F.H., 1964, Trans.Faraday Soc., 60, 589.

Carter,G., and Leck,J.H., 1959, Brit. J. Appl. Phys., 10, 364.

Clausing,P., 1932, Ann. Physik, 12, 961.

Clausing,R.E., 1961, Vacuum Symposium Transactions of the American Vacuum Society, 1, 345. (New York: Pergamon Press).

Coogan,C.K., and Gutowsky,H.S., 1962, J. Chem. Phys., 36, 110.

Datz,S., Moore,G.E., and Taylor,E.H., 1962, Third International Symposium on Rarified Gas Dynamics, Paris, p. 347.

Decker,R.W., 1954, J. Appl. Phys., 25, 1441.

Della Porta,P., and Ricca,F., 1960, Vacuum Symposium Transactions of the American Vacuum Society, (New York: Pergamon Press), p. 352.

Devonshire,A.F., 1937, Proc. Roy. Soc., A158, 269.

Dushman,S., 1921, Gen. Elec. Rev., 24, 890.

Dushman,S., 1962, Scientific Foundations of Vacuum Technique (New York: John Wiley and Sons, Inc.), 2nd Edition.

Ehrlich,G., 1956, J. Phys. Chem. Solids., 1, 1.

Ehrlich,G., 1961, J. Chem. Phys., 34, 29.

Ehrlich,G., 1961, J. Chem. Phys., 34, 39.

Ehrlich,G., 1964, Brit. J. Appl. Phys., 15, 349.

Eisinger,J., 1958, J. Chem. Phys., 28, 165.

Eisinger,J., 1958, J. Chem. Phys., 29, 1154.

Elsworth,L., and Holland,L., 1963, Brit. J. Appl. Phys., 14, 593.

Elsworth,L., Holland,L., and Laurenson,L., 1965, Vacuum, 15, 337.

Everett,D.H., and Nordon,P., 1960, Proc. Roy. Soc., A259, 341.

Feur,P., 1963, J. Chem. Phys., 39, 1311.

Foner,S.N., Mauer,F.A., and Bolz,L.H., 1959, J. Chem., Phys., 31, 546.

Frisch,R., and Stern,O., 1933, H and b.d. Phys., 22, 2, edited by H. Geiger (Berlin: Springer), p.313.

Gaede,W., 1915, Ann. Phys., Lpz., 46, 357.

Goldstone,L., 1964, Rev. Sci. Instr., 35, 1265.

Goodman,F.O., 1962, J. Phys. Chem. Solids, 23, 1269.

Goodman,F.O., 1966, Abstract of Proceedings of Fifth International Symposium on Rarified Gas Dynamics, p.253.

Gibb,T.R.P., 1962, Progress in Inorganic Chemistry 3, 315.

Gibson,R., Bergsnov-Hansen,B., Endow,N., and Pasternak, R.A., 1963, Vacuum Symposium Transactions of the American Vacuum Society (New York: Pergamon Press), p.88-92.

Gillespie,L.J., and Galstaun,L.S., 1936, J. Amer. Chem. Soc., 58, 2565.

Gomer,R., 1966, Disc. Faraday Soc., 41, 14.

Griffiths,R., 1967, Ph.D. thesis, 'An Experimental Study of Adsorption and Diffusion of Gases using Metal Filaments at Low Pressures'. (Univ.of London).

Hayward,D.O., King,D.A., and Tompkins,F.C., 1965, Chem. Comm., 178.

Hayward,D.O., and Taylor,N., 1966, J. Sci. Instr., 43, 762.

Hayward,D.O.,Taylor,N., and Tompkins,F.C., 1966, Disc. Faraday Soc., 41, 75.

Hayward,D.O., King,D.A., and Tompkins,F.C., 1967, Proc. Roy. Soc., A297, 305.

Hayward,D.O., King,D.A., and Tompkins,F.C., 1967, Proc. Roy. Soc., A297, 321.

Hayward,D.O., and Taylor,N., 1967, J.Sci. Instr., (In press).

Hickmott,T.W., 1960, J. Chem. Phys., 32, 810.

Hinchen,J.J., and Shepherd,E.F., 1966, Abstract of Proceedings of the Fifth International Symposium on Rarified Gas Dynamics, p.310.

Hoare,J.P., and Schuldiner,S., 1957, J. Phys. Chem., 61, 399.

Hint,A.L., Damm,C.C., and Popp,E.C., 1961, J. Appl. Phys., 32, 1937.

Ishii,H., and Nakayama,K., 1961, Vacuum Symposium Transactions of the American Vacuum Society, 1, 519 (New York: Pergamon Press).

Jackson,J.M., and Mott,N.F., 1932, Proc. Roy. Soc., A137, 703.

Jackson,J.M., and Howarth,A., 1933, Proc. Roy. Soc., A142, 515.

Jewett,D.N., and Makrides,A.C., 1965, Trans. Faraday Soc., 61, 932.

Josephy, B., 1933, Z. Phys., 80, 755.

Katz,O.M., and Gulbransen,E.A., 1960, Rev. Sci. Instr., 31, 615.

Kelly,K.K., 1940, J. Chem. Phys., 8, 316.

King,D.A., 1966, Disc. Faraday Soc., 41, 63.

King,D.A., 1966, Disc. Faraday Soc., 41, 109.

Kisliuk,P., 1957, J. Phys. Chem. Solids., 3, 95.

Kisliuk,P., 1958, J. Phys. Chem. Solids., 5, 78.

Kisliuk,P., 1959, J. Chem. Phys., 30, 174.

Lambert,B., and Gates,S.F., 1925, Proc. Roy. Soc., A108, 456.

Leck,J.H., 1964, Pressure Measurement in Vacuum Systems, 2nd Edition (London: Chapman and Hall).

Lindsay,W.T., and Pement,F.W., 1962, J. Chem. Phys., 36, 1229.

McCarrol,B., and Ehrlich,G., 1963, J. Chem. Phys., 38, 523.

McCarrol,B., 1963, J. Chem. Phys., 39, 1317.

McKee,C.S., and Roberts,M.W., 1965, Chem. Comm., 59.

Moore,G.E., and Allison,H.W., 1955, Phys. Rev., 96, 840.

Moore,G.E., and Unterwald,F.C., 1964, J. Chem. Phys., 40, 2626.

Morrison,J.L., and Roberts,J.K., 1939, Proc. Roy. Soc., A173, 1.

Nace,D.M., and Aston,J.G., 1957, J. Amer. Chem. Soc., 79, 3619.

Nottingham,W.B., 1954, Vacuum Symposium Transactions of the Committee of Vacuum Techniques (New York: Pergamon Press), p.76.

Pasternak,R.A., and Wiesendanger,H.U.D., 1961, J. Chem. Phys., 34, 2062.

Pasternak,R.A., Endow, N., and Bergsnov-Hansen,B., 1966, J. Phys. Chem., 70, 1304.

Pedersen,B., Krogdahl,T., and Stokkeland,O.E., 1965, J.Chem. Phys., 42, 72.

Redhead,P.A., 1959, Sixth National Symposium on Vacuum Technology Transactions p.12.

Redhead,P.A., 1961, Trans. Faraday Soc., 57, 641.

Redhead,P.A., 1962, Symposium on Electronic and Vacuum Physics; Balatonfoldvar, Hungary. p.89.

Redhead,P.A., 1963, Vacuum, 13, 253.

Ricca,F., Medana,R., and Saini,G., 1965, Trans. Faraday Soc., 61, 1492.

Rideal, Sir E.K., and Sweett,F., 1960, Proc. Roy. Soc., A257, 291.

Rigby,L.J., 1964, Canad. J. Phys., 42, 1256.

Rigby,L.J., 1965, Canad. J. Phys., 43, 1020.

Roach,D.V., and Thomas,L.B., 1966, Abstract of Proceedings of Fifth International Symposium on Rarified Gas Dynamics. p.281.

Roberts,J.K., 1935, Proc. Roy. Soc., A152, 445.

Roberts,M.W., 1963, Trans. Faraday Soc., 59, 698-712.

Rootsaert,W.J.M., van Reijen, L.L., and Sachtler,W.M.H., 1962, J. Catalysis, 1, 416.

Saba,W.G., Wallace,W.E., Sandmo,H., and Craig,R.S., 1961, J. Chem. Phys., 35, 2148.

Saini,G., Ricca,F., and Nasini,A.G., 1959, Ric. Sci. 29, 1523.

Schlier,R.E., 1958, J. Appl. Phys., 29, 1162.

Scholtus,N.A., and Hall,K.W., 1963, J. Chem. Phys., 39, 868.

Schulz,G.J., and Phelps,A.V., 1957, Rev. Sci. Instr., 28, 1051-1054.

Sears,G.W., and Cahn,J.W., 1960, J.Chem. Phys., 33, 494.

Shade,R.W., 1964, J. Chem. Phys., 40

Silberg,P.A., and Bachman,C.H., 1958, J. Chem. Phys., 29, 777.

Smith,J.N., and Fite,W.L., 1962, J. Chem. Phys., 37, 898.

Smith,J.N., and Saltsburg,H., 1966, J. Chem. Phys., 45, 2175.

Spalthoff,W., 1961, Z. Physik. Chem. (Frankfurt)., 29, 258.

Stalinski, B., 1954, Bull. Acad. Polon. Sci., 2, 245.

Stalinski,B., Coogan,C.K., and Gutowsky,H.S., 1961, J.Chem. Phys., 34, 1191.

Suhrman,R., Wedler,G., and Schumicki,G., 1959, Structure and Properties of Thin Films (eds. Neugebauer,C.A., Newkirk,J.B., and Vermilyea,D.A.) p.278. (New York: John Wiley 1959).

Suhrmann,R., Schumicki,G., and Wedler,G., 1964, Z. Phys. Chem., 42, 187.

Thomas,L.B., and Olmer,F.G., 1943, J.Am. Chem. Soc., 65, 1036.

Thomas,L.B., and Brown,R.E., 1950, J. Chem. Phys., 18, 1367.

Thomas,L.B., and Silvernail, 1966, data mentioned in paper of Roach and Thomas, q.v.

Torrey,H.C., 1958, Nuovo Cimento Suppl., 9, 95.

Trapnell,B.M.W., 1951, Proc. Roy. Soc., A206, 39.

Wachman,H.Y., 1957, 'The Thermal Accommodation Coefficient and Adsorption on Tungsten', Ph.D. Thesis University of Missouri.

Wachman,H.Y., 1962, J. Am. Rocket Soc., 32, 2.

Wachman,H.Y., 1966, Abstract of Proceedings of Fifth International Symposium on Rarified Gas Dynamics, p.305.

Wagener,S., 1950, Brit. J. Appl. Phys., 1, 225.

Wagener,S., 1951, Brit. J. Appl. Phys., 2, 132.

Wagener,S., 1952, Proc. Inst. Elec. Eng., 99 (III), 135.

Wagener,S., 1956, J. Phys. Chem., 60, 567.

Wagener,S., 1957, J. Phys. Chem., 61, 267.

Wahba,M., and Kemball,C., 1953, Trans. Faraday Soc., 49, 1351.

Waite,T.R., Wallace,W.E., and Craig,R.S., 1956, J. Chem. Phys., 24, 634.

Wasilewski,R.T., and Kehl,G.L., 1954, Metallurgia, 50, 225.

Wedler,G., and Strothenk,H., 1966, Z. Phys. Chem., 48, 86.

Winters,H.F., Denison,D.R., and Bills,D.G., 1962, Rev. Sci. Instr., 33, 520.

Worsham,J., Wilkinson,W.K., and Shull,C.G., 1957, J. Phys. Chem. Solids, 3, 303.

Wortman,R., Gomer,R., and Lundy,R., 1957, J. Chem. Phys., 27, 1099.

Zingerman,Ya,P., and Morozovskii,V.A., 1961, Soviet Physics - Solid State, 3, 760.